A Generic Assessment of Waste Disposal at Douala City Practices, Principles and Uncertainties

ABDON ATANGANA

Submitted in fulfilment of the requirements for the degree of

Doctor of Philosophy PhD

In the Faculty of Natural and Agricultural Sciences

Institute for Groundwater Studies

University of the Free State

Bloemfontein

Promoter: Professor Joseph François Botha

January 2013

DECLARATION

This thesis contains no material that has been submitted for the award of any other degree or diploma at this or any other University and contains no material previously published or written by any other person except where due reference has been made in the text. I furthermore cede copyright of the thesis in favour of the University of the Free State.

ABDON ATANGANA

ACKNOWLEGDEMENT

I wish to express my deepest appreciation to:
Prof. J.F. Botha, my supervisor, for his constant benevolent supervision, advice, encouragement and untiring assistance.
Prof. A.H.J. Cloot, my Master thesis supervisor, for his advice and assistance.
Prof. T.M. Acho for his constant advice and encouragement.
To my colleague Fannie De Lange for his assistance and companionship during my studies.
The financial support received from the National Research Foundation through a grant to my promoter.
Special words of thanks to:
My father the extraordinary plenipotentiary ambassador of Cameroon to Japan, South Korea, Australia and New Zealand his Excellency Dr Pierre Ndzengue, whose love, prayers and consistent financial support gave me the courage to complete this work.
My late mother Ngono Antoine, for her love and care.
My only and begotten complementary Ernestine Alabaraoye for her prayers, constant support, companionship and encouragement towards my education.
My entire family for their prayers, love and encouragement for my study.
To my saviour Jesus Christ for giving me life, good health and resources needed to undertake this study.

CONTENTS

LIST OF FIGURES

LIST OF TABLES

LIST OF SYMBOLS

$S_0(x,t)$ = Specific storativity
$K(x,t)$ = Hydraulic conductivity tensor of the aquifer
$S_s(x,t)$ = Specific storage of saturated porous media
V_x, V_y, V_z = Darcy velocity through the unit volume along the x, y, and z coordinate axes

W = Volumetric flux per unit volume and represents internal sources and/or sinks of water
m_s = mass of solid dissolved in a mass
m_f = mass of the fluid
v = Volume occupied by the total mass of the dissolved solids
C = Mass fractional or simply fractional concentration
c = Volumetric concentration
C^* = Mass of the substance sorbed at a mineral
K_d = Distribution coefficient
R_f = Retardation factor
a = Sorption constant
b = Maximum sorbable mass of the substance
$s(\mathrm{x,t})$ = Fraction of dissolved solids
$m_a(\mathrm{x,t})$ = Total mass of the solids that the porous matrix
$m_m(\mathrm{x,t})$ = matrix with mass
ρ_b = Dry bulk of the matrix including the adsorbed solids
$\mathrm{F}(\mathbf{x},\mathrm{t})$ = Flux of material through a unit area of the boundary, per unit of time
n = Outside unit normal vector
Serf(x) = Serf-error function
fα(x) = Alpha-stable density function
$F_m(\mathrm{x,t})$ = Molecular flux expressed as mass per unit area time
D_m = Molecular diffusion coefficient of the dissolved mass in the free fluid
T = Transmissivity Tensor
$F_h(\mathbf{x},\mathrm{t})$ = Hydrodynamic flux
J^α = Riemann-Liouville fractional integral operator of order α

D_*^α = fractional differential operator
e_{ijk} = Levi-Civita symbol
$erfc$ = Complementary error function
erf = Error function
$E_{\alpha-\beta,\beta}$ = Mittag -Leffler function
$\mathcal{L}$ = Laplace transform
α = Alpha
β = Beta
θ = Theta
μ = Mu

∇ = Nabla operator
ρ = Rho
τ = Tau
Δ = Delta
η = Eta
Γ = Gamma function
ζ = Zeta
Φ = Phi
Ω = Omega
λ = Lambda
ξ = Xi
∂ = Partial derivative
α_L and α_T = are two parameters, known as the longitude and transverse dispersivities
δ_{ij} = Kronecker delta
$\partial_{\underline{x}}^{\alpha}$ = Partial fractional derivative
$\nabla_{\underline{q}}^{\alpha}$ = Fractional Laplace operator
ρ_{f} = density of the fluid itself
$\Omega(\mathrm{x},\mathrm{t})$ = volume of partially saturated porous material
$\Omega(\mathrm{x}_0,\mathrm{t}_0)$ = Original volume of Ω
θ = Volumetric moisture of the medium
ρ = Density of the solution that is the density of the dissolved solids
$\Phi(x,t)$ = Piezometric head

Chapter 1

INTRODUCTION

1.1 GENERAL

Most of the Earth's liquid freshwater is found, not in lakes and rivers, but is stored underground in conglomerations of voids, called *aquifers*, present in the geological formations constituting the earth's mantle, where they act as reservoirs of water for rivers and streams, especially during periods of drought or low rainfall—a phenomenon commonly called *base flow*. This resource, conventionally referred to as *groundwater*; therefore forms an essential, in fact major, component of the fresh water resources, as illustrated by the fact that nearly two billion ($2\ 10^9$) people depend directly on groundwater For their drinking water, while 40% of the world's food are produced on farmlands irrigated with groundwater (Morris *et al.,* 2003). It is therefore of vital importance that this essential resource should be protected at all costs if it is to keep sustaining the human race and the various ecosystems that depend on it in the future.

One reason why groundwater, so often constitutes the main source of drinking water in many cities and towns around the world, is because it is frequently present in sufficient quantities at the point of demand. However, this seemingly advantage may sometimes be its greatest disadvantage, especially in situations where the groundwater occurs at shallow depths and the area overlying the aquifer is populated densely. This problem is particularly relevant in the present technological age with its vast quantities of waste that is often disposed in an uncontrolled manner. Such a situation occurs at Douala the economic capital of Cameroon in central Africa. The city not only hosts more than 80% of industries in the country, but also has the largest urban population of approximately 3 000 000 with a population density of approximately 350 persons per square kilometre (Eneke *et al.,* 2011) , which continue to increase at a rate of approximately 120 000 migrants per year from the rural areas (Guevart *et al*., 2006), while the groundwater level is very shallow and may sometimes rise above the soil surface, especially during floods, which occur not too infrequently.

There are essentially two difficulties that hamper the restoration of large-scale polluted aquifers. The first is that groundwater is nothing else than rainwater that infiltrated the soil surface at one time or another and therefore could contain large quantities of dissolved solids that are potentially hazardous to living organisms. The second is that groundwater is, with the exception of natural springs and other seepage faces, invisible. It is thus not always easy to detect and control groundwater pollution. Although the pollution problem is not

restricted to groundwater as such, it is aggravated here, because of the ancient belief that wastes are safely disposed of, if buried below the earth's surface. It took disasters like Love Canal and the Price Landfill (Princeton University Water Resource Program, 1984) to discover the detrimental effects that this practice may have on the population living on or near polluted aquifers. Extreme care therefore should be exercised to prevent the pollution of any aquifer that may pose problems to living organisms or to try and restore a polluted aquifer threatening the natural environment. Groundwater pollution therefore needs to be addressed once discovered with the view, to prevent its spread and to clean and restore contaminated aquifers that may pose unacceptable risks to the environment.

1.2 PURPOSE OF THIS STUDY

While the problem of groundwater pollution is nowadays recognized worldwide and many governments have started to take aggressive action to address it (Wisegeek, 2012), such investigations are often conducted in a haphazard and injudicious fashion, or simply neglected. Two reasons are often advanced to account for this state of affairs. The first that groundwater is, with the exception of natural springs and seepage faces, invisible and the second that groundwater originated from rainwater that infiltrated into the soil surface and hence dissolve any solids, some of which are hazardous to living organisms, during the infiltration process. It is thus not always easy to detect and control groundwater pollution, or to restore a polluted aquifer.

One approach to address the previously described situations would be to base the investigations of a polluted groundwater resource on a well-established and international accepted structured methodology or framework. However, environmental phenomena are complex and often site-dependent.The development of such a framework can thus be a formidable task, as can be seen from a review of the methodology developed during the coordinated research program on the Improvement of Safety Assessment Methodologies for Near Surface Disposal Facilities (ISAM) organized by the International Atomic Energy Agency (IAEA) to improve the disposal of low and intermediate level radioactive waste (IAEA, 2004a, 2004b). No attempt will therefore be made to develop such a framework for Douala. What will be done instead is to use information from the ISAM and related methodologies (Jousma and Roelofsen, 2003) to propose a set of guidelines for the future restoration of the groundwater resources of Douala and demonstrate their application to the groundwater resources.

1.3 SCOPE OF THE STUDY

The best way to develop a set of guidelines for the restoration of the groundwater resources at Douala is to have a detailed knowledge of all the factors that may contribute to the pollution. These include the origin and types of waste contributing to the pollution, the process that generates the waste, the nature of the natural environment and the effects that the waste have on humans and the natural environment. The thesis therefore begins with a discussion of these aspects, as they presently exist at Douala in Chapter 2.

One could in principle use any approach to develop a framework for the restoration of a contaminated groundwater resource. However, as a review of the ISAM and related methodologies referred to above will show, much can be gained by dividing the resource and its immediate surroundings, henceforth referred to as the site into three basic components: the *near field* or *source* (equated here with the contaminated aquifer), the *geosphere* (the geological formations in which the aquifer occurs) and the *biosphere* (the regions of the earth's crust and atmosphere surrounding the aquifer occupied by living organisms). This approach was also used in the development of the set of guidelines, proposed in Chapter 3 for the Douala aquifer.

There are many "trial–and–error" approaches that can be used to implement a framework for the remediation of a contaminated aquifer. However, experiences worldwide have shown that the most useful approach is to supplement the framework with an appropriate *computational model*, able to simulate the behaviour of the site under different conditions and stresses (National Academy of Science, 2007). One approach to develop such a model is to use the existing information and develop an appropriate *conceptual model* of the site. This conceptual model is then translated into a *mathematical model* and implemented either analytically or numerically on a computer to simulate the future behaviour of the aquifer and to study the efficiency of the guidelines proposed in Chapter 3 to clean up the aquifer. The basic mathematical principles are underlying such a model together is discussed in Chapter 4. New analytical solutions of the groundwater flow and advection dispersion equations are discussed in Chapter 5. The implementation on a computer through the commercial computer package FEFLOW (Diersch, 2009) is discussed in Chapter 6. Various methods can be used for the remediation of contaminated groundwater (U.S. Environmental Protection Agency (EPA), 2012), such as pump-and-treat methods (U.S. Geological Survey (USGS), 1999), air sparging and vacuum extraction techniques (Suthersan, 1999). The methods are, unfortunately, often costly, ineffective and needs

constant human attention and therefore may not be appropriate for every contaminated site. This applies in particular to Douala, which is situated at an elevation of 60 mamsl in the littoral province of Cameroon, approximately 50 km from the Gulf of Guinea. The city experiences in general a humid equatorial climate with a maximum annual rainfall of 4 000 mm, while daily temperatures ranges from 23°C to 33°. What seems to be required here is a method that can cope with these climatic conditions with little human intervention. A method that seems to be perfectly suitable for this purpose and has become a viable alternative to pump-and-treat methods over the past few decades is *permeable reactive trench technology* (Hudak, 2009; ITRC (Interstate Technology & Regulatory Council, 2011), also called permeable reactive boundaries or Deep Aquifer Remediation Tools (U.S.Geological Survey (USGS), 1999). This technology is discussed in more detail in Chapter 5 and its possible implementation at Douala investigated with the computational model developed for the Douala aquifer. Computational models have been used for years in groundwater investigations (Pinder and Gray, 1977; Botha, 1985), often with the assumption that results obtained from such models describe the behaviour of the aquifer accurately. However, mechanistic modelling of physical systems is often complicated by the presence of uncertainties (Isukapalli and Georgopoulos, 2001). The implications of these uncertainties are particularly important in the assessment of several potential regulatory options, for example, with respect to the selection of a strategy for the control of pollutant levels. While these uncertainties have regularly been neglected in the past, it is nowadays imperative that groundwater models be accompanied by estimates of uncertainties associated with the model. Although a large number of approaches are available for this purpose (National Aeronautic and Space Administration (NASA, 2010), they often require exorbitant computing resources. One approach based on the Latin Hypercube Sampling method (Helton and Davis, 2003) is used in Chapter 7 to derive uncertainty estimates based on the analytical solution of the one-dimensional hydrodynamic dispersion equation derived in Chapter 5. It has been known for years that the hydrodynamic dispersion equation discussed in Chapter 5, is not able to account for the long-tail plumes often observed in studies of contaminated fractured-rock aquifers. One approach that has become quite fashionable in recent years to account for this is the replacement of the ordinary spatial and temporal derivatives in the hydrodynamic equation of Chapter 4, separately or simultaneously, with fractional derivatives. This approach and its application to the hydrodynamic equation is illustrated in Chapter 8 with the help of the mathematical computer package *Mathematica* (Wolfram Research Inc., 2012).

Chapter 2

OVERVIEW OF POLLUTION IN DOUALA CITY

2.1 GEOGRAPHICAL FEATURES

Douala City is situated at latitude 4 1′ North and longitude 9 45′ East on the Wouri estuary, approximately 50 km from where the estuary opens in the Atlantic Ocean, which enhances tidal inflow of saline water along the waterfront. The estuary with its richly endowed natural and socio-economic resources is the dominant feature along the littoral zone of Cameroon.

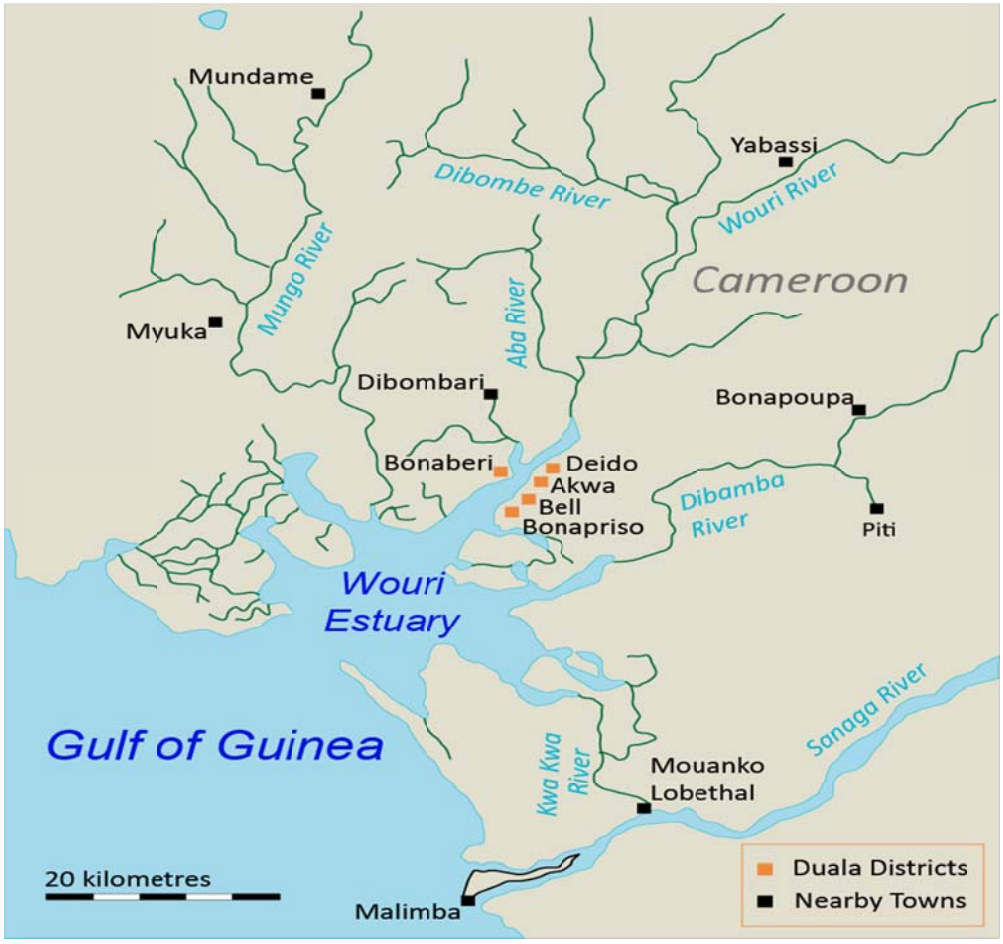

Figure 2-1: Map of the five districts of Douala and surrounding towns (Atheull *et al.*, 2009).

Douala is administratively divided into 5 districts governed by councils following the typical Cameroonian centralised command system where a government delegate appointed by the President of the Republic, presides over a council. The city houses today about 3.5 million people in a nucleated settlement pattern (Gue´vart *et al.,* 2006). The famous central area of the city, Akwa, has banks, commercial enterprises and other small-scale businesses.

The topography surrounding Douala which slopes gently from an altitude of approximately 57 m in the east towards approximately 3 m along the Wouri River in the west, see (Gue´vart *et al.,* 2006).This and the high run-off rate in the Wouri estuarine system cause groundwater levels in the city to be shallow and even above the soil surface in some areas. The city is consequently often subjected to frequent severe floods almost all year round. This applies in particular to the flood-prone areas like Mabanda and Bonendale in Bonaberi to the north and the Youpwe area in the south, as illustrated by the computer generated view of the 2010 flood in (Gue´vart *et al.,* 2006). As can be expected, such floods affect the economy of the city and life in the city adversely.

Figure 2-2: Aerial view of Douala's urban sprawl (Atheull *et al.,* 2009).

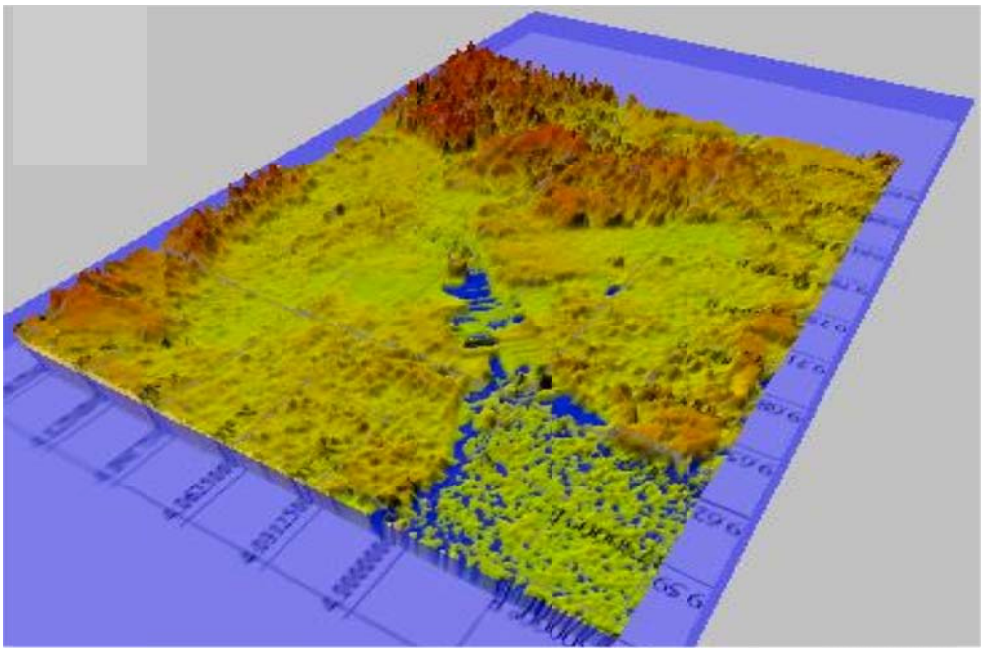

Figure 2-2: Computer generated view of the general topography of Douala.

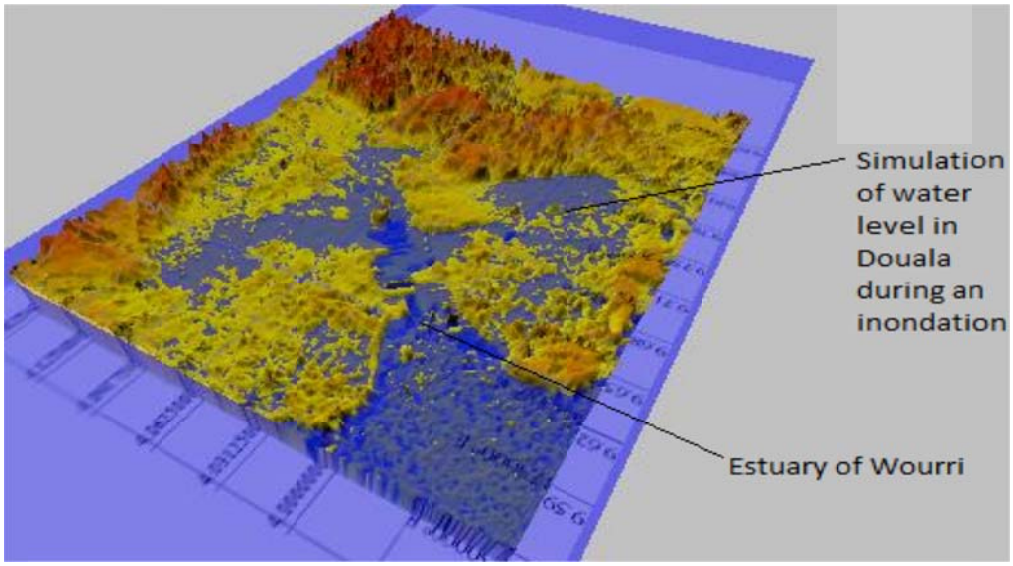

Figure 2-3**:** Computer generated view of the inundation in Douala caused by the 2010 flood.

2.2 ECONOMIC ACTIVITIES

The Douala metropolitan area—the economic hub of the Republic of Cameroon and the capital of Cameroon's Littoral Province—is not only the largest city in Cameroon, but also the nation's commercial capital. Consequently, it handles the majority of the country's chief exports, such as oil, cocoa, cotton and coffee and the trade with neighbouring landlocked

Chad and the Central African Republic. The port of Douala with its 10 km wharf is situated on the mouth of the River Wouri, 25 km from the sea. Although a commercial port, it can only handle vessels with relative shallow draughts, because of its location on an estuary. There is also a banana port in the industrial area of at Bonaberi.

Douala has two designated industrial zones Bassa and Bonaberi, situated in contrasting environments. The Bassa zone evolved on a well-drained landscape along the estuarine-creek of the Dibamba River to the east of the city, while the Bonaberi zone evolved almost entirely on marginal depressions of the aquatic terrain adjacent to the Douala lagoon, necessitating extensive land reclamation for the industrial development.

Figure 2-4: Location of the two industrial zones in Douala (In Bonaberi we have the pollution west and in Bonanjo we have the pollution East).

The industrial areas of Douala accommodate most of Cameroon's industries. These include manufacturing plants, chemical plants, including CHOCOCAM (Chocolate Cameroon)—the sole producer of quality chocolate products in the region, and breweries. The companies running the plants are often accused of not only spilling by products accidentally into the Wouri River and estuary, but also dump it deliberately. It is also alleged that gaseous emissions from the plants are responsible for the occurrence of acid rain and associated illnesses in the city. Douala also houses a number of markets, including the Marché Central

one of the biggest African style markets in Cameroon and the entire sub-Saharan region of Central Africa.

Figure 2-5: Typical scenes of buyers and sellers at Douala markets.

The market consists of thousands of shops and stores with traders from all over Africa and countries such as China, Lebanon, and Korea. Other markets include the Congo Market and the Marché De Sanaga Marché Eko Sale that concentrates on clothing and carpentry work, and household and fashions respectively Figure 2-6 shows typical scenes of buyers and sellers at Douala markets. Agriculture, which accounts for almost 50% of foreign currency earnings in Cameroon, plays an important role in the economic activities of both Douala and the surrounding coastal areas, where traditional and modern agriculture co-exist. However, the most important occupation of the rural population in the immediate vicinity of Douala is small-scale fishery, which produces more than half of the animal protein consumed in the city.

2.3 ECOLOGICAL PROBLEMS EXPERIENCED IN DOUALA

2.3.1 Pollution in Douala

The modern metropolitan area of Douala is essentially the product of the Government's policy of what may be called industrial agglomeration of economical benefits with little or no attention to the influence that the development may have on the environment. The government-supported infrastructure for controlling pollution is consequently dispersed, weak and ineffective and there is severe shortage of funding (Munde, 2011). This situation is particularly troublesome in the Bonaberi area where the major industries are related to the petroleum industry. The effluents discharged into the lagoon and surrounding areas therefore often consist of degraded petroleum products, although sources of pollution from other industries, such as pest control in cocoa, coffee and banana plantations, which are not regulated (Sama, 1996), also contribute to the overall pollution. For example, pesticides that have long been banned elsewhere in the world, such as DDT, are still used and often stored in leaky storage facilities (Munde, 2011). This poses a considerable threat to the local fishing industry and human health (Gabche and Smith, 2007).

The environmental problems in the Bonaberi area is further aggravated by the rapidly growing population and the limited availability of land, which force poor people to encroach onto wetlands (McInnes *et al.,* 2002) and the often maliciously disposal of waste. A dense mangrove swamp forest with its luxuriant palms has been almost completely destroyed since 2002, by urbanization. The houses and industrial buildings on the cleared land are poorly built, without adequate drainage. The situation is further aggravated by floods and sea-water intrusions that cause water levels to rise from the 2 m normal elevation of the area to 5m within a few minutes, destroying buildings and washing waste and raw sewage into the estuary and nearby springs and boreholes. This situation is particularly troublesome as approximately only 65 000 inhabitants out of a population of 3 million have access to clean reticulated water. The rest, including 80% of the low-income populations in the informal settlements, are forced to use springs and boreholes for their daily needs (Takem *et al* ., 2009).

Figure 2-6: Malicious disposal of waste in the Bépanda neighbourhood of Douala (Takem *et al.,* 2009)

By-products from the mainly chemical plants in the Bassa industrial zone are often discharged into the nearby estuarine creek of the Dibamba River, thereby causing the encroachment of invasive species, in the adjacent wetlands.

2.3.2 Water-borne Diseases

As could be expected from the preceding discussion water-borne diseases, ranging from simple to complex skin infections such as filarial to highly mortal diseases such as cholera, dysentery and diarrhoea are quite common in Douala (Fonteh, 2003). In fact, water-borne diseases were responsible for 15% of the deaths of children less than 5 years old that died in 2000 (Katte *et al.,* 2003), and for approximately 50% of all deaths in the country lists some of the major water-borne diseases that occur in the country.

Table 2-1:Major water-borne diseases that occur in Cameroon (Katte *et al.,* 2003)

Diseases	**Description**	**Mode of infection**	**Symptoms**	**Mode of eradication**
Hepatitis A	Viral disease that interferes with the functioning of the liver	Food or water contaminated with faecal matter	Fever, jaundice, and diarrhoea; 15% of victims have prolonged symptoms over 6-9 months	Vaccine available
Hepatitis E	Water-borne viral disease, interferes with functioning of the liver	Faecal contamination of drinking water	Jaundice, fatigue, abdominal pain, and dark coloured urine	vaccine available
Typhoid Fever	Bacterial disease	Contact with food or water contaminated by faecal matter or sewage	Victims exhibit sustained high fevers left untreated mortality rates can reach 20%	Availability of drugs
Leptospirosis	Bacterial disease that affects animals and humans	contact with water, food, or soil contaminated by animal urine	Severe fever, severe headache, vomiting, jaundice, diarrhoea	Availability of drugs
Schistosomiasis	Caused by parasitic trematode flatworm *Schistosoma*; and fresh water snails	Larval form of the parasite penetrates the skin of people exposed to contaminated water	Urinary or intestinal disease, decreased work or learning capacity;	Drugs available

Chapter 3

RESTORATION OF THE GROUNDWATER RESOURCES AT DOUALA

3.1 GENERAL

The term restoration is defined in the Oxford English Dictionary as: "*The action or process of restoring something to an unimpaired or perfect state*." While such an objective may be attainable in some situations or in an idealized world, experience shows that it is very difficult to achieve in the real world. This is especially true for what may be termed *environmental phenomena* and their related sciences. The situation here was further aggravated under the system of command-and-control regulations that dominated the environmental sciences through the mid-1980's in that regulators and industry frequently played adversarial roles. This caused a great deal of energy to be consumed in challenging the regulatory system, resulting in inefficiencies when regulators specified inappropriate technology solutions and in unpredictability when courts resolved disputes over compliance dates and other program features (NAS, 2006) (pK75). The result was that restorationprocedures were often conducted in haphazard and dubious ways a situation further aggravated by the development of the desktop computer. However, the modern shift to more collaborative market-sensitive regulatory strategies, allows an affected community to partake in the restoration and at to share responsibility for taking actions to protect human health and the environment.

Environmental phenomena are complex and often site-dependent. Various guidelines have consequently been developed in recent years to assist in the application of more collaborative market-sensitive regulatory and restorative strategies for these phenomena. As can be expected these guidelines not only vary from one phenomenon to the next, but often also mutually. Nevertheless, there is enough evidence today to conclude that no environmental restoration should be undertaken, without reference to one or more of these guidelines. This applies in particular to the field of Geohydrology, where the major constituents (water and rocks) are invisible. However, as can be seen from an evaluation of guidelines related to the assessment and monitoring of groundwater resources, e.g.(Jousma and Roelofsen, 2003; IAEA, 2004; NAS, 2006; World Meteorological Organization, 2008; Dent, 2012), the differences are often more related to details rather than principles. In fact, judging from the references quoted above, guidelines for the restoration of contaminant groundwater resources can be essentially summarized in five major recommendations.

a) Specification of the restoration context.
b) The consistent and detailed documentation of the state of the contaminated resource at the time restoration is initiated and during the restoration.
c) Identify and justify the actions and their goals that need to be taken during the restoration, and develop appropriate methods for their implementation.
d) Formulate, and implement appropriate models and use them consistently in combination with appropriate monitoring data to guide and assess the effectiveness of the restoration activities and to motivate and take corrective action where necessary.
e) Analyze the restoration results continuously and use them to build confidence in the community affected or stakeholders, as they are commonly called.

An attempt will be made in the discussion that follows to develop a preliminary methodology for the restoration of the groundwater resources at Douala based on these recommendations.

3.2 SPECIFICATION OF THE RESTORATION CONTEXT

The restoration of contaminated aquifers was in the past often conducted in a haphazard manner without a clear view of what should be achieved and what resources, including economic resources, are available for the task. The main aim of the restoration context is to try to focus the restoration by developing a well-documented framework for the project with special reference to the following not necessarily exhaustive list of objectives: purpose of the restoration and its envisaged goals or end-points; the available time frames and any regulatory constraints that need to be satisfied by the restoration or taken into account during the actual execution of the restoration procedures.

Not enough information is at present available to specify a detailed restoration context for Douala. Three aspects that would certainly have to be addressed in an actual restoration of the area are: (a) the supply of clean water to the inhabitants of the city, (b) reduction in the pollution sources and (c) a healthier biosphere.

3.3 THE DETAILED DOCUMENTATION OF THE STATE OF THE CONTAMINATED RESOURCE

The discussion can be clarified considerably by following the approach advanced in (IAEA, 2004) and divide the resource (or aquifer, as it is more commonly called) into three inter-

dependent domains.

a) The *source*—the zone of the earth's surface in direct contact with the source or sources of pollution.
b) The *geosphere*—the soil and rock formations underlying the near field that may eventually be contaminated by the pollution sources in the near field.
c) The *biosphere*—the part of the earth's crust, waters, and atmosphere that supports life.

3.3.1 The source

The available information on the disposal of waste at Douala is more of a qualitative rather than quantitive nature due to the ubiquitous sources of pollution; see Section 2.3.1 and Figure 2-7. One exception to this rule is the PK10-Génie Militaire landfill site depicted in Figure 3-1. The site, which is 10 km from Douala city centre, has been used since 2003 by the company HYSACAM ("Hygiène et Salubrité du Cameroun") under a contract with the Douala Municipality "Communauté Urbaine de Douala" or CUD to dispose municipal waste collected in the city and to manage the site. The site covers an area of approximately 63 ha of which nearly 10 ha have been used to dispose approximately 1 700 000 tonnes of waste by the end of 2011. The landfill is controlled, but there are no specific waste recovery or disposal practices in HYSACAM's operating contract with the CUD only requires that the waste be placed in successive layers 700mm thick, separated by 200mm layers of soil or inert material in cells, which are compacted and covered daily. Unfortunately, these specifications have not been strictly applied at PK10. Current practices include capping with soil material but it is not done systematically, so landfill management cannot be considered optimal. Lists of the composition and the annual quantity of Douala waste received at the PK10 landfill is given in Table (3-1)

Figure 3-1: Map of the Pk 10 landfill location near Douala (UNFCCC, 2011)

Table 3-1: Composition of the annual waste stream disposed at the Pk 10 landfill (Tonnes).

Year	Food[1]	Garden[2]	Glass[3]	Pulp[4]	Textiles	Wood[5]	Total
2003	18 389	3 009	10 241	625	669	502	33 435
2004	67 433	11 035	37 554	2 293	2 452	1 839	122 606
2005	67 240	11 003	37 447	2 286	2 245	1 834	122 055
2006	96 130	15 730	53 536	3 268	3 496	2 622	174 782
2007	96 125	15 730	53 533	3 268	3 495	2 622	174 773
2008	135 044	22 098	75 207	4 591	4 911	3 683	245 534
2009	136 033	22 260	77 758	4 625	4 947	7 710	253 333
2010	142 835	23 373	79 556	4 856	5 194	3 896	259 710
2011	149 977	24 542	83 523	5 099	5 454	4 090	272 685
Total	909 206	148 780	508 355	30 911	32 863	28 798	1 658 913
Ratio	54,8%	9,0%	30,6%	1,9%	2,0%	1,7%	100%

Food, food waste, beverages and tobacco[1]; Garden, yard and park waste[2], Glass, plastic, metal, other inert waste[3]; Pulp, paper and cardboard[4]; Wood and wood products[3]

As shown by the data in (UNFCCC, 2011), the majority of waste disposed at the PK10 site consists of organic compounds, with the result that large quantities of biogas are produced at the site. A project entitled.

Douala Landfill gas recovery and flaring project has consequently been negotiated with the United Nations Framework Convention on Climate Change (UNFCCC, 2011) as part of their Clean Development Mechanism (CDM) to install a landfill gas (LFG) recovery and flaring system at the site. This will allow HYSACAM to introduce an optimal management system for the landfill based on a feasibility study of the project by the Italian company

BIOTECNOGAS (UNFCCC, 2011). A further aspect of the study is to reshape and fully cap the landfill surface thereby improving the efficiency of LFG recovery and at the same time limit water infiltration (UNFCCC, 2011).It will take about two years (2010-2011) before the landfill management is fully optimized according to Biotecnogas' recommendations. On top of that, new waste will be placed into better-structured cells and covered regularly. Thus once optimization measures are applied, from 2012 HYSACAM will be able to stick perfectly with the contractual specifications agreed with CUD. The PK10 landfill will therefore involve a controlled placement of waste (waste is directed to specific deposition areas and there is already a control of scavenging and fires) with (i) cover material; (ii) mechanical compacting; and (iii) levelling of the waste.

3.3.2 Chemical Properties of the Water

Chemical analysis of water samples was carried out at the Indian Institute of Technology Bombay and the Water Analysis Laboratory of the Hydrologic Research Centre of Cameroon. $HC0_3^-$was determined as the total alkalinityby titrationas outlined in APHA/AWWA/WEF(Gue´vart *et al.,* 2006). Cations were analyzed by inductively coupled plasma atomic emission spectrometry (ICP-AES): Na and K, and Ca, Mg and total hardness by the EDTA titrimetric method (APHA/AWWA/WEF, 1998) (Gue´vart *et al.,* 2006). A UV-visible light spectrophotometer was used to analyze $S0_4^{2-}$by turbidimetry according to APHA/AWWA/WEF (Gue´vart *et al.,* 2006). Chloride was determined by the Ion Selective Electrode Meter (ORION). $N0_3^-$was determined by ion chromatography with the instrument model DX-120(Dionex) (Gue´vart *et al* ., 2006).

Table 3-2: Seasonal variation of the chemical content in springs (SP) and bore wells (B) February=dry and August=rainy (Gue´vart *et al* ., 2006)

Locality name	Month Sample ID	Feb pH	Aug.	Feb. $N0_3$(mg/l)	Aug.	Feb. $S0_4$(mg/l)	Aug.	Feb. Cl(mg/l)	Aug.
Bobong(II)	SP1	4.51	5.06	49.83	26.43	23.20	10.75	18.3	18.51
Genie	SP2	3.81	4.08	54.81	56.61	17.10	0.710	14.81	4.21
Ndogsimbi(CCC)	SP3	4.65	4.58	44.37	24.74	22.70	9.010	28	11.35
Ndogbong	SP4	4.01	4.04	59.80	63.03	4.520	3.330	11.3	16.54
Ndokotti(SOCARTO)	SP5	4.95	5.30	47.80	31.29	19.48	22.20	38.0	44.41
	SP6	4.10	3.98	94.30	83.16	06.30	01.22	19.6	22.06
Bonabassem	B1	4.26	4.57	0.210	0.360	0.320	0.540	2.3	01.46
Mussoke	B2	4.63	4.75	0.340	0.480	04.82	05.46	5.40	02.70
Pays Bas	B3	4.10	4.43	11.54	13.42	05.10	0.630	3.70	01.80
Genie Casmondo	B4	4.27	4.95	22.75	26.43	06.21	06.96	45.12	0.31

3.3.3 Microbial analysis

The microbiological contents in the water samples were determined using fecal coliform and fecal streptococcus as indicator bacteria. The isolation and enumeration of coliform were carried out using the membrane filtration method. Fecal streptococcus was isolated and enumerated by membrane filtration, and growth on membrane enterococcus agar (Gue´vart *et al* 2006). The following table 3-3 shows the Seasonal variation of the microbial content in springs and bore wells during the dry and rainy season in some settlement in Douala.

Table 3-3: Seasonal variation of the microbial content in springs (SP) and bore wells (B) February= dry and August=rainy(Gue´vart *et al* ., 2006)

Locality name	Month Sample ID	Feb. Aug EC(µs/cm))	Feb. FC (cfu/100 ml)	July FC (cfu/100)	Feb FS (cfu/100 ml)	July FC (cfu/100)
Bobong(II)	SP1	188.5 205	720	950	215	280
Genie	SP2	188 202	19	30	6	10
Ndogsimbi(CCC)	SP3	208 335	26	20	5	2
Ndogbong	SP4	202.4 213	500	800	420	300
Ndogbong(SOCARTO)	SP5	263 274	22	10	4	1
Bonabassem	SP6	258.4 270	27	1	13	0
Mussoke	B1	25.4 30.5	3	1	0	0
Pays Bas	B2	33.8 35.9	94	70	21	6
Genie	B3	25.2 45	633	1 200	681	800
Casmondo	B4	340 362	2 311	2.100	1 421	1 500

3.4 GEOSPHERE

As said earlier, the geosphere sometimes referred to as the near-field - the rock and unconsolidated material that lies between the near-field and the biosphere. It can consist of both the unsaturated zone which is above the groundwater table and the saturated zone which is below the groundwater table. We will then start the description here with the hydrogeology of the area under investigation.

3.4.1 Hydrogeology

Two shallow and deep aquifer units have been identified in the Douala sedimentary basin by SNEC based on the work of (Dumort, 1968) and (Regnoult, 1986). A generalized stratigraphic sequence of the major aquifer units of the Douala sedimentary basin modified from (Mafany, 1999) and (Regnoult, 1986) is given in Fig.1. The shallow aquifer is made up of the Mio-Pliocene sands at the base and the Quaternary alluvium at the top (Fig. 3.2), which together form the Wouri Formation. It consists of fine- to coarse-grained sand and gravel mixed with silt and clay, and lies on top of the Miocene shale of the Matanda

Formation, which serves as an aquicludes. According to (Djeuda-Tchapnga et al, 2001), the aquifer's thickness ranges between 50 and 60 m. Several lentils of channel-filled sands, hosted in clay layers, occur within this main aquifer, which act as perched aquifers. The water table is generally less than 10 m below the surface (Gue´vart *et al.,* 2006). Bore-well discharges of 80 m3/h well have also been reported (Gue´vart *et al* ., 2006). The aquifer is mainly recharged by precipitation. Waste water from drainage channels also infiltrates into this aquifer. Several streams drain the area and may also recharge the aquifer depending on the season and the water levels. Average groundwater level fluctuations range between 0.3 and 2.1 m between the dry and wet seasons. The aquifer is highly exploited by dug wells that record water levels of approximately 1–20 m. Many springs flow from valleys at the base of small cliffs where the topography intersects the water table in the shallow aquifer. These perennial springs are the major source of drinking water in the sub-urban settlements, though their yields have not been measured. However, because of poor sanitation facilities, there are several potential sources of pollution mixing together at close proximity to the springs. During the rainy season, the area surrounding the springs is flooded with solid and liquid waste from the pit latrines, stagnant surface water from puddles located upstream, leachate from solid waste dumps, waste water from washing cloths and wastewater mixed with human feces and animal dung. The deep aquifer consists of the Basal sandstones of the Moundeck Formation, underlain by the Precambrian granites and overlain by shale and marl of the Logbaba Formation and the Palaeocene sands of the Nkappa Formation (Fig. 3.2). The Palaeocene aquifer of this area has a thickness of about 200 m see in (Gue´vart *et al.,* 2006).

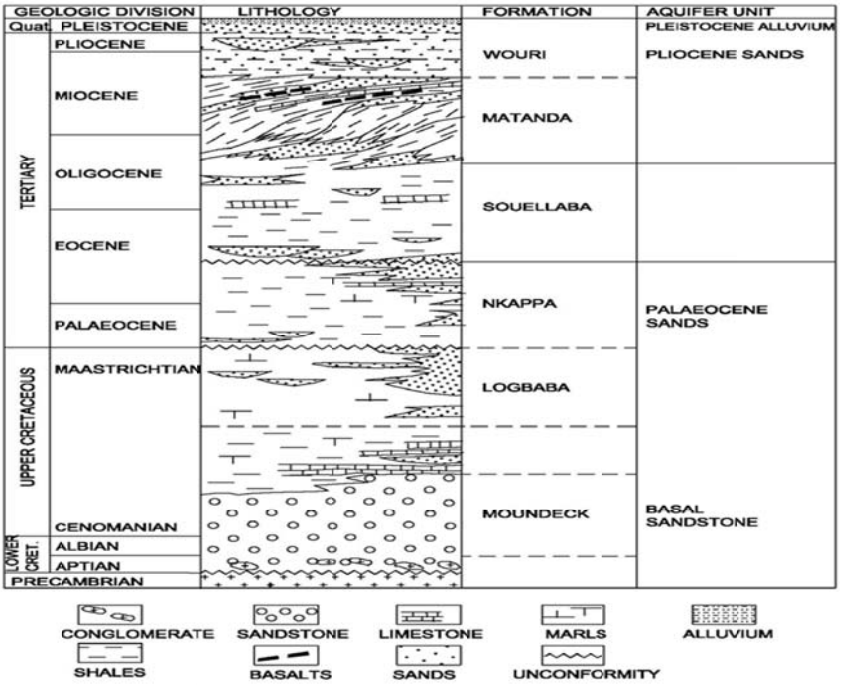

Figure 3-2: Chrono-stratigraphic column of the Douala basin showing the four major aquifer units (Modified from Mafany, 1999; Regnoult, 1986)

3.4.2 Geological setting

The study area is part of the Phanerozoic Cretaceous-Quaternary Douala Sedimentary Basin, covering an area of about 7,000 km square with a maximum width of 60 km (Mafany, 1999; Regnoult, 1986). It is one of the several divergent margin basins along the Southwest African Coast whose origin and structure are associated with the opening of the South Atlantic Ocean during the breakup of the Gondwana. The geology of this basin has been described by several researchers (Mafany, 1999; Regnoult 1986, Tamfu and Batupe 1995). The stratigraphic of the Douala sedimentary basin, according to (Tamfu and Batupe 1995), consists of Precambrian basement, unconformable overlain by a sedimentary sequence ranging in age from Cretaceous to Recent (Fig. 3-2). The city of Douala rests directly on the Mio-Pliocene to Recent alluvial sediments of this basin, which constitute the Wouri Formation of the Douala basin. The entire study area is dominated by this formation. It generally consists of unconsolidated fine- to coarse-grained sand and gravel mixed with silt and clay in various proportions. The alluviums composed predominantly of quartz and kaolinite (Regnoult, 1986), with a general thickness that ranges between 50 and 60 m (Djeuda-Tchapnga *et al.,* 2001).

3.4.3 Spring location

The anthropogenic activities (washing of clothes and kitchen utensils, garbage dumps, etc.) around the springs (about 10–30 m radius) (Ndogsimbi, Bonabassem, Bobong II) were found to have an impact on the water quality. Several pit latrines are located adjacent to and at times up gradient of these springs at a distance of less than 30 m, a phenomenon that is common to suburban communities in Cameroon (Tanawa *et al.*, 2002). Domestic waste water disposal in the open area adjacent to the springs is a common practice. Some springs are located at the base of small hills on which are found overcrowded houses with solid waste scattered on hill slopes together with stagnant water, and in some cases storm water runoff from the neighbouring up-gradient area flowing into these springs. The area around some of these springs (Bonabassem, Bobong II, SOCARTO and Genie; Fig. 3.3) usually is flooded, especially during the rainy season, because of poor drainage.

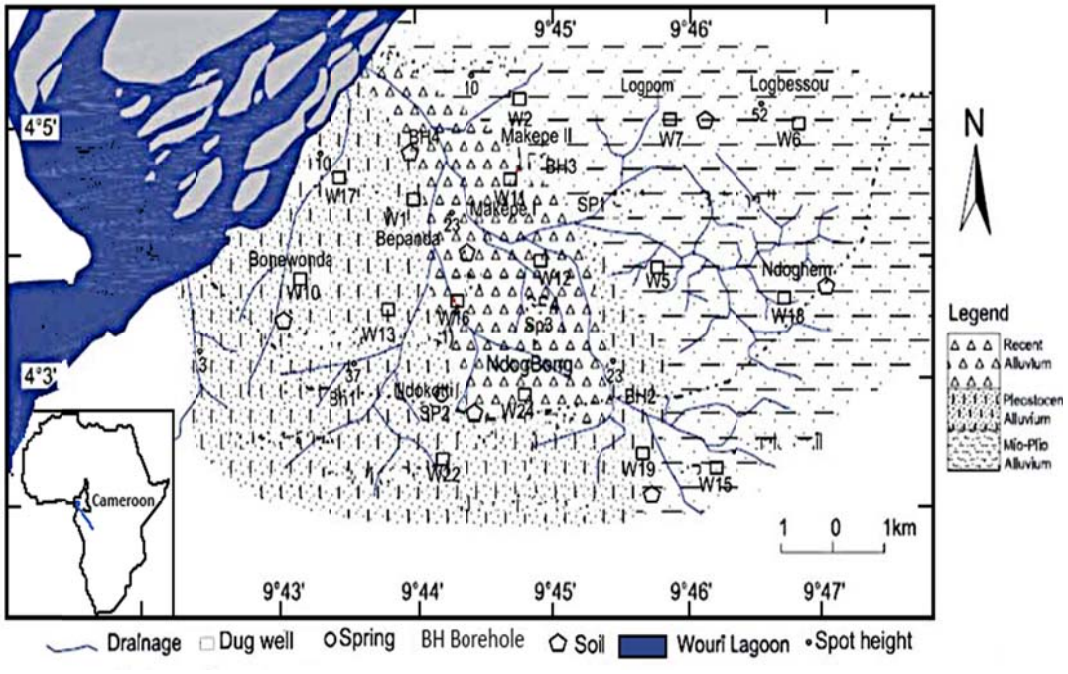

Figure 3-3: Geology drainage and sample points of Douala (Olirvy, 1986)

3.4.4 Hydro-geochemistry

Chemical reactions determine occurrence, distribution, and behaviour of aquatic species. Aquatic species are defined as organic and inorganic substances dissolved in water in contrast to colloids (1-1000 nm) and particles (> 1000 nm). This definition includes free anions and cations sensu strictu as well as complexes. The term complex applies to

negatively charged species such as OH^- , $HCO3^-CO_3^-$, SO_4^{2-} , NO_3^{2-},PO_4^{3-}, positively charged species such as $ZnOH^+$+,$CaH2PO4^+$, $CaCl^+$, and zero-charged species such as CaCO3, FeSO4 or NaHCO3 as well as organic ligands. Interactions of different species within the aqueous phase, with gases and solid phases (minerals) as well as Equilibrium reactions 5 transport and decay processes (biological decomposition, radioactive decay) are fundamental in determining the hydro-geochemical composition of ground and surface water. Hydro-geochemical reactions involving only a single phase are called homogeneous, whereas heterogeneous reactions occur between two or more phases such as gas and water, water and solids, or gas and solids. In contrast to open systems, closed systems enable only exchange of energy, not constituents with the surrounding environment. The ability of solid substances to exchange cations or anions with cation or anions in aqueous solution is called ion-exchange capacity. In natural systems anions are exchanged very rarely, in contrast to cations, which exchange more readily forming a succession of decreasing intensity: Ba^{2+}> Sr^{2+}> Ca^{2+} > Mg^{2+}> Be^{2+} and Cs^+> K^+> Na^+> Li^+. Generally, multivalent ions (Ca^{2+}) are more strongly bound than monovalent ions (Na^+), yet the selectivity decreases with increasing ionic strength (Stumm and Morgan, 1996). Large ions like Ra^{2+} or Cs^+ as well as small ions like Li^+ or Be^{2+} are merely exchanged to a lower extent. The H^+ proton, having a high charge density and small diameter, is an exception and is preferentially absorbed. The following table shows the major ion composition of water sample in Douala city. The hydro-geochemical characteristics of the water samples were studied using the data from the samples from the year 2009 shown in Table 3-4 (Gue´vart *et al.,* 2006).

Table 3-4: Major ion composition of water sample collected in January 2006

Sample Name	pH	Cond (µs/cm)	Na^+ (mg/l)	K^+ (mg/l)	Ca^{2+} (mg/l)	Mg^{2+} (mg/l)	Cl^- (mg/l)	HCO_3^- (mg/l)	SO_4^{2-} (mg/l)
SP1	4.5	220	14.4	4.51	4	2.4	18.6	10	15.5
SP2	4	199	11.09	4.53	8	2.4	15.2	5	18.4
SP3	5	242	27.48	4.07	8	2.4	33.4	10	25.1
SP4	4.1	188	11.53	5.1	8	0.0	15.4	5	3.6
SP5	4.4	265	16.88	6.1	12	2.4	35.3	10	19.3
SP6	4.4	261	13.28	4.53	8	2.4	19.9	10	6.3
B1	4.3	30.2	0.54	1.62	8	0.0	3.1	5	15.7
B2	4.65	34.3	0.73	2.5	12	2.4	4.6	10	16.2
B3	4.24	50.1	4.1	1.85	8	0.0	4.3	5	17.8
B4	4.3	356	38.34	6.39	12	0.0	45.1	10	19.1
W1	6.1	54.2	3.12	2.3	12	0.0	2.27	35	2.26
W2	6.4	74.8	5.5	1.36	12	2.43	3	40	11.11

The pH of water ranged from 4.1 to 6.5. There was no marked difference in pH between the springs and bore wells as the water is generally acidic. The acidic nature of groundwater could be due to the organic acids in the soil as well as from atmospheric sources (Chapman, 1996). Although chemical data about the rainwater are not available, considering the number of industrial establishments present in the region, it is assumed that the rainfall is acidic due to the continuous emission of SO2 and NO2. The sandy nature of the soils and short residence time of groundwater in the aquifer provide less time for water-rock interaction, thereby allowing the groundwater to maintain the pH of the rainwater (Chapman, 1996). Electrical conductivity varied from 54.2 µs/cm in W1 to 356 µs/cm in B4 (Table 6), whereas a background electrical conductivity of 50 µs/cm was reported by (Kamta, 1999). The springs showed high conductivity (199–265 µs/cm) compared to bore wells (30.2–50.1 µs/cm), except for B4 (356 µs/cm). A similar situation was observed with respect to major ions and nitrate (Table 3-4).

3.4.5 Tectonic and seismic conditions

The Douala basin is bordered by Precambrian basement to the East and Northeast and by the mount Cameroon volcanic line to the West and Northwest. It extends south into the offshore across the shadow sheft off Cameroon into the deepwater area of Equatorial Guinea. The area is divided into two sub-areas, comprising an uplifted Cretaceous platform in the southern shallow water region, the Kribi-Campo sub-basin and the onshore and offshore Cretaceous / tertiary Douala sub-basin in the North (Lakin, 2010).

3.4.6 Tectonic setting

The Douala basin developed during the Cretaceous break-up of Gondwana and the separation of Africa from South America. The initial rifting phase may have commenced during very Early Cretaceous time (Berritasian-Hauterivian) but the principal rifting episode in these areas occurred from late Barremian-Aptain time (Lakin, 2010). The initial formation of oceanic crust as the continents separated is believed to have commenced during the late-Aptian-late Albian interval. It would appear that the rifting was asymmetrical, as many of the syn-rift features that would normally be expected are not apparent at depth in this area, but they are abundant in the correspondent South American segment (Lakin, 2010). Several additional tectonic events occurred during the passive “drift” phase of the continent margin evolution at 84 Ma (Santonian), 65 Ma (K/T boundary) and 37 Ma (late Eocene) (Lakin, 2010). These events, resulting in uplift, deformation and erosion at the basin margins, are generally attributed to change in the plate motion and

intraplate stress fields due to convergent and collision events between Africa and Europe (Lakin, 2010). The Santonian uplift and possibly the late Eocene events also appear to have resulted in significant mass wasting of the continental margin by gravity sliding, Contribution towards reservoir formation (Lakin, 2010). The final uplift event relates to growth of the Cameroon Volcanic Line (CVL) and effectively lasts from 37 Ma through to present day on the northwest margin of the basin (Lakin, 2010). This relatively recent volcanic activity is important as heat flows resulting from it are through to be instrumental in pushing younger source rocks into oil window (Lakin, 2010)

3.4.7 Seismic conditions

The Uniform Building Code (UBC) lists Cameroon, specially the cities of Douala and Yaoundé, as being in seismic zone zero (UBC, 1997). The design basis ground motion that has a 10 percent change of being exceeded in 50 years as determined by a site-specific hazard analysis or which may be determined from a hazard map. This corresponds to a 475 years recurrence interval. Nevertheless seismic zone zero is essentially aseismic.

3.5 BIOSPHERE

As we said earlier the biosphere is the physical media (atmosphere, soil, sediments and surface water) and the living organisms including humans that interact with them. The biosphere - e.g. climate and atmosphere, water bodies, human activity, biota, near surface lithostratigraphy, topography, geographical extent and location. Hence we will start our description with climate and the atmosphere of the area under investigation.

3.5.1 Climate and atmosphere

Douala features a tropical monsoon climate, with relatively constant temperatures throughout the course of the year. The city typically features warm and humid conditions. Douala sees plentiful rainfall during the course of the year, experiencing on average roughly 3850 mm of precipitation of rainfall per year. Its driest month is December where on average 33 mm of precipitation falls while its wettest month is August when on average nearly 800 mm of rain falls. The following graph shows the yearly and monthly precipitations in Douala (World Weather Information Service Douala ,2012).

Month	J	F	M	A	M	J	J	A	S	O	N	D	Year
[mm]	37	65	175	231	264	426	671	786	601	408	150	33	3847
[°C]	26.8	27.6	27.2	27.0	26.8	25.7	24.8	24.6	25.1	25.5	26.4	26.8	26.2

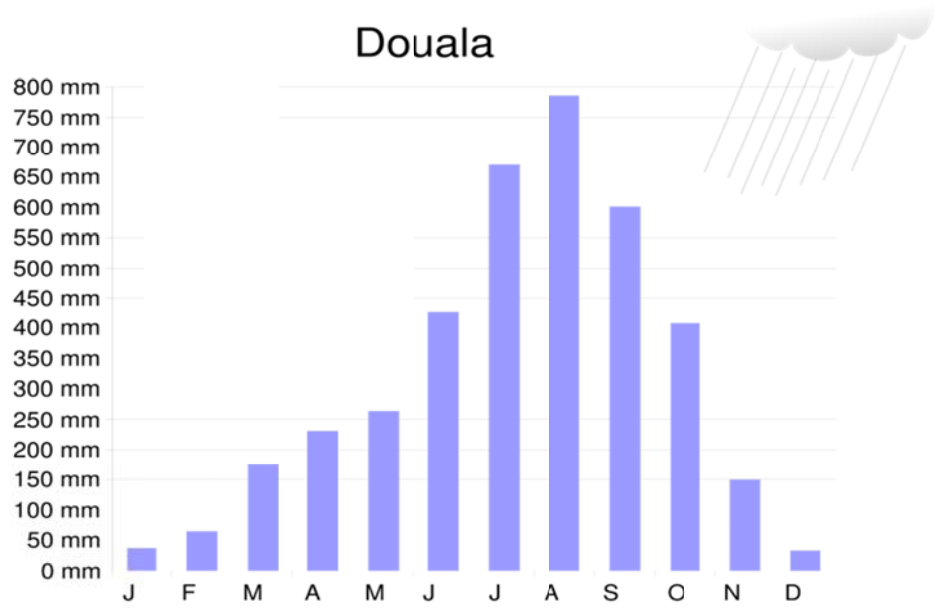

Figure 3-4: Precipitations Douala.svg: (World Weather Information Service Douala ,2012).

3.5.2 Water bodies

The Wouri estuary, or Cameroon estuary is a large tidal estuary in Cameroon where several rivers come together, emptying into the Bight of Biafra. Douala, The area under assessment, is at the mouth of the Wouri River where it enters the estuary. The estuary contains extensive mangrove forests. The estuary lies to the east of Mount Cameroon and empties into the Bight of Biafra. It is fed by the Mungo, Wouri and Dibamba Rivers see (Fig, 2-1). The estuary lies in the Douala Basin, a low-lying depression about 30 meters (98 ft) on average above sea level, with many creeks, sand bars and lagoons (Yerima, 2005). The Plio-Pleistocene Wouri alluvial aquifer, a multi-layer system with alternating sequences of marine sands and estuarine mud and silt lies below the estuary and surrounding region and is an important source of well water. The upper aquifer in this system is an unconfined sandy horizon that is hydraulically connected to the brackish waters of the estuary and to the coastal wetlands (Yébalé (17.3km)) .

Figure 3-5: Dibamba River, which flows into the estuary (Atheull *et al.*, 2009).

The spring tides at the mouth of the estuary are 2.8 meters (9.2 ft). Rainfall is from 4,000 millimetres (160 in) to 5,000 millimetres (200 in) annually. Salinity is very low, particularly during the rainy season. Surface salinity of 0.4% is common around Douala throughout the year (Hughes, 1992). Mungo River splits into numerous small channels that empty into the estuary complex (Yerima, 2005). The tidal wave in the bay travels as far as 40 kilometres (25 mi) up the Mungo. In this section of the river, large flats and sand banks are exposed at low tide (Yerima, 2005). The Wouri is affected by the tides for 45 kilometres (28 mi) above Douala, with blocks of tidal forest along its shores throughout this stretch.

3.5.3 Biota

The Douala-Edea hosts an important wildlife reserve in the Littoral Region of Cameroon. It is located on either side of the mouth of the Sanaga River along the shores of the Bight of Biafra opposite the island of Bioko. 80% of the reserve is covered by tropical lowland equatorial forest and 15% by Atlantic mangrove forests (Ngea, 2012). The Mouanko reserve between the Sanaga and the Wouri estuary holds about 15,000 hectares (37,000 acres) of mangrove forests (Ramsar, 2011). The mangroves form a buffer against coastal erosion, and are a refuge for 80% of the local

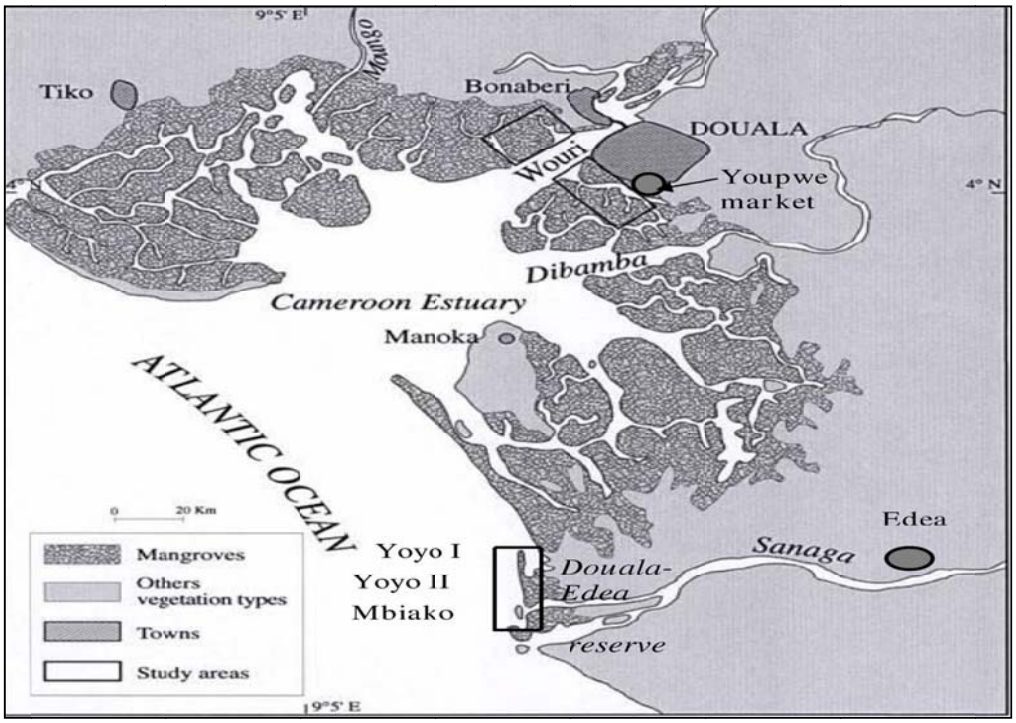

Figure 3-6: Mangrove of Douala forest (Din *et al.*, 2002)

marine and aquatic species for at least part of their lifecycle. They are threatened by logging for construction timber and for firewood used in fish smoking, as well as by urban infrastructure development (Ninan, 2009). Fauna include forest elephants, primates (chimpanzees, monkey species such as BLACK COLUBUS), antelopes (SITATUNGA, blue duiker, etc), West African manatees, sea turtles, dolphins, crocodiles, alligator, many fish species, terrestrial and water bird species (Ngea, 2010).The RED-CAPPEDMANGABEY was reported to be common in the reserve in 1972 (Lee, 1988). The endangered Red-Eared Nose-Spotted Guenon was reported in the Lombé part of the reserve in densities of 2-3 groups per square kilometres, but populations had dropped elsewhere due to hunting (Lee, 1988). Animals in the reserve are poorly protected and poaching is widespread (Ramsar, 2011). Central chimpanzees in the reserve are threatened by hunters.

3.5.4 Near surface stratigraphic

The following picture shows the cross section of Douala basin. We chose a point A and point B near the Southern pollution source and then we join the two points by a line. With the appropriate software, we generate the cross section underlying the location under investigation as showing in Figure 3-7.

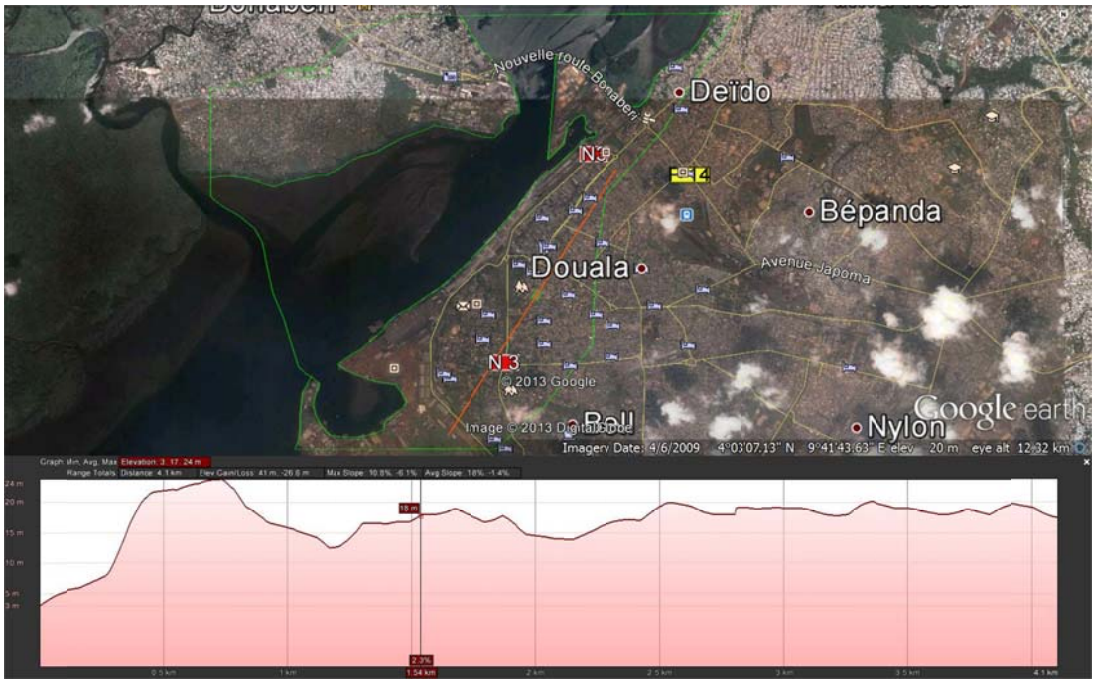

Figure 3-7: cross section of Douala Basin, demonstrates vertical and lateral changes in rock type as well as geologic structures such as faults.

The basic stratigraphic of the Douala Basin is interpreted to include of rift, transition and drift mega-sequences related to the tectonic evolution over Africa cratonic basement and associated Atlantic margin (Lakin, 2010 in). Regional stratigraphic and tectonics can be summarised in four main phases of evolution related to pre, syn and post rift separation of Africa from South America (Lakin, 2010).

Phase 1 (Pre-rift) Basement: Earlier interpretations of the Douala basin place the transition between Oceanic and continental crust approximately along the present coastline, but Bowleven believe that asymmetric rifting took place, with much of the pre-rift sediment moving South-Westwards towards present day South America (Lakin, 2010).

Phase 2 Rift and Transition (Early Cretaceous Berriasian-Aptian): The Early Cretaceous sequences are not fully understood, as the high pressure experienced in the Upper Cretaceous sediments have limited deep drilling. They have, nevertheless, been identified in the Rio Muni Basin immediately to the South in Equatorial Guinea and from this; the rift mega sequence is expected to include predominantly basal fluvial and alluvial sandstones and conglomerates of the Lower Mundeck formation, similar to those encountered in fields south of the permit at depths between 1000m and 2000m (Lakin, 2010). They are expected to be thick and laterally continuous and will constitute a good secondary reservoir target. These possibly pass upwards into lacustrine claysones, which may have secondary source

potential (Lakin, 2010).

Phase 3 Transitions (Mid Cretaceous: Albian-U.Cenomanian/ Turonian): The transitional mega sequence is expected to include predominantly clay stones of the Upper Mundeck formation deposited in deepening water environments that may initially have been lacustrine, and which passed through restricted, possibly evaporitic, marine conditions to open, deepwater marine. The mega sequence is increasingly truncated towards the edge of the basin in the northern part of the permit by the effects of the Santonian uplift. In the shallow basement area of OLHP-1, this unit occurs in a more marginal "top set" facies comprising alterations of arkosic and glauconitic sands passing up through limestone into shale.

Phase 4 Post-Rift (Late Cretaceous; Santonian-Campanian): The Douala Basin came into separate being during the Santonian, When thick clastic deposits were laid down in the centre, thinning rapidly and becoming increasingly shaly to the east and south of the permit area. Erosion took place around the basin margin during the Santonian uplift, removing some previous reservoir facies, so the Campanian in these areas is resting on older rocks or directly on basement. It is postulated that the eroded sediments were re-deposited in the centre of the basin, in close proximity to Cenomanian-Turonian source rocks. Gravity sliding may have created localised accommodation space to pond some of these reworked sands in hanging wall growth structures or on the landward side of associated toe-thrusts detaching in the lower Cretaceous above the syn-rift blocks.

3.5.5 Geographical context

The Douala coastal environment describes a barrier island lagoon formation. A number of such old barrier island were colonized by the following districts (Akwa, Deido, Bépanda, Bassa, Bonamoussadi) which today supports the high population density metropolitan area of Douala (Gabche et al., 2007). The lagoon system is about 50 km away and has a broad embayment as it opens in to the Atlantic Ocean, which greatly enhances tidal movement, often leading to the inflow of saline waters. The area is characterized by low-lying geomorphic features with faint slopes almost at sea level. Geographically Douala is located at latitude 4 1′ North and longitude 9 45′ East. It is subdivided into 5 councils which are governed following the typical Cameroonian centralised command system where a government delegate appointed by the President of the Republic, rules over the councils′ mayors. This city of about 3.5 million inhabitants today, displays a nucleated settlement pattern (Gue′vart *et al.*,2006). The famous central town called Akwa, has banks, commercial enterprises and other small scale businesses like hackers and street vendors. It also has two

major designated industrial zones called Bassa and Bonaberi amongst few other smaller ones. These two zones are located peripherally at the Eastern and Western fringes of the city albeit they are both situated in areas containing easily contaminated streams and brooks as well as below sea level. The two companies charged by the municipality to dispose waste are HYSACAM and CAMHYGIENE. , The Douala coastal lagoon complex is easily the dominant feature with richly endowed natural and socio-economic resources along the littoral zone of Cameroon. It is fed mainly by the River Wouri, evolving a maze of creeks and lagoons about 50 km from the Atlantic Ocean, with its largest surface extent north of Bonaberi, to the north west of metropolitan Douala see (Fig, 2-5).

3.5.6 Human activities

Douala city is considered as the economic lung of Cameroon because it hosts about 70% of the economic activities of the entire country. Most of the essential infrastructure is found in the coastal region: roads, ports, airports, telecommunication, schools, hospitals etc. With respect to national averages, this region has fewer jobs in the primary sector and more in the secondary and tertiary sectors: 36.9% of the active population is engaged in the primary sector as against 71.9% for the whole country: 21.4% and 41.7% work in the secondary and tertiary sectors respectively (Asangwe, 2006). Being the seat of Cameroon's largest port and its major international airport, Douala Airport, it is the nation's commercial capital hence indisputably the largest city in Cameroon as well as the capital of Cameroon's Littoral Province. Consequently, it handles the majority of the country's chief exports, such as oil, cocoa and cotton, coffee, as well as trade with neighbouring landlocked Chad and the Central African Republic. It is also home to the Eko Market, not only the country's largest market but also the largest in the whole CEMAC Central African sub region. The port of Douala is situated on the mouth of the River Wouri, 25 km from the sea, and this poses a problem of siltation, thus demanding constant dredging. It is essentially a commercial port which receives only vessels with little draught, considering its location on an estuary. The port has a 10 km wharf. Upstream, there is a banana port at Bonaberi, in the vicinity of which is located the industrial zone. The following figure (3-8) shows, the industrial activities taking place in Douala port.

Figure 3-8: Ship at the Douala Port with goods from abroad .

The industrial zone of Douala including, PILCAM (Societe Camerounaise de Fabrication des Piles Electriques); CCC (Cameroon Chemical Complex)is the biggest soap manufacturer in the nation; SCDP (Societe Camerounaise des Depot Petroliers) otherwise called in English Cameroon Petroleum Products Depot Corporation has been alleged that their hydrocarbon/petroleum products are not only occasionally accidentally spilled over during their transportation processes, but also deliberately dumped into the River Wouri; ALPICAM is a wood treatment facility whose usually nocturnal gaseous emissions have caused severe acid rain and hence illnesses to its neighbourhood; SIPLAST is dealing with the recycling and production of plastic materials and products; SMALTO is a paint manufacturer; CHOCOCAM (Chocolate Cameroon) is a cacao beans processed products - Sole producer of quality chocolate of in the region. Products include Cocoa Butter, Cocoa Powder, Black Cocoa; SOCAPALM processes palm kernels, coconut and cotton seed to produce Crude Palmoil, Coconut Oil, Cotton Seed Oil; NoSuCa (NoSuCa - Nouvelle Sucrieres du Cameroun) both refined and crude sugar; Brasserie du Cameroun is a beer brewery company producing various brands of Cameroon beers and soft soda drink products; Cimencam (Cement of Cameroon) is the sole producer of quality cement for construction in the sub-Saharan region of central Africa. When one get to a typical African market in Douala, one may think the whole world is gathered there. Some popular market of Douala including, Marché de Lagos (intersection of Rue de New Bell and Rue Congo Pariso); Marché Central (Douala Central

market located at the intersection of Rue de New Bell and Rue Congo Pariso close to the Akwa Shopping centres) one of the biggest African style markets in Cameroon and the entire sub-Saharan region of Central Africa. The Douala Central Market holds thousands of shops and store with traders from all over Africa. Prominent amongst these traders are Cameroon, Benin, China, Mali, Nigerian, Togo, Lebanese, Koreans, Moroccans, Senegal and several others nations. All items of interest can be found at the Douala Central market household appliances, electronics such as cell phones, cameras, television screens…, textile, leather products, groceries and countless others; Congo Market at Entrée Camp Bertau consisting of clothing and carpentry work; Marché De Sanaga Marché EkoSale of household goods to fashion accessoceries; Marché Bobbi Score **-** A typical Supermarket model in western fashion; Marché de Fleur (off Ave Charles de Gaulle) Sale of crafts work - wood carvings, masks, African wooden drums, special designer tablecloths stone jewelleries; Centre Artisanal de Douala Sale of Cameroonian artworks - sculptors, masks and various crafts. Has a good collect of arts from all cultures and regions of Cameroon. The following photo shows some items sole in some Douala markets. In this coastal zone, the most important occupation of the rural population is undoubtedly small-scale fishery. Fishery contributes more than half of the animal protein consumed in Douala. The exploitable species of the aquatic fauna consist essentially of fishes, shrimps and mollusks. Agriculture accounts for almost 50% of foreign currency earnings in Cameroon. Thus, it plays an important role in the economic activities of this coastal zone both in feeding the population and raising family revenues. Traditional and modern agriculture co-exist in this coastal area see (Fig, 2-6).

3.5.7 Topography

Topography generally drops from East to West towards the Wouri River and leads to flooding of the area. The altitude is about 57m in the East, passing on to 23m in the Centre and dropping to 3 m in the West towards the Wouri River. The high magnitude of run-off from the River Wouri estuarine system in to the land-water interface leads to a high water table which leads to flooding of the area see (Fig, 2-2; 2-3).

3.5.8 Inundation

In Douala, severe flooding affected life, economy and, floods are the most common natural disasters. In recent years, floods have received much media attention. Many poor neighbourhoods got flooded so they went in debt to pay the price of repairing homes. Douala's vulnerability to flooding was highlighted by the loss of life and economic damage from flooding events in flood-prone zones like Mabanda and Bonendale localities of

Bonaberi to the north and Youpwe locality to the south (Asangwe, 2006). In addition, summer flooding of the New Bell streams and waterways resulted in some of the worst floods seen in the city in 2010. The consequences were death, drowning, injury and destruction of property. Crops and businesses which residents depend on to make money were destroyed. Vulnerable groups within communities are the elderly, disabled, children, women, ethnic minorities, and those on low incomes (Asangwe, 2006).

Douala presents an array of varying creeks, lagoons, sand and rocky beaches, coastal plains, wetlands and with faint slopes. Flooding is a major consequence of this scenario exhibited by the dynamism of the River Wouri on the Douala metropolitan area all years round. This ensures that the water table remain high and thus effect constant inundation. Geographers say though the newly built up areas of Bonamoussadi, Makepe and Logpom are about 50 kilometres away from the Atlantic Ocean, it is just over 16 meters above sea level, while the rapidly growing districts of the metropolis, like Bonaberi which includes Mabanda, Ndobo are just between 3-7 meters above sea level. The low lying nature of the city provoking floods is observed in the general lack of flowing drains in the core built up areas like Mabanda and Akwa, resulting in stagnant water due to constantly high water table which has a further consequence of increasing high rate of subsidence and tilting of residential housing structures (Asangwe, 2006) . This has frequently inundated hazardous areas like Mabanda, Bonendale and Youpwe, which offer spaces for the development of slum settlements and now suffer subsidence of residential housing structures (Asangwe, 2006). Figure 2-3 and 2-4 show the area affected by this natural disaster in the city of Douala.

3.6 SCENARIO DESCRIPTIONS

The ecology of Douala is under threat from growing pollution from industry, farming and households, threatening both fish yields and human health (Gabche, 2007). Sources of pollution include electroplating and oil refinery industries, pest control in cocoa, coffee and banana plantations, and waste organic oils from land transport, process industries and power generation (Sama, 1996). The bulk of human-generated sewage is also released into the estuary without treatment. The government infrastructure for controlling pollution is dispersed, weak and ineffective, and there is severe shortage of funding (Munde, 2011). Agriculture is the mainstay of the Cameroon economy. Pesticides are not regulated, and also contribute to pollution. Pesticides that have long been banned elsewhere are still in use, or are being held in leaky storage facilities (Munde, 2011). The growing population is increasing production of export crops such as coffee, cocoa, bananas, palm oil and cotton,

using imported pesticides and fertilizers. Typically fertilizers contain urea, ammonia, and phosphorus. Pesticides applied are mostly DDT and other derivatives of organ halogens (Sama, 1996). About 80% of Cameroon's industries are based in or around Douala. Their liquid waste is released into the estuary with little or no treatment (Sama, 1996). Douala's Bassa industrial zone ends in the estuarine creek formation of the Dibamba River, discharging pollutants. The wetlands are quickly being colonized by invasive species, and a great number of phytoplankton species has been identified, some of which are caused by the pollution. The Bonaberi suburb of Douala, with a rapidly growing population of over 500,000, illustrates the urban environmental problems. More than 75% of Bonaberi is 2 metres (6.6 ft) above sea level on average. With limited land, poor people have encroached into wetlands (McInnes *et al.*, 2002). As of 2002, the dense mangrove swamp forest, which included luxuriant growths of palms, was undergoing extinction due to urbanization. The houses and industrial buildings on the cleared land are poorly built, without adequate drainage. Pools of stagnant water are breeding grounds for disease. Human and industrial wastes end up in the channels of the Wouri, reducing its rate of flow. River floods and sea incursions may cause rises of water level from 2 metres (6.6 ft) to 5 metres (16 ft) within a few minutes, destroying buildings and washing raw sewage into the wells. Waterborne diseases such as typhus and dysentery are common causes of death (McInnes *et al.*, 2002) see (Fig.; 2-7). The inadequate supply of pipe-borne water, with approximately 65,000 persons connected out of the 3 million inhabitants (Gue´vart *et al.*, 2006), pushes the suburban population to depend on springs and borehole (Takem *et al.*, 2010). 80% of the low-income populations in the informal settlements use springs and borehole water for part or all of their drinking and other domestic needs (Takem *et al.*, 2010). Such settlements in Douala are Bapanda-Makepe, Ndogbong, Bonabassem, Ndogsimbi, Genie Millitaire and Bobong II (Takem *et al.*, 2010). The following picture shows relatively the scenario of ground-water pollution in Douala.

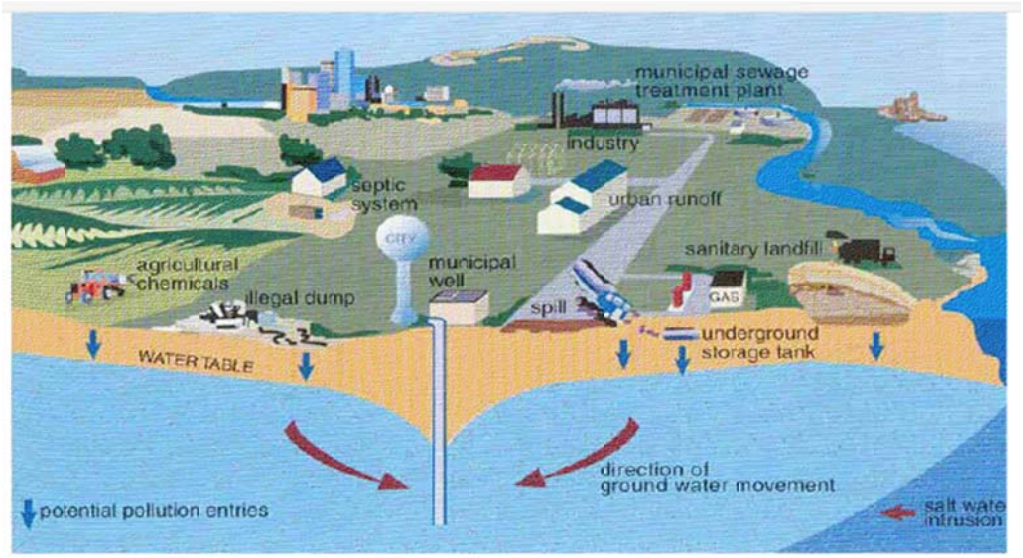

Figure 3-9: Scenario of Groundwater pollution in Douala.

The target audience (stakeholders) for this situation of case is assumed to be a hypothetical regulatory body and staff involved in producing the safety assessment. Other possible stakeholders such as the public or other interest groups will be considered at this stage (IAEA, 2004a).

Groundwater resource is an environmental restoration. However, the concept of restoration awaits more precise definition, and the science of ecosystem restoration is in its infancy. Nevertheless, it is clear that restoration is a call for water resources management that accommodates and benefits from, rather than controls, annual and multiyear variability in the patterns and timing of river flows and the extremes of flood and drought (NAS, 2004)

The purpose of the Working Group is to promote the appropriate and consistent use of mathematical models in the remediation and restoration process at sites containing—or contaminated with— radioactive and/or mixed waste materials. This report demonstrates a thorough approach to documenting model applications in a consistent manner and is intended to assist technical staff responsible for identifying and implementing flow and transport models in support of cleanup decisions at radioactive and hazardous waste sites. It is hoped that adoption of the tenets in the report will enhance the understanding between modelers and their managers of what may be expected in model documentation; facilitate the peer-review process by ensuring that modeling documentation is complete; ensure the institutional memory is preserved; and institute greater consistency among modeling reports (EPA, 1996).

Chapter 4

CLASSICAL MATHEMATICAL FORMULATION OF GROUNDWATER POLLUTION

There is no universal view of how science proceeds in the development of a theory (Louie, 1983). Nevertheless, as a survey of the history of Physics (in contrast to more philosophical concepts) will show the development of the "superb theories" of Physics can be conveniently summarized in four steps, see e.g. (Davies, 1973; Louie, 1983).

Step1 Observe the phenomenon through the human senses, aided by suitable auxiliary instruments, if necessary, and identifies at least one interaction (Botha, 1984).

Step2 Measure whatever properties of the observed interactions in the phenomenon, commonly known as observables, are measurable and try to relate the observables conceptually to one another, thereby establishing conceptual visualization for the phenomenon. (Such a visualization can be presented formally in the form of a manuscript, drawing or any other appropriate medium, but often consists of a mere mental image, or simple sketch.) (Botha, 1984)

Step3 Apply the rules of mathematical analysis to the observable(s) included in the conceptual visualization of the phenomenon and try to synthesize (Ritchey, 1996) a framework, or hypothesis, able to predict the behaviour of the phenomenon, under different conditions than that used in synthesizing the hypothesis.

Step4 Compare the behaviour of the phenomenon predicted by the hypothesis, established in Step 3, with new observations of the phenomenon. It is only when the two sets of data agreed satisfactorily that the hypothesis is regarded as a theory for the phenomenon. Otherwise, one has to repeat the analysis, in many cases also the observations to try to find a new hypothesis—hence theory. In the following section we are going to establish step 3, which is we are going to discuss the development of mathematical model that explains the measurement of the concentration of pollution in the groundwater (Botha, 1984).

The description of transport is closely related to the terms convection, diffusion, dispersion, and retardation as well as decomposition of the solute in the water. First, it is assumed that there are no interactions between the species dissolved in water and the surrounding solid phase. Furthermore, it is assumed that water is the only fluid phase. Multiphase flow, e.g. in the systems water-air, water-organic phase (e.g. oil or DNAPL) or water-gas-organic phase,

is not considered here. Convection (also known as advection) is the vector, which results from the DARCY or the RICHARDS equations. It describes the flow velocity or the flow distance for a certain time t. In general, convection has the major influence on mass transport. Magnitude and direction of the convective transport are controlled by:

- The development of the flow field.
- The distribution of the hydraulic permeability within the flow field.
- The development of the groundwater table or the potentiometric surface.
- The presence of sources or sinks.

Concentration gradients are levelled out by diffusion by means of molecular movement. The vector of diffusion is generally much smaller than the vector of convection in groundwater. With increasing flow velocity diffusion can be neglected. In sediments, in which the k_f value is very low, and consequently the convective proportion is very small or even converging towards zero (e.g. for clay), the diffusion could become the controlling factor for mass transport. The third term in mass transport is dispersion. The dispersion describes the mass flow, which results from velocity variations due to the geometry and the structure of the rock system. From this definition it follows that the smaller the vector of convection the smaller the effect of dispersion. The other way round, an increasing effect of dispersion occurs with higher flow velocity. Consequently, the mathematical description of the species distribution is an overlap of convection, diffusion, and dispersion. All phenomena that cause species not to spread with the velocity of the water in soil or in groundwater are called retardation. Retardation is possible without any mass decrease. Frequently, though, retardation is combined with degradation. This “degradation” of the concentration of a species can occur by means of radioactive decay of a radionuclide or biological degradation of an organic substance. Also sorption and cation exchange can be included in this definition of “degradation”, because the considered element is entirely or partially removed from the aqueous phase.

4.1 CLASSICAL GROUNDWATER FLOW EQUATION

Used in hydrogeology, the groundwater flow equation is the mathematical relationship which is used to describe the flow of groundwater through an aquifer. The transient flow of groundwater is described by a form of the diffusion equation, similar to that used in heat transfer to describe the flow of heat in a solid (heat conduction). The steady-state flow of groundwater is described by a form of the Laplace equation, which is a form of potential flow and has analogy in numerous fields. The groundwater flow equation is often derived

for a small representative elemental volume (REV), where the properties of the medium are assumed to be effectively constant. A mass balance is done on the water flowing in and out of this small volume, the flux terms in the relationship being expressed in terms of head by using the constitutive equation called Darcy's law, which requires that the flow is slow. A mass balance must be performed, and used along with Darcy's law, to arrive at the transient groundwater flow equation. This balance is analogous to the energy balance used in heat transfer to arrive at the heat equation. It is simply a statement of accounting, that for a given control volume, aside from sources or sinks, mass cannot be created or destroyed. The conservation of mass states that for a given increment of time (Δt) the difference between the mass flowing in across the boundaries, the mass flowing out across the boundaries, and the sources within the volume, is the change in storage.

4.1.1 Hydraulic head

The estimation of near-field water flow is an important element of near-field modelling since it is the driving force for the release of pollution in the liquid phase. Its aim in this thesis is to the flow rate in the near-field for each phase of the near-field disposal facility's existence. The model flow hence is based on a numerical solution of the conventional saturated groundwater flow equation for density-independent flow.

$$S_0(x,t)\partial_t\Phi(x,t) = \nabla.[\boldsymbol{K}(x,t)\nabla\Phi(x,t)] + f(x,t) \tag{4.1}$$

where, $S_0(x,t)$ is the specific storativity

$\boldsymbol{K}(x,t)$ is the hydraulic conductivity tensor of the aquifer

$\Phi(x,t)$ is the piezometric head.

$f(x,t)$ is the strength of any source or sink, with $x\ and\ t$ the usual spacial and time coordinates.

∇ being the gradient operator.

This model showed that the dominant flow field in these aquifers is vertical and linear and not horizontal and radial as commonly assumed. As a review of the derivation of Eq. (4.1) will show, Darcy law:

$$q(x,t) = -\boldsymbol{K}\Phi(x,t) \tag{4.2}$$

is used as a keystone in the derivation of Eq. (4.1). This law proposed by Darcy early in the 19th century, is relying on experimental results obtained from the flow of water through a one-dimensional sand column. Alternatively, Darcy's law states that the rate of flow through a porous medium is proportional to the loss of head, and inversely proportional to the length of the flow path. Note that the specific discharge $q(x,t)$ has the dimensions of a velocity. The concept specific discharge assumes that the water is moving through the entire

porous medium, solid particles as well as pores, and is thus a macroscopic concept. The great advantage of this concept is that the specific discharge can be easily measured.

4.1.2 Velocity field

Assume that the density of groundwater is constant. Consider a unit volume of a porous medium and apply Darcy's law and the law of conservation of mass. The three dimensional form of the partial differential equation for transient groundwater flow in saturated porous media can be expressed as

$$\frac{\partial V_{Sx}}{\partial x} + \frac{\partial V_{Sy}}{\partial x} + \frac{\partial V_{Sz}}{\partial x} - w = S_S \frac{\partial h}{\partial t} \qquad (4.3)$$

where: $V_x, V_y,\ and\ V_z$ are values of the specific discharge (or Darcy velocity) through the unit volume along the x, y, and z coordinate axes, w [1/T] is a volumetric flux per unit volume and represents internal sources and/or sinks of water; S [1/L] is the specific storage of saturated porous media; h [L] is the hydraulic head; and t [T] is time.

4.2 DEVELOPMENT OF CLASSICAL MATHEMATICAL MODELS OF HYDRODYNAMIC DISPERSION EQUATION

4.2.1 General

The primary mechanism for the transport of improperly discarded hazardous waste through the environment is by the movement of water through the subsurface and surface waterways. Study this movement requires that one must be able to measure the quantity of waste present at a particular point in space time. The measure universally for chemical pollution is the concentration, conventionally expressed in terms of either a mass fraction or mass volume. Experimental evidence indicates that this dependence is rather weak, if the fractional concentration is small. The density of the solute may thus be considered as independent of the concentration when working with low concentration, or watery, solutions. It has, therefore, become a custom to use the volumetric concentration (c), which contain the solute density for high concentration solutions. However, this is not a fast rule and one can use the two measures interchangeably, but not simultaneously (Botha, 1996).

4.2.2 Interactions between dissolved solids and a porous medium

Groundwater is, by its nature, always in contact with the matrix of the aquifer (Botha, 1996). There is thus a possibility that the solutes may interact with the rock matrix, and one another. A true mathematical model of groundwater pollution must therefore be able to account for interactions between the dissolved and matrix of the aquifer. It will thus be advantageous to look at the nature of interaction between dissolved solids and a porous medium that may be expected in groundwater pollution. Experimental evidence indicates

that when a dissolved solid comes in contact with the matrix of porous medium it may:

d) Pass through the medium with no apparent effect

e) Be absorbed by the porous matrix and

f) Reacts with the porous matrix and other substances dissolved in the fluid. The dissolved solids encountered in porous flow are, for this raison, often classified as conservative, non-conservative and reactive tracers. This behaviour implies that the quantity of dissolved solids in a porous medium depends not only on the flow pattern, but also the nature of the porous matrix and the solution.

The reactions of inorganic compounds with aquifer material are relatively well-known (Garrels and Christ, 1965) (Hem, 1970) (Kauskopf, 1967). Some of more common types of reactions encountered in practice include, for example: (a) adsorption (including ion exchange), (b) oxidation and reduction and (c) conversion of compounds to other oxidation states. However, this is not the case with the many organic compounds occurring in effluents, storm water and others sources (Zoeteman and Piet, 1980). This applied especially to some of the modern biodegradable organic compounds that are compounds that tend to degrade under natural conditions to simpler compounds such as carbon dioxide and water. However, these compounds all tend to leave non-degradable fractions, which persist in the water, and ultimately appear in the groundwater. This behaviour of organic compounds, described by the term persistence, defined by (Zoeteman and Piet, 1980) as: "The *capacity of an aquatic pollution to resist to a reduction of the original concentration in the water place, after a certain period of time, while undergoing a variety of physical, chemical and biological processes"* does not depend only on their chemistry, but also on the nature of the particular ecosystem. A comparison of particular compounds from rivers and aquifers has shown that most organic compounds are more persistent in groundwater, even a hundred times more persistent, than in surface water (Zoeteman and Piet, 1980). This persistence of organic compounds creates a considerable problem for the use of groundwater source, since many of these occur in modern household detergents and chemicals. It will clearly be formidable to task to develop a mathematical model for groundwater pollution that takes the complexity of all possible interactions into account, even if the model is restricted only to those compounds that have been identified hazardous (Botha, 1996). Fortunately, the interactions do not all occur simultaneously in every polluted aquifer. The mathematical model, discussed below, will therefore be restricted to the adsorption of hydrophobic compounds and the decay of radioactive isotopes, which

cover a considerable number of interactions of importance in groundwater pollution. Nevertheless, this model may not be valid for all practical situations (Abriola and Pinder, 1985 a) (Abriola and Pinder, 1985 b).

The full derivation of this can be found in (Botha, 1996). The differential equation is therefore nothing else than another expression of mass conservative and is given below as.

$$D_t(\theta c + \rho_b s) + \nabla.\{\mathrm{v}(\theta c + \rho_b s)\} + \lambda(\theta s + \rho_b s) + \nabla.F = 0. \qquad (4.4a)$$

In the previous discussion no account was taken of sources and sinks in the derivation of Equation (4.4). Nevertheless, this oversight can be easily rectified by simply adding the flux term, $f(\mathbf{x},\mathrm{t})$ with c_0 the concentration and $f(x,t)$ the strength of the source, to the right-hand side of Equation (4.4). This yields the so-called hydrodynamic dispersion equation

$$D_t(\theta c + \rho_b s) + \nabla.\{\mathrm{v}(\theta c + \rho_b s)\} + \lambda(\theta s + \rho_b s) + \nabla.F = c_0 f(\mathbf{x},t), \qquad (4.4b)$$

which is the equation of customary used as mathematical model for mass transport in a porous medium.

4.2.3 The Dispersion coefficient

Substitution of dispersion coefficient into Equation (4.4), yields the equation

$$D_t(\theta c + \rho_b s) + \nabla.\{\mathrm{v}(\theta c + \rho_b s)\} + \lambda(\theta s + \rho_b s) + \nabla.(c\bar{q}^* - \rho\theta \mathrm{D}\nabla \mathrm{C}) = c_0 f(\mathbf{x},t), \qquad (4.5)$$

where

$$D = D_h + D_m \qquad (4.6)$$

is known as hydrodynamic dispersion coefficient, or simply the dispersion coefficient. Notice that the explicit dependence of D (and other variables) on the spatial coordinates has been suppressed in Equation (4.5), for ease of notation.

The molecular diffusion coefficient for ordinary substances in water is not very large, as indicated by the numerical values in Table 4-1. Molecular diffusion has consequently often been neglected in the studies of groundwater pollution, by simply ignoring $\mathrm{D_m}$ in Equation (4.5). However, studies of pollution transport in heterogeneous and fractured rock aquifers in the last two decades have shown that molecular diffusion may retard the movement of pollutants considerably in these aquifers (Sudicky, 1983).

To illustrate the behaviour of the molecular diffusion, consider the situation of a heterogeneous aquifer, consisting of two layers with different hydraulic conductivities. The higher hydraulic conductivity of Layer 2 will obviously cause this layer to form a preferential flow path in the aquifer. Advection will there tend to transport any pollutant that enters Layer 2 along this preferential flow path. However, this will create a concentration gradient between the water in Layer 1 and 2. This gradient will not only cause

the pollutants to diffuse into Layer 1, but also decrease the concentration of the pollutant.

Table 4-1: Molecular diffusion coefficients of selected substances in water, at a pressure of 100kpa (Botha, 1996)

Diffusing Substance	$\mathbf{D_m}(m^2s^{-1})$	**Temperature** (C^0)
O_2.	$1{,}3.10^{-9}$ $2{,}0.10^{-9}$	10 20
Na^+	$1{,}3.10^{-9}$	20
Cl^-	$2{,}0.10^{-9}$	20
NaCl	$1{,}2.10^{-9}$	18
NH_4^+	$1{,}8.10^{-9}$	15
HCOOH	$1{,}1.10^{-9}$	12
CH_3COOH CH_3OH	$0.9.10^{-9}$ $1{,}3.10^{-9}$	12 20

In Layer 2, thereby effectively retarding its motion, and smooth out any variations in the concentrations of the two layers. The rate of longitudinal spreading in a heterogeneous aquifer can thus be quite complex time-dependent process.

4.2.4 Mass Conservation in Hydrodynamic Dispersion

Equation (2.4) is nothing more than an expression for the mass conservation of the dissolved solids, fluid and matrix combined. Since each of these components must also satisfy the law of mass conservation separately, the possibility exists that Equation (2.4) may contain a number of redundant terms. In this connection, it is interesting to note that the terms containing the fluid motion fraction can also be expressed in the equivalent form.

$$D_t(\theta c) + \nabla.(\mathrm{v}\theta c) = \rho\theta\{D_t C + \mathrm{v}.\nabla C\} + C\{D_t(\rho\theta) + \nabla.(\rho\theta\mathrm{v})\}$$

where C is the mass fraction concentration . The time derivative in the second term on the right-hand side of this equation can now be replaced by its equivalent expression given below

$$D_t[\rho_b(\mathrm{x},\mathrm{t})] = \nabla.[\rho_b \mathrm{v}_m(\mathrm{x},\mathrm{t})] \tag{4.6}$$

to obtain

$$D_t(\theta c) + \nabla.(\mathrm{v}\theta c) = \rho\theta\{D_t C + \mathrm{v}.\nabla C\} + C\{-\nabla.\rho q + \rho f)\} \tag{4.7}$$

where

$$q(\mathbf{x},\mathrm{t}) = -K\nabla\Phi,$$

is the ordinary Darcy velocity, associated with the piezometric head Φ(x,t). The terms relating to the mass $s(x,t)$ can be expresses similarly as

$$D_t(\rho_b s) + \nabla.\{\mathrm{v}(\rho_b s)\} = s\{D_t\rho_b + \nabla.\rho_b\mathrm{v}\} + \rho_b\{D_t s + \mathrm{v}.\nabla s\}.$$

The expression in the brackets, in the first term on the right-hand side of the equation,

expresses nothing else than the law of mass conservation for the absorbed mass fraction s(x, t) and the porous matrix. It must therefore vanish, according to the second equation in Equation (4.6), so that

$$D_t(\rho_b s) + \nabla.\{\mathrm{v}(\rho_b s)\} = \rho_b\{D_t\mathrm{s} + \mathrm{v}.\nabla\mathrm{s}\}. \tag{4.8}$$

Substitution of Equations (4.6) and (4.8) into Equation (4.4), using the definition of the generalized Darcy velocity given below

$$q_t(\mathrm{x},t) = -K\nabla\varphi(\mathrm{x},t) + \theta\mathrm{v}_m(\mathrm{x},t),$$

to obtain

$$\nabla.(c\bar{q}^*) = C\nabla.(\rho q + \rho\theta\mathrm{v}) + \rho(q + \theta\mathrm{v}).\nabla C,$$

yields

$$[\rho\theta D_t C + \rho_b D_t s + \rho q.\nabla C] + (\rho\theta\mathrm{v}.\nabla C + \rho_b\mathrm{v}.\nabla s) = \nabla.(\rho\theta\mathrm{D}\nabla C) - \lambda(\theta\rho C + \rho_b s) + \rho f(\mathrm{x},t)(C_0 - C) - C\nabla.(\rho\theta\mathrm{v}) - \rho\theta\mathrm{v}.\nabla C. \tag{4.9}$$

This is the most general equation for description of density-dependent mass transport in a consolidating porous medium.

Equation (4.9) is quite complex and therefore seldom, if ever, applied in practice. Fortunately, it is seldom necessary to consider consolidating media in studies of groundwater pollution. The terms containing the matrix velocity, v, can therefore be safely discarded in such studies. This yields the equation (4.10)

$$[\rho\theta D_t C + \rho_b D_t s + \rho q.\nabla C] + (\rho\theta\mathrm{v}.\nabla C + \rho_b\mathrm{v}.\nabla s) = \nabla.(\rho\theta\mathrm{D}\nabla C) - \lambda(\theta\rho C + \rho_b s) + \rho f(\mathrm{x},t)(C_0 - C),$$

that has to be used in modelling density-dependent mass transport, such as the phenomenon of sea-water intrusion, for example. However, the equation can be simplified farther, if one is only interested in the study of problems where the density remains approximately constant. In such situations Equations (4.10) can be expressed in its more usual form

$$\theta D_t c + \rho_b D_t s + q.\nabla c = \nabla.(\theta\mathrm{D}\nabla c) - \lambda(\theta c + \rho_b s) + (c_0 - c)f(\mathrm{x},\mathrm{t}). \tag{4.11}$$

The practicable application of the hydrodynamic dispersion equation in Equation (4.11), to actual groundwater pollution problems, is not without its difficulties. For examples, there are indications that it does not describe the physics of the groundwater pollution accurately (Nguyen, and Pinder 1981). Nevertheless, it is the equation normally used for this purpose. It worth noting that the hydrodynamic dispersion equation (4.11) representing the variations of concentration of pollution in the aquifer in space and time is a partial differential equation of integer orders.

4.2.5 Hydraulic head

Groundwater flow directions are determined using a water-table or potentiometric surface map based on water-level measurements made at the site. Groundwater flow is perpendicular to the equipotential lines expressed on a map as contours of water-table or potentiometric surface elevation. For simple flow fields, groundwater flow directions may be determined using a three point problem approach. At most sites, however, sufficient measurements should be taken to delineate localized variations in the flow field using contour maps. Maps should be constructed for several different measurement events to determine the range of seasonal hydraulic variations at the site. The final design of the PRB should incorporate the effect of maximum variation in flow directions to avoid future situations where the plume may bypass the barrier.

The estimation of near-field water flow is an important element of near-field modelling since it is the driving force for the release of pollution in the liquid phase. Its aim in this thesis is to the flow rate in the near-field for each phase of the near-field disposal facility's existence. The model flow hence is based on a numerical solution of the conventional saturated groundwater flow equation for density-independent flow.

$$S_0(x,t)\partial_t\Phi(x,t) = \nabla.[\boldsymbol{K}(x,t)\nabla\Phi(x,t)] + f(x,t)$$

where, $S_0(x,t)$ is the specific storativity, $\boldsymbol{K}(x,t)$ is the hydraulic conductivity tensor of the aquifer; $\Phi(x,t)$ is the piezometric head, $f(x,t)$ is the strength of any source or sink, with $x\ and\ t$ the usual spacial and time coordinates; ∇ being the gradient operator.

4.2.6 Velocity field

Hydrologic or groundwater flow parameters are important in PRB design because these parameters determine the groundwater capture zone, and the location, orientation, configuration, and dimensions of the PRB. The objectives of taking hydrologic measurements are to estimate the groundwater flow velocity and direction in the prospective PRB location. These objectives can be achieved through measurement of aquifer properties and the use of Darcy's Law, through tracer testing, or through direct measurement with appropriate probes. Most available probes are in various stages of development and evaluation; therefore, at most sites, the most reliable method of estimating groundwater velocity and direction involves using water-level measurements along with Darcy's Law. The use of the Darcy's Law equation is the most common approach for determining groundwater velocity in the aquifers.

Assume that the density of groundwater is constant. Consider a unit volume of a porous medium and apply Darcy's law and the law of conservation of mass. The three dimensional

form of the partial differential equation for transient groundwater flow in saturated porous media can be expressed as

$$\frac{\partial V_{Sx}}{\partial x}+\frac{\partial V_{Sy}}{\partial x}+\frac{\partial V_{Sz}}{\partial x}-w=S_S\frac{\partial h}{\partial t}$$

where ,$V_x, V_y,\ and\ V_z$are values of the specific discharge (or Darcy velocity) through the unit volume along the x, y, and z coordinate axes, w[1/T] is a volumetric flux per unit volume and represents internal sources and/or sinks of water; S [1/L] is the specific storage of saturated porous media; h [L] is the hydraulic head; and t [T] is time.

4.3 ANALYTICAL SOLUTIONS OF GROUNDWATER FLOW AND ADVECTION DISPERSION EQUATIONS

Our concern here is to provide a solution to a model that describes more accurately the events that take place in the aquifers; we first start with the test of aquifer parameters using the groundwater flow equation or the Theis equation, following by the advection dispersion equation.

4.3.1 Analytical solution of groundwater flow equation

In 1935, Theis was the first to developed an equation for unsteady state flow which introduced the time factor and the storativity as

$$\partial_r^2\Phi(r,t)+\frac{1}{r}\partial_r\Phi(r,t)-\frac{S_0}{T}\partial_{\mathrm{t}}\Phi(r,t)=0. \qquad (4.12)$$

Several solutions of the above partial differential equation have been proposed; see for example (Theis, 1935) (Cooper-Jacob, 1952)(Atangana, Botha, 2012). On one hand Theis solution was an exact solution to the partial differential equation and this solution is given below as: (4.13)

$$\Phi(r,t)=\frac{Q}{4\,\pi\,T}\int_{\frac{r^2S}{4Tt}}^{\infty}\frac{e^{-y}}{y}dy.$$

However, for practical purpose this solution is very difficult to implement. On the other hand (Cooper Jacob, 1952) proposed an approximate solution of the partial differential equation for a latter time and this solution is given below as (4.14)

$$\Phi(r,t)=\frac{2.30\,Q}{4\,\pi K}Log\left[\frac{2.25\,K\,t}{r^2S}\right]$$

The Cooper Jacob is the most used in groundwater studies because, at the time the solution was proposed, it was easier to handle it with the Log paper than the exponential integral ,but now day many computational software are available to handle Theis without Log paper.

Nevertheless the Cooper Jacob solution has limitations, because his solution is a large time approximation of the Theis non-equilibrium solution. The approximation involves truncations of an infinite series expansion for the Theis well function that is valid when the variable: $\frac{r^2 S_0}{4\,T\,t}$ is small enough which the case in groundwater study is not always. Actually the one-dimensional groundwater flow equation and its solution were first proposed by (Terzaghi, 1923). Recently (Atangana and Botha, 2012) proposed an analytical solution using the Homotopy Decomposition Method (HDM), their approximated analytical solution is given below as:

$$\Phi(r,t) = \frac{2.30\,Q}{4\,\pi K} Log\left[1 + \frac{2.20\,K\,t}{r^2 S}\right]. \qquad (4.15)$$

The following figure shows the graphical representation of the solutions for different values of theoretical properties of the aquifer. The red line is the graphical representation of the solution proposed by Cooper Jacob, the green line is the graphical representation of the solution proposed by the author and the blue line is the graphical representation of the solution proposed by Theis.

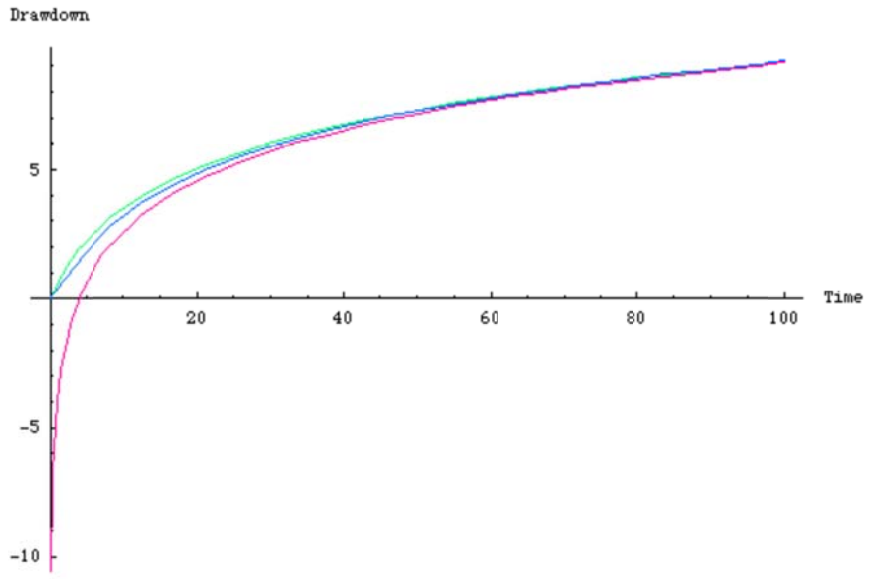

Figure 4-1: Comparison for Q = 4.50 m/s, S= 0.001091 $\boldsymbol{m^{-1}}$, T= 0.1265 $\boldsymbol{m^2}$/day and r = 32.039 m

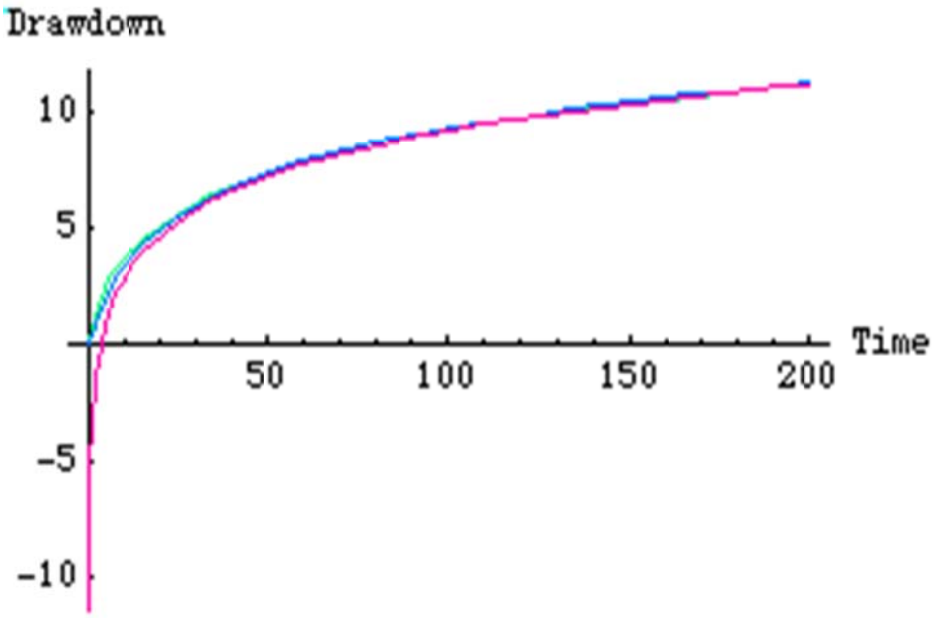

Figure 4-2: Comparison for Q = 4.50 m/s, S= 0.001091 $\boldsymbol{m^{-1}}$, T= 0.1265 $\boldsymbol{m^2}$/day and r = 32.039 m

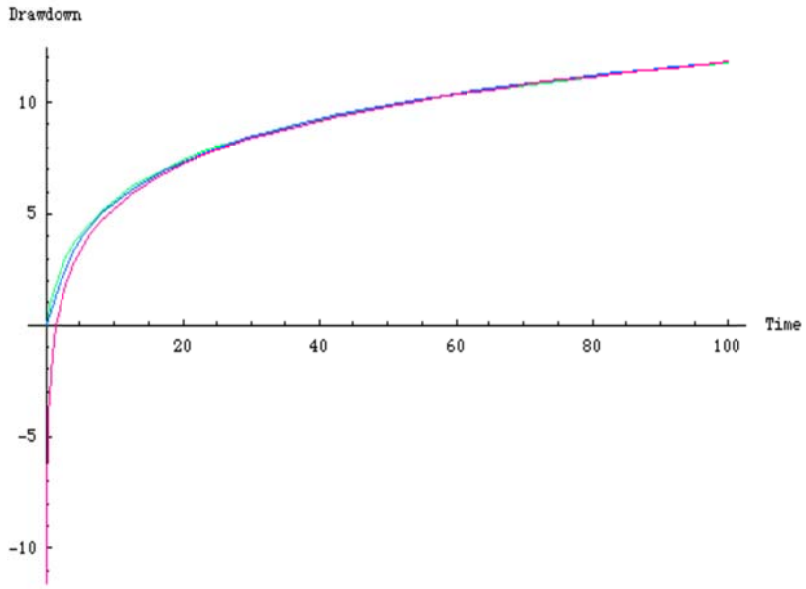

Figure 4-3: Comparison for Q = 4.50 m/s , S= 0.001091 $\boldsymbol{m^{-1}}$, T= 0.1265 $\boldsymbol{m^2}$/day and r = 20 m

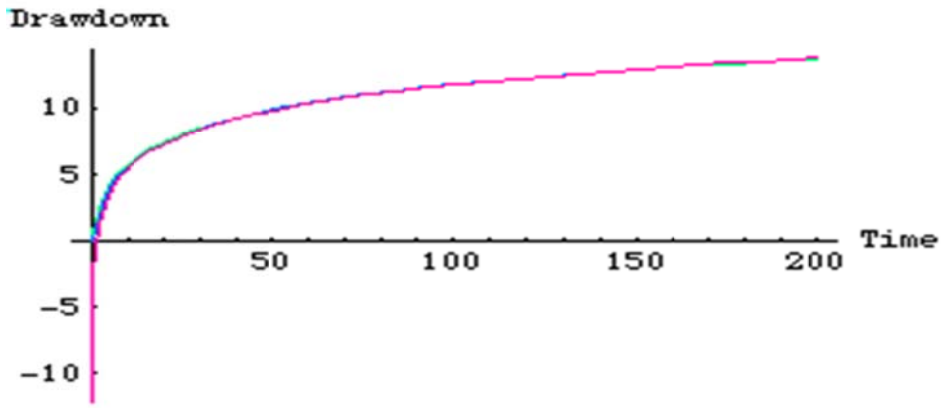

Figure 4-4: Comparison for Q = 4.50 m/s, S= 0.001091 $\boldsymbol{m^{-1}}$, T= 0.1265 $\boldsymbol{m^2}$/day and r = 20 m

The above figure shows that for large distance from the observation borehole, the Cooper Jacob is not valid for Theis equation, meaning fitting a set of experimental data with this solution under this condition will lead to a wrong estimation of aquifer parameters under investigation, or in the same condition one can see that the solution proposed approximate successfully Theis solution.

4.3.2 Comparison with experimental data

In order to examine the validation of this solution, the above asymptotic solution is compared with 2 sets of experimental see figure 4-5 and figure 4-6. Figure 4-5 shows the comparison between experimental data from a pumping test conducted in the polder 'Oude Korendijk', south of Rotterdam with Cooper Jacob, Theis and the proposed solutions. Here the transmissivity was determined as T =360 m^2 per day, the storativity $S = 0.179\ m^{-1}$ and for a constant discharge rate of Q = 9.12 l/s at a distance of r = 90 m. The above shows the comparison between experimental data from a pumping test conducted in the 'Oude Korendijk', south of Rotterdam with Cooper Jacob, Theis and the proposed solutions. Here the transmissivity was determined in Figure 4-3 as T =360 m^2 per day, the storativity S = 0.9 m^{-1} and for a constant discharge rate of Q = 9.12 l/s at a distance of r = 215 m. The graphical representations of the comparison revealed a good agreement of experimental data with the proposed solution.

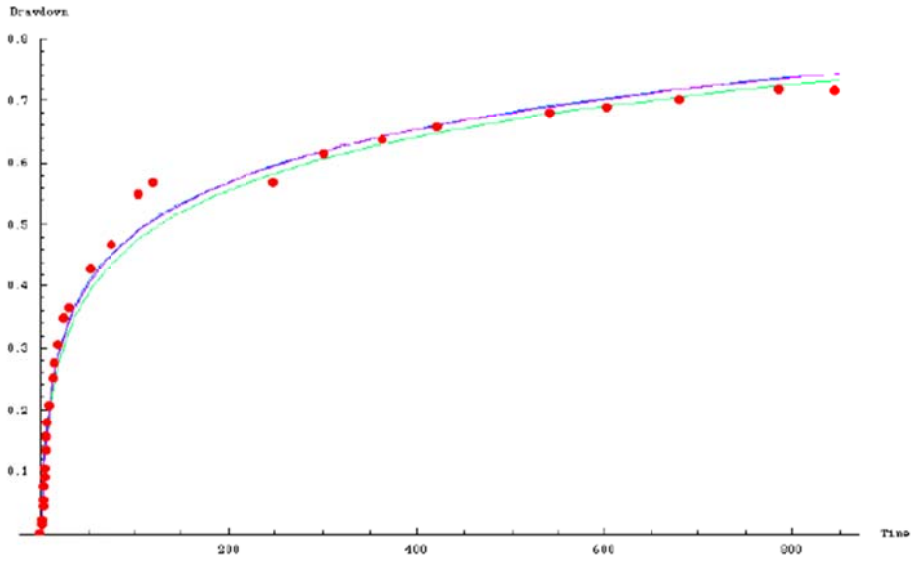

Figure 4-5: Comparison between the existing, real world data and the proposed solution, where the red point represent the data and the rest as said before in Fig 4-1 and Fig 4-3

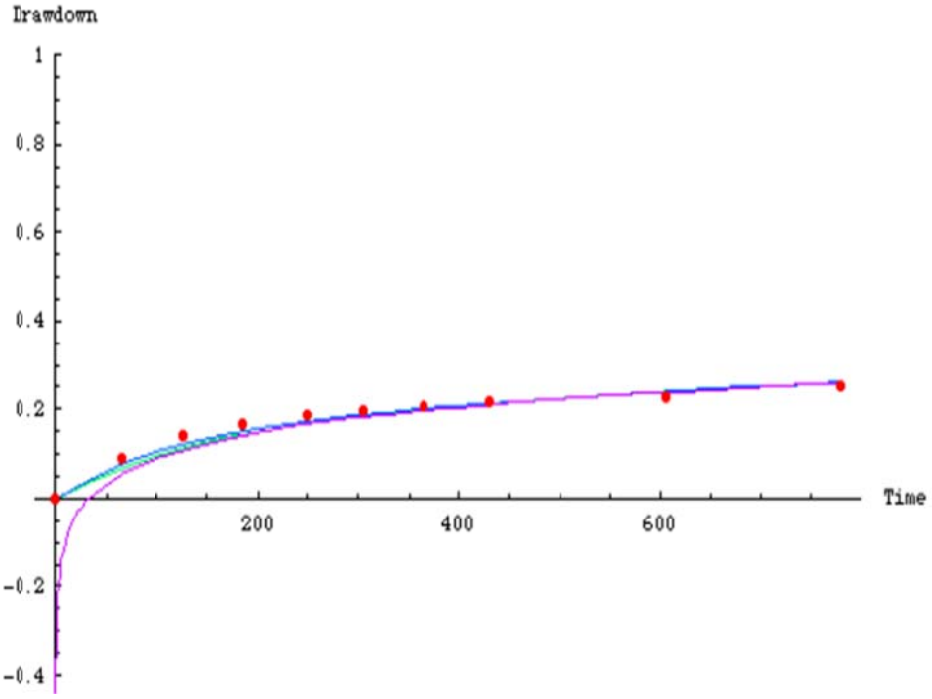

Figure 4-6: Comparison between the existing, real world data and the proposed solution, where the red point represent the data and the rest as said before.

4.4 ANALYTICAL SOLUTIONS OF ADVECTION DISPERSION EQUATION OF A POLLUTED SITE

It is commonly assumed that aquifer system is initially free of chemical substances before any injection of pollution. However this situation is unrealistic for the case of Douala, because we do not know the history of the aquifer underlying the city of Douala. Therefore, we must assume that this aquifer is not initially free of chemical, but instead there is a certain value of concentration, c_0 initial found in this aquifer and chemical companies inject chemical from one side of the aquifer.

4.4.1 Analytical solution

In this section we investigate the solution of the hydrodynamic dispersion equation subject to the following initial and boundary conditions:

initials conditions

$$c(x,0) = c_0, \tag{4.16}$$

and boundary conditions

$$c(0,t) = c_1 \exp(-\gamma t) \quad \text{for } t > 0 \quad \text{and } \partial_x c(x,t) \to 0 \text{ as } x \to \infty. \tag{4.17}$$

Hence we assume that the groundwater is initially contaminated with c_0 (case of Douala) as initial concentration and boundaries conditions are the same as prescribed by Dirichlet.

To solve this equation we first apply the Laplace transform on both sides, as follows

$$\mathcal{L}\left(\partial_t c(x,t) + \mathrm{q_r}\partial_x \mathrm{c}(x,t) - \mathrm{D_r}\partial_x^2 c(x,t) + \lambda c(x,t)\right) = \mathcal{L}(0) \tag{4.18}$$

where the symbol $\mathcal{L}$ is the Laplace transform operator, and yields to

$$sC(x) - C(0) + \left(\mathrm{q_r}\partial_x C(x) - \mathrm{D_r}\partial_x^2 C(x) + \lambda C(x)\right) = 0 \text{ with } C(x) = \mathcal{L}\big(c(x,t)\big). \tag{4.19}$$

Here s is the Laplace transform variable with respect to time variable and $C(0) = c_0$. We have from the above that, the partial differential equation becomes an ordinary non-homogeneous differential equation of order 2 because the partial derivative here becomes a total derivative and we have that, Equation (4.18) reduced to:

$$-\mathrm{D_r}C'' + \mathrm{q_r}C' + (s+\lambda)C = c_0 \tag{4.20}$$

The homogeneous solution associated to the above equation is given as

$$C_h(x) = A_1 \exp(r_1 x) + A_2 \exp(r_2 x) \tag{4.21}$$

where $A_1$and A_2 are arbitrary constants,

$$r_2 = \frac{\mathrm{q_r} + \sqrt{({q_r}^2 + 4\mathrm{D_r}(s+\lambda)}}{2\mathrm{D_r}}$$

$$r_1 = \frac{\mathrm{q_r} - \sqrt{({q_r}^2 + 4\mathrm{D_r}(s+\lambda)}}{2\mathrm{D_r}}$$

A particular solution associate to the equation is given by

$$C_p(x) = A_1(x)\exp(r_1 x) + A_2(x)\exp(r_2 x) \tag{4.22}$$

where $A_1(x)$ and $A_2(x)$ are function to be determined from the following system of equation

$$\begin{cases} A_1'(x)\exp(r_1 x) + A_2'(x)\exp(r_2 x) = 0 \\ r_1 A_1'(x)\exp(r_1 x) + r_2 A_2'(x)\exp(r_2 x) = g(x) \end{cases}$$

Hence the particular solution is given by (4.23)

$$C_p(x) = \frac{c_0}{\lambda + s}$$

Thus the solution of the ordinary non-homogeneous differential equation is given as

$$C(x) = A_1\exp(r_1 x) + A_2\exp(r_2 x) + \frac{c_0}{(\lambda+s)} \tag{4.24}$$

To determine the coefficient A_1andA_2 we need to put our initial and boundaries conditions in Laplace space as follows: (4.25)

$$\mathcal{L}\big(c(0,t)\big) = \frac{c_1}{\gamma + s}.$$

Applying the following boundary condition $\lim_{x\to\infty} \partial_x C(x) \to 0$ we have

$$A_2 = 0.$$

Further, using the initial condition, (4.25) we have (4.26)

$$A_1 = -\frac{c_0}{\lambda + s} + \frac{c_1}{\gamma + s}.$$

It follows the solution of the ordinary differential equation is given as

$$\frac{c_0}{\lambda + s} + ex\,p\left(x\frac{q_r - \sqrt{q_r^2 + 4D_r(\lambda + s)}}{2D_r}\right)\left[\frac{c_1}{\gamma + s} - \frac{c_0}{\lambda + s}\right].$$

Therefore the solution of the hydrodynamic dispersion equation is given as (4.27)

$$c(x,t) = \mathcal{L}^{-1}(C(x))$$

where $\mathcal{L}^{-1}$ is the inverse Laplace transform operator. The first term of the sum is invertible and gives: (4.28)

$$\mathcal{L}^{-1}\left(\frac{c_0}{\lambda + s}\right) = c_0\exp(-\lambda t).$$

To find the inverse Laplace of the second term of the sum we need to use the convolution theorem since we have the product of two functions namely

$$\left[\frac{c_1}{\gamma + s} - \frac{c_0}{\lambda + s}\right],$$

and

$$ex\,p\left(x\frac{q_r-\sqrt{q_r^2+4D_r(\lambda+s)}}{2D_r}\right).$$

The inverse Laplace of the above expression is obtained and is given below as

$$\mathcal{L}^{-1}\left(exp\left(x\frac{q_r-\sqrt{q_r^2+4D_r(\lambda+s)}}{2D_r}\right)\right)=\frac{xexp\left(-\frac{(-q_rt+x)^2-t\lambda}{4D_rt}\right)}{2\sqrt{\frac{\pi}{D_r}}t^{3/2}}=f(t).$$

and (4.29)

$$\mathcal{L}^{-1}\left\{\frac{c_1}{\gamma+s}-\frac{c_0}{\lambda+s}\right\}=c_1\exp(-\gamma t)-c_0\exp(-\lambda t)=g(t).$$

The inverse Laplace of the second term of the sum can then be expressed as

$$\int_0^t f(\xi)g(\xi-t)d\xi.$$

Using the table of integrals we find that the above integral yields to

$$\frac{c_1\exp[-\gamma t]}{2}\left\{exp\left(x\frac{q_r-u_r}{2D_r}\right)erfc\left(\frac{x-u_rt}{2\sqrt{D_rt}}\right)+exp\left(x\frac{q_r+u_r}{2D_r}\right)erfc\left(\frac{x+u_rt}{2\sqrt{D_rt}}\right)\right\}$$
$$-\frac{c_0\exp(-\lambda t)}{2}\left\{erfc\left(\frac{x-q_rt}{2\sqrt{D_rt}}\right)+exp\left(x\frac{q_r}{D_r}\right)erfc\left(\frac{x+q_rt}{2\sqrt{D_rt}}\right)\right\},$$

where (4.30)

$$u_r=\sqrt{q_r^2+4D_r(\lambda-\gamma)}$$

and $erfc(x)=\frac{2}{\sqrt{\pi}}\int_x^\infty \exp(-v^2)\,dv$ is known as complementary error function. Therefore the analytical solution of the hydrodynamic dispersion equation subject to the prescribed initial and boundaries conditions is given as: (4.31)

$$c(x,t)=\frac{c_1\exp[-\gamma t]}{2}\left\{exp\left(x\frac{q_r-u_r}{2D_r}\right)erfc\left(\frac{x-u_rt}{2\sqrt{D_rt}}\right)+exp\left(x\frac{q_r+u_r}{2D_r}\right)erfc\left(\frac{x+u_rt}{2\sqrt{D_rt}}\right)\right\}$$
$$-\frac{c_0\exp(-\lambda t)}{2}\left\{erfc\left(\frac{x-q_rt}{2\sqrt{D_rt}}\right)+exp\left(x\frac{q_r}{D_r}\right)erfc\left(\frac{x+q_rt}{2\sqrt{D_rt}}\right)\right\}+c_0\exp(-\lambda t).$$

Here one can notices that if $c_0=0$, then the analytical solution of the hydrodynamic dispersion equation is the same as the one given by (Clearly and Ungs 1978), that is, (4.32)

$$c(x,t)=\frac{c_1\exp[-\gamma t]}{2}\left\{exp\left(x\frac{q_r-u_r}{2D_r}\right)erfc\left(\frac{x-u_rt}{2\sqrt{D_rt}}\right)+exp\left(x\frac{q_r+u_r}{2D_r}\right)erfc\left(\frac{x+u_rt}{2\sqrt{D_rt}}\right)\right\}.$$

In the following section, graphical representation of this solution will be investigated for various parameters and this will be successfully achieved via the software Mathematica. For given set of parameters the software will provide a surface represents a solution associated

with respect to time and space. The used values for this purposed are arbitrary and not result from specific field observation.

4.4.2 Numerical results

The following figures show the behaviour of the analytical solution of the advection dispersion equation of the aquifer which is initially polluted with a certain concentrationc_0. The parameters used for the simulation are theoretical.

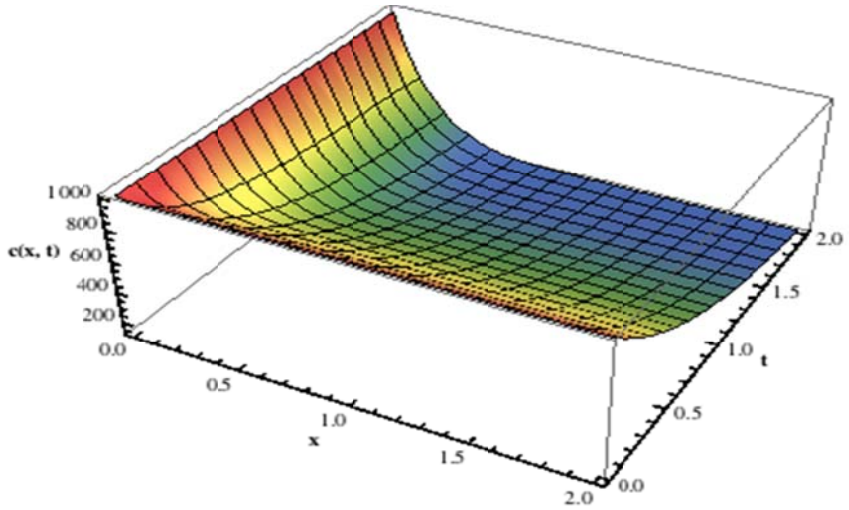

Figure 4-7: Surface showing the concentration for t in [0, 2] and $\boldsymbol{x}$ in [0, 2],γ=0 and $\boldsymbol{c(0,t) = c1 = 1000}$ $\boldsymbol{c(x,0) = c0 = 990, \rho_b = 1800, K_d = 1, q = 2}$, λ=1, and $\boldsymbol{D = 80}$

The above figure shows that if one assume that the concentration at the origin for all $t > 0$ the concentration is a constant, that is γ=0 and $c(0,t) = c1 = 1000$, the concentration at all the position of the aquifer for $t = 0$, that is $c(x,0) = c0 = 990$, the dry bulk density of the matrix $\rho_b = 1800$, the volumetric moisture content of the medium $\theta = 1$, the volumetric distribution coefficient $K_d = 1$, the Darcy velocity $q = 2$, the decay constant λ=1 and the dispersion coefficient $D = 80$, then the concentration near the origin first increases respect to time but decreases respect to position. Later on the concentration increases respect to the position and decreases respect to time. The practical meaning of this is that, the pollution observed at certain distance from the industry that continuously releases the hazardous waste in the aquifer, is the mixture of the concentration from the industry and the initial concentration that was already in the groundwater.

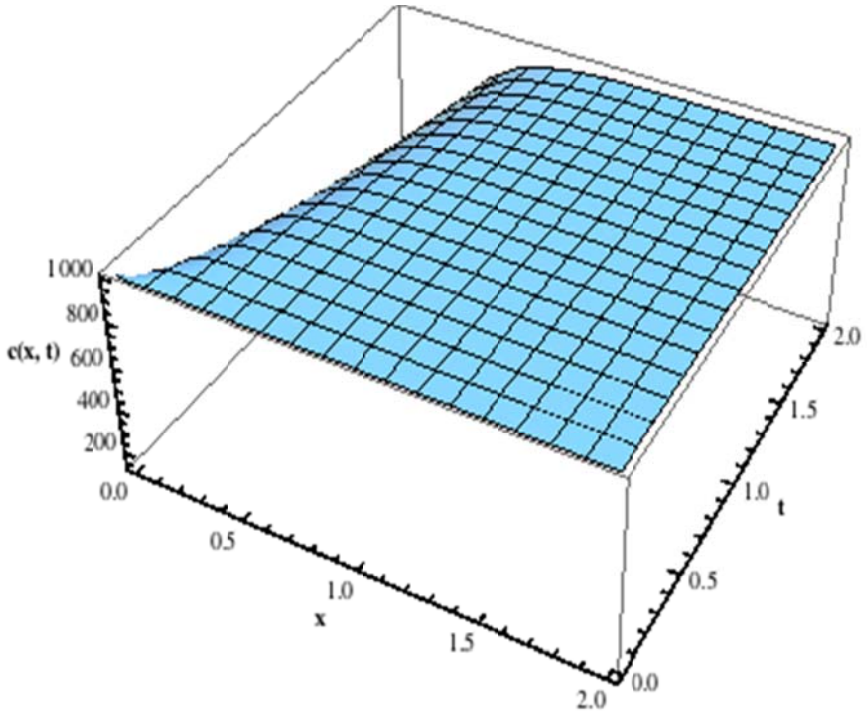

Figure 4-8: Surface showing the concentration for x in [0 2] and t in [0 2] $\boldsymbol{c(0.t) = c1 = 1000exp(-t)}$, $\boldsymbol{c(x,0) = c0 = 990, \rho_b = 1800, K_d = 1, q = 2}$, , λ=1, and $\boldsymbol{D = 80}$.

The above figure shows that if one assume that, the concentration at the origin for all t>0 the concentration is not a constant, but a decreasing function of time, that is $\gamma = 1$ and $c(0.t) = c1 = 1000exp(-t)$, the concentration at all the position of the aquifer for $t = 0$, that is $c(x,0) = c0 = 990$, the dry bulk density of the matrix $\rho_b = 1800$, the volumetric moisture content of the medium $\theta = 1$, the volumetric distribution coefficient $K_d = 1$, the Darcy velocity $q = 2$, the decay constant $\lambda = 0$, that is, there is no presence of radioactive in the pollution and the dispersion coefficient $D = 80$, then the concentration of pollution in groundwater will increase respect to time and respect to near the origin and the decreases slowly in time and position.

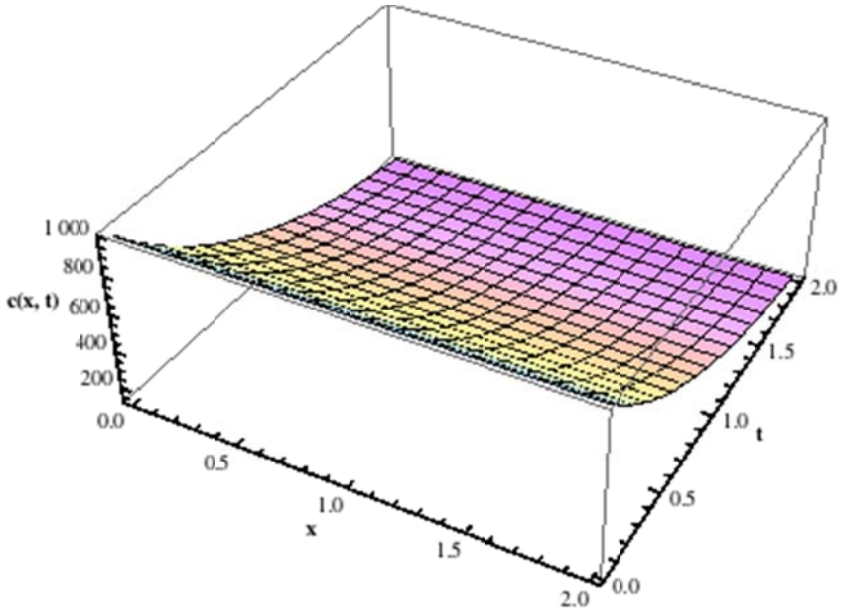

Figure 4-9: Surface showing the concentration for x in [0 2] and t in [0 2], $\boldsymbol{c(0,t) = c1exp(-t) = 1000exp(-t)}$, $\boldsymbol{c(x,0) = c0 = 990}$, $\boldsymbol{\rho_b = 1800}$, $\boldsymbol{K_d = 1}$, $\boldsymbol{q = 2}$, λ=1, and $\boldsymbol{D = 80}$

The above figure shows that if one suppose that the concentration at the origin for all $t > 0$ the concentration is not a constant, but a function of time, that is $\gamma = 1$ and $c(0,t) = c1exp(-t) = 1000exp(-t)$, the concentration at all the position of the aquifer for $t = 0$, that is $c(x,0) = c0 = 990$, the dry bulk density of the matrix $\rho_b = 1800$, the volumetric moisture content of the medium $\theta = 1$, the volumetric distribution coefficient $K_d = 1$, the Darcy velocity $q = 2$, the decay constant $\lambda = 1$ and the dispersion coefficient $D = 80$, then the concentration near the origin first increases respect to time and decreases respect to position. Later on the concentration increases respect to the position and decreases respect to time. The practical meaning of this is that, the pollution observed at certain distance from the industry that continuously releases the hazardous waste in the aquifer, is the mixture of the concentration from the industry and the initial concentration that was already in the groundwater. Here we realise that this situation is not too different from the situation described in figure 4-1

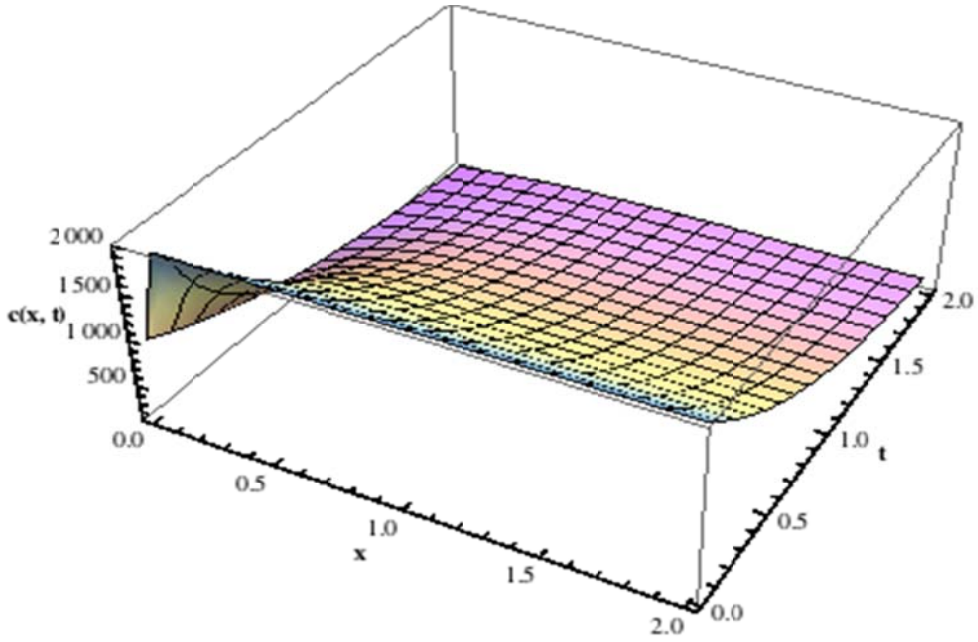

Figure 4-10: Surface showing the concentration for $\boldsymbol{x}$ in [0 , 2] and t in [0 2] $\boldsymbol{c(0,t) = c1exp(-t) = 1000exp(-t)}$, $\boldsymbol{c(x,0) = c0 = 990}$, $\boldsymbol{\rho_b = 1800}$, $\boldsymbol{K_d = 1}$, $\boldsymbol{q = 2}$, λ=1, and $\boldsymbol{D = 80}$.

The above figure shows that if one suppose that the concentration at the origin for all $t > 0$ the concentration is not a constant, but a function of time, that is $\gamma = 1$ and $c(0,t) = c1exp(-t) = 1000exp(-t)$, the concentration at all the position of the aquifer for $t = 0$, that is $c(x,0) = c0 = 990$, the dry bulk density of the matrix $\rho_b = 1800$, the volumetric moisture content of the medium $\theta = 1$, the volumetric distribution coefficient $K_d = 1$, the Darcy velocity $q = 2$, the decay constant $\lambda = 1$ and the dispersion coefficient $D = 80$, then the concentration will increase in space and decrease in time. The practical meaning of this is that, the pollution observed at certain distance from the industry that continuously releases the hazardous waste in the aquifer, is the mixture of the concentration from the industry and the initial concentration that was already in the groundwater since the initial concentration in the groundwater is greater than the one releases by the industry, it follows that the mixture will increase in space but at the same time as the time passes the mixture will decrease slowly.

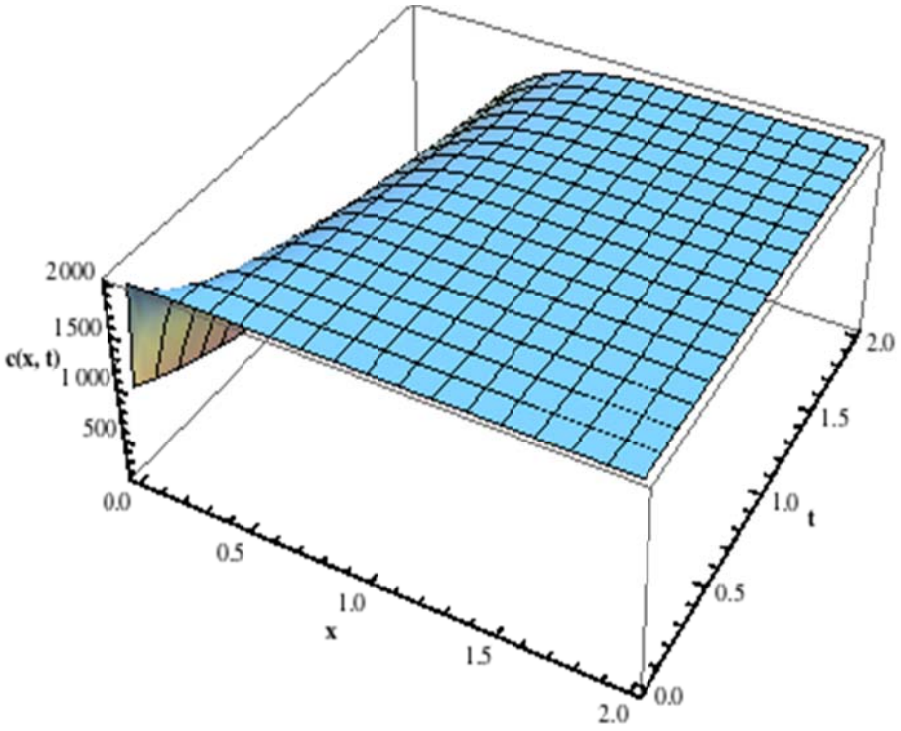

Figure 4-11: Surface showing the concentration for x in [0 2] and t in [0 2] $\boldsymbol{c(0,t) = c1exp(-t) = 1000exp(-t)}$, $\boldsymbol{c(x,0) = c0 = 1990}$,, $\boldsymbol{\rho_b = 1800}$, $\boldsymbol{K_d = 1}$, $\boldsymbol{q = 2}$, λ=1, and $\boldsymbol{D = 80}$.

The above figure shows that if one assume that, the concentration at the origin for all $t > 0$ the concentration is not a constant, but a decreasing function of time, that is $\gamma = 1$ and $c(0,t) = c1 = 1000exp(-t)$, the concentration at all positions of the aquifer for $t = 0$, that is $c(x,0) = c0 = 1990$, the dry bulk density of the matrix $\rho_b = 1800$, the volumetric moisture content of the medium $\theta = 1$, the volumetric distribution coefficient $K_d = 1$, the Darcy velocity $q = 2$, the decay constant $\lambda = 0$, that is, there is no presence of radioactive in the pollution and the dispersion coefficient $D = 80$, then the concentration of pollution in groundwater will increase rapidly respect to time near the origin and the decreases slowly in time and position

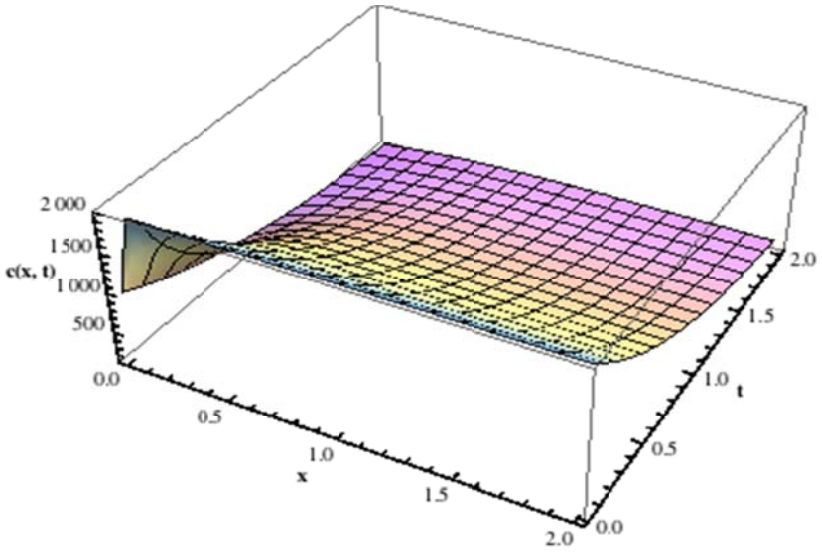

Figure 4-12: Surface showing the concentration for x in [0 2] and t in [0 2] $\boldsymbol{c(0,t)} = \boldsymbol{c1exp(-t)} = \boldsymbol{1000}, \boldsymbol{c(x,0)} = \boldsymbol{c0} = \boldsymbol{1990}, , \boldsymbol{\rho_b} = \boldsymbol{1800}, \boldsymbol{K_d} = \boldsymbol{1}, \boldsymbol{q} = \boldsymbol{2}$, λ=1, and $\boldsymbol{D} = \boldsymbol{80}$

The above figure shows that if one suppose that the concentration at the origin for all $t > 0$ the concentration is a constant, that is $\gamma = 0$ and $c(0,t) = c1 = 1000$, the concentration at all the position of the aquifer for $t = 0$, that is $c(x,0) = c0 = 1990$, the dry bulk density of the matrix $\rho_b = 1800$, the volumetric moisture content of the medium $\theta = 1$, the volumetric distribution coefficient $K_d = 1$, the Darcy velocity $q = 2$, the decay constant $\lambda = 1$ and the dispersion coefficient $D = 80$, then the concentration near the origin first increases rapidly respect to time and position. Later on the concentration increases respect to the position and decreases respect to time. The practical meaning of this is that, the pollution observed at certain distance from the industry that continuously releases the hazardous waste in the aquifer, is the mixture of the concentration from the industry and the initial concentration that was already in the groundwater, since the initial concentration in the groundwater is greater than the one releases by the industry, if follows that this mixture will be more important at the site than everywhere else. The first remark here is that the concentration behaviour is sensible to the present or absence of radioactive nuclide in the system. The second one is that the initial concentration plays a key role in the model. To have a proper sensitivity of the parameters involved in this solution, in the following section our discussion will be based on uncertainties and sensitivity analysis.

Chapter 5

GROUNDWATER REMEDIATION TECHNIQUES

Groundwater contamination, as one of the most important health-related environmental problems, has brought serious adverse effects on the environment and human health and attracted more and more attention around the world. Groundwater remediation is one of the major technical and environmental challenges in the field of water resources because completion of groundwater remediation often needs to undergo a relatively long time horizon of up to several decades or more. This involves removing or containing the plume of contaminants within an aquifer. Many methods have been devised and used to treat the many types of contaminants in the many types of aquifers. Eight of the more common remediation methods are discussed below. Interested readers are referred to the following references for more detail (Stewart, 2008)(Miller, 1980)(Hayman and Dupont, 2001)(Air Sparging, 2009) and (Bob, 2009).

5.1 REMEDIATION METHODS

The method for remediation depends on the several factors: (a) Hydro-geological setting; (b) Contaminant characteristics; (c) Physical properties (sink or float); (d) Chemical properties (solubility, sorption); (e) Subsurface access, land use; (f) Toxicity-risk; (g) Cost. All are expensive, and some are much more expensive than others (Stewart, 2008) .

Many remediation methods are used to clean the polluted aquifer, the more common are:

Pump-and-treat

This involves removing contaminated groundwater from strategically placed wells, treating the extracted water after it is on the surface to remove the contaminates using mechanical, chemical, or biological methods, and discharging the treated water to the subsurface, surface, or municipal sewer system.

Hydraulic Containment

Pumping water from wells can be done in such a way that it changes the flow of water through an aquifer in ways to keep contaminants away from wells used for cities or farms. The technique works if the flow through the aquifer is relatively simple, so the plume of contaminated water does not divide into different paths. It is often used together with pump and treat, and it has the same limitations.

Air Sparging/Soil-Vapour Extraction

The limitations include: (a) difficulty flushing in low permeability zones, (b) difficulty

operating below 9m (30ft), (c) difficulty extracting multi-component phases.

In-situ Oxidation

This method injects an oxidant such as hydrogen peroxide (H2O2) into the contaminated aquifer. The contaminant is oxidized, primarily producing carbon dioxide and water.

Permeable Reactive Barriers

These methods use a trench backfilled with reactive material such as iron filings, activated carbon, or peat, which absorb and transform the contaminant as water from the aquifer passes through the barrier. This works only for relatively shallow aquifers.

Phyto-remediation

Some plants accumulate heavy metals and metal like elements, such as arsenic, lead, uranium, selenium, cadmium, and other toxins such as nutrients, hydrocarbons, and chlorinated hydrocarbons. Chinese Ladder fern Pteris vittata, also known as the brake fern, is a highly efficient accumulator of arsenic. Genetically altered cottonwood trees suck mercury from the contaminated soil in Danbury Connecticut and, transgenic Indian mustard plants to soak up dangerously high selenium deposits in California. The remediation consists of growing such plants so their roots tap the groundwater. Then, the plants are harvested and disposed. The method is limited to remediation of groundwater that is close enough to the surface that it can be reached by plant roots.

Natural Attenuation

Sometimes natural processes remove contaminants with no human intervention. The removal may involve dilution, radioactive decay, sorption (attachment of compounds to geologic materials by physical or chemical attraction), volatization, or natural chemical reactions that stabilize, destroy, or transform contaminants.

Intrinsic and Enhanced Bioremediation

Biodegradation is the breakdown of carbon-based contaminants by microbial organisms into smaller compounds. The microbial organisms transform the contaminants through metabolic or enzymatic processes. Biodegradation processes vary greatly, but frequently the final product of the degradation is carbon dioxide or methane. Biodegradation is a key process in the natural attenuation of contaminants at hazardous waste sites.

The most widely used method of groundwater remediation is a combination of extraction, ex-situ treatment, and discharge of the treated water, commonly known as pump and treat. Pump-and-treat methods are costly and often ineffective in meeting long-term protection standards (Travis and Doty, 1990) (Gillham and Burris, 1992). A potentially cost-effective technology for the removal of organic and inorganic compounds from contaminated aquifers that will be used in the model described in Chapter 6 is Deep Aquifer

Remediation Tools (DART's), more specifically its shallow aquifer equivalent Permeable Reactive Barriers (PRB's), which will now be described in more detail.

5.2 PERMEABLE REACTIVE BARRIERS

Instead of pumping water to the surface for ex-situ treatment, a tool has been developed to take advantage of the natural groundwater gradient to channel groundwater into highly permeable reactive material(s) (David *et al*, 1999). These Deep Aquifer Remediation Tools (DARTs) are used in conjunction with non-pumping wells and offer a low-cost and virtually maintenance-free alternative to ex-situ treatment methods. As the ground water passes through the permeable reactive material, the contaminant is immobilized or transformed to a non-toxic form by a variety of chemical reactions depending on the reactive material and contaminant of concern (Davis *et al*, 1999) The DARTs are deployed into an aquifer and corresponding contaminant

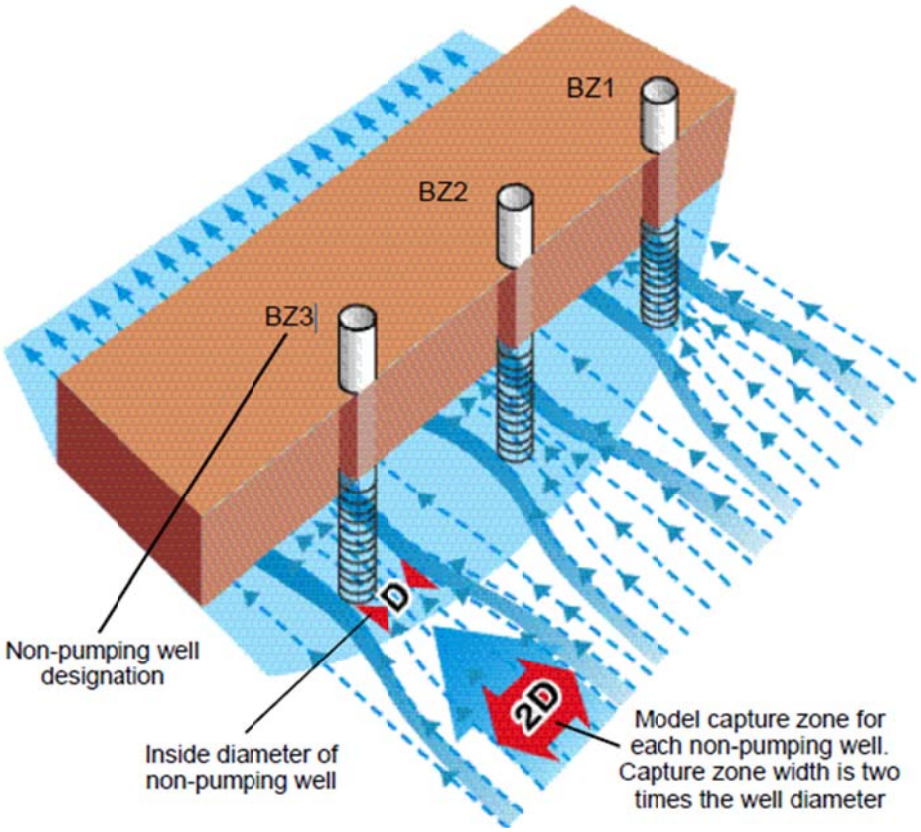

Figure 5-1: Schematic diagram showing non-pumping wells containing DARTs and modelled pollution capture zone; Fry Canyon. Utah, 2004 (David *et al*., 1999).

plume through a series of non-pumping wells. (Wilson and Mackay, 1997) have found that ground water will converge to arrays of un-pumped wells in response to the difference in

hydraulic conductivity between the well and aquifer. Numerical simulations conducted during DART development indicate that each well typically intercepts ground water in the up-gradient part of the aquifer that is approximately twice the inside diameter of the well (David *et al.,* 1999). Trenching techniques are commonly used to emplace permeable reactive barriers (PRBs) for in-situ contaminant removal in shallow aquifers (Manz and Quinn, 1997) and (Schmithorst and Vardy, 1997). Trench emplacement of PRBs has a number of disadvantages that include: (1) limited to shallow treatment zones; (2) requires specialized trenching equipment; (3) increased health and safety concerns during installation; and (4) replacement and disposal costs of reactive material after breakthrough (David *et al.*, 1999). Because DARTs are deployed through non-pumping wells, in-situ treatment of deeper contaminant plumes (greater than 100 feet below land surface) that could not be treated with currently available trenching technologies is now possible (David *et al.*, 1999). In addition, DARTs allow for easy retrieval, replacement, and disposal of reactive material after chemical breakthrough. DARTs are designed to fit a variety of well dimensions and plume geometries. A DART is composed of three basic components: (1) a rigid PVC shell with high-capacity flow channels to contain the permeable reactive material; (2) flexible wings to direct the flow of ground water into the permeable reactive material; and (3) passive samplers to determine the quality of the treated water (David *et al.*, 1999). Multiple DARTs can be joined together for the treatment of thicker contaminant plumes. DARTs also allow for "vertical stacking" of different reactive materials for the treatment of chemically segregated contaminant plumes.

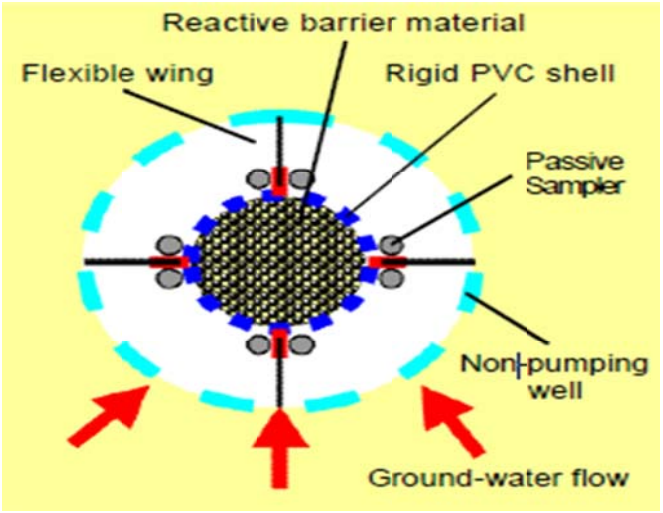

Figure 5-2: Schematic diagram of deep Aquifer Remediation Tool (DART) (David *et al.*, 1999)

Since 1997, several DART prototypes have been field tested in non-pumping wells for the removal of uranium (U) from groundwater at sites in Utah and Wyoming (David *et al*, 1999). The reactive material used during these field tests consisted of a mixture of bone charcoal and iron oxide pellets. The probable mechanism for U removal in this mixture is sorption or precipitation of insoluble uranyl precipitates. Results from the latest DART field test completed in July 1999 indicate an order of magnitude reduction in U concentrations compared to pre-treatment water samples (David *et al.*, 1999). Additional field tests of the DARTs are currently (September 1999) in progress and include the testing of an additional barrier material (zero valent iron) (David *et al.*, 1999). Previous research with zero-valent iron (installed using trenching techniques) has indicated greater than 99.9 percent U removal rates over extended field operations (David, *et al.*, 1999). Note that in a shallow aquifer, the boreholes are replaced by a barrier.

5.3 OBJECTIVE OF THE TECHNIQUE

The use of permeable reactive barriers for the restoration of contaminated groundwater has evolved from innovative to accepted, standard practice, for the containment and treatment of a variety of contaminants in ground water. Like any remedial technology, the decision to use PRBs will be conditioned by the nature of the natural system, the target contaminants, and the treatment objectives. As with any technology used to treat or extract contaminants in the subsurface, successful implementation will be contingent on effective site characterization, design, and construction. Our studies on long-term performance of the technology at a number of sites have shown the following with respect to ensuring (designing) and verifying (monitoring) that the PRB meets performance objectives (USEPA, 1988; 1998a, 1998b, 2000a, 2000b, 2008a):

• Adequate site characterization is necessary on the scale of the PRB. Site characterization approaches, typical of remedial feasibility investigations, are oftentimes not adequate. Additional localized characterization of the plume distribution in four dimensions (including time), understanding of local hydrogeology, and knowledge of the geochemistry of the site is required.

• Understanding of site hydrology has emerged as the most important factor for successful implementation. This is not surprising given the nature of the technology. The PRB must be located to intercept the plume. Once located in the subsurface, it cannot be moved, so an understanding of how the PRB will impact the prevailing flow patterns is important. It is imperative that the selected design allow for capture of the plume in its present configuration, as well as allow for variations in flow direction, depth, velocity, and

concentrations of contaminants, which may vary over time.

• There is a need to develop contingency plans in case a system fails to meet design objectives. This requires specification of design criteria, performance objectives, and what constitutes a failure in order to clearly trigger the activation of contingency plans, i.e., alternative technologies or remedies to the installed PRB system.

Performance goals should target the adequacy of plume capture and contaminant treatment such that acceptable down gradient water quality is achieved in a reasonable time frame. Short-term objectives generally involve establishment of adequate residence time of the contaminant(s) in the reactive media to achieve treatment goals, while long-term objectives revolve around longevity or lifetime expectations for the system, which in turn, affect cost.

Specific criteria need to be established for all these concerns, and both parties (site owner and regulator) need to be clear on what triggers contingency plans. Maximum contaminant level (MCL) concentrations for contaminants in ground water are often used as criteria at points of compliance. This approach becomes complicated when contaminant levels already exceed goals at the point of compliance, and meeting these goals is contingent on desorption of residual contaminants or flushing over time. A time period needs to be specified in such a case that is reasonable given site characteristics and known contaminant behaviour.

Performance goals are usually developed for the site as a whole and contingent upon plume and barrier location relative to compliance points and/or site boundaries. The performance goals can be numeric, regulatory-driven targets and may have system design features including remedial measures, such as natural attenuation, down gradient of the barrier location. The time horizon for sustaining performance goals will depend on site-specific factors related to chemical, physical and microbiological processes, but also such factors as the extent of source removal, source containment or expected lifetime of the source as a plume generator.

In many cases, contingency plans are required in the event that the PRB fails to meet performance criteria. Such plans may range from minor modifications of the PRB to use of an alternative technology. If the PRB fails to capture a portion of the plume, an extension to the PRB may be prescribed. If concentrations of contaminants exiting the PRB are higher than expected, then an additional wall may be required down gradient of the first wall. In some installations, monitored natural attenuation of contaminants down gradient of the wall is expected and designed into the system to help meet compliance goals. This will be explicitly observed with the numerical results via FEFLOW in the next Chapter 6.

Chapter 6

SUGGESTED NUMERICAL MODEL FOR GROUNDWATER POLLUTION AT DOUALA CITY

In this chapter, the software "FEFLOW" is used to generate the numerical solution of groundwater in the city of Douala. Any pre-existing geological background and site information should be assembled and a preliminary conceptualization of the subsurface geologic features should be completed. This model should have general information on the site-wide lithology, various aquifer layers and confining units, contaminant plume configuration, and factors such as precipitation. A conceptualization of the lithologic variations also should be developed. These variations have a significant impact on aquifer heterogeneity, which may be the most important control on the groundwater flow system and placement of the PRB. This preliminary assessment should be used as a basis for further delineation of the local geology for PRB installation. This was done earlier in chapter two

The topography of this area is generated by Google-Map. With the help of the software "Surfer" the topography's image is discredited to have the numerical data. 31×31 points were selected to be used in FEFLOW, some assumption were made for this matter, including, aquifer recharge, hydraulic conductivity and the specific storativity. The area under investigation measures a distance about 40 kilometres from Nouvelle route de Bonaberi to Yassa and 17.7 kilometres (11 miles) from the Wouri estuary to Logbessou-Sunshine city. However, for the simulation purposed, we will only consider, from north to south a distance of 5603 m and from East to west a distance of 5256 m.

6.1 MASS TRANSPORT AND VELOCITY FIELDS

In this section, we will describe the hydraulic head and the vector fields of Douala, and we start this description with the hydraulic head following by the velocity field, the numerical solution of this will be obtained via the software FEFLOW. The aquifer parameters used for these simulation, are theoretical except the topography coordinates that are given by Google-Earth.

From the numerical solution generated by FEFLOW one can see that the elevation of water in this area varies between 0 and 15 meters. Note that the number zero here in the below figure 6-3 corresponds to the elevation at the sea. The figure 6-4 below shows two zone of convergence of water flow, the first zone here includes, Bonassama, Deido, Akwa I, Bonamikengue and the bay of Bonaberi and the second zone including, New Bell, Douala

International Airport and the Wouri estuary which is found in the mangrove, this mangrove. Since the water flow is the driving force for the release of pollution in the liquid phase, it follows that the high concentration of groundwater pollution released from different waste disposal in Douala may possibly be found in these two zones. The following Figure (6-1) shows the finite element mesh used for the model. To set up our model we considered here two points of pollutions, one in the Bonaberi area and another one in the New Bell near the estuary. This network is the base of the models that will be simulated throughout this thesis. The model network was generated by making use of a 3D finite element ground water modelling software package FEFLOW, developed by the German based DHI WASY Institute for Water Resources Planning and Systems Research GmbH. The basic premise on which all numerical models are based is that the area in question can be discredited into smaller areas, also referred to as elements. In the case of Douala city, the two major areas were discredited into 393,860 elements (795044 elements x 1 layer), with 217,074 nodal positions (795608 nodes x2 slices). Different zones and layers were assigned in order to compensate for hydro geological differences in characteristics over the area due to geology and/or gradient at depth. No rotation of the model grid was required as it was assumed that the natural flow occurs from South to North in the model domain. Two sources of contaminations were introduced, one at industrial zone of Bonaberi and one in industrial zone of Bassa as indicated in Figure (6-1) in chapter 2. From north to south we have a distance of 5603 m and from East to west we have a distance of 5256 m, these distances were measures via WISH.

We have placed the western source of groundwater pollution at the Bonaberi industrial zone. We placed the Eartern source of groundwater pollution in the Bassa zone industrial, between Bonanjo and Akwa, as display in figure (6-1). Figure (6-3) shows the initial head run as transient state. The black areas between the two industrial zones correspond to the estuary and will not take into account. Figure (6-4) shows the velocity field of Douala's groundwater flow. This figure is in perfect agreement with the topography and the hydraulic head field show the convergent zones. It is worth noting the upper part of the area under study shows that the water from the springs and rivers recharge the aquifer, but near the industrial zone including, Bonassama, Deido, Akwa I, Bonamikengue and the bay of Bonaberi, the groundwater flows toward the river Wouri.

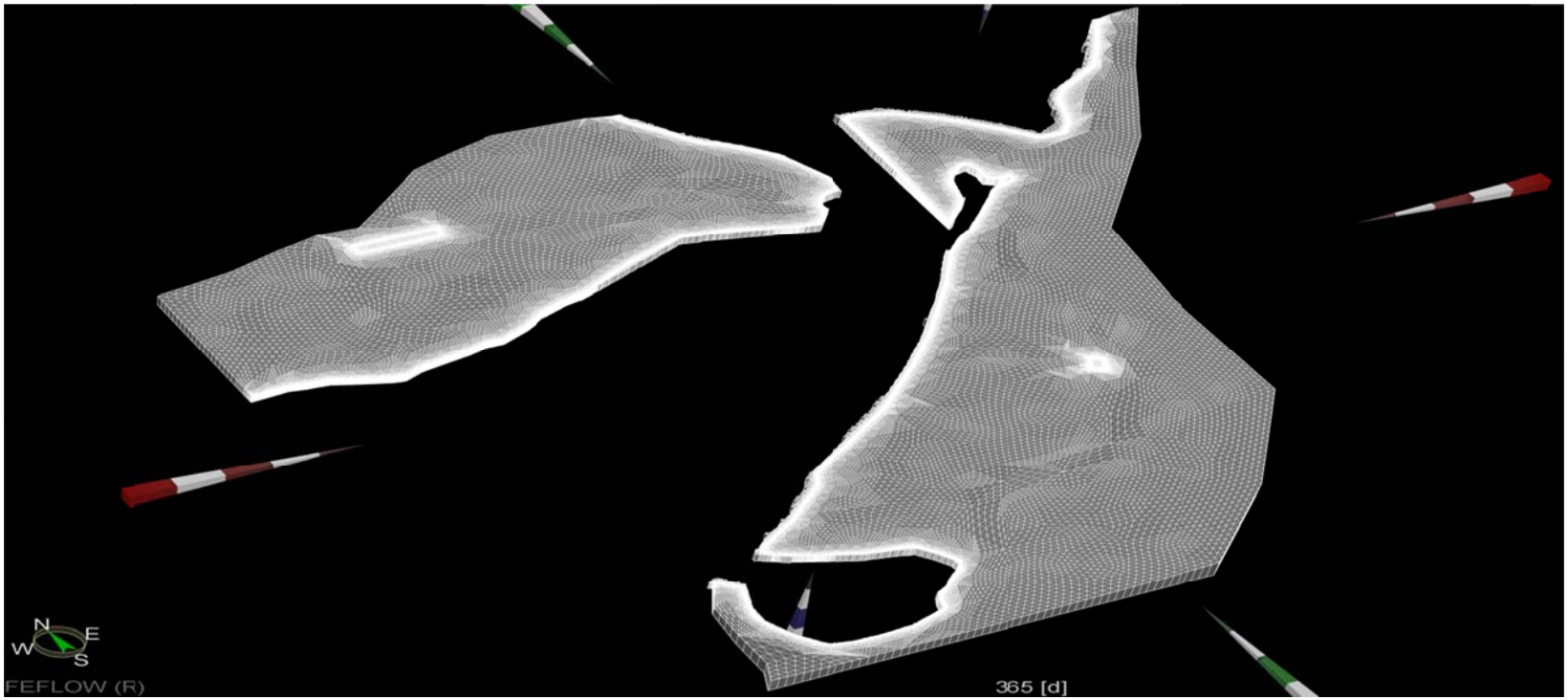

Figure 6-1 Network of the numerical model at Douala city

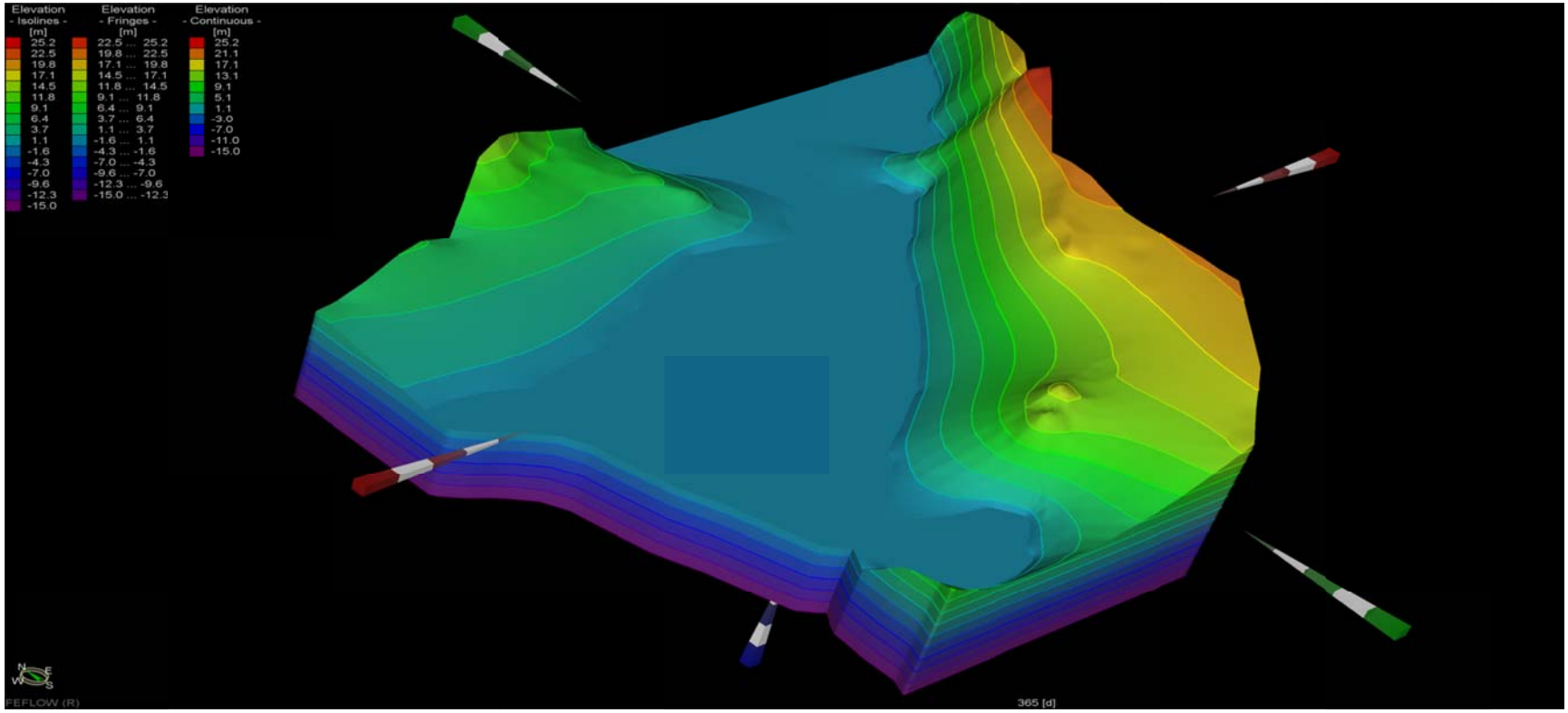

Figure 6-2: Elevation contour map, the elevation ranges from -15 to 0 and from 0 to 25.2, where 0 corresponds to the sea, -15 m corresponds to the elevation below the sea and 25 m above the sea.

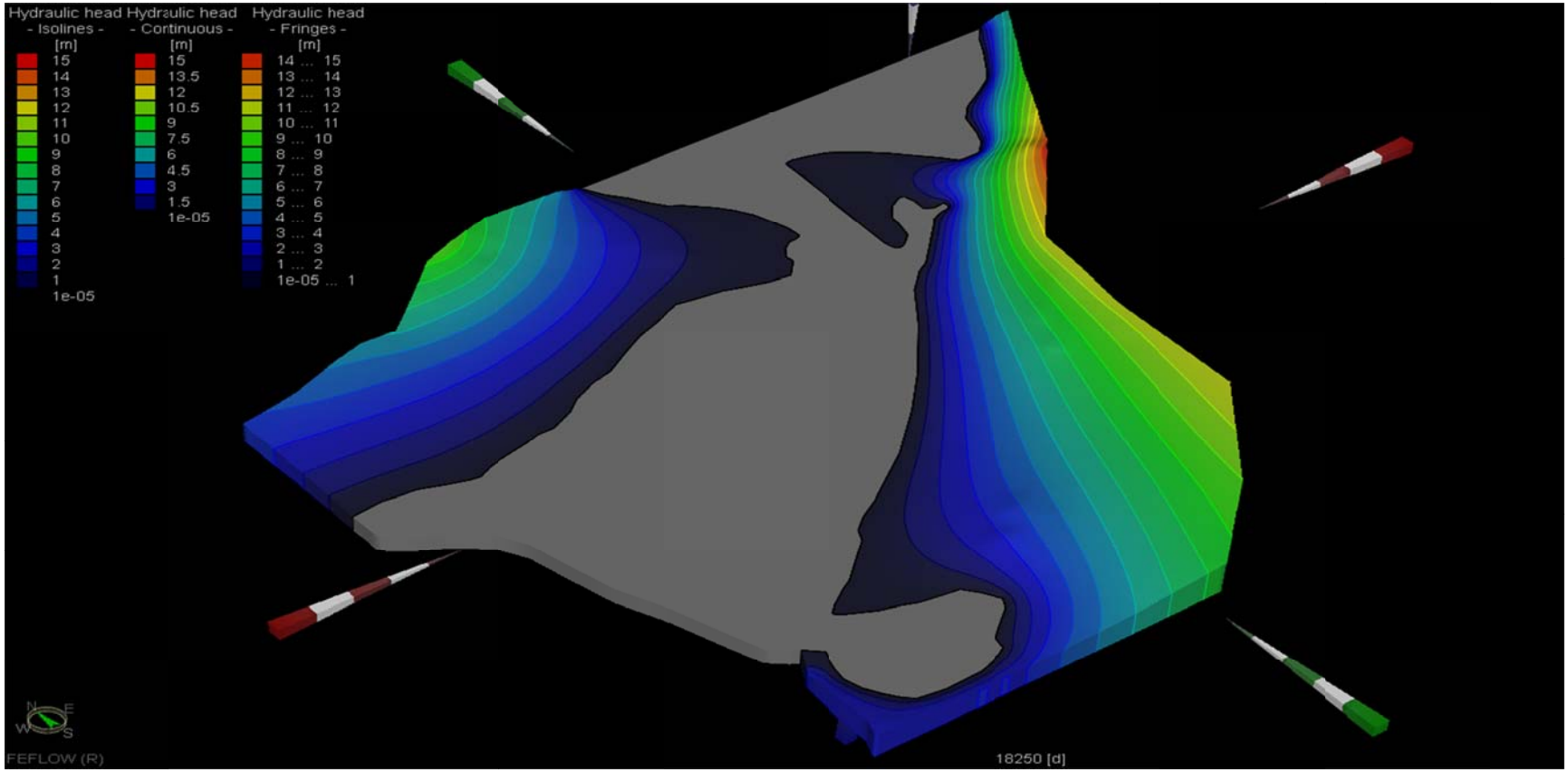

Figure 6-3: Hydraulics Head in Douala generated by FEFLOW, with the hydraulic head ranging between from 0 to 15 m. Where the number zero corresponds to the level of water at the Wouri estuary

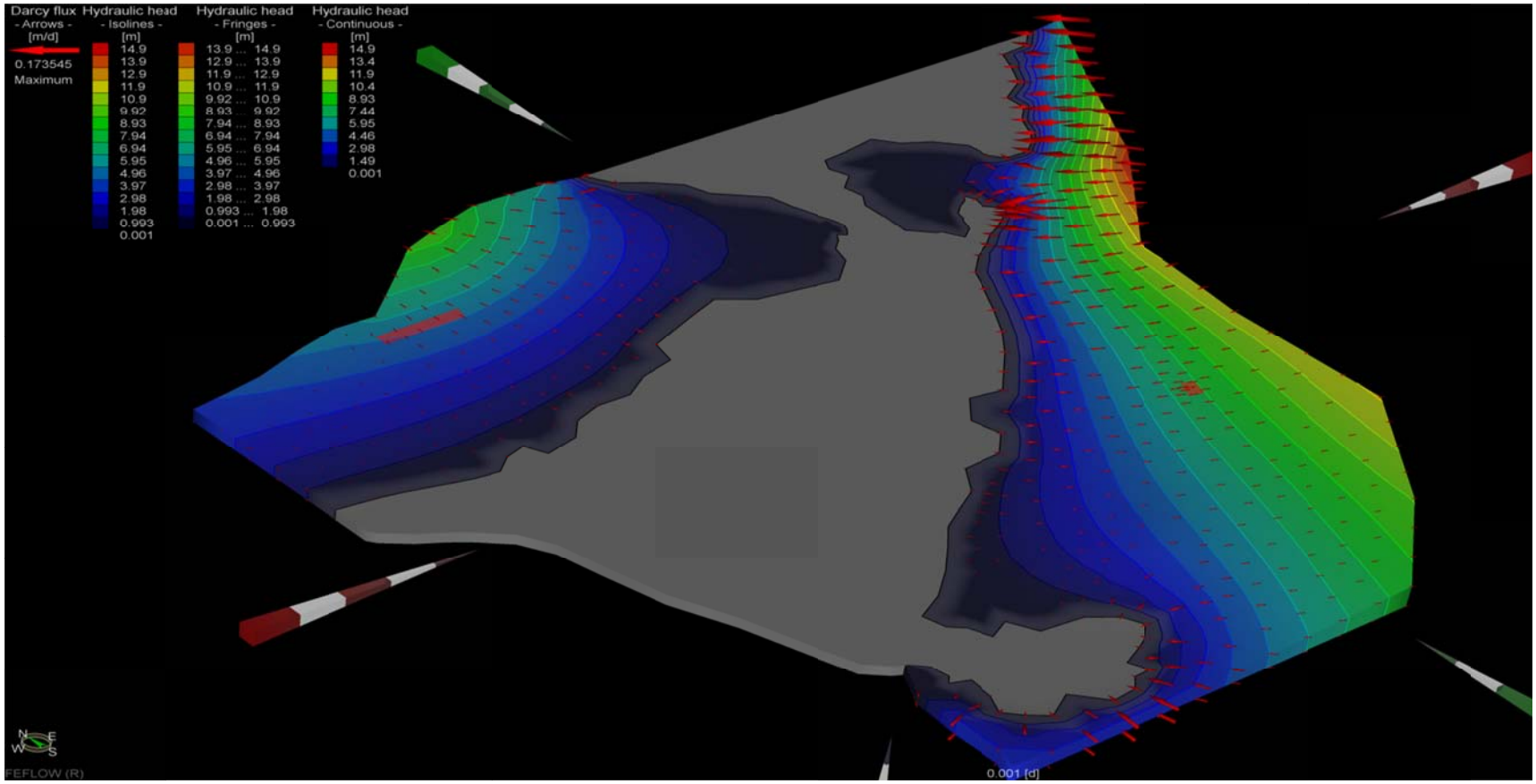

Figure 6-4: Velocity field of the area under study (Douala). The accumulation of the velocity corresponds to the convergence point of the groundwater flow from the main aquifer to the Wouri estuary. The direction of the flow is more effective in the Eastern part of the model

This is in perfect agreement with what was predicted from the hydraulic head; see Fig (6-3). Therefore, these velocities will be used in the solution of the mass transport equation.

6.2 NUMERICAL IMPLEMENTATION OF THE GROUNDWATER RESTORATION AT DOUALA CITY VIA OF PRB

The permeable reactive barrier (PRB) technology has gained acceptance as an effective ground-water remediation strategy for the treatment of a variety of chlorinated organic and inorganic compounds. The technology combines subsurface fluid-flow management with contaminant treatment by chemical, physical or biological processes, or by combinations of these three principal process categories. The PRB methodology has advantages over traditional pump-and-treat systems in that it is passive and a large plume can be treated in a cost-effective manner. More than one hundred implementations of the technology worldwide have proven that passive reactive barriers can be cost-effective and efficient approaches to remediate a variety of compounds of environmental concern. Yet, few case studies are available that evaluate the long-term performance of these *in-situ* systems, especially with respect to the long-term efficiency of contaminant removal, the build-up of mineral precipitates, and the build-up of microbial biomass. On the Eastern source of contamination we will accurately place the barrier to intercept the plume, but on the western part the barrier will not be placed accurately for the sake of clarity. This choice is to illustrate how important is to place adequately the barrier to intercept all the pathway of the plume in the aquifer. The numerical simulations of the mass transport equation in Douala cit obtained via FEFLOW have been depicted in Figure 6-7, Figure 6-8, Figure 6-9, Figure 6-10, Figure 6-11 and Figure 6-12. In Figure 6-7 we placed the barrier between the pollution source and the estuary and then we run the model for few days to see the effect of the barrier to the pollution pathway. The similar scenario was done in the simulation of Figure 6-8, Figure 6-9, Figure 6-10.

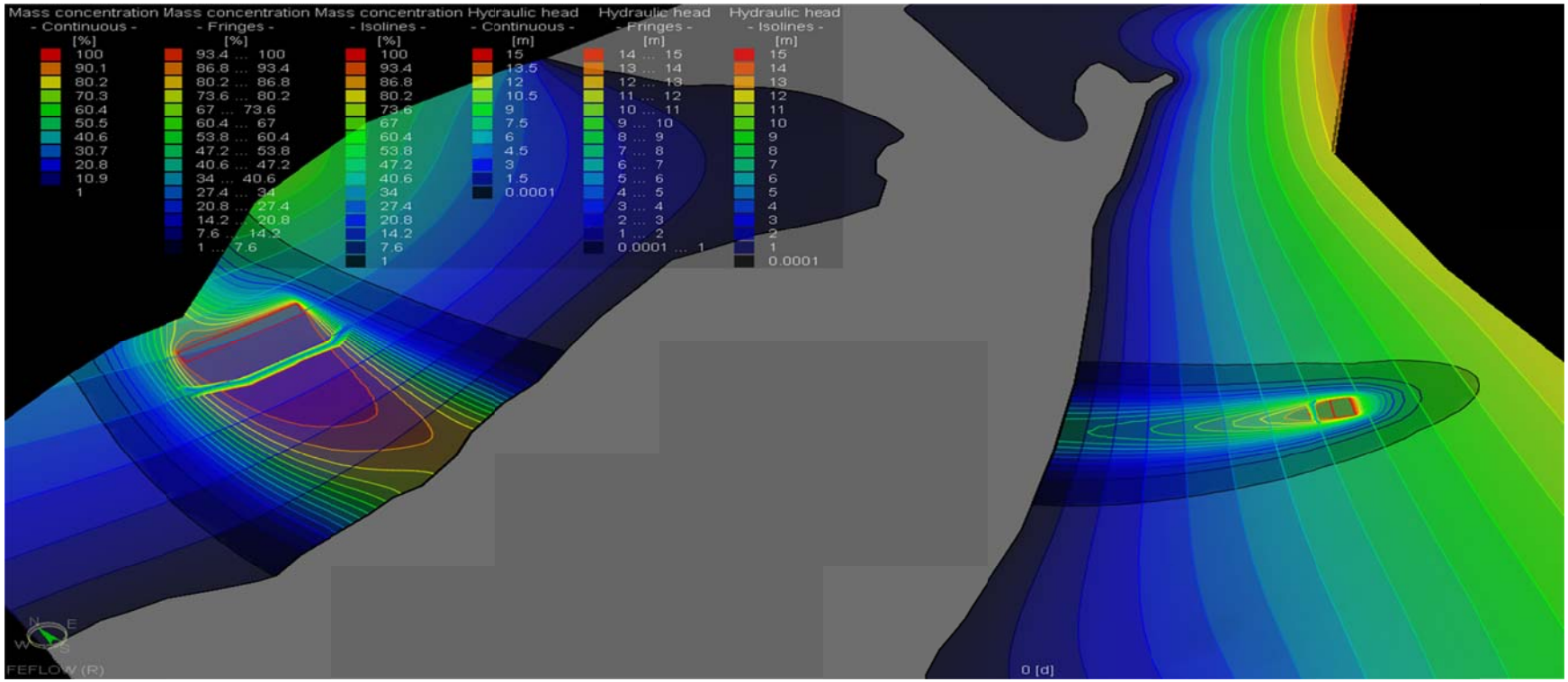

Figure 6-5: clean up for year zero, 100% of the mass concentration, the hydraulic head continuous ranging from 0 to 15 m and the hydraulic head isolines ranging from 0.0001 to 15 m and mass concentration fringes ranging from [1-7.6] to [93.4-100]

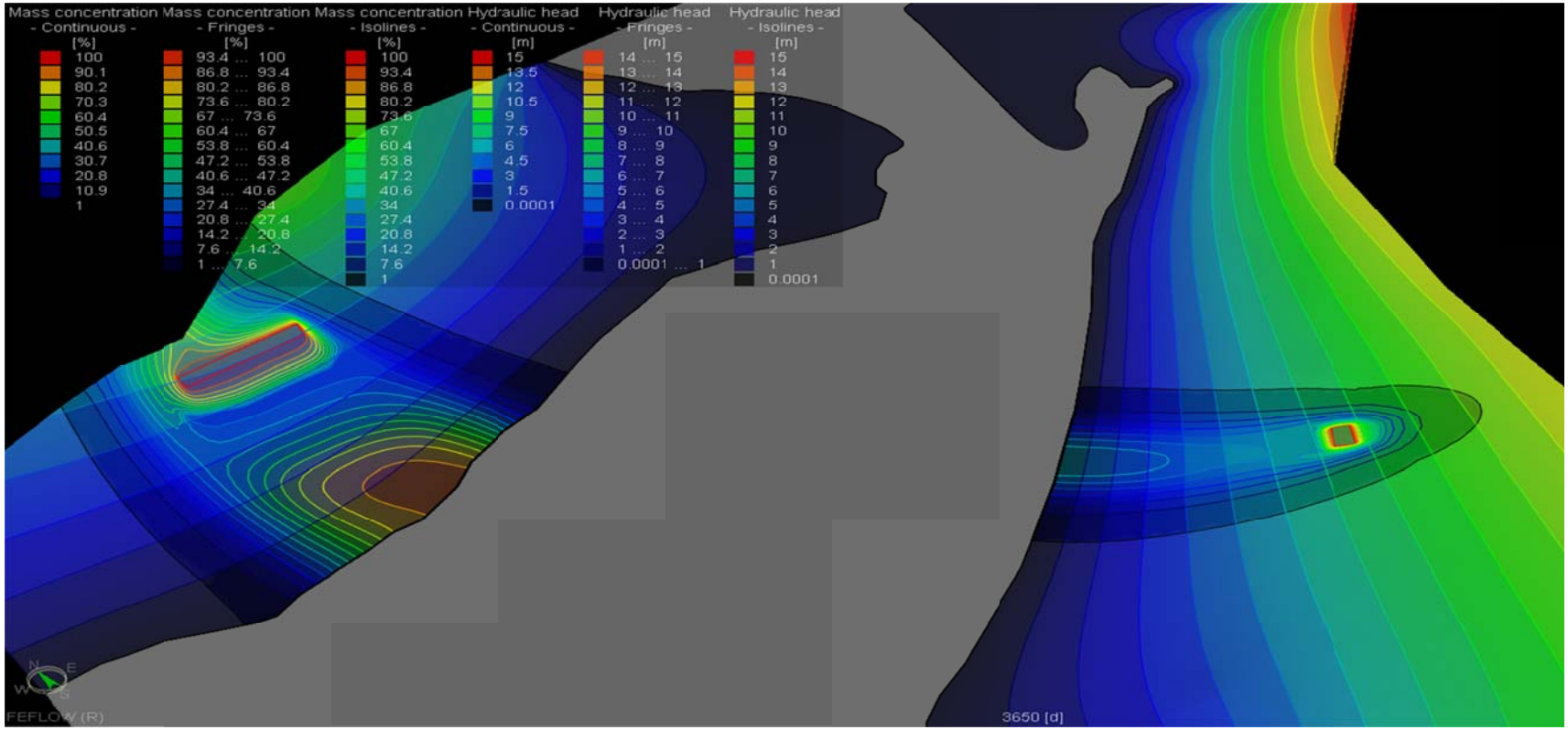

Figure 6-6: Clean up after 10 years 100% of the mass concentration, the hydraulic head continuous ranging from 0 to 15 m and the hydraulic head isolines ranging from 0.0001 to 15 m and mass concentration fringes ranging from [1-7.6] to [93.4-100]

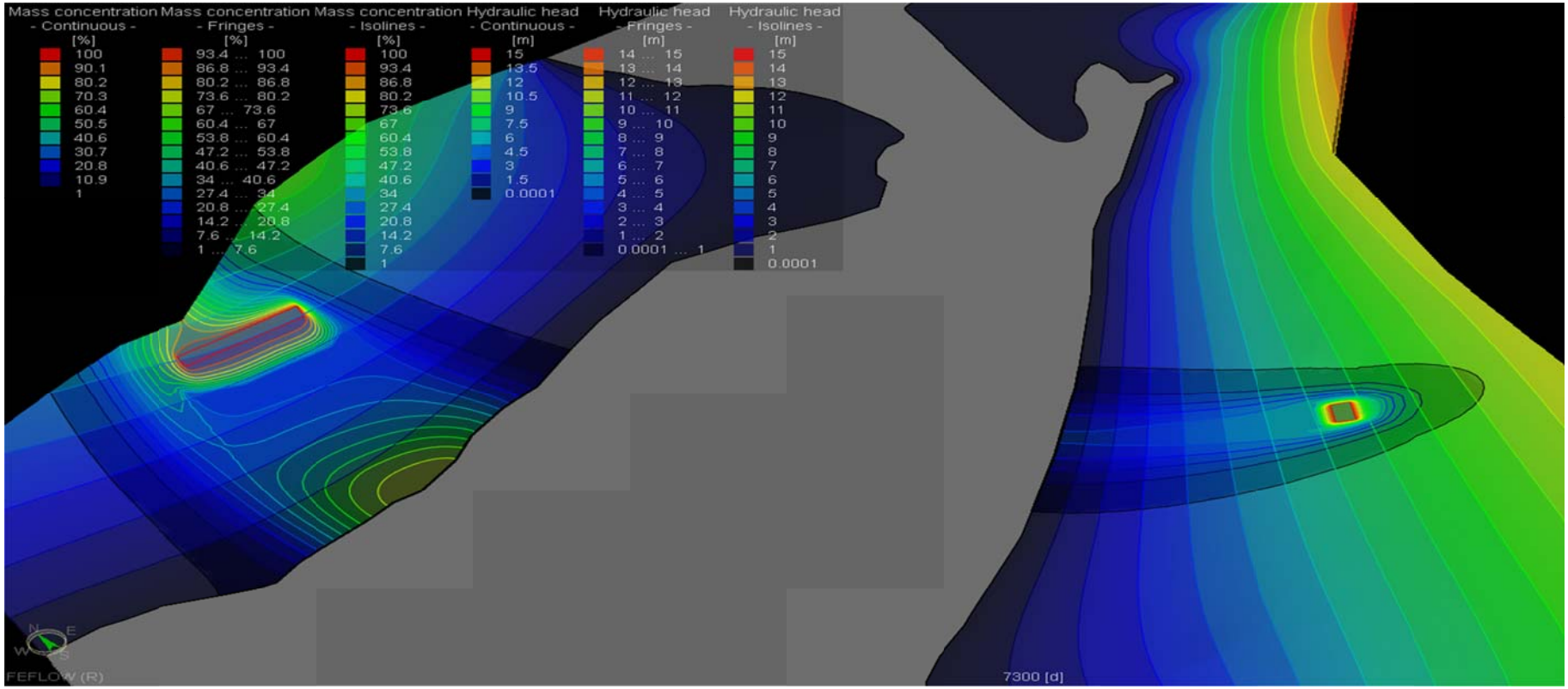

Figure 6-7: Clean up after 20 years, 100% of the mass concentration, the hydraulic head continuous ranging from 0 to 15 m and the hydraulic head isolines ranging from 0.0001 to 15 m and mass concentration fringes ranging from [1-7.6] to [93.4-100]

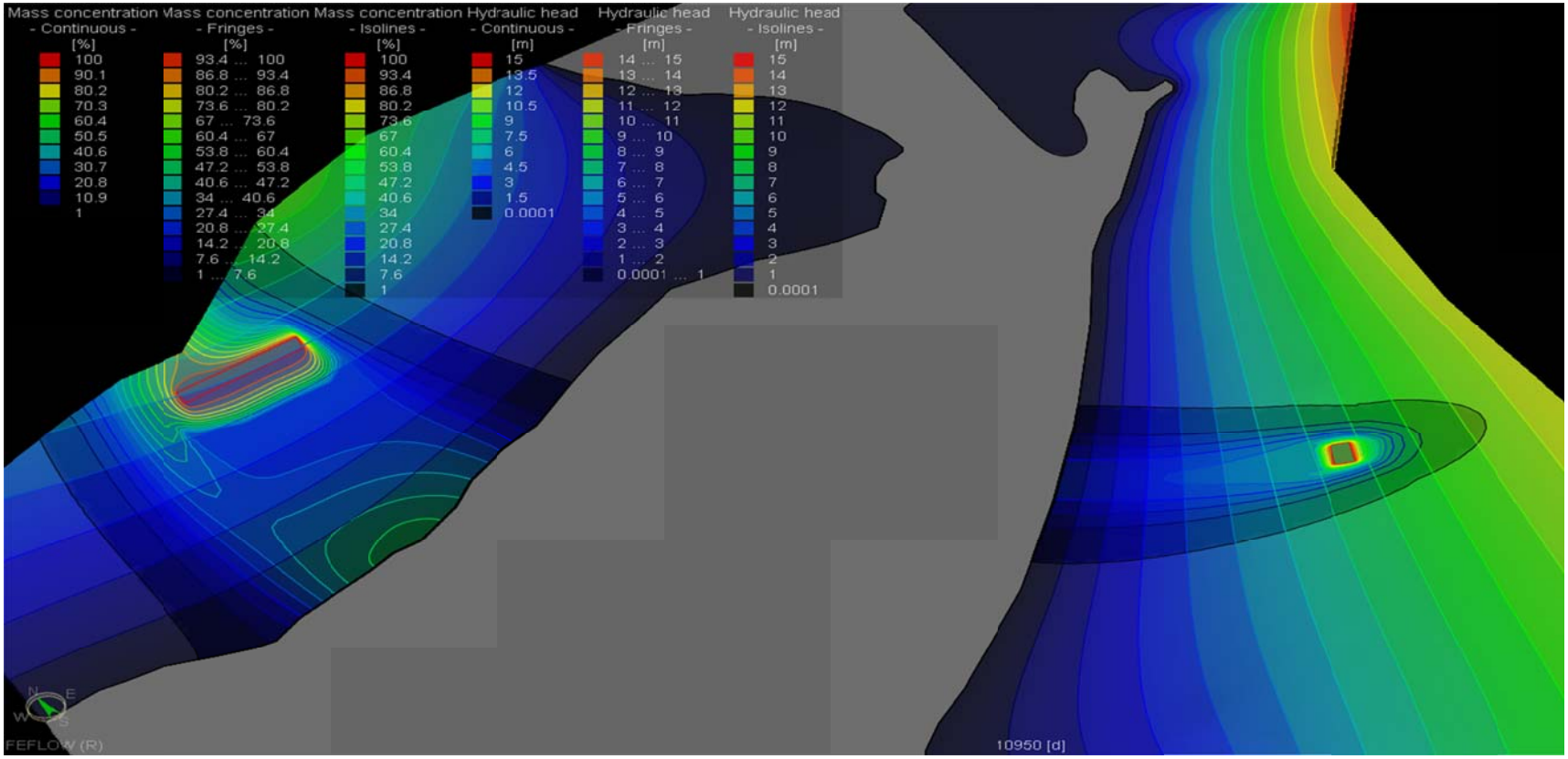

Figure 6-8: Clean up after 30 years, 100% of the mass concentration, the hydraulic head continuous ranging from 0 to 15 m and the hydraulic head isolines ranging from 0.0001 to 15 m and mass concentration fringes ranging from [1-7.6] to [93.4-100]

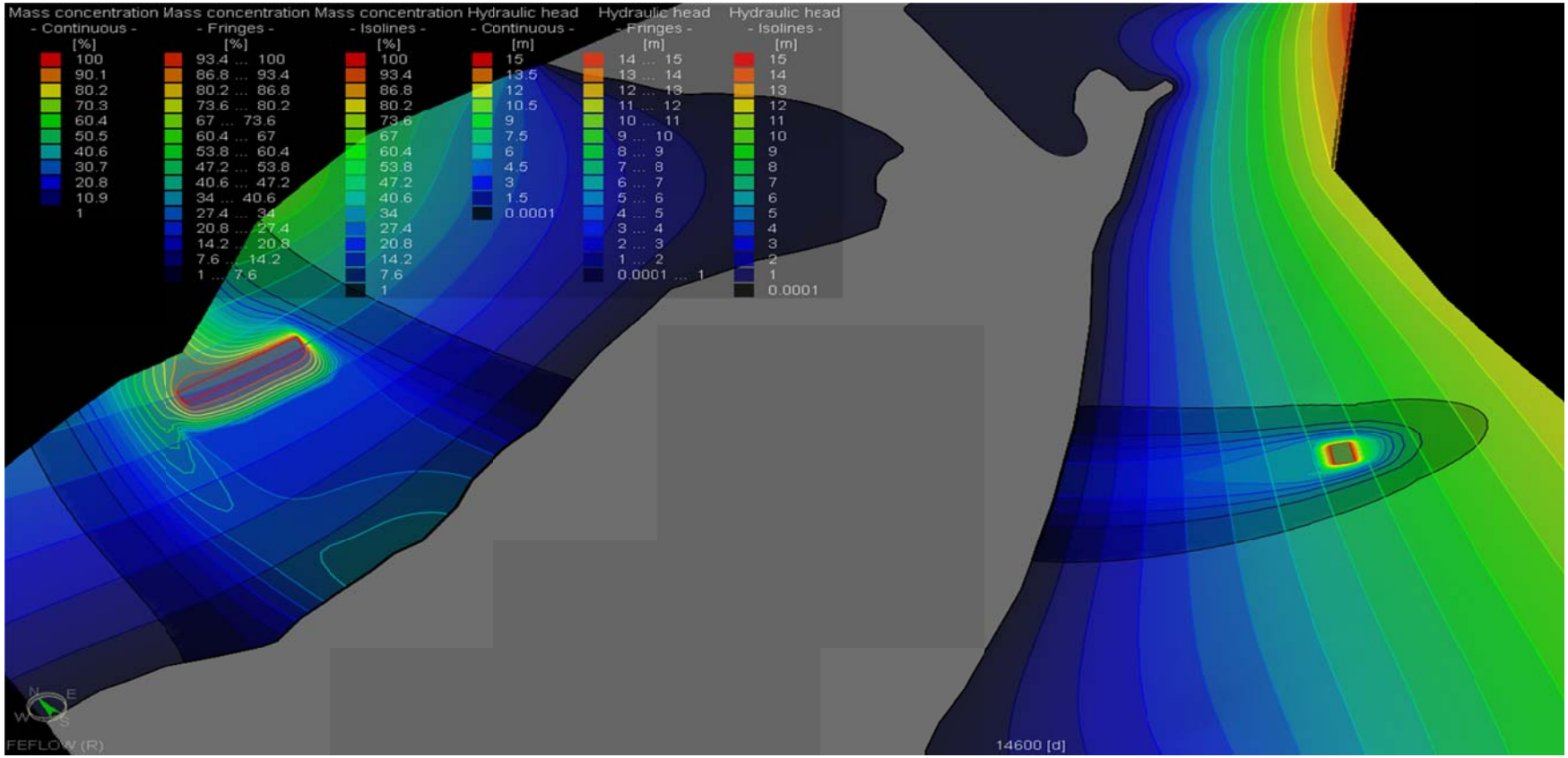

Figure 6-9: Clean up after 40 years, 100% of the mass concentration, the hydraulic head continuous ranging from 0 to 15 m and the hydraulic head isolines ranging from 0.0001 to 15 m and mass concentration fringes ranging from [1-7.6] to [93.4-100]

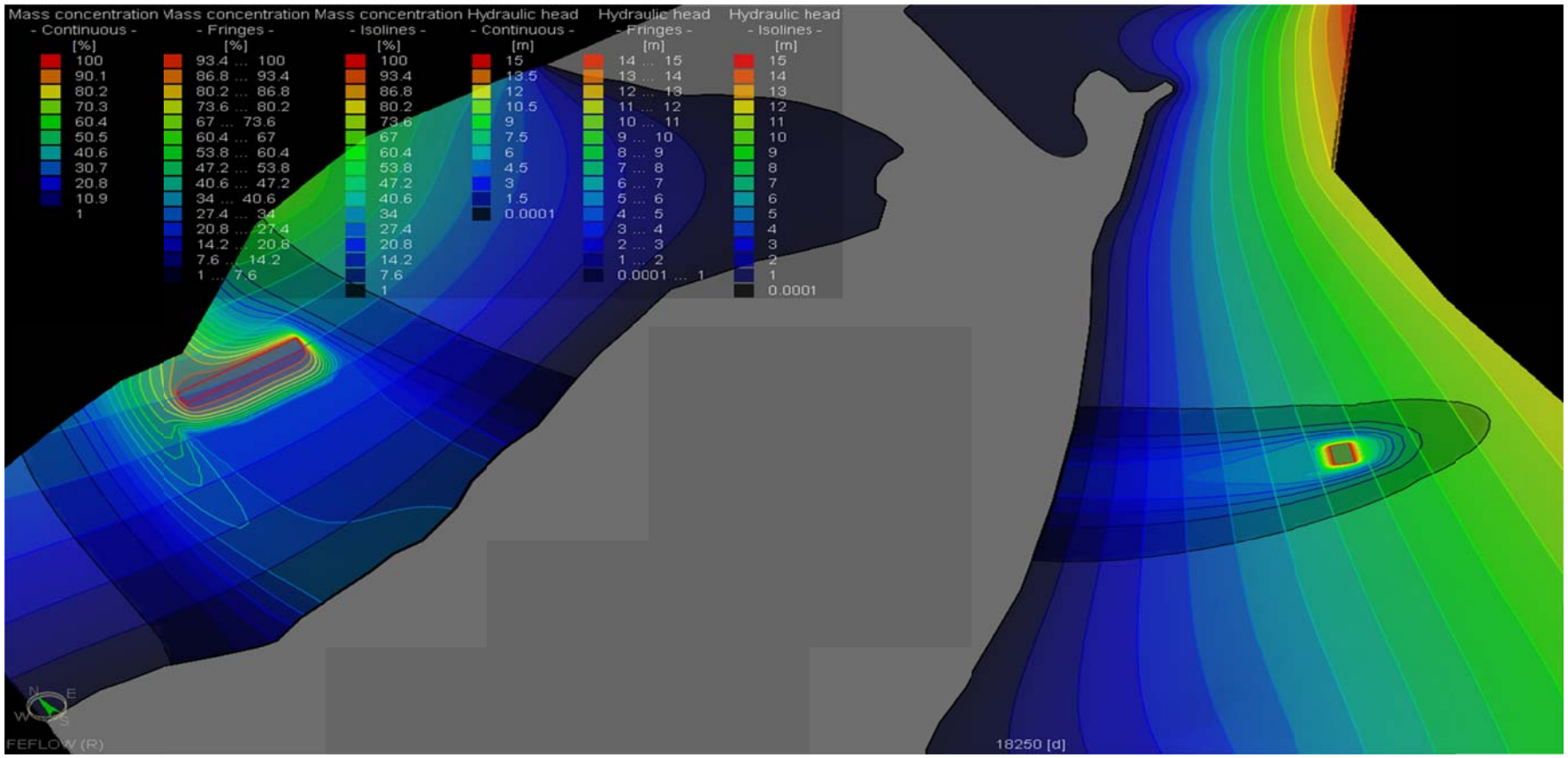

Figure 6-10: Clean up after 50 years, 100% of the mass concentration, the hydraulic head continuous ranging from 0 to 15 m and the hydraulic head isolines ranging from 0.0001 to 15 m and mass concentration fringes ranging from [1-7.6] to [93.4-100]

The above figure show that after a period of 30 years there will be no pollution after the barrier in the Eastern part and after a period of 50 years no pollution will be observed after the barrier in the western part. Note that if the barrier was placed accurately in the western part, after 30 years no pollution will be observed as in the case of Eastern part. Therefore care needs to be taken when placing the interceptor barrier.

6.3 REMARKS AND DISCUSSIONS

From the numerical our results via FEFLOW, one can see that, in many cases, contingency plans are required in the event that the PRB fails to meet performance criteria. Such plans may range from minor modifications of the PRB to use of an alternative technology. If the PRB fails to capture a portion of the plume, an extension to the PRB may be prescribed. If concentrations of contaminants exiting the PRB are higher than expected, then an additional wall may be required down gradient of the first wall see for example the barrier placed in Bonaberie. In some installations, monitored natural attenuation of contaminants down gradient of the wall is expected and designed into the system to help meet compliance goals. As with any groundwater remediation technology, adequate hydro-geological characterization must be done to understand flow patterns and the distribution of the contaminant plume, which was the main raison of the mass transport solution Figure 7-6. This is particularly important for PRBs as the treatment system is immovable or passive, yet it must intercept and capture the contaminant plume for effective treatment. Information to be obtained includes advective velocity parameters such as the gradient, the hydraulic conductivity, porosity, and other parameters collected as part of a hydro-geological characterization program. It is also important to understand temporal changes in flow direction and flux due to processes such as recharge, pumping of adjacent wells or other disturbances. Observed changes in flow direction at the Douala City site, for example, have ranged as high as 15 degrees from time to time.

In addition to the hydrology, the stratigraphic and lithology of the site is important to understand and will dictate effective PRB design. If a low permeability layer exists at the site, the PRB can be keyed into this layer. If it does not exist, then a hanging wall design must be chosen which may add to the uncertainty of plume capture. If the site has low permeability layers through which the PRB must be constructed, care must be taken during construction to avoid smearing of such layers. This could impact hydraulic contact between the formation and the reactive media. A thorough understanding of site stratigraphic is especially important or helpful in choosing a particular construction method. Use of sheet

piling to construct a reactive gate may not be a good choice where low permeability layers exist because of the smearing potential and increased difficulty in re-establishing good hydraulic contact between aquifer sediments and the reactive zone.

Characterization of contaminant concentrations in four dimensions is required for successful implementation of a PRB. In addition to knowledge of the plume in the three-dimensional space, it is also imperative to understand variability in plume shape and direction over time. Plumes deviate in direction and location over time and may change shape due to attenuation, degradation, mixing with other plumes, dilution, recharge, and other natural and anthropogenic-induced disturbances.

PRBs are often located within plumes. This requires some understanding of the impact of construction on plume behaviour, both up gradient and down gradient of the barrier. For example, it is essential to verify that hydraulic contact between the plume and reactive media is established. If a PRB is located below an impermeable surface structure such as a parking lot, will the surface be repaved immediately or will recharge be allowed to occur over the PRB? Some understanding of natural attenuation processes at the site is important in being able to interpret the subsequent response of the natural system to the presence of the PRB. This is most often manifested in trying to estimate how long the down gradient aquifer will require to achieve cleanup goals. A key question to address is the length of time required before contaminants located down gradient of the barrier flush out of the sediments or degrade naturally.

Chapter 7

SENSITIVITY AND UNCERTAINTY ANALYSIS

In more general terms uncertainty and sensitivity analysis investigate the robustness of a study when the study includes some form of statistical modelling. Sensitivity analysis can be useful to computer modellers for a range of purposes, including:

- Support decision making or the development of recommendations for decision makers (e.g. testing the robustness of a result);
- Enhancing communication from modellers to decision makers (e.g. by making recommendations more credible, understandable, compelling or persuasive);
- Increased understanding or quantification of the system (e.g. understanding relationships between input and output variables); and Model development (e.g. searching for errors in the model)

In the following sections sensibilities and uncertainties we are discussed.

7.1 SENSITIVITY ANALYSIS

The aim of sensitivity analysis is to estimate the rate of change in the output of a model with respect to change in model inputs. Such knowledge is important for (a) evaluating the applicability of the model, (b) determining parameters for which it is important to have more accurate values, and (c) understanding the behaviour of the system being modelled. The choice of a sensitivity analysis method depends to a great extent on (a) the sensitivity measure employed, (b) the desired accuracy in the estimates of the sensitivity measure, and (c) the computational cost involved.

In general, the meaning of the term “sensitivity analysis” depends greatly on the sensitivity measure that is used. Based on the choice of sensitivity metric and the variation in the model parameters, sensitivity analysis methods can be broadly classified into the following categories: Variation of parameters or model formulation: In this approach, the model is run at a set of sample points (different combinations of parameters of concern) or with straightforward changes in model structure (e.g., in model resolution).

Sensitivity measures that are appropriate for this type of analysis include the response from arbitrary parameter variation, normalized response and extrema. Of these measures, the

extreme values are often of critical importance in environmental applications.

Domain-wide sensitivity analysis: Here, the sensitivity involves the study of the system behaviour over the entire range of parameter variation, often taking the uncertainty in the parameter estimates into account.

Local sensitivity analysis: Here, the focus is on estimates of model sensitivity to input and parameter variation in the vicinity of a sample point. This sensitivity is often characterized through gradients or partial derivatives at the sample point. In the following paragraph, local sensitivity analysis will be used in the case of our work.

7.1.1 Linear (first-order) sensitivity coefficients

The analytical solution of the advection dispersion equation subject to the prescribed initial and boundaries conditions described in chapter 5 was given as:

$$c(x,t) = \frac{c_1 \exp[-\gamma t]}{2}\left\{exp\left(x\frac{q_r - u_r}{2D_r}\right)erfc\left(\frac{x-u_r t}{2\sqrt{D_r t}}\right) + exp\left(x\frac{q_r + u_r}{2D_r}\right)erfc\left(\frac{x+u_r t}{2\sqrt{D_r t}}\right)\right\}$$
$$- \frac{c_0 \exp(-\lambda t)}{2}\left\{erfc\left(\frac{x-q_r t}{2\sqrt{D_r t}}\right) + exp\left(x\frac{q_r}{D_r}\right)erfc\left(\frac{x+q_r t}{2\sqrt{D_r t}}\right)\right\} + c_0 \exp(-\lambda t).$$

From this solution one can see that the concentration is a function of the parameters γ, $q_r, u_r, D_r$and λ, thus we can write the concentration as follows

$$c = c(q_r, u_r, D_r, \gamma, \lambda, x, t) \tag{7.1a}$$

Note that because u_r is not an independent parameter and should thus be excluded from the sensitivity analysis. Therefore, the concentration depends on the following physical parameters and the independent variables x and . Then, Equation (7.1a) can be reproduced as:

$$c = c(\alpha, \gamma, \lambda, \theta, \rho, K, q_r, x, t) \tag{7.1b}$$

A common assumption in uncertainty analyses is that the independent variables are perfectly known and therefore excluded from such analyses. The same applies to λ as it denotes the rate at which a given chemical reaction proceed and is usually well-known or can be determined quite accurately in the laboratory.

Let $(\alpha_i, i = 1 \ldots 5)$ be the set of all parameters involve in Equation (7. 1) then we have that c can be written as

$$c = c(\alpha_i, x, t) \tag{7.2}$$

Consider the first-order sensitivity coefficients defined as

$$c_{\alpha_i}(x,t) = \frac{\partial c(\alpha,x,t)}{\partial \alpha_i},\ i = 1,2..5 \tag{7.3}$$

It is a straightforward matter to differentiate Equation (7.1) respect to each parameter. Hence we begin with, (7.4)

$$c_{\alpha_1} = c_{q_r} = -\frac{1}{2}c_0\, exp[-t\,\lambda]\left[\frac{exp\left[-\frac{(-q_r t+x)^2}{4D_r t}\right]t}{\sqrt{\pi D_r t}} - \frac{exp\left[\frac{q_r x}{D_r} - \frac{(-q_r t+x)^2}{4D_r t}\right]t}{\sqrt{\pi D_r t}} + \frac{exp\left[\frac{q_r x}{D_r}\right] xErfc\left[\frac{q_r t+x}{2\sqrt{D_r t}}\right]}{D_r}\right] + \frac{1}{2}c_1 exp[-\gamma\, t]\left[\frac{exp[x]xErfc\left[\frac{-u_r t+x}{2\sqrt{D_r t}}\right]}{2D_r} + \frac{exp[x]xErfc\left[\frac{u_r t+x}{2\sqrt{D_r t}}\right]}{2D_r}\right]$$

The normalized solution of the above equation is illustrated graphically in the below figure for different values of q_r.

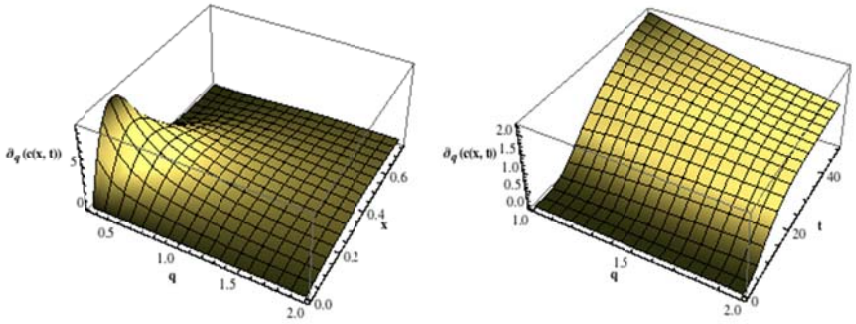

Figure 7-1: Variation of the concentration as function of seepage velocity

It is worth noting from the graphs that,$c_{\alpha_1}(x,t)$ is a positive function for all values of the retarded velocity vectorq_r. Thus the concentration is an increasing function of the retarded velocity vector q_r, in time and space.

We follow here with, (7.5)

$$c_{\alpha_2} = c_{u_r} = \frac{1}{2}c_1 exp[-t\lambda]t\left[\frac{exp\left[-\frac{(-q_r t+x)^2}{4D_r t}\right]t}{\sqrt{\pi D_r t}} - \frac{exp\left[\frac{q_r x}{D_r} - \frac{(-q_r t+x)^2}{4D_r t}\right]}{\sqrt{\pi D_r t}} + \frac{exp\left[\frac{q_r x}{D_r}\right] xErfc\left[\frac{q_r t+x}{2\sqrt{D_r t}}\right]}{D_r}\right].$$

The normalized solution of the above equation is illustrated graphically in the below figure

for different values of γ

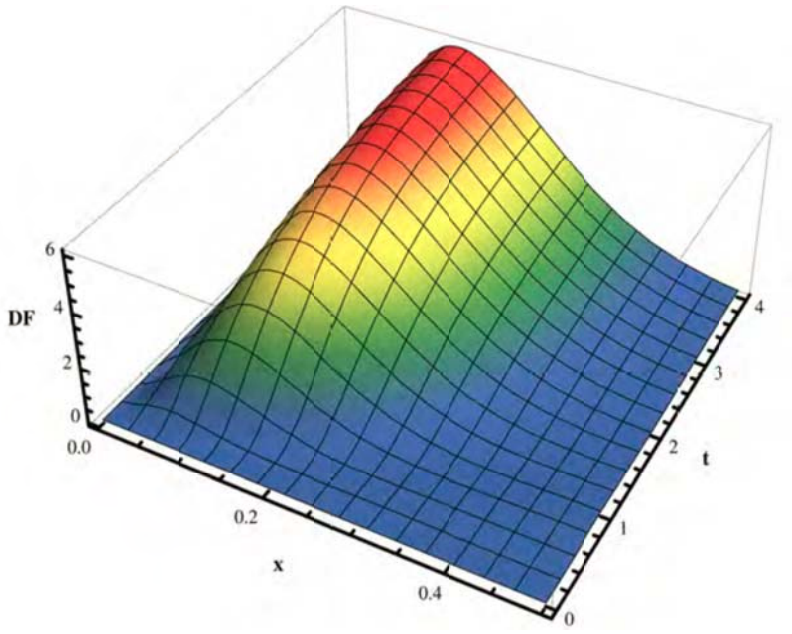

Figure 7-2: Variation of the concentration as function of the parameter$\boldsymbol{\gamma}$

It is worth noting from the graphs that, $c_{\alpha_2}(x,t)$ is a positive function for all values of the retarded velocity vectorq_r. Thus the concentration is an increasing function of the retarded velocity vector γin time and space.

For the next parameters, in the concentration, we have (7.6)

$$c_{\alpha_3} = c_{D_r} = -\frac{1}{2}c_0 exp[-t\lambda]\left[-\frac{exp\left[-\frac{(-q_r t+x)^2}{4D_r t}\right]t^2}{2\sqrt{\pi}(D_r t)^{3/2}} + \frac{exp\left[\frac{q_r x}{D_r} - \frac{(-q_r t+x)^2}{4D_r t}\right]t^2}{2\sqrt{\pi}(D_r t)^{3/2}}\right.$$
$$+\frac{exp\left[-\frac{(-q_r t+x)^2}{4D_r t}\right](-q_r t+x)^2}{4\sqrt{t\pi}(D_r)^{3/2}} + \frac{exp\left[\frac{q_r x}{D_r} - \frac{(-q_r t+x)^2}{4D_r t}\right]tx(q_r t+x)}{2D_r\sqrt{\pi}(D_r t)^{3/2}}$$
$$-\frac{exp\left[\frac{q_r x}{D_r} - \frac{(-q_r t+x)^2}{4D_r t}\right]t\left[\frac{q_r x}{{D_r}^2} - \frac{(-q_r t+x)^2}{4{D_r}^2 t}\right]}{2\sqrt{\pi D_r t}} - \frac{exp\left(\frac{q_r x}{D_r}\right)xErfc\left[\frac{q_r t+x}{2\sqrt{D_r t}}\right]}{D_r^2}$$
$$\left.-\frac{exp\left(\frac{q_r x}{D_r}\right)x^2 Erfc\left[\frac{q_r t+x}{2\sqrt{D_r t}}\right]}{D_r^3}\right]$$

$$+\frac{1}{2}c_1 exp[-t\gamma]\left[\frac{exp\left[-\frac{(-q_r t+x)^2}{4D_r t}\right]\exp[tx](-u_r t+x)}{4D_r\sqrt{\pi}(D_r t)^{3/2}}\right.$$
$$+\frac{exp\left[-\frac{(-q_r t+x)^2}{4D_r t}\right]\exp[tx](u_r t+x)}{4D_r\sqrt{\pi}(D_r t)^{3/2}}-\frac{exp\left(\frac{q_r x}{D_r}\right)xErfc\left[\frac{-u_r t+x}{2\sqrt{D_r t}}\right]}{D_r^2}$$
$$\left.-\frac{exp\left(\frac{q_r x}{D_r}\right)xErfc\left[\frac{u_r t+x}{2\sqrt{D_r t}}\right]}{D_r^2}\right]$$

We further have, (7.7)

$$\partial_{\alpha_4}c=c_\gamma=\frac{1}{2}c_1 exp[-t\,\gamma]\left[-\frac{exp\left[-\frac{(x-tu_r)^2}{4D_r t}\right]exp[tx]}{\sqrt{\pi u_r D_r t}}+\frac{exp\left[-\frac{(x+tu_r)^2}{4D_r t}\right]exp[tx]}{\sqrt{\pi u_r D_r t}}\right]$$
$$-\frac{1}{2}c_1 exp[-t\gamma]\left[\frac{exp[x]Erfc\left[\frac{x-tu_r}{2\sqrt{D_r t}}\right]}{2D_r}+\frac{exp[x]Erfc\left[\frac{x+tu_r}{2\sqrt{D_r t}}\right]}{2D_r}\right].$$

The normalized solution of the above equation is illustrated graphically in the below figure for different values of γ.

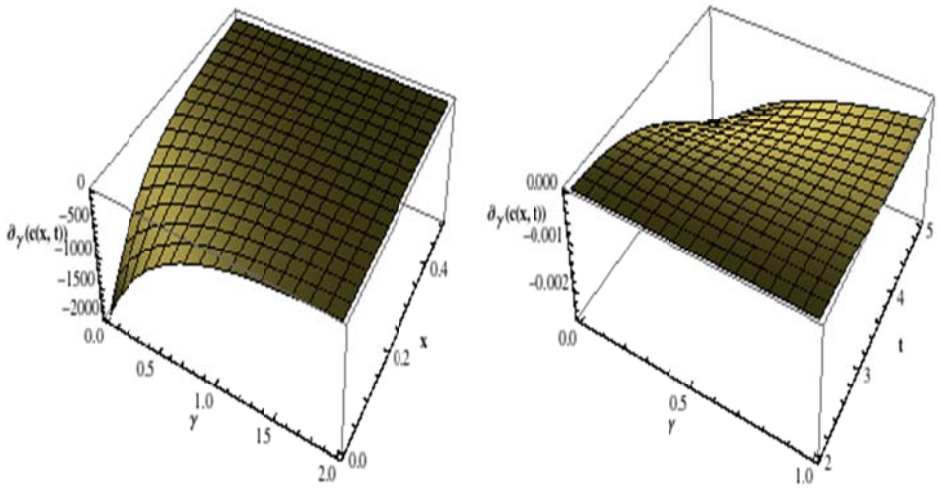

Figure 7-3: Variation of the concentration as function of the parameter $\boldsymbol{\gamma \geq 0}$

The above figure shows that for $\gamma \geq 0$, $\partial_{\alpha_4}c(x,t)$ is a negative function implying, the function $c = c(x,t,D_r)$ is decreasing in time and space respect to γ.

Finally, we have for the last parameter (7.8)

$$c_{\alpha_5} = c_\lambda = \frac{1}{2}c_1 exp[-t\gamma]\left[\frac{exp\left[-\frac{(x-u_r t)^2}{4D_r t}\right]exp[t\ x]}{\sqrt{\pi D_r t}u_r} - \frac{exp\left[-\frac{(x+u_r t)^2}{4D_r t}\right]exp[t\ x]}{\sqrt{\pi D_r t}u_r}\right] + \frac{1}{2}c_0 exp[-\lambda\ t]t\left[\frac{exp\left[-\frac{(x-q_r t)^2}{4D_r t}\right]t}{\sqrt{\pi D_r t}} - \frac{exp\left[\frac{q_r x}{D_r} - \frac{(x+u_r t)^2}{4D_r t}\right]}{\sqrt{\pi D_r t}} + \frac{exp\left[\frac{q_r x}{D_r}\right]xErfc\left[\frac{q_r t+x}{2\sqrt{D_r t}}\right]}{D_r}\right].$$

The normalized solution of the above equation is illustrated graphically in the below figure for different values of λ.

If one consider, $R = \theta + \rho\ K$ (retardation factor), we obtain the following sign of the partial derivative.

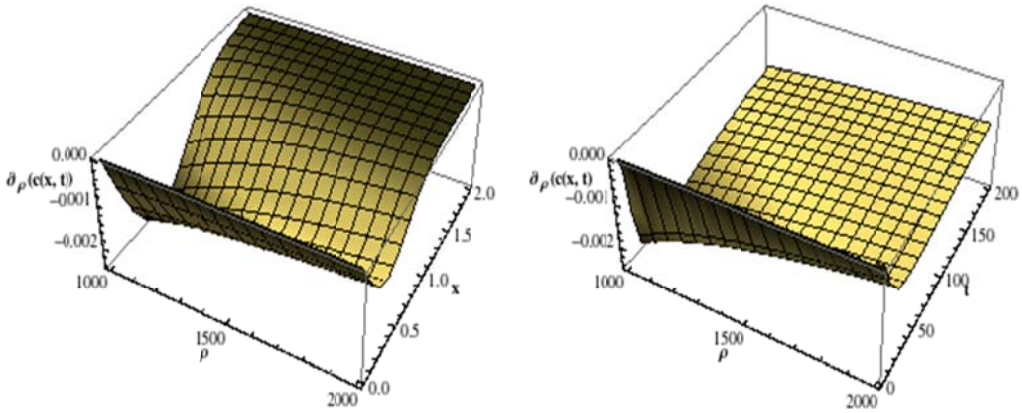

Figure 7-4: Derivative of the concentration as function of $\boldsymbol{\rho}$

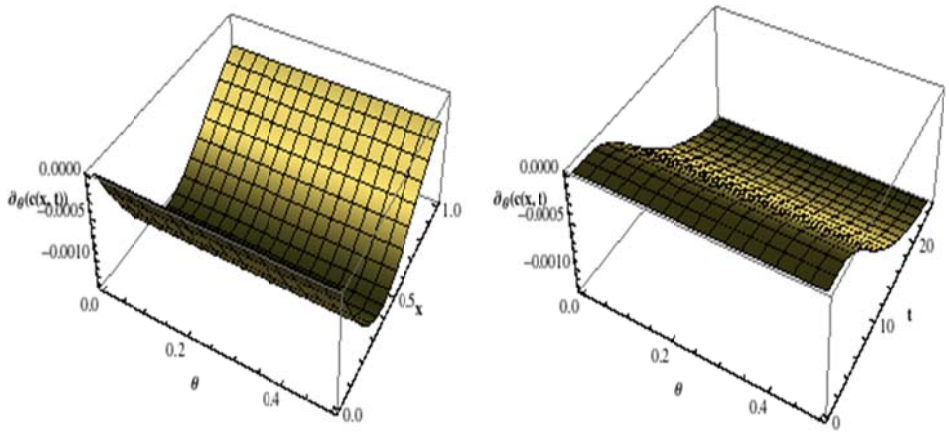

Figure 7-5: Derivative of the concentration as function of $\boldsymbol{\theta}$

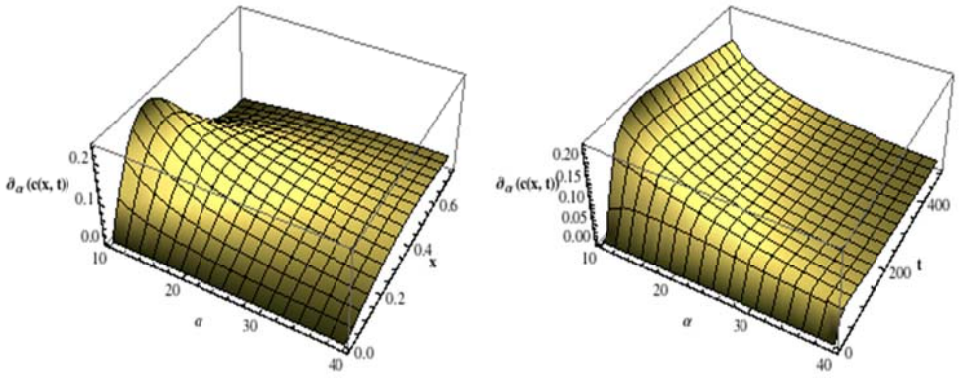

Figure 7-6: Derivative of the concentration as function of $\boldsymbol{\alpha}$

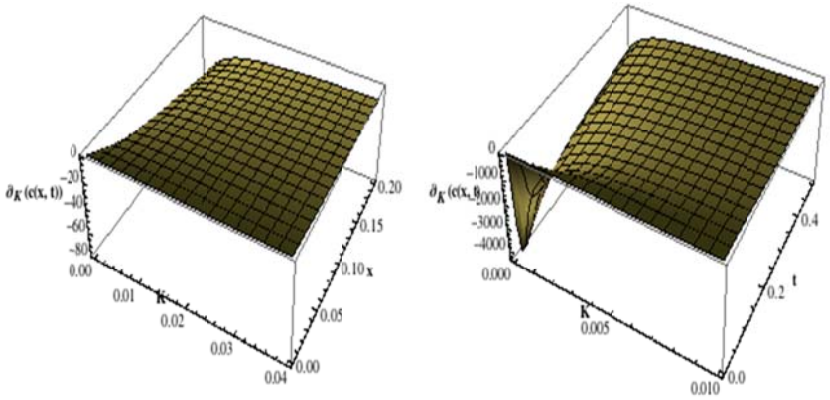

Figure 7-7: Derivative of the concentration as function of $\boldsymbol{K}$

One can conclude from the above investigation that for the first order coefficient sensitivity, the value of the retarded hydrodynamic dispersion coefficient must be measured very accurately because the investigation shows that the concentration of pollution in space time is more sensitive to the value of the retarded hydrodynamic dispersion coefficient than other parameters involved in the solution.

7.1.2 Linear (Second-order) sensitivity coefficient

We will probably remember that with a function of one variable we looked at the second derivative to establish whether a point was a maximum or a minimum or a point of inflection. For functions of two variables, it's a little more complicated, because we don't just have one second derivative any more, in fact we have three. For a function f(x, y), we can differentiate twice with respect to x to find this second derivative: f_{xx}. Or we could differentiate twice with respect to y to get this second derivative: f_{yy}. Or we could differentiate once with respect to x and then once with respect to y (or the other way round

- it gives the same answer) to get this second derivative: f_{xy} So how can we use all those second derivatives to decide the nature of a point? This is the rule: If $f_{xx}f_{yy}$-f_{xy}^2 is negative, then the point is neither a max nor a min, it is a saddle point. If $f_{xx}f_{yy}$-f_{xy}^2 is positive, and f_{xx} and f_{yy} are both negative, the point is a maximum. If $f_{xx}f_{yy}$-f_{xy}^2 is positive, and f_{xx} and f_{yy} are both positive, the point is a minimum. So let's try out those rules on a function under investigation, that is $c(\alpha_{i,}\alpha_j), (i,j) \in \{1, \dots \dots ,5\} \times \{1, \dots \dots ,5\}$. Hence the sign of $f_{xx}f_{yy}$-f_{xy}^2 will be given for a few values of $(\alpha_{i,}\alpha_j)$ and for all $x, t > 0$. We start this investigation by given some second order partial derivatives as follows. (7.9)

$$\partial_{q_r}^2 c = -\frac{1}{2}c_0 exp[-\lambda t]\left(-\frac{exp\left[\frac{q_r x}{D_r} - \frac{(q_r t+x)^2}{4D_r t}\right] tx}{D_r\sqrt{\pi D_r t}} + \frac{exp\left[-\frac{(q_r t+x)^2}{4D_r t}\right] t(-q_r t + x)}{2D_r\sqrt{\pi D_r t}} - \frac{exp\left[\frac{q_r x}{D_r} - \frac{(q_r t+x)^2}{4D_r t}\right] t\left(\frac{-q_r t}{D_r} + \frac{x}{2D_r}\right)}{\sqrt{\pi D_r t}} + \frac{exp\left[\frac{q_r x}{D_r}\right] x^2 Erf\left[\frac{q_r t+x}{2\sqrt{D_r t}}\right]}{D_r^2}\right).$$

The sign of this derivative will not be investigated. But one can still go in detail in this study by given the sign of this second order derivative which can be used to determine in which interval one will have the maximum or minimum for a given set of $(\alpha_{i,}\alpha_j)$.

We follow here with: (7.10)

$$\partial_{q_r,\alpha}^2 c = -\frac{1}{2}c_0 exp[-\lambda\, t]\left[-\frac{exp\left[-\frac{(x-tq_r)^2}{4D_r t}\right] t^2}{2\sqrt{\pi}(D_r t)^{3/2}} + \frac{exp\left[\frac{q_r x}{D_r} - \frac{(x-tq_r)^2}{4D_r t}\right] t^2}{2\sqrt{\pi}(D_r t)^{3/2}} + \frac{exp\left[-\frac{(x-tq_r)^2}{4D_r t}\right](tq_r + x)^2}{4D_r^2\sqrt{\pi D_r t}} + \frac{exp\left[\frac{q_r x}{D_r} - \frac{(x-tq_r)^2}{4D_r t}\right] tx(q_r t + x)}{2\sqrt{\pi}(D_r t)^{3/2}} - \frac{exp\left[\frac{q_r x}{D_r} - \frac{(x-tq_r)^2}{4D_r t}\right] t\left(\frac{q_r x}{{D_r}^2} - \frac{(x-tq_r)^2}{4{D_r}^2 t}\right)}{\sqrt{\pi D_r t}} - \frac{exp\left[\frac{q_r x}{D_r}\right] xErfc\left[\frac{q_r t+x}{2\sqrt{D_r t}}\right]}{D_r^2} - \frac{exp\left[\frac{q_r x}{D_r}\right] x^2 q_r Erfc\left[\frac{q_r t+x}{2\sqrt{D_r t}}\right]}{D_r^3}\right]$$

$$+\frac{1}{2}c_1 exp[-t\,\gamma]\left[\frac{exp\left[-\frac{(x-tq_r)^2}{4D_r t}\right] Exp[t\,x](-tu_r + x)}{4D_r\sqrt{\pi}(D_r t)^{3/2}} + \frac{exp\left[-\frac{(x+tu_r)^2}{4D_r t}\right] Exp[t\,x](tu_r + x)}{4D_r\sqrt{\pi}(D_r t)^{3/2}} - \frac{exp[x]Erfc\left[\frac{-tu_r+x}{2\sqrt{D_r t}}\right]}{2D_r^2} - \frac{exp[x]Erfc\left[\frac{tu_r+x}{2\sqrt{D_r t}}\right]}{2D_r^2}\right]$$

Note that $c_{D_{r,}D_r}$was calculated but due to the length of the expression we decided to save

page by leaving that expression out, but it will we be used in this work.

Let $f_{\alpha,q_r}(x,t) = c_{\alpha,\alpha}(x,t)c_{q_r,q_r}(x,t) - (c_{\alpha,q_r}(x,t)).^2$

Note that several figures were obtained for different values of (α, q_r), but not mention here. From the above three figures we can see that $f_{D_r,q_r}(x,t) < 0$, then according to the rule, we conclude that the set of $(D_r, q_r) > (0,0)$ are saddle points.

We follow here with: (7.11)

$$\partial_{\lambda,\lambda}c = c_0 exp[-t\lambda]t^2 - \frac{1}{2}c_0 exp[-t\lambda]t^2\left[Erfc\left[\frac{-q_r t + x}{2\sqrt{D_r t}}\right] + exp\left[\frac{q_r x}{D_r}\right]Erfc\left[\frac{q_r t + x}{2\sqrt{D_r t}}\right]\right].$$

and

$$\partial_{\lambda,D_r}c = \frac{1}{2}c_0 exp[-\lambda\, t]t\left[\frac{exp\left[-\frac{(-tq_r+x)^2}{4D_r t}\right]t(-tq_r + x)}{2\sqrt{\pi}(D_r t)^{3/2}} + \frac{exp\left[\frac{q_r x}{D_r} - \frac{(tq_r+x)^2}{4D_r t}\right]t(tq_r + x)}{2\sqrt{\pi}(D_r t)^{3/2}} - \frac{exp\left[\frac{q_r x}{D_r}\right]q_r x Erfc\left[\frac{q_r t+x}{2\sqrt{D_r t}}\right]}{D_r^2}\right]$$

Let $f_{\alpha,\lambda}(x,t) = c_{\alpha,\alpha}(x,t)c_{\lambda,\lambda}(x,t) - (c_{\alpha,\lambda}(x,t))^2$

The normalized solution of the above equation is illustrated graphically in the below figure for different values of (α, λ).

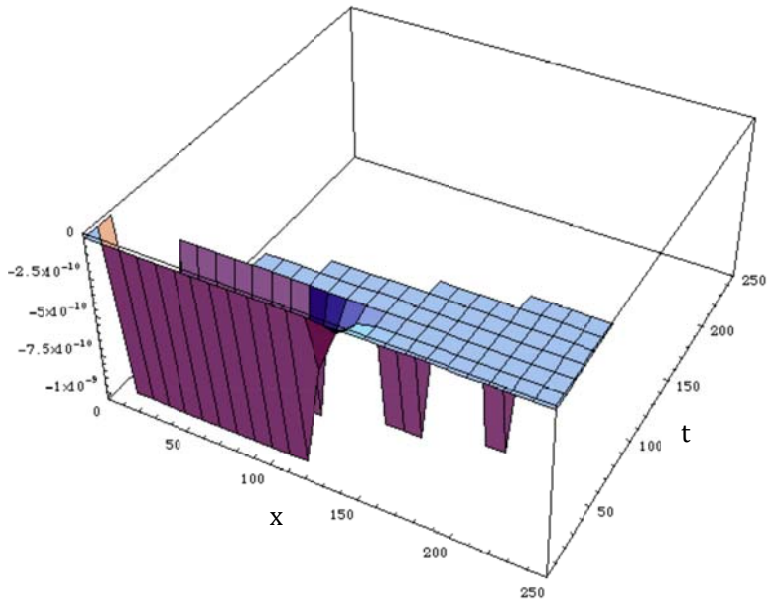

Figure 7-8: Second derivative of the concentration for $\boldsymbol{\alpha = 80,\ \lambda = 1}$

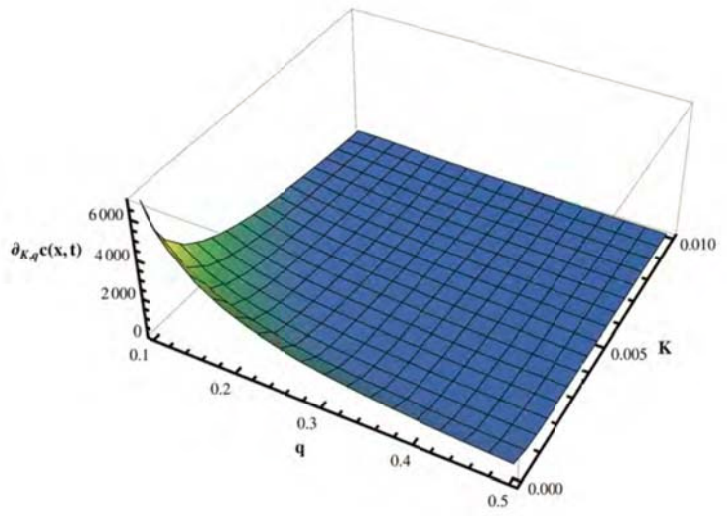

Figure 7-9: second partial derivative of the concentration for $\boldsymbol{\alpha = \frac{80}{1801}}$, $\boldsymbol{K = 0.4}$

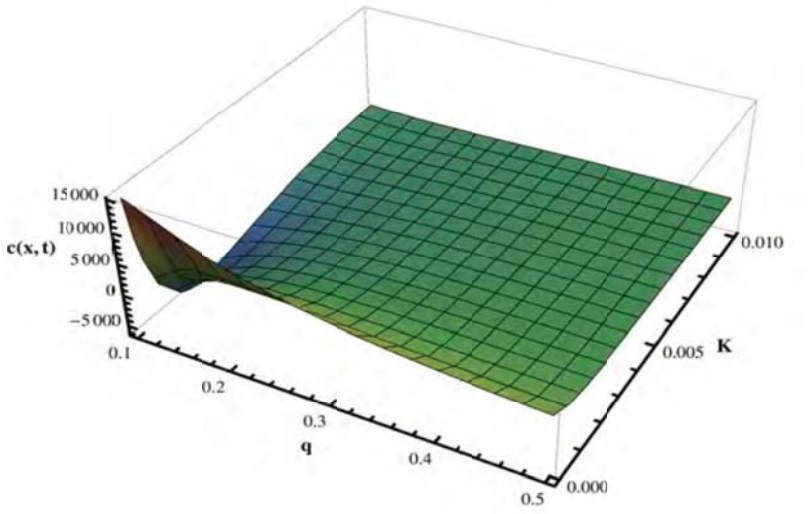

Figure 7-10: second partial derivative of the concentration for $\boldsymbol{\alpha = 1, K = 0.5}$

Note that several figures were obtained for different values of (α, λ), but the above three were chosen to illustrate the behavior of the function under investigation. From the above three figure one can see that there exists a set $S_0 = \{(\alpha, \lambda)\epsilon[0, \rightarrow) \times [0, 1]: f_{\alpha,\lambda}(x, t) > 0 \; for \; all \; t, x > 0\}$ of Maximum or minimum depending on whether $c_{\lambda,\lambda}$ and c_{D_r,D_r} are both negative, or are both positive. And there exists a set $S_1\{(\alpha, \lambda)\epsilon[0, \rightarrow) \times [0, 1]: f_{\alpha,\lambda}(x, t) < 0 \; for \; all \; t, x > 0\}$ of saddle points.

We follow with: (7.12)

$$\partial_{\gamma,\gamma}c = \frac{1}{2}c_1 exp[-t\,\gamma]t^2\left[\frac{exp[q_r-u_r]xErfc\left[\frac{-t\,u_r+x}{2\sqrt{D_r t}}\right]}{2D_r}+exp[q_r+u_r]xErfc\left[\frac{t\,u_r+x}{2\sqrt{D_r t}}\right]\right]$$

$$\partial_{\alpha,\gamma}c = -\frac{1}{2}c_1 exp[-t\,\gamma]t\left[\frac{exp\left[-\frac{(-tu_r+x)^2}{4D_r t}\right]exp[t](q_r-u_r)x(-tu_r+x)}{4D_r\sqrt{\pi}(D_r t)^{3/2}}\right.$$
$$+\frac{exp\left[-\frac{(tu_r+x)^2}{4D_r t}\right]exp[t](q_r+u_r)x(tu_r+x)}{4D_r\sqrt{\pi}(D_r t)^{3/2}}-\frac{exp[q_r-u_r]xErfc\left[\frac{-tu_r+x}{2\sqrt{D_r t}}\right]}{2D_r^2}$$
$$\left.-\frac{exp[q_r+u_r]xErfc\left[\frac{tu_r+x}{2\sqrt{D_r t}}\right]}{2D_r^2}\right].$$

Let $f_{\alpha,\gamma}(x,t) = c_{\alpha,\alpha}(x,t)c_{\gamma,\gamma}(x,t) - (c_{\alpha,\gamma}(x,t))^2$. The normalized solution of the above equation is illustrated graphically in the below figure for different values of (α,γ).

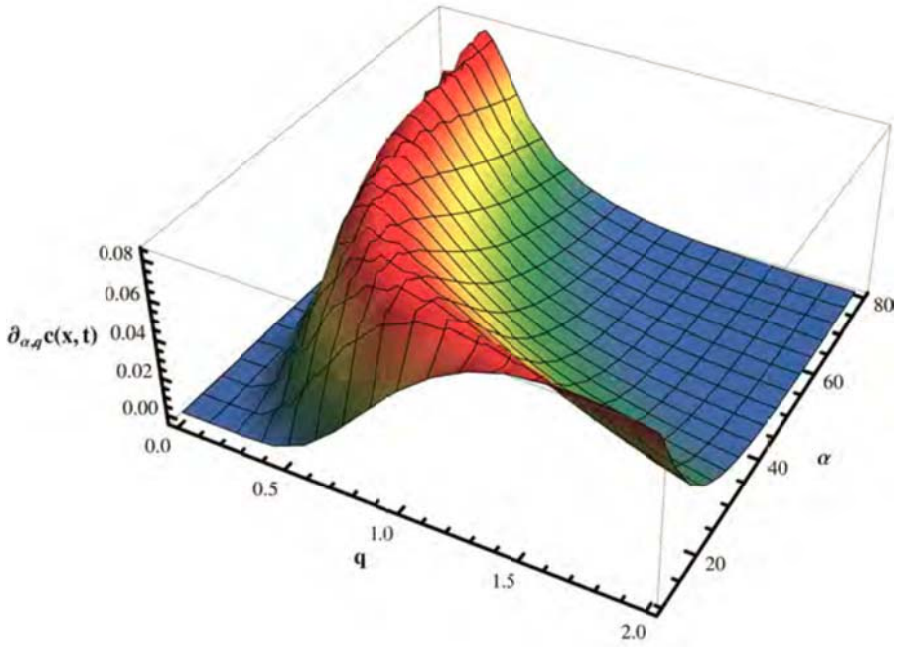

Figure 7-11: Second partial derivative of the concentration for ($\boldsymbol{\alpha}$, $\boldsymbol{\lambda}$)

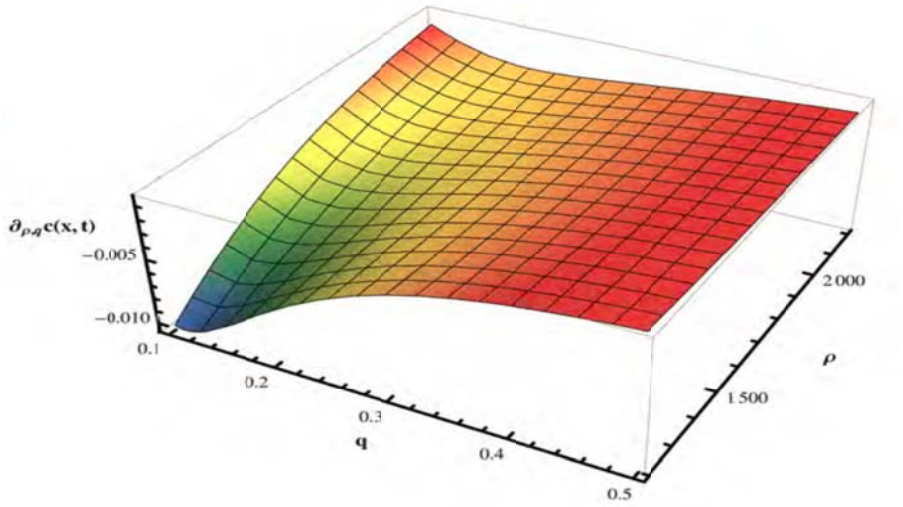

Figure 7-12: Second partial derivative of the concentration for ($\boldsymbol{\rho}$, $\boldsymbol{q}$)

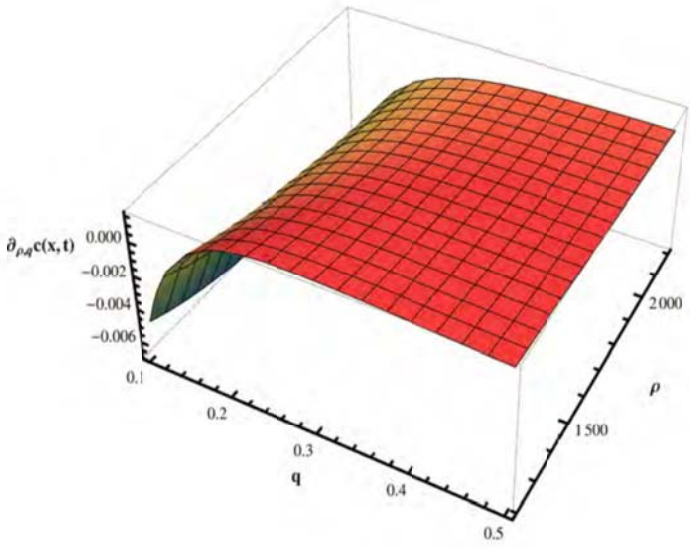

Figure 7-13: Second partial derivative of the concentration for ($\boldsymbol{\rho}$, $\boldsymbol{q}$).

Note that several figures were obtained for different values of (α, γ), but the above three were chosen to illustrate the behavior of the function under investigation. From the above three figure one can see that there exists a set $S_2 = \{(\alpha,\gamma)\epsilon[0,\rightarrow) \times [0,1]: f_{\alpha,\gamma}(x,t) > 0 \; for \; all \; t, x > 0\}$ of Maximum or minimum depending on whether $c_{\lambda,\lambda}$ and c_{D_r,D_r} are both negative, or are both positive. And there exists a set $S_3\{(\alpha,\gamma)\epsilon[0,\rightarrow) \times [0,1]: f_{\alpha,\gamma}(x,t) < 0 \; for \; all \; t, x > 0\}$ of saddle points.

We end here with: (7.13)

$$\partial_{u_r,u_r}c = \frac{1}{2}c_1 exp[-t\gamma]\left[-\frac{exp\left[-\frac{[-tu_r+x]^2}{4D_rt}\right]exp[tx]}{D_r\sqrt{\pi D_r t}} - \frac{exp\left[\frac{-[tu_r+x]^2}{4D_rt}\right]exp[tx]}{D_r\sqrt{\pi D_r t}} + \frac{exp\left[-\frac{[-tu_r+x]^2}{4D_rt}\right]exp(t)(q_r-u_r)x(x-tu_r)}{4D_r^2\sqrt{\pi t D_r}} + \frac{exp\left[\frac{[tu_r+x]^2}{4D_rt}\right]exp(t)(q_r+u_r)x(x+tu_r)}{4D_r^2\sqrt{\pi t D_r}}\right]$$

Let $f_{\alpha,\rho}(x,t) = c_{\alpha,\alpha}(x,t)c_{\rho,\rho}(x,t) - (c_{\alpha,\rho}(x,t))^2$. The normalized solution of the above equation is illustrated graphically in the below figure for different values of (α,ρ).

Note that several figures were obtained for different values of (α,ρ), but the above two were chosen to illustrate the behavior of the function under investigation. From the above two figures, one can observe that there exists a set $S_4 = \{(D_r,u_r)\epsilon[0,\rightarrow)\times[0,1]: f_{D_r,u_r}(x,t) > 0\ for\ all\ t,x>0\}$ of Maximum or minimum depending on whether c_{u_r,u_r} and c_{D_r,D_r} are both negative, or are both positive. And there exists a set $S_5\{(D_r,u_r)\epsilon[0,\rightarrow)\times[0,1]: f_{D_r,u_r}(x,t) < 0\ for\ all\ t,x>0\}$ of saddle points.

The above analysis show that all aquifer parameters are bounded, that is has a lower and upper bound. For practical purpose one will go to the field and measure the aquifer parameters for each parameter, one will possibly be able to determine the upper and the lower bound of these parameters. Knowing the upper and the lower bound of each parameter, the uncertainty analysis will be followed. In the next section, aleatory and epistemic uncertainties will be presented.

7.2 UNCERTAINTY ANALYSIS OF GROUNDWATER POLLUTION

We start this section by quoting (Feynman, 1956) "Any difference. But to get a law that is right, or at least one that keeps going through the successive sieves, that goes on for many more observations, requires a tremendous intelligence and imagination and a complete revamping of our philosophy, our understanding of space and time. I am referring to the relativity theory. It turns out that the tiny effects that turn up always require the most revolutionary modifications of ideas. Scientists, therefore, are used to dealing with doubt and uncertainty. All scientific knowledge is uncertain. This experience with doubt and uncertainty is important. I believe that it is of very great value, and one that extends beyond the sciences. I believe that to solve any problem that has never been solved before, you have

to leave the door to the unknown ajar. You have to permit the possibility that you do not have it exactly right. Otherwise, if you have made up your mind already, you might not solve it. Doubt is clearly a value in the sciences. Whether it is in other fields are an open question and an uncertain matter. I expect in the next lectures to discuss that very point and to try to demonstrate that it is important to doubt and that doubt is not a fearful thing, but a thing of very great value*".* Uncertainties can be classified into different categories:

1. Aleatory or statistical uncertainties are unknowns that differ each time we run the same experiment. Statistical uncertainties are therefore something an experimenter cannot do anything about: they exist, and they cannot be suppressed by more accurate measurements.
2. Epistemic or systematic uncertainties are due to things we could in principle know but don't in practice. This may be because we have not measured a quantity sufficiently accurately, or because our model neglects certain effects, or because particular data are deliberately hidden.

In real life applications, for instance in groundwater pollution, both kinds of uncertainties are often present. Uncertainty quantification intends to work toward reducing type 2 uncertainties to type 1. The quantification for the type 1 uncertainty is relatively straightforward to perform. Techniques such as Monte Carlo methods are frequently used. Pdf (Probability density function) can be represented by its moments (in the Gaussian case, the mean and covariance suffice), or more recently, by techniques such as Karhunen-Loève and polynomial chaos expansions. To evaluate type 2 and 3 uncertainties, the efforts are made to gain better knowledge of the system, process or mechanism. Methods such as fuzzy logic or evidence theory (Dempster–Shafer theory - generalization of Bayes theory) are used.

In this section uncertainty is carried out to investigate the predictive accuracy of the concentration models for describing the transport of improperly discarded hazardous waste through the environment that is the movement of water through the subsurface and surface waterway in the aquifer.

Uncertainty in groundwater hydrology originates from different sources. Neglecting uncertainty in groundwater problems can lead to incorrect results and misleading output, generally, there are various sources of uncertainty of the model outputs, such as the input uncertainty reflecting the lack of knowledge or accuracy of the model inputs, and the structural uncertainty related to the mathematical interpretation of the model (Bradford and Toride, 2007). From the uncertainty analysis, a probability distribution of model

outputs can be obtained, including the mean value, the variances and the quantiles (McKay *et al* 1999)(J.C. Helton, 1993) The uncertainties of the groundwater pollution model may come from the following sources:

1) Conceptual Model Uncertainties

a) Geological uncertainties

(i) The approximation of the geometry of the aquifer.

(ii) The heterogeneity or anisotropy of sediments or bedrock within the aquifer.

b) Physico-chemical Uncertainties

(iii) Lack of understanding physical mechanisms responsible for the mass flux.

(iv) The contaminant transport mechanisms and chemical reactions.

(v) The approximation of particle velocity by the average pore water velocity; it has been observed that the particles of different sizes may travel faster or slower that the carrying fluid in porous media (R.L. Iman and J.C. Helton, 1988).

(vi) Estimation of dispersion coefficients by fitting to experiments; for highly heterogeneous porous media the observed breakthrough curves are more dispersed and contain more scattered points(R.L. Iman and J.C. Helton. 1985).

(vii) The approximation of the density in most general the equation describing the density as being a constant.

2) Mathematical Model Uncertainties

(viii) Derivation of the mathematical model from the conceptual model. The approximation made in the most general equation for the description of density–dependent mass transport in a consolidating porous medium which consist of discarding the terms containing the matrix velocity.

(ix) The assumption made in finding the analytical of the hydrodynamic dispersion equation including, there is no discharge from or recharge to the aquifer, the Darcy velocity, and dispersion tensor are constant, and the matrix of dissolved can be represented by the Freundlish isotherm.

(x) The boundaries conditions to the problem frame.

(xi) The domain V spanned by x and its boundary $\neq$V is not known

(xii) The relational parameters, such as $S_0(x, t)$ and $K(x, t)$ is not well known at all points x in V and any time t for which the differential equation has to be solved.

(xiii) Any forcing functions that appear in the differential equation describing the hydrodynamic dispersion equation are well known

(xiv) Boundary conditions, appropriate values of the dependent variable, are not known at all points along ≠V and again at any time t for which differential equation has to be solved.

(xv) Initial conditions, appropriate values of dependent variable are not usually well known across V for a suitable time, $t_0 = 0$ say.

3) Parameters Model Uncertainties

Parameter uncertainty can be defined as uncertainty that arises in selecting values for parameters in the various models. There are many parameters in this assessment that are uncertain. First, there are insufficient data about the site climatic, geological and hydrological conditions. As a result, such parameters as sorption coefficients, moisture content, river flow rate, river depth and width, hydraulic gradient in the aquifer and erosion rate are taken from the general literature. Some parameters used need to be specified more accurately, e.g. evaporation or distance between the disposal facility and the river, and between the disposal facility and residences. On the other hand, the sensitivity analysis aims at quantifying the individual contribution from each parameter's uncertainty to the uncertainty of outputs. Correlations between parameters may also be inferred from sensitivity analysis. It is a frequent routine and recommended to perform the uncertainty and sensitivity analysis in tandem (Bradford *et al*, 2004) (Sin *et al*.,2009a) (Sin *et al*., 2009b) and (Helton, 1997).

Several approaches have been developed to cope with uncertainty including; Data uncertainty engine (DUE);Error propagation equations; Expert elicitation; Extended peer review (review by stakeholders); Inverse modelling (parameter estimation);Inverse modelling (predictive uncertainty); Monte Carlo analysis; Multiple model simulation; NUSAP; Quality assurance, Scenario analysis; Sensitivity analysis; Stakeholder involvement and Uncertainty matrix.

The most widely used methods in uncertainty analysis are Monte Carlo simulation (MCS) and Latin hypercube sampling (LHS), developed from MCS. Despite the simplicity of MCS, many runs are required to achieve a reliable result. In this thesis we are using the Latin hypercube sampling Monte Carlo to address the uncertainties issues.

7.2.1 Method history and description

The method of LHS is an extension of quota sampling (Steinberg, 1963), and can be viewed as an dimensionalextension of Latin square sampling (Raj and Des, 1968). This method first was used in "Uncertainty Analysis" by selecting input values $x = (x_1, x_2, \ldots, x_n)$ n

(random variable) of a function $y = h(\boldsymbol{x})$, inorder to estimate the cumulative distribution function (c.d.f.) and mean value of y (McKay*et al* , 1979a)(Iman and Conover ,1980)(Iman and Helton, 1988). This sampling approach ensures that each of the input variables has all portions of its range represented. LHS is computationally cheap to generate and can cope with many input variables. In what follows the generation and application of LHS in MC yield estimation is presented.

7.2.2 Samples Generation

The LHS method (McKay *et al.,* 1979b) is a type of stratified MC sampling (Hocevar *et al .,* 1983) . The sampling region is partitioned into a specific manner by dividing the range of each component of x. We will only consider the case where the components of x are independent or can be transformed to an independent base. Moreover, the sample generation for correlated components with Gaussian distribution can be easily achieved (Iman and Conover, 1982).

As originally described, in the following manner, LHS operates to generate a sample size N from the n variables $x_1, x_2, , , , , , x_n$. The range of each variable is partitioned into N non overlapping intervals on the basis of equal probability size 1/N. One value from each interval is selected at random with respect to the probability density in the interval. The N values thus obtained for $x_1$are paired in a random manner with the N values of x_2 . These N pairs are combined in a random manner with the N values of x_3 to form N triplets, and so on, until a set of N n-tuples is formed.This set of n-tuples is the Latin hypercube sample. Thus, for given values of N and n, there exist $(N!)^{n-1}$ possibles interval combinations for a LHS. A 10-run LHS for 3 normalized variables (range [-1,1]) with the uniform p.d.f. is listed below. In this case the equal probability spaced values are -1,-0.8... 0.8, 1.

7.2.3 Efficiency of LHSMC

Consider the case that $x$denotes an n-vectors random variable with p.d.f. $f_x(x)$for$x \epsilon S$. Let$h$denote an objective function given by $h = q(x)$. Consider now the following class of estimators

$$T = \frac{1}{N}\sum_{i=1}^{N} g(H_i). \qquad (7.14)$$

where g(.) is an arbitrary known function and $H_i = q(x_i)$. If $g(h) = h$that is if h a fixed point for g, then T represents an estimator of $[h]$. If $g(h) = H_i$one obtains the rth sample moment. By choosing $g(h) = u(c - h)$ ($u(.)$ is astep function), one achieves the empirical distribution function of $h$at the point c. Now consider the following theorems

Theorem 7.1: *If $x^{i\prime}s$ are generated by LHS method. Then, the statistic T Equation* (7.14) *is an unbiased estimator of the mean of* (h)*. That is,*

$$E[T] = E[g(h)]. \quad (7.15)$$

Proof: This is a special case of Theorem 7.1 in (Iman and Conover, 1980). It should be emphasized that even if the variables are correlated LHS estimator will be unbiased. Let T_R denote estimator (7.14) with standard random sampling of, and T_L denote the estimator with the LHS generator of x. Now consider the following theorem related to the variances of T_R and T_L.

Theorem 7.2: *If* $h = q(x_1, x_2, \ldots, x_n)$ *is monotonic at least in* $(n-1)$ *of its arguments, and if* $g(h)$ *isa monotonic function of h, then the variance of LHSMC estimator is less than that of PMC, that is, in order words*

$$Var\ (T_R) \geq Var(T_L). \text{ (Keramat, 1996)}$$

The goodness of an unbiased estimator of yield can be measured by the size of its variance. From Theorem 7.2, it is seen that for the monotonic function $q(.)$ for $n-1$ variables and a monotonic $g(.)$ the LHSMC method gives better estimate than that of the random sampling, without any significant additional computational costs.

Theorem 7.3: *If* $h = q(x_1, x_2, \ldots, x_n)$ *is monotonic in each of its arguments and if* $g(h)$ *is amonotonic function of h, then a lower bound of the variance differences between the LHSMC and the PMC estimators is* m

$$Var(T_L) - Var(T_R) \leq -\frac{1}{N}\max_{I\epsilon[1,\ldots\ldots n]}\{Var(E_{\bar{I}_l}(\mu_c))\}. \quad (7.16)$$

where $\bar{I}_l = I_{1\ldots.l-1,l+1\ldots\ldots,n}$ and $\mu_c(I_1, I_2, \ldots, I_n) = \int g(h) f_x(x)dx$ in which I_l presents the ith component of the cell I (the interval number in direction x_l)(Keramat, 1996) It should be emphasized that the monotonicity conditions of Theorem 9.2 and Theorem 9.3 are sufficient condition and are not necessary. Consider now the following theorem with no assumption of monotonicity in the two-dimensional space.

Theorem 7.4: *If* $h = q(x_1, x_2)$ *and* $g(h)$ *are arbitrary functions, then the difference of variances between the LHSMC and the PMC estimators is* (Keramat, 1996) (7.17)

$$Var(T_L) - Var(T_R) = \frac{1}{N(N-1)}\left[Var(\mu_c) - N\sum_{l=1}^{2} Var\left[E_{I_l}(\mu_c)\right]\right].$$

In order to compare two different estimation methods, an efficiency measure is introduced as the product of the ratio of the respective variances with the ratio of the respective computation times (Hocevar *et al* , 1983) (7.18)

$$\eta = \frac{\sigma_R^2 \tau_R}{\sigma_L^2 \tau_L},$$

where τ_R and σ_R^2 denote the computation time and the variance of the PMC estimator.

τ_L and σ_L^2 are the computation time and the variance of the LHSMC respectively

7.3 APPLICATIONS

Iman and Helton (Iman and Helton, 1988) applied the LHS approach to cumulative distribution function (c.d.f.) estimation of the three computer models: 1) Environmental radionuclide movement, 2) Multi-component aerosol dynamics, and 3) Salt dissolution in bedded salt formations. They reported a good agreement of c.d.f. estimations. In this section, the application of Latin Hypercube Sampling Monte Carlo to groundwater pollution will be discussed.

7.3.1 Latin hypercube sampling of parameters involved in the solution of advection dispersion equation

The generation of an LHS is presented here for $\alpha = [D_r, q_r, u_r, \gamma, \lambda]$ and $nS = 5$. D_r assigned a triangular distribution and a mode of 1 on [0,2],) q_r assigned a triangular distribution and a mode of 0.875 on [0, 1.75], λ and γ assigned a uniform distribution on [0, 1]. The range of the five parameters are subdivided into five intervals of equal probability, with this represented by lines that originate at 0.2, 0.4, 0.6 and 0.8 on the ordinates Fig (6-20, 6-21, 6-22 and 6-23), extend horizontally to the CDFs (Cumulative Distribution Function), and then drop vertically to the abscissas to produce the five indicated intervals. Random values $D_r(1), D_r(2), \dots, D_r(5)$; $q_r(1), q_r(2), q_r(3), \dots, q_r(5)$; $q_r(1), q_r(2), \dots, u_r(5)$
$\lambda(1), \lambda(2), \dots, \lambda(5)$and $\gamma(1), \gamma(2), \dots, \gamma(5)$ are then sampled from these intervals. The sample of these random values is implemented by (i) sampling $RD_r(1), Rq_r(1), Ru_r(1), R\lambda(1)$and $R\gamma(1)$ from a uniform and a triangular distribution on [0,0.2], $RD_r(1), Rq_r(1), Ru_r(1), R\lambda(1)$and $R\gamma(1)$ from a uniform and triangular distribution on [0.2, 0.4], and so on, and then (ii) using the CDFs to identify(i.e. sample) the corresponding D_r, q_r, u_r, γ and λ values, with this identification represented by the lines that originate on the ordinates of Fig (6-20, 6-21, 6-22 and 6-23), extend horizontally to the CDFs, and then drop vertically to the abscissas to produces
$D_r(1), D_r(2), \dots, D_r(5)$; $q_r(1), q_r(2), q_r(3), \dots, q_r(5)$; $q_r(1), q_r(2), \dots, u_r(5)$
$\lambda(1), \lambda(2), \dots, \lambda(5)$ and $\gamma(1), \gamma(2), \dots, \gamma(5)$. The generation of the LHS is then completed by randomly pairing without replacement the resulting values for D_r, q_r, u_r, γa nd λ. As this pairing is not unique, many possible LHSs can be result. In this case, we have 3125 possible LHS's. Note that, improbability and statistics, the triangular distribution is a continuous probability distribution with lower limit a, upper limit b and mode c, where $a < b$ and $a \leq c \leq b$. The probability density function is given by: (7.20)

$$f(x) = \begin{cases} 0 \; for \; x < a \\ \frac{2(x-a)}{(b-a)(c-a)} \quad for \; a \leq x < c \\ \frac{2}{(b-a)} \quad for \;\; x = c \\ \frac{2(b-x)}{(b-a)(b-c)} \quad for \; c < x \leq b \\ 0 \;\; for \; b < x \end{cases}$$

and the Cumulative Distributive Function associated to this probability density function is given by:

$$CDF = \begin{cases} 0 \; for \; x < a \\ \frac{(x-a)^2}{(b-a)(c-a)} \quad for \; a \leq x < c \\ \frac{c-a}{(b-a)} \quad for \;\; x = c \\ 1 - \frac{(b-x)^2}{(b-a)(b-c)} \quad for \; c < x \leq b \\ 1 \quad for \; b \; < x \end{cases}$$

On the other hand the Cumulative Distribution Function associated to a normal distribution on [a, b] is given by: The following figures show an example of CDF for some parameters.

$$\begin{cases} 0 \; for \quad x < a \\ \frac{x-a}{b-a} \quad for \; a \leq x \leq b \\ 1 \; for \; x \geq b \end{cases}$$

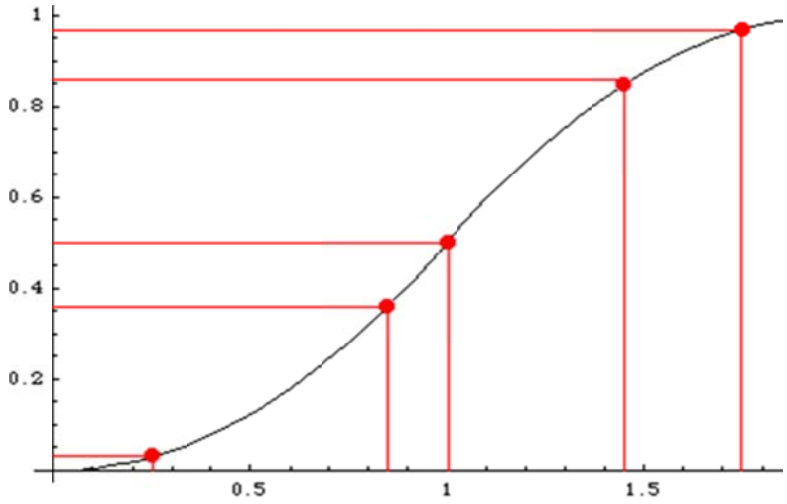

Figure 7-14: CDF of the triangular distribution of $\boldsymbol{\theta}$ in [0, 1.75] and mode 0.875

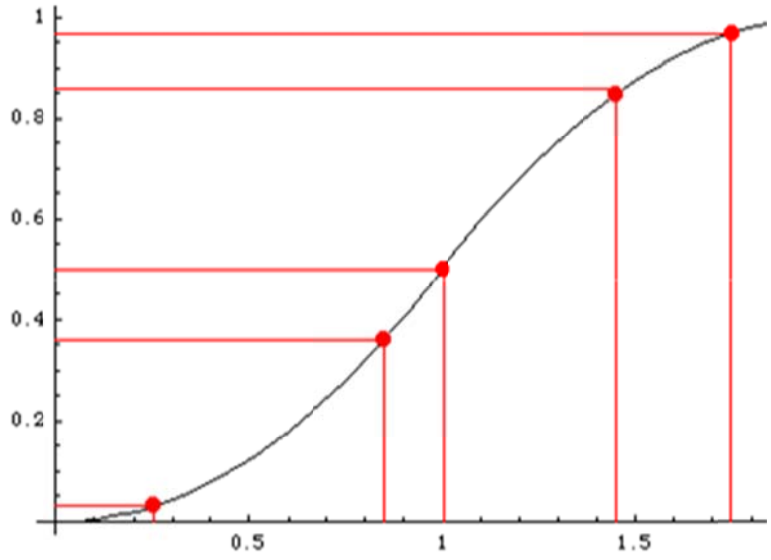

Figure 7-15: CDF of the triangular distribution of $\boldsymbol{\theta}$ in [0, 2] and mode 1

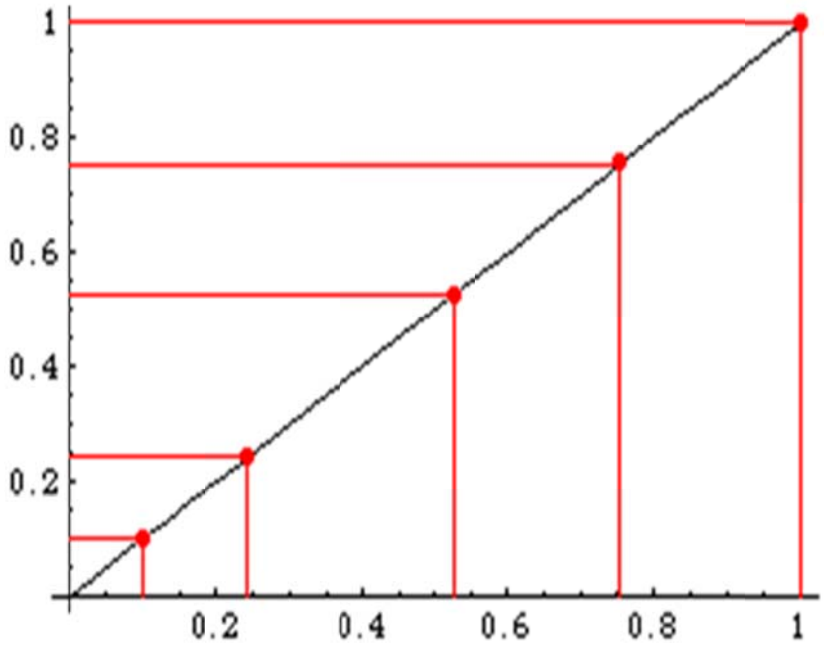

Figure 7-16: CDF of the uniform distribution of $\boldsymbol{\theta}$ in [0, 2] and mode 1

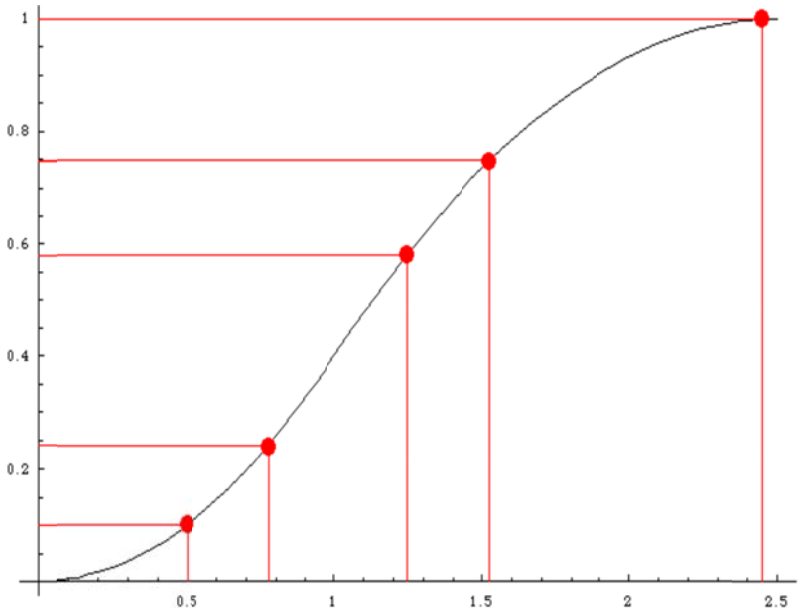

Figure 7-17: CDF of a triangular distribution of $\boldsymbol{u_r}$ in [0, 2.5] and mode 1.

Table 7-1: Latin Hypercube sampling parameters from above distribution

n	θ	α	q_r	K	ρ
1	0.2	10	0.1	1	1200
2	0.4	20	0.4	20	1400
3	0.6	40	0.6	40	1800
4	0.8	60	0.8	60	2000
5	1	80	1	100	2200

As we said before, the pairing is not unique, and many possible LHSs can result. Without loss of generality, the following Table shows the set of 5-tuples used in this work and for each element of the set we associate a solution to a model.

Table 7-2: Latin Hypercube Sampling (pairing)

Con1	0.2	20	0.6	60	2200
Con2	1	60	0.6	20	1200
Con3	0.4	10	0.1	1	1800
Con4	0.8	80	0.8	100	1400
Con5	0.6	40	0.1	40	2000
Con6	0.4	20	01	20	2200
Con7	0.2	60	0.4	01	1200
Con8	0.8	10	0.1	100	1400
Con9	01	80	01	100	2200
Con10	0.6	40	0.6	40	2000

The preceding sampling procedures are probabilistically based in the sense that weights

$$w_i, \qquad i = 1, \dots \dots \dots \dots nS,$$

exist such that the result obtained with sample element $x_i$can be used in conjunction with the weight $w_i$to obtain quantities such as expected values, variances and other entities that derive from integration over the space of probability associated(J.C. Helton, F.J. Davis, 2003). For random sampling and also Latin hypercube sampling, $w_i$is the reciprocal of the sample size, that is $w_i = \frac{1}{nS}$ and hence for our case $w_i = \frac{1}{10}$

7.3.2 Analysis inputs to analysis results

Once the sample is generated, evaluation of the concentration creates the following mapping from analysis inputs to analysis results.$[\alpha_i, c_i(x,t)]$, $i = 1, \dots \dots, 10$

Table 7-3: Parameter sets 1 and 2

c_o,	c_1	α	γ	λ	θ	ρ_b	K	q
990	1 000	20	0	1	1/5	2 200	60	3/5,
990	1 000	60	0	1	1	1 200	20	3/5

x	t	c_1(x, t)	c_2(x, t)
0.10	0.50	600.465 357	600.465 353
0.10	1.00	364.210 719	364.202 496
0.10	1.50	221.053 143	220.944 828
0.10	2.00	134.580 366	134.208 805
0.10	2.50	82.567 359	81.833 507
0.10	3.00	51.397 512	50.298 374
x	**t**	**c_1(x, t)**	**c_2(x, t)**
0.20	0.50	600.465 353	600.465 353
0.20	1.00	364.200 647	364.200 647
0.20	1.50	220.898 859	220.898 859
0.20	2.00	133.981 934	133.981 931
0.20	2.50	81.264 201	81.264 153
0.20	3.00	49.289 518	49.289 233
x	**t**	**c_1(x, t)**	**c_2(x, t)**
0.30	0.50	600.465 353	600.465 353
0.30	1.00	364.200 647	364.200 647
0.30	1.50	220.898 859	220.898 859
0.30	2.00	133.981 930	133.981 930
0.30	2.50	81.264 149	81.264 149
0.30	3.00	49.289 198	49.289 198

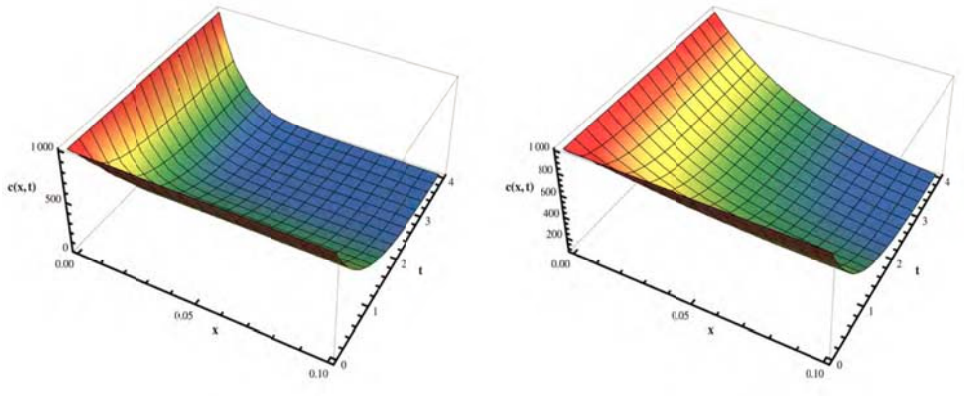

Figure 7-18: Output for set 1 and 2

Table 7-4: Parameter sets 3 and 4

co,	c1	α	γ	λ	θ	ρb	K	q
990	1 000	10	0	1	2/5	1 800	1	1/10
990	1 000	80	0	1	4/5	1 400	100	4/5

x	t	$c_1(x, t)$	$c_2(x, t)$
0.10	0.50	600.466 107	600.465 440
0.10	1.00	364.381 161	364.254 870
0.10	1.50	222.150 424	221.418 769
0.10	2.00	137.256 283	135.579 581
0.10	2.50	86.926 745	84.299 223
0.10	3.00	57.197 792	53.788 658
x	**t**	**$c_1(x, t)$**	**$c_2(x, t)$**
0.20	0.50	600.465 353	600.465 353
0.20	1.00	364.200 647	364.200 647
0.20	1.50	220.898 886	220.898 86
0.20	2.00	133.982 590	133.982 003
0.20	2.50	81.268 416	81.264 835
0.20	3.00	49.303 233	49.292 099
x	**t**	**$c_1(x, t)$**	**$c_2(x, t)$**
0.30	0.50	600.465 353	600.465 353
0.30	1.00	364.200 647	364.200 647
0.30	1.50	220.898 859	220.898 859
0.30	2.00	133.981 930	133.981 930
0.30	2.50	81.264 149	81.264 149
0.30	3.00	49.289 200	49.289 198

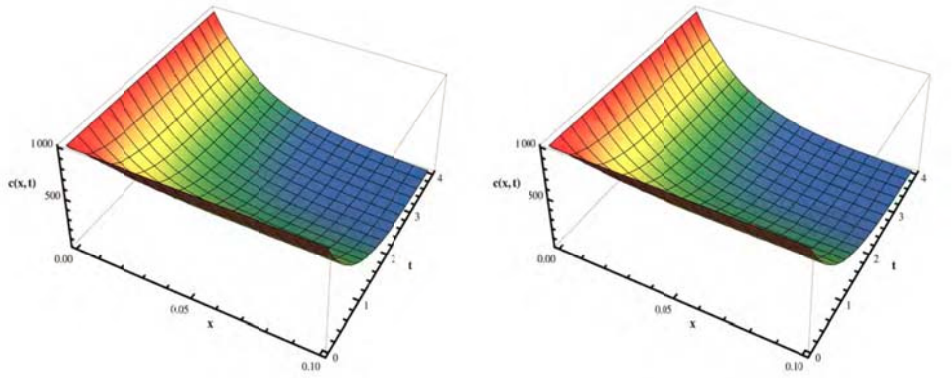

Figure 7-19: Output of set 3 and 4

Table 7-5: Parameter sets 5 and 6

c_o,	c_1	α	γ	λ	θ	ρ_b	K	q
990	1 000	40	0	1	3/5	2 000	40	1/10
990	1 000	20	0	1	2/5	2 200	20	5/5

x	t	$c_1(x, t)$	$c_2(x, t)$
0.10	0.50	600.465 353	600.465 434
0.10	1.00	364.200 647	364.252 940
0.10	1.50	220.898 859	221.405 532
0.10	2.00	133.981 930	135.547 007
0.10	2.50	81.264 149	84.246 384
0.10	3.00	49.289 198	53.718 886
x	**t**	**$c_1(x, t)$**	**$c_2(x, t)$**
0.20	0.50	600.465 353	600.465 353
0.20	1.00	364.200 647	364.200 647
0.20	1.50	220.898 859	220.898 860
0.20	2.00	133.981 930	133.981 998
0.20	2.50	81.264 149	81.264 799
0.20	3.00	49.289 198	49.291 969
x	**t**	**$c_1(x, t)$**	**$c_2(x, t)$**
0.30	0.50	600.465 353	600.465 353
0.30	1.00	364.200 647	364.200 647
0.30	1.50	220.898 859	220.898 859
0.30	2.00	133.981 930	133.981 930
0.30	2.50	81.264 149	81.264 149
0.30	3.00	49.289 198	49.289 198

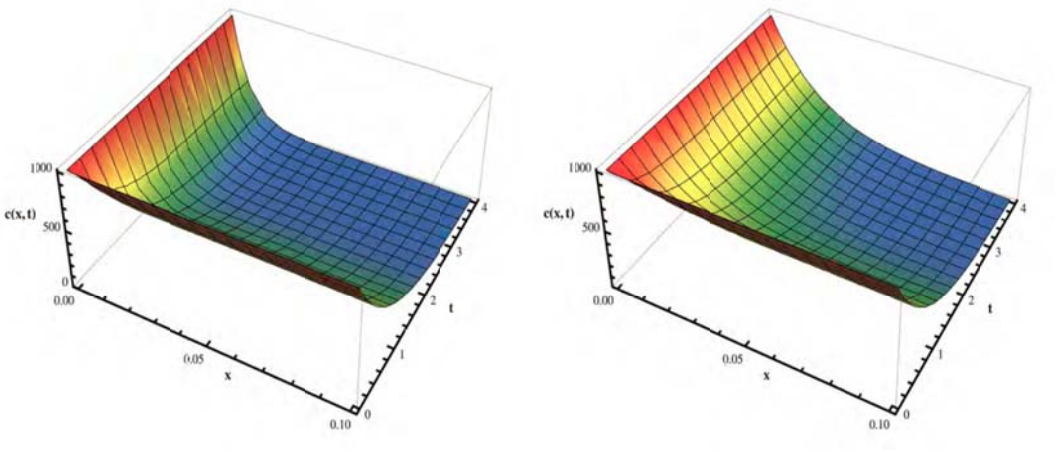

Figure 7-20: Output of set 5 and 6

Table 7-6: Parameter Sets 7 and 8

c_o,	c_1	α	γ	λ	θ	ρ_b	K	q
990	1 000	60	0	1	1/5	1 200	1	2/5
990	1 000	10	0	1	4/5	1 400	100	1/10

x	t	$c_1(x, t)$	$c_2(x, t)$
0.10	0.50	704.987 753	600.465 353
0.10	1.00	600.179 033	364.200 647
0.10	1.50	550.359 324	220.898 859
0.10	2.00	524.673 999	133.981 930
0.10	2.50	510.888 768	81.264 149
0.10	3.00	503.309 636	49.289 198
x	t	$c_1(x, t)$	$c_2(x, t)$
0.20	0.50	620.975 852	600.465 353
0.20	1.00	441.794 161	364.200 647
0.20	1.50	351.209 771	220.898 859
0.20	2.00	303.239 341	133.981 930
0.20	2.50	277.103 149	81.264 149
0.20	3.00	262.593 907	49.289 198
x	t	$c_1(x, t)$	$c_2(x, t)$
0.30	0.50	603.340 468	600.465 353
0.30	1.00	386.298 579	364.200 647
0.30	1.50	268.420 488	220.898 859
0.30	2.00	203.693 756	133.981 930
0.30	2.50	167.657 008	81.264 149
0.30	3.00	147.362 470	49.289 198

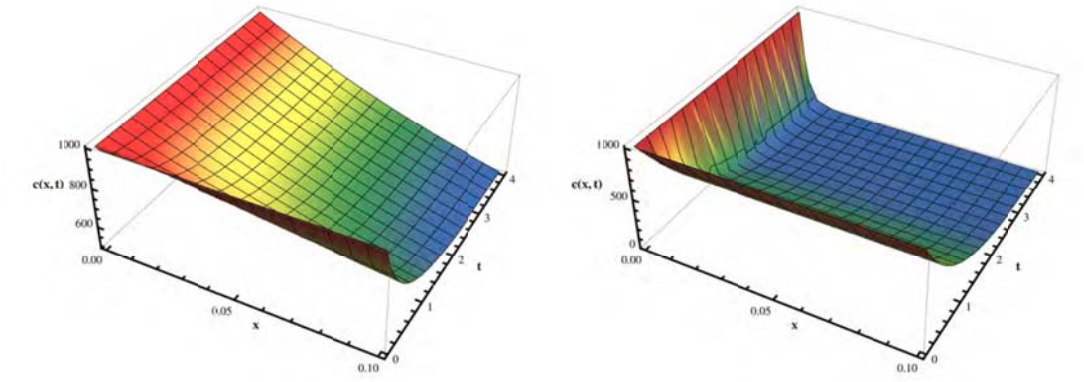

Figure 7-21: Output of set 7 and 8

Table 7-7: Parameter Sets 9 and 10

c_o	c_1	α	γ	λ	θ	ρ_b	K	q
990	1 000	80	0	1	1/5	1 200	100	5/5
990	1 000	40	0	1	4/5	2 000	40	3/5

x	t	c1(x, t)	c2(x, t)
0.10	0.50	600.465 357	600.465 353
0.10	1.00	364.210 719	364.202 496
0.10	1.50	221.053 143	220.944 828
0.10	2.00	134.580 366	134.208 805
0.10	2.50	82.567 359	81.833 507
0.10	3.00	51.397 512	50.298 374
x	**t**	**$c_1(x, t)$**	**$c_2(x, t)$**
0.20	0.50	600.465 353	600.465 353
0.20	1.00	364.200 647	364.200 647
0.20	1.50	220.898 859	220.898 859
0.20	2.00	133.981 934	133.981 931
0.20	2.50	81.264 201	81.264 153
0.20	3.00	49.289 518	49.289 233
x	**t**	**$c_1(x, t)$**	**$c_2(x, t)$**
0.30	0.50	600.465 353	600.465 353
0.30	1.00	364.200 647	364.200 647
0.30	1.50	220.898 859	220.898 859
0.30	2.00	133.981 930	133.981 930
0.30	2.50	81.264 149	81.264 149
0.30	3.00	49.289 198	49.289 198

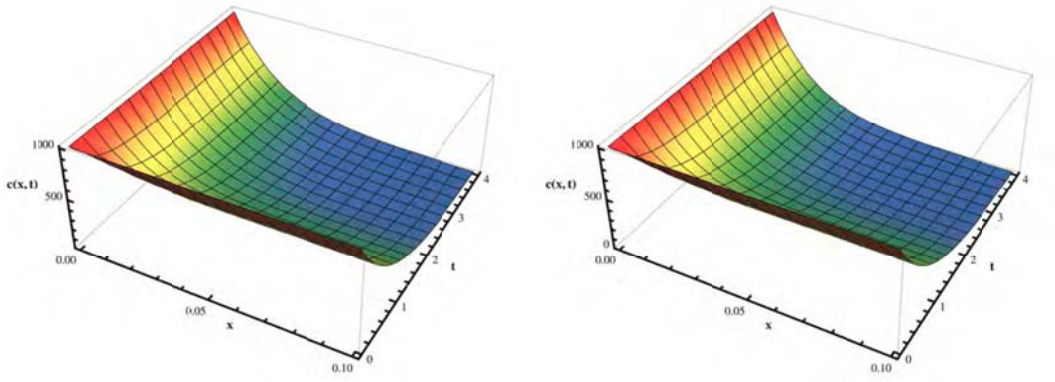

Figure 7-22: Output of set 9 and 10

7.3.3 Cumulative distribution function

The distribution for the concentration is presented as a cumulative distribution function (CDF) or as a complementary cumulative distribution function (CCDF), which is simply one minus the CDF (Helton and Davis, 2003). Hence in our case the cumulative distribution function can be approximated as follows: (7.21)

$$prob\big(c(\alpha,x,t) > C(\alpha,x,t)\big) = \sum_{i=1}^{10} \delta_{C(\alpha,x,t)}\left(c_i(x,t)\right)\frac{1}{10},$$

where $\delta_{C(\alpha,x,t)}(c_i(x,t)) = \begin{cases} 1 & if\ \ c_i(x,t) > C(\alpha,x,t) \\ 0 & if\ \ c_i(x,t) < C(\alpha,x,t). \end{cases}$

and $prob\big(c(\alpha,x,t) > C(\alpha,x,t)\big)$ is the probability that a value larger than $C(\alpha,x,t)$ will occur. The distribution function approximated above provides the most complete representation of the uncertainty in the concentration that derives from the distributions.

Let $C(\alpha,x,t) = C(\frac{80}{1801}, \frac{2}{1801}, 0.875,\ \lambda = 1,\ \gamma = 0.85, x, t)$. We shall choose a set of (x,t) to calculate the probability, and we will then calculate the mean of those probability. For $(x,t) = (1,1)$ we have:

Table 7-8: Concentration for $(\boldsymbol{x},\boldsymbol{t}) = (\mathbf{1},\mathbf{1})$

$c_1(\alpha,x,t)$	58.2577
$c_2(\alpha,x,t)$	74.8909
$c_3(\alpha,x,t)$	60.6521
$c_4(\alpha,x,t)$	58.0343
$c_5(\alpha,x,t)$	40.0718
$c_6(\alpha,x,t)$	46.8954
$c_7(\alpha,x,t)$	92.2647
$c_8(\alpha,x,t)$	28.3879
$c_9(\alpha,x,t)$	44.8966
$c_{10}(\alpha,x,t)$	77.9576
$C(\alpha,x,t)$	33.0835

then the probability is given by (7.22)

$$prob\big(c(\alpha,x,t) > C(\alpha,x,t)\big) = \sum_{i=1}^{10} \delta_{C(\alpha,x,t)}\left(c_i(x,t)\right)\frac{1}{10} = \frac{9}{10}$$

For $(x,t) = (20,20)$ we have:

Table 7-9: Concentration for $(\boldsymbol{x},\boldsymbol{t}) = (\mathbf{20},\mathbf{20})$

$c_1(\alpha,x,t)$	0.00176227
$c_2(\alpha,x,t)$	0.634651
$c_3(\alpha,x,t)$	0.00250054
$c_4(\alpha,x,t)$	0.00131972
$c_5(\alpha,x,t)$	0.0000131415
$c_6(\alpha,x,t)$	12.3906
$c_7(\alpha,x,t)$	62.123
$c_8(\alpha,x,t)$	1.76417×10^{-7}
$c_9(\alpha,x,t)$	5.40976×10^{-6}
$c_{10}(\alpha,x,t)$	1.00504
$C(\alpha,x,t)$	1.85504×10^{-7}

then, the probability is given by

$$prob\big(c(\alpha,x,t) > C(\alpha,x,t)\big) = \sum_{i=1}^{10} \delta_{C(\alpha,x,t)}\left(c_i(x,t)\right)\frac{1}{10} = \frac{9}{10}$$

For $(x,t) = (100,100)$ we have:

Table 7-10: Concentration for $(\boldsymbol{x},\boldsymbol{t}) = (\mathbf{100},\mathbf{100})$

$c_1(\alpha,x,t)$	5.35161×10^{-22}
$c_2(\alpha,x,t)$	2.02342×10^{-9}
$c_3(\alpha,x,t)$	1.42489×10^{-21}
$c_4(\alpha,x,t)$	8.70786×10^{-22}
$c_5(\alpha,x,t)$	1.14739×10^{-31}
$c_6(\alpha,x,t)$	1.48021
$c_7(\alpha,x,t)$	52.9736
$c_8(\alpha,x,t)$	3.34787×10^{-42}
$c_9(\alpha,x,t)$	4.73136×10^{-33}
$c_{10}(\alpha,x,t)$	1.02619×10^{-8}
$C(\alpha,x,t)$	3.34807×10^{-42}

then ,the probability is given by

$$prob\big(c(\alpha,x,t) > C(\alpha,x,t)\big) = \sum_{i=1}^{10} \delta_{C(\alpha,x,t)}\left(c_i(x,t)\right)\frac{1}{10} = \frac{9}{10}$$

For $(x,t) = (200,200)$ we have:

Table 6-11: Concentration for $(x,t) = (200,200)$

$c_1(\alpha,x,t)$	3.29798×10^{-45}
$c_2(\alpha,x,t)$	4.71079×10^{-20}
$c_3(\alpha,x,t)$	2.25591×10^{-44}
$c_4(\alpha,x,t)$	1.51925×10^{-44}
$c_5(\alpha,x,t)$	2.63774×10^{-64}
$c_6(\alpha,x,t)$	0.137565
$c_7(\alpha,x,t)$	57.4742
$c_8(\alpha,x,t)$	1.24551×10^{-85}
$c_9(\alpha,x,t)$	1.33147×10^{-66}
$c_{10}(\alpha,x,t)$	1.05306×10^{-18}
$C(\alpha,x,t)$	1.2455×10^{-85}

then, the probability is given by

$$prob\big(c(\alpha,x,t) > C(\alpha,x,t)\big) = \sum_{i=1}^{10} \delta_{C(\alpha,x,t)}\left(c_i(x,t)\right)\frac{1}{10} = 1.$$

For $(x,t) = (2500,2500)$ we have:

Table 6-12: Concentration for $(\boldsymbol{x},\boldsymbol{t}) = (\mathbf{2500},\mathbf{2500})$

$c_1(\alpha,x,t)$	1.3525×10^{-579}
$c_2(\alpha,x,t)$	8.8894×10^{-265}
$c_3(\alpha,x,t)$	8.76466×10^{-569}
$c_4(\alpha,x,t)$	8.416153×10^{-569}
$c_5(\alpha,x,t)$	8.32007×10^{-816}
$c_6(\alpha,x,t)$	0
$c_7(\alpha,x,t)$	83.3925
$c_8(\alpha,x,t)$	1.652×10^{-1084}
$c_9(\alpha,x,t)$	0×10^{-828}
$c_{10}(\alpha,x,t)$	1.90842×10^{-248}
$C(\alpha,x,t)$	1.652×10^{-1085}

then, the probability is given by:

$$prob\big(c(\alpha,x,t) > C(\alpha,x,t)\big) = \sum_{i=1}^{10} \delta_{C(\alpha,x,t)}\left(c_i(x,t)\right)\frac{1}{10} = \frac{4}{5}.$$

Therefore the mean of those probabilities is given by

$$\overline{prob\big(c(\alpha,x,t) > C(\alpha,x,t)\big)} = \frac{9}{10}$$

As said before, the distribution function approximated above provides the most complete representation of the uncertainty in the concentration that derives from the distributions.

7.3.4 Expected value of the sampling

For Latin hypercube sampling method, the form for the estimator of the expected value of the concentration is given by (Helton and Davis, 2003): (7.23)

$$\bar{c}(x,t) = \frac{1}{10}\sum_{i=1}^{10} c_i(x,t),$$

where $c_i(x,t) = c(D_r(i), q_r(i), u_r(i), \lambda(i), \gamma(i), x, t)$ and $D_r(i), q_r(i), u_r(i), \lambda(i)$and $\gamma(i)$ the values are given in the tables above. The expected value approximated here provides a summary of this distribution but with the inevitable loss of resolution that occurs when the information contained in 20 numbers. The following surface shows the response of the expected values as function of space and time.

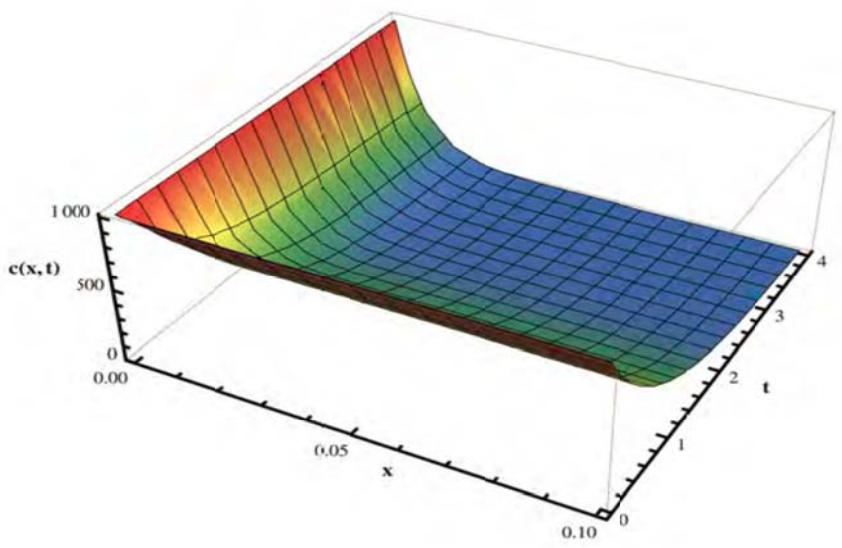

Figure 7-23: Expected values of the sample as function of space and time

7.3.5 Variance of the sampling and Repeatability Uncertainty

Variance of the sample

The form for estimator of the variance of $c(x,t)$ is given by (7.24)

$$Var(c(x,t)) = \frac{1}{10-1}\sum_{i=1}^{10}(c_i(x,t) - \bar{c}(x,t))^2$$

The goodness of an unbiased estimator can be measured by its variance. The variance approximated here provides a summary of this distribution but with the inevitable loss of resolution that occurs when the information contained in 20 numbers (J.C. Helton, F.J. Davis, 2003). The following graph shows the cross section ($x = 25$) of the variance for

$0.001 \leq t \leq 25$ and the surface shows the respond of the variance of the distribution as function of space and time

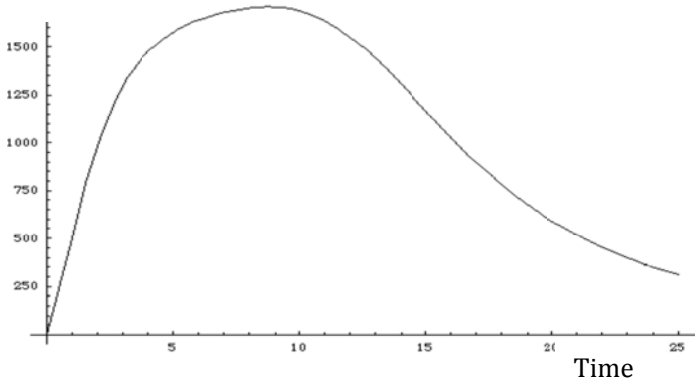

Figure 7-24: Cross section ($\boldsymbol{x = 25}$) of the variance for a fixed value of $\boldsymbol{x}$

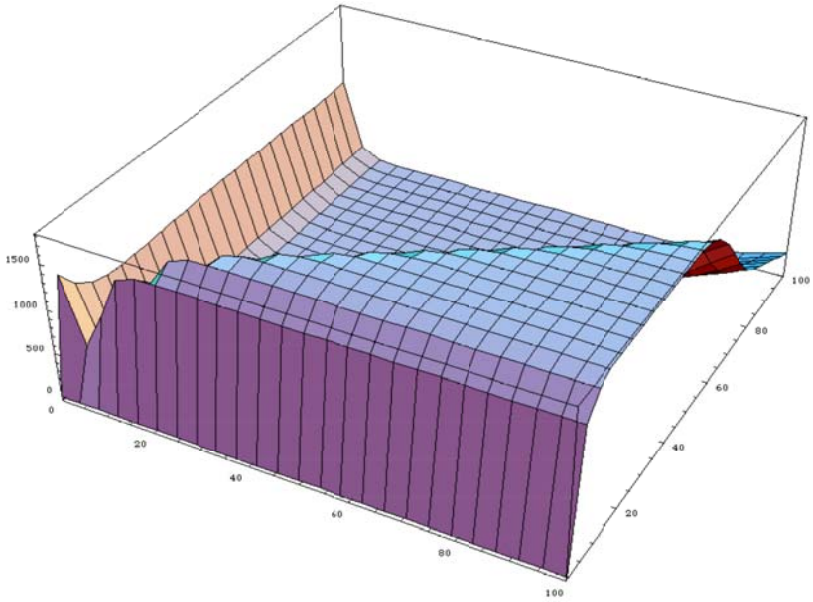

Figure 7-25: Variance of the sample as function of time and space

Repeatability Uncertainty

It is important noting that repeatability uncertainty is equal to the standard deviation of the sample data (NASA HANDBOOK, 2010). In the case under investigation, the mathematical expression is given as (7.25)

$$S(c(x,t)) = \sqrt{\frac{1}{10-1}\sum_{i=1}^{10}(c_i(x,t) - \bar{c}(x,t))^2}.$$

The normalized solution of the above equation is illustrated graphically in the below figure.

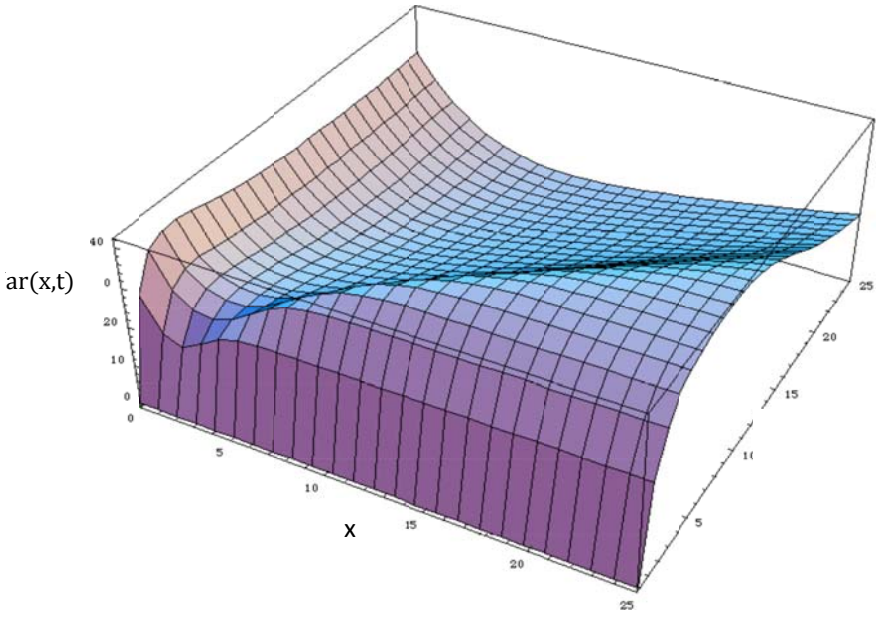

Figure 7-26: Repeatability uncertainty.

7.3.6 Develop the Error Model

An error model is an algebraic expression that defines the total error in the value of a quantity in terms of all relevant measurement process or component errors. The error model for the quantity$c(\alpha, x, t)$, the concentration of pollution that was calculated here is given below as (NASA, 2010),

$$\varepsilon_{c(\alpha,x,t)} = \varepsilon_{D_r} c_{D_r}(x,t) + \varepsilon_{q_r} c_{q_r}(x,t) + \varepsilon_{u_r} c_{u_r}(x,t) + \varepsilon_{\lambda} c_{\lambda}(x,t) + \varepsilon_{\gamma} c_{\gamma}(x,t) \qquad (7.26)$$

where

$\varepsilon_{c(\alpha,x,t)}$is the error in the concentration; $\varepsilon_{D_r}$is the error in the retarded hydrodynamic dispersion coefficient; $\varepsilon_{q_r}$is the error in the retarded velocity vector; $\varepsilon_{u_r}$is the error in u_r; $\varepsilon_{\gamma}$is the error in γ; $\varepsilon_{\lambda}$is the error in therate of decay of the radionuclide;

and $c_{D_r}, c_{q_r}, c_{u_r}, c_{\gamma}$ and c_{λ} are the first order sensitivity coefficients that determine the relative contribution of the errors in D_r, q_r, u_r, γ and λ to the total error in$c(\alpha, x, t)$. The first order sensitivity coefficients are the same as the one defined in section 6.1.

For this purpose we chose the following definition of error, (7.27)

$$\varepsilon_{\alpha_i} = \frac{maximum\ value - minimum\ value}{maximum\ value\ \times 100}, \qquad i = 1,..5.$$

Then,

$\varepsilon_{D_r} = 0.008571428, \varepsilon_{q_r} = 0.008601823,\ \varepsilon_{u_r} = 0.007959183 \varepsilon_{\gamma} = 0.0091$, and $\varepsilon_{\lambda} = 0.009$.

Here we also chose

$$\alpha_i = \frac{1}{5}\sum_{k=1}^{5} \alpha_{i_k}, i = 1 \dots 5.$$

Thus $D_r = 1.06,\ q_r = 0.98, u_r = 1.299, \gamma = 0.5462$ and $\lambda = 0.5245$ which implies that

$$\alpha = (1.06, 0.98, 1.299, 0.5462, 0.5245).$$

And the error in the concentration equation (7.8) becomes:

$\varepsilon_{c(\alpha,x,t)} = 0.008571428c_{D_r}(x,t) + 0.008601823c_{q_r}(x,t) + 0.007959183c_{u_r}(x,t) +$
$0.009c_{\lambda}(x,t) + 0.0091c_{\gamma}(x,t).$

The following surface plot shows the error in the concentration of the sample as a function of time and space.

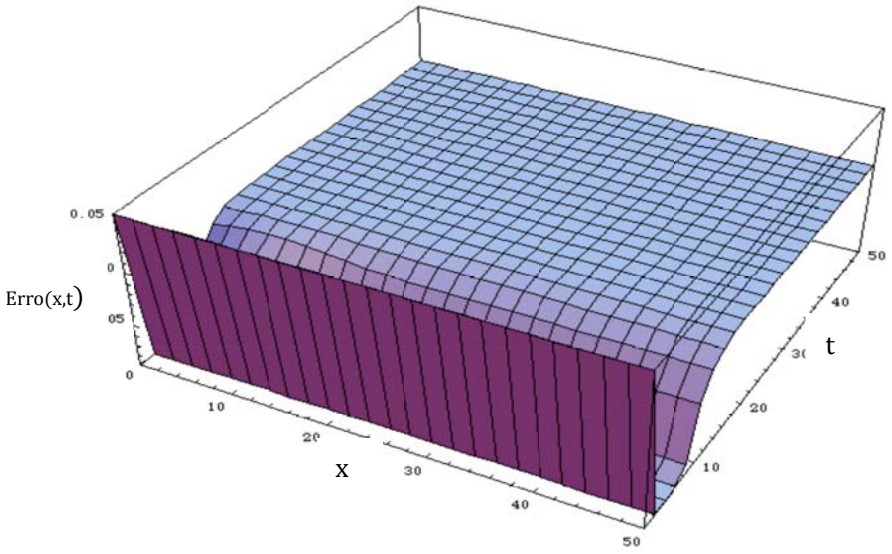

Figure 7-27: Model error as function of space and time

7.3.7 Uncertainty in quantities or variables

The uncertainty in a quantity or variable is the square root of the variable's mean square error or variance. In mathematical terms, this is expressed as (NASA, 2010): (7.28)

$$u_{c(\alpha,x,t)} = \sqrt{\varepsilon^2{}_{D_r} c^2{}_{D_r}(x,t) + \varepsilon^2{}_{q_r} c^2{}_{q_r}(x,t) + \varepsilon^2{}_{u_r} c^2{}_{u_r}(x,t) + \varepsilon^2{}_{\lambda} c^2{}_{\lambda}(x,t) + \varepsilon^2{}_{\gamma} c^2{}_{\gamma}(x,t)}.$$

Providing that the correlation coefficients for the error in D_r, q_r, u_r, γ and λ are equal to zero. The response of this analytical expression is shown in the following surface.

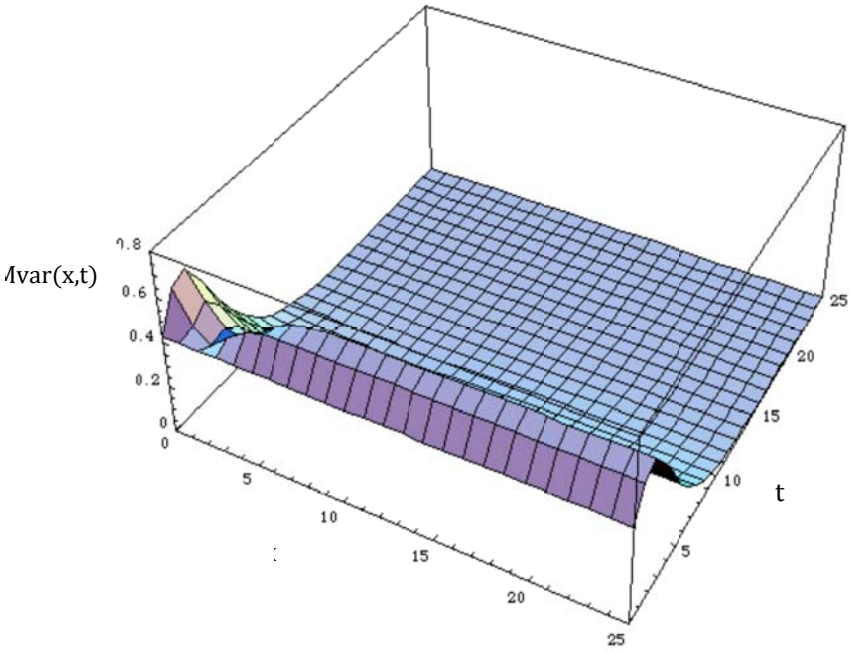

Figure 7-28: Variable's mean square error as function of time and space.

7.3.8 Skewness and Kurtosis Tests

Descriptive statistics, such as skewness and kurtosis, can provide relevant information about the normality of the data sample. Skewness is a measure of how symmetric the data distribution is about its mean. Kurtosis is a measure of the "peakedness" of the distribution (NASA, 2010). In mathematical terms for the case under investigation, these are expressed as: Since $c_1(\alpha, x, t), \ldots, c_{10}(\alpha, x, t)$are our sampled functions from a sample of size 10,with mean $\bar{c}(x,t)$and standard deviation $var(x,t)$, then, the sample coefficient of skewness c_3 and coefficient of kurtosis c_4 are given by (NASA , 2010) (7.29)

$$c_3 = \frac{\frac{1}{10-1}\sum_1^{10}(c_i(x,t) - \bar{c}(x,t))^3}{var[(c(x,t))^3}.$$

The following surface shows the respond of the analytical expression of the sample coefficient of skewness, as function of time and space

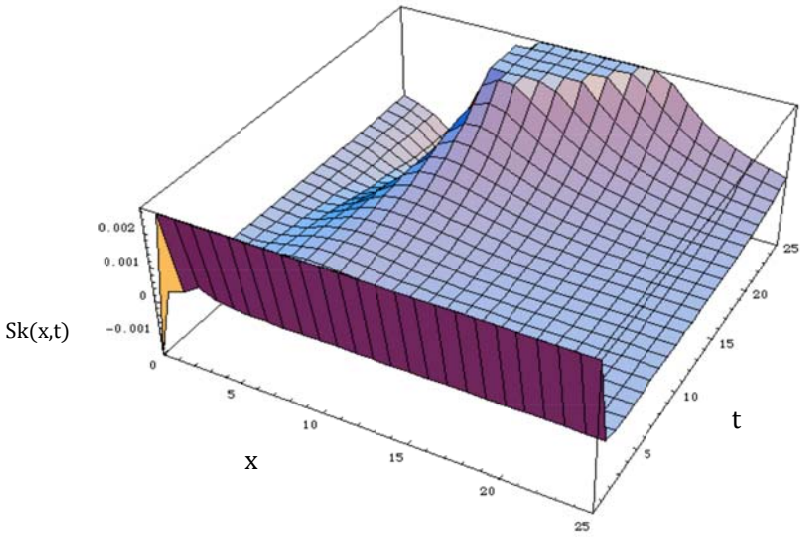

Figure 7-29: Sample coefficient of skewness

and (7.30)

$$c_4 = \frac{\frac{1}{10-1}\sum_1^{10}(c_i(x,t) - \bar{c}(x,t))^4}{var(x,t)^4}$$

The following surface shows the respond of the analytical expression of the sample coefficient of kurtosis as function of time and space

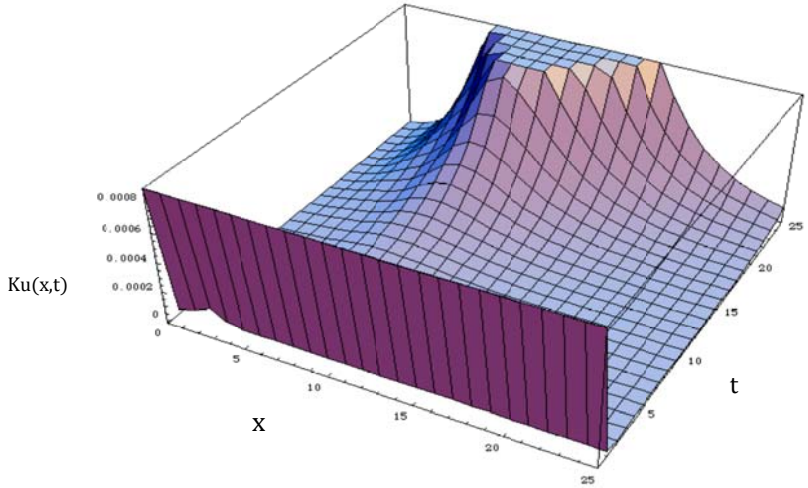

Figure 7-30: Sample coefficient of Kurtosis.

The above study is very important in groundwater study, very important because to have a clear knowledge of aquifer parameters, several measurement of each parameter must be done, and once these parameters are known they can be exposed to aleatory uncertainty analysis.

Chapter 8

THE CONCEPT OF NON-INTEGER ORDER DERIVATIVES

It is commonly believed that, the concept of fractional calculus stemmed from a question rose in the year 1695 by Marquis de L Hospital (1661-1704) to Gottfried Wilhelm Leibniz (1646-1716), which sought the meaning of Leibniz's currently popular notation

$$\frac{d^n y}{dx^n},\ n \in \mathbb{N}_0 := \{0, 1, 2, \dots \dots\} \tag{8.1}$$

for derivative of order when $\boldsymbol{n}$ (What if $\boldsymbol{n} = \frac{\mathbf{1}}{\mathbf{2}}$). In his reply, dated 30 September 1695, Leibniz wrote to L' Hospital as follows: " *This is an apparent paradox from which, one day, useful consequences will drawn…..".*

Starting from these speculation of G .W. Leibniz and others such as Leonard Euler (1730) and George Bernard Friederich Riemann, the fractional calculus (FC) has been developed progressively up to now. The fractional calculus therefore may be considered an old and yet novel topic. However, it is only since about 1970 that the subject has been consistently in the physical and engineering sciences (Ross, 1975). The topic is consequently not well known in many branches of physical and engineering sciences. The discussion below therefore begins with a brief overview of the history of fractional order derivatives.

8.1 BRIEF HISTORY OF FRACTIONAL ORDER DERIVATIVES

It is worth nothing that the standard mathematical models of integer-order derivatives, including nonlinear models, do not work adequately in many cases. In the recent years, fractional calculus has played a very important role in various fields such as mechanics, electricity, chemistry, biology, economics, notably control theory, and signal and image processing. Major topics include anomalous diffusion; vibration and control; continuous time random walk; Levy statistics, fractional Brownian motion; fractional neutron point kinetic model; power law; Riesz potential; fractional derivative and fractals; computational fractional derivative equations; nonlocal phenomena; history-dependent process; porous media; fractional filters; biomedical engineering; fractional phase-locked loops; fractional variational principles; fractional transforms; fractional wavelet; fractional predator-prey system; soft matter mechanics; fractional signal and image processing; singularities analysis and integral representations for fractional differential systems; special functions related to fractional calculus; non-Fourier heat conduction; acoustic dissipation, geophysics;

relaxation; creep; viscoelasticity; rheology; fluid dynamics; chaos and groundwater problems.. An excellent literature of this can be found in (Oldham and Spanier, 1974; Podlubny,1999; Caputo, 1967; Atangana, 2012). These models are making use of the fractional order derivatives that exist in the literature. However there are many of these definitions in the literature nowadays, but few of them are commonly used, including Riemann-Liouville (Kilbas et al, 2006; Samko, 1993), Caputo (Caputo, 1967), Weyl (Atangana, 2012; Botha and Cloot, 2006, Atangana and Kilicman, 2013), (Atangana and Secer, 2013)and Guy Jumarie (Jumarie, 2005, 2006), Hadamard (Podlubny,1999), Matt Davison and Christopher Essex (Essex and Matt, 1998), Riesz (Oldham and Spanier, 1974), Erdelyi-Kober (Magin, 2006) and Coimbra (Coimbra; 2003). All these fractional derivatives definitions have their advantages and disadvantages. The purpose of this note is to present the result of fractional order derivative for some function and from the results, establish the disadvantages and advantages of theses fractional order derivative definitions. We shall start with the definitions.

8.1.1 Definitions

There exists a vast literature on different definitions of fractional derivatives. The most popular ones are the Riemann–Liouville and the Caputo derivatives. For Caputo we have

(8.2)

$$ {}_0^C D_x^\alpha\big(f(x)\big) = \frac{1}{\Gamma(n-\alpha)}\int_0^x (x-t)^{n-\alpha-1}\frac{d^n f(t)}{dt^n}dt. $$

In the case of Riemann-Liouville we have the following definition (8.3)

$$ D_x^\alpha\big(f(x)\big) = \frac{1}{\Gamma(n-\alpha)}\frac{d^n}{dx^n}\int_0^x (x-t)^{n-\alpha-1} f(t)dt. $$

Guy Jumarie proposed a simple alternative definition to the Riemann–Liouville derivative.

(8.4)

$$ D_x^\alpha\big(f(x)\big) = \frac{1}{\Gamma(n-\alpha)}\frac{d^n}{dx^n}\int_0^x (x-t)^{n-\alpha-1}\{f(t)-f(0)\}dt. $$

For the case of Weyl we have the following definition (8.5)

$$ D_x^\alpha\big(f(x)\big) = \frac{1}{\Gamma(n-\alpha)}\frac{d^n}{dx^n}\int_x^\infty (x-t)^{n-\alpha-1} f(t)dt. $$

With the Erdelyi-Kober type we have the following definition: (8.6)

$$ D_{0,\sigma,\eta}^\alpha\big(f(x)\big) = x^{-n\sigma}\left(\frac{1}{\sigma x^{\sigma-1}}\frac{d}{dx}\right)^n x^{\sigma(n+\eta)} I_{0,\sigma,\eta+\sigma}^{n-\alpha}(f(x)). $$

here (8.7)

$$I^{\alpha}_{0,\sigma,\eta+\sigma}(f(x)) = \frac{\sigma x^{-\sigma(\eta+\alpha)}}{\Gamma(\alpha)} \int_0^x \frac{t^{\sigma\eta+\sigma-1} f(t)}{(t^{\sigma}-x^{\sigma})^{1-\alpha}} dt.$$

With Hadamard type, we have the following definition (8.8)

$$D^{\alpha}_0\big(f(x)\big) = \frac{1}{\Gamma(n-\alpha)}\Big(x\frac{d}{dx}\Big)^n \int_0^x \Big(log\frac{x}{t}\Big)^{n-\alpha-1} f(t)\frac{dt}{t}.$$

With Riesz type, we have the following definition (8.9)

$$D^{\alpha}_x\big(f(x)\big) = -\frac{1}{2\cos\left(\frac{\alpha\pi}{2}\right)}\left\{\frac{1}{\Gamma(\alpha)}\Big(\frac{d}{dx}\Big)^m\left(\int_{-\infty}^{x}(x-t)^{m-\alpha-1} f(t)dt + \int_x^{\infty}(t-x)^{m-\alpha-1} f(t)dt\right)\right\}.$$

We will not mention the Grunward-Letnikov type here because it is in series form. This is not more suitable for analytical purpose.

In 1998, (Davison and Essex, 1998) published a paper which provides a variation to the Riemann-Liouville definition suitable for conventional initial value problems within the realm of fractional calculus. The definition is as follows (8.10)

$$D^{\alpha}_0 f(x) = \frac{d^{n+1-k}}{dx^{n+1-k}} \int_0^x \frac{(x-t)^{-\alpha}}{\Gamma(1-\alpha)} \frac{d^k f(t)}{dt^k} dt$$

In an article published by (Coimbra, 2003), a variable order differential operator is defined as follows: (8.11)

$$D^{\alpha(t)}_0(f(x)) = \frac{1}{\Gamma\big(1-\alpha(x)\big)} \int_0^x (x-t)^{-\alpha(t)} \frac{df(t)}{dt} dt + \frac{\big(f(0^+)-f(0^-)\big)x^{-\alpha(x)}}{\Gamma\big(1-\alpha(x)\big)}$$

8.2 ADVANTAGES AND DISADVANTAGES

8.2.1 Advantages

It is very important to point out that all these fractional derivative order definitions has theirs advantages and disadvantages, here we shall include, Caputo, variational order, Riemann-Liouville, Jumarie and Weyl. We shall examine first the variation order differential operator. Anomalous diffusion phenomena are extensively observed in physics, chemistry and biology fields (Solomon *et al.*, 1993; Bhalekar *et al.*, 2011; Magin *et al.*, 2008; Magin, 2006). To characterize anomalous diffusion phenomena, constant-order fractional diffusion equations are introduced and have received tremendous success. However, it has been

found that the constant order fractional diffusion equations are not capable of characterizing some complex diffusion processes, for instance, diffusion process in inhomogeneous or heterogeneous medium (Chechkin *et al.*, 2005). In addition, when we consider diffusion process in porous medium, if the medium structure or external field changes with time, in this situation, the constant-order fractional diffusion equation model cannot be used to well characterize such phenomenon (Santamaria *et al.*, 2006; Sun *et al.*, 2009). Still in some biology diffusion processes, the concentration of particles will determine the diffusion pattern (Sun *et al.*, 2009; de Azevedo *et al.*, 2006). To solve the above problems, the variable-order (VO) fractional diffusion equation models have been suggested for use (Chechkin *et al.*, 2005; Sun *et al.*,2011; Umarov and Steinberg, 2009).

The ground-breaking work of VO operator can be traced to Samko *et al.* by introducing the variable order integration and Riemann–Liouville derivative in 1993 (Samko and Ross,1993; Ross and Samko, 1995). It has been recognized as a powerful modelling approach in the fields of viscoelasticity (Coimbra, 2003), viscoelastic deformation (Ingman and Suzdalnitsky, 2005), viscous fluid (Pedro *et al.*, 2008), anomalous diffusion (Kobelev *et al.*, 2003), Schrödinger equation (Atangana and Cloot, 2013) and groundwater flow (Atangana and Botha, 2013) etc.....

With the Jumarie definition which is actually the modified Riemann-Liouville fractional derivative, an arbitrary continuous function needs not to be differentiable; the fractional derivative of a constant is equal to zero and more importantly it removes singularity at the origin for all functions for which $f(0) = \text{constant}$ for instance the exponentials functions, Mittag-Leffler functions and so on.

With the Riemann-Liouville fractional derivative, an arbitrary function needs not to be continuous at the origin and it needs not to be differentiable.

One of the great advantages of the Caputo fractional derivative is that, it allows traditional initial and boundary conditions to be included in the formulation of the problem. In addition its derivative for a constant is zero.

It is customary in groundwater investigations to choose a point on the centreline of the pumped borehole as a reference for the observations and therefore neither the drawdown nor its derivatives will vanish at the origin, as required (Cloot and Botha, 2006). In such situations where the distribution of the piezometric head in the aquifer is a decreasing function of the distance from the borehole the problem may be circumvented by rather using the complementary, or Weyl, fractional order derivative (Cloot and Botha, 2006) (Atangana, 2012).

8.2.2 Disadvantages

Although these fractional derivative display advantages, they are not applicable in all the situations however. We shall begin with the Liouville-Riemann type(Atangana and Secer, 2013) .

The Riemann-Liouville derivative has certain disadvantages when trying to model real-world phenomena with fractional differential equations. The Riemann–Liouville derivative of a constant is not zero. In addition, if an arbitrary function is a constant at the origin, it fractional derivatives has a singularity at the origin, for instance exponential and Mittag-Leffler functions. Theses disadvantages reduce the field of application of the Riemann-Liouville fractional derivative.

Caputo's derivative demands higher conditions of regularity for differentiability: to compute the fractional derivative of a function in the Caputo sense, we must first calculate its derivative. Caputo derivatives are defined only for differentiable functions while functions that have no first order derivative might have fractional derivatives of all orders less than one in the Riemann–Liouville sense (Atangana and Secer, 2013) .

With the Jumarie fractional derivative, if the function is not continuous at the origin, the fractional derivative will not exist, for instance, the fractional derivative of $\ln(x)$, $x^{-1/2}$ and many other one.

Variation order differential operator cannot easily be handled analytically. However, they can be useful for numerical purposes.

Although Weyl fractional derivative found its place in groundwater investigation, its still display a significant disadvantage, because the integral defining these Weyl derivatives are improper, greater restrictions must be placed on a function. For instance the Weyl derivative of a constant is not defined. In addition, general theorem about Weyl derivatives are often more difficult to formulate and prove, as in the case of their corresponding theorems for Riemann-Liouville derivatives (Atangana and Secer, 2013a) .

8.3 DERIVATIVES REVISITED

8.3.1 Variational order differential operator revisited

Let $f: \mathbb{R} \longrightarrow \mathbb{R}, x \longrightarrow f(x)$ denotes a continuous but necessary differentiable, let $\alpha(x)$ be a continuous function in $(0, 1]$. Then its variational order differential in [a,∞) is defined as:

(8.12)

$$D_a^{\alpha(t)}(f(x)) = FP\left(\frac{1}{\Gamma(1-\alpha(x))}\frac{d}{dx}\int_a^x (x-t)^{-\alpha(t)}(f(t)-f(a))\,dt\right).$$

Where FP means finite part of the variation order operator (Atangana and Secer, 2013).
Notice that, the above derivative meets all the requirement of the variational order differential operator; in additional the derivative of the constant is zero, which was not possible with the standard version.

8.3.2 Variational order fractional derivatives via fractional difference revisited

Let $f: \mathbb{R} \longrightarrow \mathbb{R}, x \longrightarrow f(x)$ denotes a continuous but necessary differentiable, let $\alpha(x)$ be a continuous function in (0, 1] and $h > 0$ denote a constant discretization span. Define the forward operator FWh by the expression: (8.13a)

$$FW(h)\big(f(x)\big) \coloneqq f(x+h).$$

Note that, the symbol means that the left side is defined by the right side. Then the variation order fractional difference of order $\alpha(x)$ of $f(x)$ is defined by the expression (8.13b)

$$\Delta^{\alpha(x)} f(x) = (FW-1)^{\alpha(x)} = \sum_{k=0}^{\infty} (-1)^k \frac{1}{\Gamma\big(k-\alpha(x)\big)} f(x-(\alpha(x)-k)h).$$

And its variational order fractional derivative of order $\alpha(x)$ is defined by the limit (8.13c)

$$f^{\alpha(x)}(x) = \lim_{h\to 0} \frac{\Delta^{\alpha(x)}(f(x)-f(0))}{h^{\alpha(x)}}$$

8.3.3 Jumarie fractional derivative revisited

Recently, Guy Jumarie proposed a simple alternative definition to the Riemann–Liouville derivative. His modified Riemann–Liouville derivative has the advantages of both the standard Riemann–Liouville and Caputo fractional derivatives: it is defined for arbitrary continuous (non-differentiable) functions and the fractional derivative of a constant is equal to zero. However if the function is not defined at the origin, the fractional derivative will not exist, therefore in order to circumvent this defeat we propose the following definition (Atangana and Secer, 2013).
Let $f: \mathbb{R} \longrightarrow \mathbb{R}, x \longrightarrow f(x)$ denotes a continuous but necessary at the origin and not necessary differentiable, then its fractional derivative is defined as: (8.14)

$$D_0^{\alpha}(f(x)) = FP\left(\frac{1}{\Gamma(1-\alpha)} \frac{d^n}{dx^n} \int_0^x (x-t)^{n-\alpha-1}(f(t)-f(0))\,dt\right).$$

Where FP means finite part of the variational order operator.
Notice that, the above derivative meets all the requirement of the fractional derivative

operator; the derivative of the constant is zero, in addition the function needs not to be continuous at the origin. With this definition, the fractional derivative of $ln(x)$ is given as

$$D_0^{\alpha}(ln(x)) = -\frac{x^{-\alpha}(EulerGamma + \pi Cot[\pi\,\alpha] - ln(x) + PolyGamma[0,\alpha])}{\Gamma(1-\alpha)}$$

Remark: It is very important to notice that all existing fractional derivation has theirs advantages and disadvantages depending on the function under investigation. These fractional derivatives must be used with care, in particular one will needs to chose a fractional derivative according to the support of the function (Atangana and Secer, 2013a).

8.4 DEFINITIONS AND PROPERTIES

Definition 1 A real function $f(x), x > 0$, is said to be in the space $C_{-\mu}$, $\mu\epsilon\mathbb{R}$ if there exists a real number $p > \mu$, such that $f(x) = x^p h(x)$, where $h(x)\,\epsilon C\,[0,\infty)$, and it is said to be in space C_{μ}^{m} if $f^{(m)}\epsilon\, C_{\mu}$, m∈ℕ

Definition 2 The Riemann-Liouville fractional integral operator of order α≥0, of a function $f\epsilon C\_\mu, \mu \geq -1$, is defined as (8.15)

$$J^{\alpha} f(x) = \frac{1}{\Gamma(\alpha)}\int_0^x (x-t)^{\alpha-1} f(t)dt, \;\; \alpha > 0, x > 0$$

$$J^0 f(x) = f(x).$$

Properties of the operator can be found in (Luchko and Groneflo, 1998) (Oldham and Spanier, 1974) we mention only the following:

For $f\epsilon\, C_{\mu}$, $\mu \geq -1$, $\alpha,\ \beta \geq 0$ and $\gamma > -1$:

$$J^{\alpha}J^{\beta} f(x) = J^{\alpha+\beta} f(x), \qquad J^{\alpha}J^{\beta} f(x) = J^{\beta}J^{\alpha} f(x) \text{and } J^{\alpha}x^{\gamma} = \frac{\Gamma(\gamma+1)}{\Gamma(\alpha+\gamma+1)}x^{\alpha+\gamma} \qquad (8.16)$$

The Riemann-Liouville derivative has certain disadvantages when trying to model real-world phenomena with fractional differential equations. Therefore, we shall introduce a modified fractional differential operator D_{*}^{α} proposed by Caputo in his work on the theory of viscous-elasticity (Caputo, 1967).

Definition 3

The fractional derivative of $f(x)$ in the Caputo sense is defined as (8.17)

$$ {}_a^c D_x^{\alpha} f(x) = J^{m-\alpha} D^m f(x) = \frac{1}{\Gamma(m-\alpha)}\int_a^x (x-t)^{m-\alpha-1} f^m(t)dt,$$

$$m-1 < \alpha \leq m, m \in \mathbb{N}, x > 0, f \in C_{-1}^{\mu}.$$

also, we need here two of its basic properties.

Lemma 1 If $m-1 < \alpha \leq m, m \in \mathbb{N}$ *and* $f \in C_{\mu}^{m}, \mu \geq -1$, *then*

$$ {}_a^c D_x^{\alpha} J^{\alpha} f(x) = f(x) \text{and } J^{\alpha} D_0^{\alpha} f(x) = f(x) - \sum_{k=0}^{m-1} f^{(k)}(0^+)\frac{x^k}{k!}\ ,\ x > 0. \qquad (8.18)$$

Definition 4: Partial Derivatives of Fractional order

Assume now that $f(\boldsymbol{x})$ is a function of n variables $x_i\ i = 1, \dots \dots, n$ also of class C on D∈ $\mathbb{R}_n$. As an extension of definition 3 we define partial derivative of order α for f respect to x_i the function (8.19a)

$$ {}_a^c\partial_{\underline{x}}^{\alpha} f = \frac{1}{\Gamma(m-\alpha)} \int_a^{x_i} (x_i - t)^{m-\alpha-1}\, \partial_{x_i}^m f(x_j)|_{x_j=t} dt. $$

If it exists, where $\partial_{x_i}^m$ is the usual partial derivative of integer order m. Hence, the Caputo fractional derivative is considered because it allows traditional initial and boundaries conditions to be included in the formulation of the problem (Podlubny, 2002).

8.5 FUNDAMENTALS OF THE FRACTIONAL CALCULUS IN MULTIPLE DIMENSIONS

In this section the basic operators and definitions regarding to the calculus in more than one dimension are generalized to the case of derivatives of fractional orders.

8.5.1 Clairaut's theorem for partial derivatives of fractional orders

Assume that $f(\underline{\boldsymbol{x}})$ *is a function which* ${}_{c_i}^{c}\partial_{x_i}^{\alpha}\left[c_j \partial_{x_j}^{\beta} f\right]$ *and* ${}_{c_i}^{c}\partial_{x_j}^{\beta}\left[c_i \partial_{x_i}^{\alpha} f\right]$ *exist are continuous over a domain* $D \in \mathbb{R}_n$ *then* (8.19b)

$$ {}_{c_i}^{c}\partial_{x_i}^{\alpha}\left[c_j \partial_{x_j}^{\beta} f\right] = {}_{c_i}^{c}\partial_{x_j}^{\beta}\left[c_i \partial_{x_i}^{\alpha} f\right], i \neq j $$

Proof: Writing $\alpha = m_i - r_i; \beta = m_j - r_j; 0 < r_i, r_j \leq 1$, we have on one hand that (8.20)

$$ \begin{aligned} {}_{c_i}^{c}\partial_{x_i}^{\alpha}\left[c_j \partial_{x_j}^{\beta} f\right] &= \frac{1}{\Gamma(\mathrm{r_i})\Gamma(\mathrm{r_j})} \int_{c_j}^{x_i} (x_i - t)^{r_i - 1}\, c_i \partial_{x_i}^{m_i} \left[\int_{c_j}^{x_j} \left(x_j - s\right)^{r_j - 1}\, c_j \partial_{x_j}^{m_j} f(\underline{x})|_{s=x_j} ds \right] dt \\ &= \frac{1}{\Gamma(\mathrm{r_i})\Gamma(\mathrm{r_j})} \int_{c_i}^{x_i} [\int_{c_j}^{x_j} (x_i - t)^{r_i} \left(x_j - s\right)^{r_j - 1} c_i \partial_{x_i}^{m_i} [c_j \partial_{x_j}^{m_j}\ f(\underline{x})|_{s=x_j} ds] dt \\ &= \frac{1}{\Gamma(\mathrm{r_i})\Gamma(\mathrm{r_j})} \int_{c_i}^{x_i} \int_{c_j}^{x_j} (x_i - t)^{r_i - 1} \left(x_j - s\right)^{r_j - 1} c_i \partial_{x_i}^{m_i} c_j \partial_{x_j}^{m_j}\ f(\underline{x})|_{s=x_j} ds dt \end{aligned} $$

and on the other hand we have the following (8.21)

$$ \begin{aligned} {}_{c_i}^{c}\partial_{x_j}^{\beta}\left[c_i \partial_{x_i}^{\alpha} f\right] &= \frac{1}{\Gamma(\mathrm{r_j})\Gamma(\mathrm{r_i})} \int_{c_j}^{x_j} (x_j - t)^{r_j - 1}\, c_j \partial_{x_j}^{m_j} \left[\int_{c_i}^{x_i} (x_i - s)^{r_i - 1}\, c_i \partial_{x_i}^{m_i} f(\underline{x})|_{s=x_i} ds \right] dt \\ &= \frac{1}{\Gamma(\mathrm{r_j})\Gamma(\mathrm{r_i})} \int_{x_j}^{x_j} [\int_{c_i}^{x_i} (x_i - t)^{r_i} \left(x_j - s\right)^{r_j - 1} c_j \partial_{x_j}^{m_j} [c_i \partial_{x_i}^{m_i}\ f(\underline{x})|_{s=x_i} ds] dt \\ &= \frac{1}{\Gamma(\mathrm{r_j})\Gamma(\mathrm{r_i})} \int_{x_j}^{x_j} \int_{x_i}^{x_i} (x_i - t)^{r_i} \left(x_j - s\right)^{r_j - 1} c_j \partial_{x_j}^{m_j} c_i \partial_{x_i}^{m_i}\ f(\underline{x})|_{s=x_i} ds dt \end{aligned} $$

Using the continuity hypothesis we have, according to Clairaut (James, 1966) and Fubini (Thomas and Finney, 1996) theorems that the right hand side and identical and thus so are

the left hand sides therefore (8.22)

$$ {}_{c_i}^{c}\partial_{x_i}^{\alpha}\left[c_j\partial_{x_j}^{\beta}f\right] = {}_{c_i}^{c}\partial_{x_j}^{\beta}\left[c_i\partial_{x_i}^{\alpha}f\right],, i \neq j. $$

8.5.2 Gradient, divergence and curl of fractional order

Consider the scalar field $f(\underline{\boldsymbol{x}})$ and the vector field $\underline{\boldsymbol{F}}(\underline{\boldsymbol{x}})$ that are assume to possess partial derivatives of α with respect to all the Cartesian coordinates $x_i\ i = 1, 2,3$. We define the gradient of order α as being the vector field (8.23)

$$ \underline{\mathrm{c}}\nabla_{\underline{x}}^{\alpha}f = \sum_{i=1}^{3}(c_i\partial_{x_i}^{\alpha}f)\,\underline{\boldsymbol{e_i}}. $$

where $\underline{e_i}$ is the unit vector in the "i" direction. The divergence of order α as being the scalar field

$$ \underline{\mathrm{c}}\nabla_{\underline{x}}^{\alpha}.\underline{F} = \sum_{i=1}^{3}c_i\partial_{x_i}^{\alpha}F_i. $$

and the curl of orderαas being the vector field is hence defined as follows. (8.24)

$$ \underline{\mathrm{c}}\nabla_{\underline{x}}^{\alpha}\times\underline{F} = \sum_{i=1}^{3}\left[\sum_{j=1}^{3}\sum_{k=1}^{3}e_{ijk}c_j\partial_{x_j}^{\alpha}F_k\right] $$

where e_{ijk} is the Levi-Civita symbol.

8.5.3 Fundamental relation for gradient, divergence and curl of fractional order

Assuming that the different operations for the scalar and vector fields exist, we have

1. $\underline{\mathrm{c}}\nabla_{\underline{\mathrm{x}}}^{\alpha}(\alpha f+\beta g)=\alpha\underline{\mathrm{c}}\nabla_{\underline{x}}^{\alpha}f+\ \beta\underline{\mathrm{c}}\nabla_{\underline{x}}^{\alpha}g$
2. $\underline{\mathrm{c}}\nabla_{\underline{\mathrm{x}}}^{\alpha}.\left(\alpha\underline{F}+\beta\underline{G}\right)=\alpha\underline{\mathrm{c}}\nabla_{\underline{x}}^{\alpha}.(\underline{F})+\ \beta\underline{\mathrm{c}}\nabla_{\underline{x}}^{\alpha}.(\underline{G}).$ (8. 25)
3. $\underline{\mathrm{c}}\nabla_{\underline{\mathrm{x}}}^{\alpha}\times\left(\alpha\underline{F}+\beta\underline{G}\right)=\ \alpha\underline{\mathrm{c}}\nabla_{\underline{x}}^{\alpha}\times(\underline{F})+\ \beta\underline{\mathrm{c}}\nabla_{\underline{x}}^{\alpha}\times(\underline{G})$
4. $\underline{c}\nabla_{\underline{x}}^{\alpha}.\left[\underline{c}\nabla_{\underline{x}}^{\alpha}\times\underline{F}\right]=0$
5. $\underline{c}\nabla_{\underline{x}}^{\alpha}\times\left[\underline{c}\nabla_{\underline{x}}^{\alpha}f\right]=0$

The first three relations are direct consequences of the linear characteristic of the different operations are fairly trivial to establish. The last two relations rely on Clairaut's result. Consider for example relation (4). We have from the definition of the divergence and curl of fractional order. (8.26)

$$\underline{c}\nabla_{\underline{x}}^{\alpha}.\left[\underline{c}\nabla_{\underline{x}}^{\alpha}\times\underline{F}\right]=\sum_{i=1}^{3}\sum_{j=1}^{3}\sum_{k=1}^{3}e_{ijk}c_i\partial_{x_i}^{\alpha}c_j\nabla_{x_j}^{\alpha}F_{k.}$$

But the Levi-Civita symbol equals to zero whenever two or more indexes take the same value and the triple sum in the relation reduces to

$$\sum_{i=1}^{3}\sum_{j=1}^{3}\sum_{k=1}^{3}e_{ijk}c_i\partial_{x_i}^{\alpha}c_j\,\partial_{x_j}^{\alpha}F_k=\sum_{i=1}^{3}\left(e_{ijk}c_i\partial_{x_i}^{\alpha}\left[c_j\,\partial_{x_j}^{\alpha}F_k-c_k\partial_{x_k}^{\alpha}F_j\right]\right);i\neq j\neq k$$

or (8.27)

$$\underline{c}\nabla_{\underline{x}}^{\alpha}.\left[\underline{c}\nabla_{\underline{x}}^{\alpha}\times\underline{F}\right]=c_i\partial_{x_i}^{\alpha}\left[c_j\,\partial_{x_j}^{\alpha}F_k-c_k\partial_{x_k}^{\alpha}F_j\right]+c_j\partial_{x_j}^{\alpha}\left[c_k\,\partial_{x_k}^{\alpha}F_i-c_i\partial_{x_i}^{\alpha}F_k\right]$$
$$+c_k\partial_{x_k}^{\alpha}\left[c_i\,\partial_{x_i}^{\alpha}F_j-c_j\partial_{x_j}^{\alpha}F_i\right]=0$$

by direct application of the generalized version of Clairaut's theorem. Relation 5 is established using similar arguments as for relation 4.

8.5.4 Directional derivatives of fractional orders

Let $f(\underline{x})$ be a function of n variables for which the gradient of the fractional order α,$\underline{c}\nabla_{\underline{x}}^{\alpha}f$, exists over a domain D of $\mathbb{R}_n$. Then we define the directional derivatives of fractional order α for the function f in the direction $\underline{\theta}$ to be the function (8.28)

$$\underline{c}D_{\underline{\theta}}^{\alpha}f=\underline{c}\nabla_{\underline{x}}^{\alpha}f.\underline{\theta};\left\|\underline{\theta}\right\|=1$$

8.5.5 The generalized Divergence theorem

To recall, let the vector field $\underline{F}$ have continuous derivatives on an open region of the space D containing the volume V and S be the boundary surface of V positively outward orientated. Then we have (8.29)

$$\iiint_{\mathrm{V}}\nabla.\underline{F}d\mathrm{V}=\int\int_{S}\underline{F}.\underline{n}dS.$$

Within the framework of fractional derivatives this theorem can be rephrased as following:

Notation

Let the vector field $\underline{F}$ having partial fractional derivatives of order β with respect to all variables $\underline{x}=(x_1,\ldots.,x_n)^T$ on D. Then we denote by $\underline{c}D_{\underline{x}}^{\beta}\underline{F}$ the vector (8.30)

$$\underline{c}D_{\underline{x}}^{\beta}\underline{F}=\sum_{i=1}^{n}(\underline{e}_{x_i}^{T}\left[\underline{c}\nabla_{\underline{x}}^{\beta}\left(\underline{F}\right)^{T}\right].\underline{e}_{x_i})\,\underline{e}_{x_i}$$

$$= \sum_{i=1}^{n} c_i \partial_{x_i}^{\beta} F_{x_i} \underline{e}_{x_i}$$

Theorem 8.1

Let the vector field $\underline{F}$ *have continuous fractional derivatives of order α on an open region of the space D containing the volume V and S be the boundary surface of V positively outward orientated. Then we have* (8.31)

$$\iiint_V \underline{c}\nabla_{\underline{x}}^{\beta}.\underline{F}dV = \iint_S \underline{c}\mathrm{D}_{\underline{x}}^{\beta-1}\underline{F}.\underline{n}dS.$$

Proof:

The proof of this is very easy once one realize that

$$\underline{c}\nabla_{\underline{x}}^{\beta}.\underline{F} = \nabla_{\underline{x}}.\underline{c}D_{\underline{x}}^{\beta-1}\underline{F}$$

We have then by direct application of the classical version of the divergence theorem (7.32)

$$\iiint_V \underline{c}\nabla_{\underline{x}}^{\beta}.\underline{F}dV = \iint_S \nabla_{\underline{x}}.\underline{c}\mathrm{D}_{\underline{x}}^{\beta-1}\mathrm{F}.\mathrm{n}dS$$

In the similar way, the well known theorems of Green and Stokes of classical vector calculus may be suitable rewritten to accommodate directly the concept of derivatives of fractional orders. We have the following expressions:

Theorem 2: Generalized Green's theorem

Let C be a simple positively orientated, piecewise-smooth, closed curve in $\mathbb{R}_2$*, say the x-y plane, further more let D be the interior of C. If* $f(x,y)$, $g(x,y)$ *are two functions having continuous partial derivatives of fractional order α on D then* (8.33)

$$\iint_D c_x \partial_x^{\alpha} g - c_y \partial_y^{\alpha} f dS = \int_C c_y \partial_y^{\alpha-1} f dx + c_x \partial_x^{\alpha-1} g dy$$

Proof

This is clearly a direct application of the classical version of Green's theorem. Since,

$$\iint_D c_x \partial_x^{\alpha} g - c_y \partial_y^{\alpha} f dS = \iint_D \partial_x (c_x \partial_x^{\alpha-1} g) - \partial_y (c_y \partial_y^{\alpha-1} f) dS \quad (8.34)$$

Hence applying Green's theorem yields (8.35)

$$\iint_D c_x \partial_x^{\alpha} g - c_y \partial_y^{\alpha} f dS = \int_C c_y \partial_y^{\alpha-1} f dx + c_x \partial_x^{\alpha-1} g dy$$

Note that for further purposes, this relation into the plane can be expressed in term of the curl of fractional order α of the vector field $\underline{F} = (f, g, h)$, h being an arbitrary function defined in D.

$$\iint_D \underline{c}\nabla_{\underline{x}}^{\alpha} \times \underline{F}.\underline{n}dS = \int_C c_y \partial_y^{\alpha-1} f dx + c_x \partial_x^{\alpha-1} g dy, \quad (8.36)$$

where $\underline{n}$ is the outward normal to the x-y plane pointing in the direction of $\underline{e_z}$.

Theorem 3: Generalized Stokes's theorem

Let S be a regular surface of class C^2 *described by the parametric equations*

$$\underline{P}(u,v) = \big(x(u,v), y(u,v), z(u,v)\big); u, v \in S, \tag{8.37}$$

where x, y, z *are the Cartesian coordinates. Consider a simple positively orientated, piecewise-smooth, closed curve* C_k *in the* $u - v$ *plane, and let K be the interior of* C_k*. S and C are images of the domain K and its boundary* C_k *in the Cartesian space and* $\underline{F}$ *is a vector field having continuous partial derivatives of fractional order α on S then* (8.38)

$$\iint_S \big[\underline{c}\nabla_{\underline{x}}^{\alpha} \times \underline{F} + \big(\partial_x\big[\underline{c}A_{\underline{x}}^{\alpha-1}\big].F_y\underline{e_y}\big)\underline{e_x} + \big(\partial_y\big[\underline{c}A_{\underline{x}}^{\alpha-1}\big].F_z\underline{e_z}\big)\underline{e_y} + \big(\partial_y\big[\underline{c}A_{\underline{x}}^{\alpha-1}\big].F_x\underline{e_x}\big)\underline{e_z}\big].\underline{n}dS$$
$$= \int_C c_z\partial_z^{\alpha-1}F_x dx + c_x\partial_x^{\alpha-1}F_y dy + c_y\partial_y^{\alpha-1}F_z dz.$$

Hence $\underline{c}A_{\underline{x}}^{\alpha}$ *stands for the differential operator*

$$\underline{c}A_{\underline{x}}^{\alpha} = -1\underline{c}\nabla_{\underline{x}}^{\alpha} \tag{8.39}$$
$$= \big(c_y\partial_y^{\alpha} - c_z\partial_z^{\alpha}\big)\underline{e_x} + (c_z\partial_z^{\alpha} - c_x\partial_x^{\alpha})\underline{e_y} + \big(c_x\partial_x^{\alpha} - c_y\partial_y^{\alpha}\big)\underline{e_z}.$$

While $\underline{n}$ *is the unit positive outside normal to S*

Proof

It is easy to prove this by splitting the line integral

$$\int_C c_z\partial_z^{\alpha-1}F_x dx + c_x\partial_x^{\alpha-1}F_y dy + c_y\partial_y^{\alpha-1}F_z dz.$$

Into 3 components including, $\int_C c_z\partial_z^{\alpha-1}F_x dx$, $\int_C c_x\partial_x^{\alpha-1}F_y dy$ and $\int_C c_y\partial_y^{\alpha-1}F_z dz$. We consider the component $\int_C c_z\partial_z^{\alpha-1}F_x dx$ without loss of generality. Let us assume, for clarity of this purpose, that the boundary C_k can be described by the mean of one single parametric relation C_k:$\big(u(t), v(t)\big); t \in [a,b]$ then the corresponding curve C in the Cartesian space of coordinates is given by

$$\underline{P}(t) = \Big(x\big(u(t), v(t)\big), y\big(u(t), v(t)\big), z\big(u(t), v(t)\big)\Big). \tag{8.40}$$

Therefore, defining ,$f_1 = c_z\partial_z^{\alpha-1}F_x$, we have the following

$$\oint f_1\, dx = \int_a^b f_1((u(t), v(t)))\frac{dx(u(t), v(t))}{dt}dt$$
$$= \int_a^b f_1(u(t), v(t))\,\partial_u x\frac{du}{dt}dt + f_1(u(t), v(t))\partial_v x\frac{dv}{dt}dt$$

$$= \int_{c_k} f_1(u,v)\partial_u x du + f_1(u,v)\partial_v x dv.$$

Hence, applying the Green's theorem in its classical version to this last result gives (8.41)

$$\int_c f_1 dx = \iint_K \partial_u[f_1(u,v)\partial_v x] - \partial_v[f_1(u,v)\partial_u x]dudv = \iint_K \partial_u[f_1\partial_v x] - \partial_v[f_1\partial_u x]dudv$$

$$= \iint_K \left[\partial_x f_1 \partial_u x + \partial_y f_1 \partial_u y + \partial_z f_1 \partial_u z\right]\partial_v x$$

$$- \left[\partial_x f_1 \partial_v x + \partial_y f_1 \partial_v y + \partial_z f_1 \partial_v z\right]\partial_u x du dv$$

$$= \iint_S [\partial_z f_1 \left|\frac{\partial(z,x)}{\partial(u,v)}\right| - \partial_z f_1 \left|\frac{\partial(x,y)}{\partial(u,v)}\right|]dudv$$

$$= \iint_S \left[\partial_z f_1 n_y - \partial_y f_1 n_z\right]dS.$$

Hence $n_y$and n_z are the components of the normal to S, that is (8.42)

$$\underline{n} = (n_x, n_y, n_z) = \frac{\partial_u \underline{x} \times \partial_v \underline{x}}{\left|\partial_u \underline{x} \times \partial_v \underline{x}\right|},$$

or explicitly

$$\int_c c_z \partial_z^{\alpha-1} F_x dx = \iint_S \left[\partial_z (c_z \partial_z^{\alpha-1} F_x) n_y - \partial_y (c_z \partial_z^{\alpha-1} F_x) n_z\right]dS.$$

Repeating the same analogy for the two others line integral components yields (8.43)

$$\int_c c_x \partial_x^{\alpha-1} F_y dy = \iint_S \left[\partial_x (c_x \partial_x^{\alpha-1} F_y) n_z - \partial_z (c_x \partial_x^{\alpha-1} F_y) n_y\right]dS$$

and

$$\int_c c_y \partial_y^{\alpha-1} F_z dz = \iint_S \left[\partial_y (c_y \partial_y^{\alpha-1} F_z) n_x - \partial_x (c_y \partial_y^{\alpha-1} F_z) n_y\right]dS.$$

Now adding those 3 relations and rearranging the terms with respect to the components of the normal vector yields (8.44)

$$\int_C c_z \partial_z^{\alpha-1} F_x dx + c_x \partial_x^{\alpha-1} F_y dy + c_y \partial_y^{\alpha-1} F_z dz$$

$$= \iint_S \partial_z (c_z \partial_z^{\alpha-1} F_x) n_y - \partial_y (c_z \partial_z^{\alpha-1} F_x) n_z$$

$$+ \left[\partial_y \left(c_y \partial_y^{\alpha-1} F_z\right) n_x - \partial_x \left(c_y \partial_y^{\alpha-1} F_z\right) n_y\right] + [\partial_x (c_x \partial_x^{\alpha-1} F_y) n_z$$

$$- \partial_z (c_x \partial_x^{\alpha-1} F_y) n_z] dS.$$

Finally the expected result is obtained by adding to the kernel of the surface integral the term of null value

$$(c_z \partial_z^{\alpha} F_y - c_z \partial_z^{\alpha} F_y) n_x + \left[(c_x \partial_x^{\alpha} F_z) - (c_x \partial_x^{\alpha} F_z)\right] n_y + (c_y \partial_y^{\alpha} F_x - c_y \partial_y^{\alpha} F_x) n_z$$

Indeed we have then that

$$\int_C c_z \partial_z^{\alpha-1} F_x dx + c_x \partial_x^{\alpha-1} F_y dy + c_y \partial_y^{\alpha-1} F_z dz$$

$$= \iint_S \partial_z (c_z \partial_z^{\alpha-1} F_x) n_y - \partial_y (c_z \partial_z^{\alpha-1} F_x) n_z$$

$$+ \left[\partial_y \left(c_y \partial_y^{\alpha-1} F_z\right) n_x - \partial_x \left(c_y \partial_y^{\alpha-1} F_z\right) n_y\right] + [\partial_x (c_x \partial_x^{\alpha-1} F_y) n_z$$

$$- \partial_z (c_x \partial_x^{\alpha-1} F_y) n_z] dS.$$

That is (8.45)

$$\int_C c_z \partial_z^{\alpha-1} F_x dx + c_x \partial_x^{\alpha-1} F_y dy + c_y \partial_y^{\alpha-1} F_z dz$$
$$= \iint_S \left[\underline{c}\nabla_{\underline{x}}^{\alpha} \times \underline{F} + \left(\partial_x \left[\underline{c} A_{\underline{x}}^{\alpha-1}\right].F_y \underline{e}_y\right)\underline{e}_x + \left(\partial_y \left[\underline{c} A_{\underline{x}}^{\alpha-1}\right].F_z \underline{e}_z\right)\underline{e}_y \right.$$
$$\left. + \left(\partial_y \left[\underline{c} A_{\underline{x}}^{\alpha-1}\right].F_x \underline{e}_x\right)\underline{e}_z\right].\underline{n} dS.$$

8.5.6 The Laplace operator of fractional order

With the concept of the gradient of fractional order leads to a possible generalization of the Laplacian of a scalar function. By definition we call the Laplacian of fractional order (α, β) of a scalar functions F the differential operator. (8.46)

$$\underline{c}\nabla_{\underline{q}}^{\alpha}.\left[\underline{c}\nabla_{\underline{q}}^{\beta}\right] = \frac{1}{h_1 h_2 h_3}\left\{\partial_{q_1}\left[\frac{h_1 h_2}{h_1^{\alpha-1}} c_1 \partial_{q_1}^{\alpha-1}\left\{\frac{1}{h_1^{\beta}}(c_1 \partial_{q_1}^{\beta} F)\right\}\right] + \partial_{q_2}\left[\frac{h_1 h_3}{h_2^{\alpha-1}} c_2 \partial_{q_2}^{\alpha-1}\left\{\frac{1}{h_2^{\beta}}(c_2 \partial_{q_2}^{\beta} F)\right\}\right]\right.$$
$$\left. + \partial_{q_3}\left[\frac{h_2 h_3}{h_3^{\alpha-1}} c_3 \partial_{q_3}^{\alpha-1}\left\{\frac{1}{h_3^{\beta}}(c_3 \partial_{q_3}^{\beta} F)\right\}\right]\right\}.$$

In following section the concept of fractional derivative will be used to generalize first the standard form the groundwater flow equation and secondly, the hydrodynamic dispersion equation. An asymptotic solution of this new equation will be investigated via the Adomian decomposition (Atangana, 2012a), Variational Iteration (He, 1977) methods and straightforward resolution of this equation will be investigated in term of Mittag-Leffler function.

8.6 A GENERALIZATION OF THE GROUNDWATER FLOW AND ADVECTION DISPERSION EQUATIONS USING THE CONCEPT OF FRACTIONAL DERIVATIVES ORDERS

Fractional Calculus has been used to model physical and engineering processes, which are found to be best described by fractional differential equations. It is worth nothing that the standard mathematical models of integer-order derivatives, including nonlinear models, do not work adequately in many cases. In the recent years, fractional calculus has played a very important role in various fields such as mechanics, electricity, chemistry, biology, economics, notably control theory, and signal and image processing. Major topics include anomalous diffusion; vibration and control; continuous time random walk; Levy statistics, fractional Brownian motion; fractional neutron point kinetic model; power law; Riesz potential; fractional derivative and fractals; computational fractional derivative equations; nonlocal phenomena; history-dependent process; porous media; fractional filters; biomedical engineering; fractional phase-locked loops; fractional variational principles; fractional transforms; fractional wavelet; fractional predator-prey system; soft matter

mechanics; fractional signal and image processing; singularities analysis and integral representations for fractional differential systems; special functions related to fractional calculus; non-Fourier heat conduction; acoustic dissipation, geophysics; relaxation; creep; viscoelasticity; rheology; fluid dynamics; chaos. An excellent literature of this can be found in (Oldham and Spanier, 1974) (Podlubny, 1999) (Kilbas *et al*., 2006) (Caputo, 1967) (Miller and B. Ross, 1993) (Samko et al, 1993) (Zaslavsky, 2005).

8.6.1 Generalization of groundwater flow equation

A problem that arises naturally in groundwater investigations is to choose an appropriate geometry for the geological system in which the flow occurs. For example, one can use a model based on percolation theory to simulate the flow in a fractured rock system with a very large fracture density or the parallel plate model to simulate flow through a single fracture. However, there are many fractured rock aquifers where the flow of groundwater does not fit conventional geometries. This is in particular the case with the Karoo aquifers in South Africa, characterised by the presence of a very few bedding parallel fractures that serve as the main conduits of water in the aquifers. Attempts to fit a conventional radial flow model to the observed drawdown always yield a fit that underestimates the observed drawdown at early times and overestimates it at later times. The deviation of observations from theoretically expected values is usually an indication that the theory is not implemented correctly, or does not fit the observations. Recent investigations (Van Tonder et al., 2001) suggest that the flow is also influenced by the geometry of the bedding parallel fractures, a feature that Theis cannot account for. It is therefore possible that Theis equation may not be applicable to flow in these fractured aquifers. In an attempt to circumvent this problem, Barker (Barker, 1988) introduced a model in which the geometry of the aquifer is regarded as a fractal. Although this model has been applied with reasonable success in the analysis of hydraulic tests from boreholes in Karoo aquifers (Van der Voort, 2001), it introduces parameters for which no sound definition exist in the case of non-integer flow dimensions.

The law, proposed by Darcy early in the 19thcentury, is relying on experimental results obtained from the flow of water through a one-dimensional sand column, the geometry of which differs completely from that of a fracture. There is therefore a possibility that the Darcy law may not be valid for flow in fractured rock formations but is only a very crude idealisation of the reality. Nevertheless, the relative success achieved by Botha, (Botha et al.,

1998), to describe many of the properties of Karoo aquifers, suggests also that the basic principle underlying this law may be correct: the observed drawdown is to be related to either a variation in the hydraulic conductivity of the aquifer, or a change in the piezometric head. Any new form of the law should therefore reduce to the classical form under the more common conditions. Because $\underline{K}$ is essentially determined by the permeability of the rocks, and not the flow pattern, the gradient term in Theis is the most likely cause for the deviation between the observed and theoretical drawdown observed in the Karoo formations. In this Possibility is further investigated for a radially symmetric form of Theis by replacing the classical first order derivative of the piezometric head by a complementary derivative. It is customary in groundwater investigations to choose a point on the centreline of the pumped borehole as a reference for the observations and therefore neither the drawdown nor its derivatives will vanish at the origin, as required. In such situations where the distribution of the piezometric head in the aquifer is a decreasing function of the distance from the borehole the problem may be circumvented by rather using the complementary, or Weyl, fractional order derivative.

Broadly seen the generalised version of the Darcy law is affecting conceptually the physical content of Darcy's work in mainly two ways. Firstly, the new generalised constitutive equation is not, unlike the usual Darcy relation, satisfying the popular principle of local (spatial) action that postulates that the evolution of a system at a given spatial position and at a given time is only affected by the behaviour of the different variables in the direct neighbourhood around that point. Within the frame of Darcy's law this principle implies that the Darcy velocities may only be expressed as relations containing the value, at that point, of the piezometric head and/or its derivatives. The use of a constitutive relation based on a spatial integration of the piezometric head over the half infinite line is breaking away from this postulate and is allowing for the consideration of more general situations where the groundwater flow at a given point of the aquifer is governed not only by the properties of the piezometric field at that specific position but also depends on the global spatial distribution of that field in soil matrix. Note that there is a close relation between, the flow equation and the mass transport (Advection Dispersion Equation). The successful application of the fractional order derivative to groundwater flow equation lead us to the mass transport equation. The following section deals with the fractional advection equation.

8.7 GENERALIZED ADVECTION DISPERSION EQUATION USING THE CONCEPT OF FRACTIONAL ORDER DERIVATIVES

Dispersion of aqueous tracers in natural systems including heterogeneous soils, aquifers, and rivers, is typically observed to Benon-Fickian, also called ‘‘anomalous”. Anomalous transport is very often found at all scales – from pore scale simulations (Zhang XX, Mouchao , 2007), soil cores (Bromly and Hinz , 2004)(Cortis and Berkowitz , 2004), laboratory experiments (Hatano and Hatano 1998)(Klise *et al.*, 2004) to field scale observations see for example (Adams and Gelhar , 1992) (Benson *et al.*, 2000) and (Deng, 2004). Anomalous transport may be characterized by trailing edges (also called heavy tails) of a plume emanating from a point source, or nonlinear growth of the centred second moment. If the growth rate is faster than linear, the transport is anomalous super-diffusion; slower than linear growth rate is sub-diffusion (Bouchaud and Georges , 1990).The extreme heavy tails of the solute transport dominate problems associated with toxic chemicals: early arrivals pose the most risk, while late arrivals dominate the cost and strategy of cleanup. Proper modelling of anomalous transport of tracers is a truly important step that has not been achieved completely, even after decades of effort. Anomalous transport behaviour may be due to different mechanisms. First, the complex flow velocity in natural, multi-scale heterogeneous media leads to anomalous spreading of a conservative tracer that deviates significantly from a Fickian model. For example, preferential flow paths can enhance spreading of the plume front, resulting in anomalous super-diffusion. Second, mass exchange between relatively mobile and immobile zones can retard the movement of aqueous tracers and result in heavy tails concentration profile, which is typically referred to as a sub-diffusive process (Bouchaud and Georges A, 1990). The second mechanism is due to chemical reactions (including sorption/desorption), where the diffusion and dispersion of solute in the mobile phase can still be Fickian. See also the recent discussion by (Berkowitz et al, 2008).

Numerous numerical experiments indicate that anomalous dispersion cannot be described by the traditional second-order advection– dispersion equation (ADE) without extremely detailed information on the connectivity of high and low hydraulic conductivity (K) sediments (Eggleston and Rojstaczer , 1998) (Zheng and Gorelick, 2003). Five alternative, nonlocal transport techniques have been developed for the use of the general hydrology community. These techniques are the Stochastic Averaging of the classical ADE (SA-ADE) method, the (single- and) multiple-rate mass transfer (MRMT) method, an interested reader can find this method in the recent work (Haggerty *et al.*, 2000) (Haggerty *et al.*,

2002)(Harvey and Gorelick, 1995)(Harvey and Gorelick 2000), also see (Brusseau et al ,1995)(Carrera et al, 1997)(Coats and Smith, 1964)(Gerke and van Genuchten.,1993) the continuous time random walk (CTRW) method (Dentz and Berkowitz , 2003)(Dentz *et al.*, 2004) (Montroll and Weiss, 1965), the time fractional advection–dispersion equation (fADE) method with the time scale index $0 < c < 1$ (Zhang et al, 2006)(Schumer R et al 2003)(Meerschaert and Scheffler, 2004)(Becker-Kern P, 2004), and the space fADE method (Benson *et al.*, 2000, 2001)(Clarke, 2005)(Schumer *et al.,* 2000)(Zhang, 2007). These alternative conceptual models describe nonlocal dependence on either time or space, or both, to explain the development of anomalous dispersion. Here the nomenclature ‘‘nonlocal” follows the definition given by Cushman (Coats and Smith, 1964): ‘‘If the constitutive variable depends on what is happening at a point in space–time or a very small neighbourhood of the point, the variable is said to be local and derived from a local theory . . . On the other hand, if information is needed to define the constitutive variables from regions of space and time distinct from a neighbourhood of the space–time point where evaluation of the variables is to be made, then the theories and constitutive variables are said to be nonlocal in character”. More specifically, the concentration change at some location in time might depend on a wide variety of locations upstream meaning space nonlocality (Cushman and Ginn , 2000)(Molz, 2002)(Schumer *et al.,* 2001)(Zhang, 2007), and it also might depend on the temporal history of concentration ‘‘loading” at that location (time-nonlocality)(Cushman JH, 1991)(Cushman *et al.*, 1994)(Dentz and Berkowitz, 2003)(Dentz *et al.,* 2004) (Neuman, 1993)(Schumer *et al.*, 2003). The temporal nonlocality can be physically attributed to mass transfer of solute between relatively immobile and mobile phases meaning the sorption or desorption mechanism discussed above (Dentz and Berkowitz, 2003)(Dentz *et al.*, 2004) and transport in segregated regions of high and low permeability (Benson DA et, 2001)(Zinn and Harvey, 2003) (Benson DA et al, 2000)(Berkowitz and Scher, 1998). The spatial nonlocality might be due to the high variation and long-range dependence (or long spatial autocorrelation) of permeability (Grabasnjak, 2003)(Herrick, 2002)(Kohlbecker, 2006)(Trefry, 2003) and (Zhang, 2007), including the preferential flow paths discussed above. In this thesis we focus our investigation on the fractional advection dispersion equation (FADE).

With the fundamental of Fractional Calculus in multiple Dimensions we have introduced in the previous section, a possible generalization of dispersion equation can be introduced as follows. From the following equation:

$$\theta D_t c + \rho_b D_t s + q.\nabla c = \nabla.(\theta \mathrm{D}\nabla c) - \lambda(\theta c + \rho_b s) + (c_0 - c) f(\mathrm{x,t}).$$

Hence D_t and ∇c can be replaced by $o\partial_t^\alpha$ and $o\nabla_x^\alpha$ respectively and become

$$\theta o\partial_t^\alpha c + \rho_b o\partial_t^\alpha s + q.o\nabla_x^\alpha c = \quad \nabla(\theta \mathrm{D} o\nabla_x^\alpha c) - \lambda(\theta c + \rho_b s) + (c_0 - c) f(\mathrm{x,t}). \tag{8.57}$$

Where α is a real number lying in (0, 1] and the above equation in this thesis will be called the generalized hydrodynamic dispersion equation. The hydrodynamic dispersion equation in Equation (8.57) is quite complex, from the mathematical point of view, and must be usually be solved numerically in practice until we find a suitable mathematical method to solve it analytically.

The majority of the available analytical solutions for Equation (8.57) are based on three assumptions:

a) There is no discharge from the recharge to the aquifer
b) The Darcy's velocity, q and the dispersion tension, D, are constant
c) The matrix fraction, s(x , t), of dissolved solids can be represented by the Freundlish isotherm.

g) $s(x,t) = K_d\, c(x,t)$

where K_d is the volumetric distribution coefficient. With these assumptions Equation (8.57) can be written in more compact form as

$$R_d D_t c + q.\nabla c = \nabla.(\theta \boldsymbol{D_h} \nabla c) - \lambda R_d c, \tag{8.58}$$

for the standard case . In order to include explicitly the possible effect of the flow geometry into the mathematical model the Cartesian component of the gradient of the concentration, Δc is replaced here by Caputo fractional derivative $o\nabla_x^\alpha$ of order α. This provides a generalized form of the classical equation governing the dispersion (8.58)

$$R_d o\partial_t^\beta c + q.o\nabla_x^\alpha c = \nabla(\theta \boldsymbol{D_h} o\nabla_x^\alpha c) - \lambda R_d c. \tag{8.59}$$

This integro-differential equation does contain the additional parameters including, βandα, which can be viewed as a new physical parameters that characterizes the dispersion through the geological formations and hence also,

$$R_d = \theta + \rho_b K_d \tag{8.60}$$

is known as the retardation factor. Two particular important sets of problems, that satisfy these assumptions, are the set of the one-dimensional problems, characterized by

$$q = iq_x \text{ and} \theta D_h = \alpha_L \mathrm{q} \tag{8.61}$$

and the set of two-dimensional problems characterized by

$$q = iq_x + q_y j \quad \text{and} \quad \theta D_h = i\alpha_L q_x + j\alpha_T q_y = iD_L + jD_T.$$

In these cases Equation (7.59) can be divided through by R_d to obtain

$$\partial_t^\beta c + \mathrm{q_r}.o\nabla_x^\alpha c = \nabla(\theta \mathrm{D_r} o \nabla_x^\alpha c) - \lambda c. \tag{8.62}$$

For the generalized form and here

$$\mathrm{q_r} = \frac{\mathrm{q}}{\mathrm{R_d}} \quad \text{and} \quad \mathrm{D_r} = \frac{\mathrm{D}}{R_d}$$

are the retarded velocity vector and hydrodynamic dispersion coefficient, respectively. Notice that since $R_d \geq \theta$, and $\mathrm{q_r} \leq \mathrm{q}$, the Darcy velocity of the fluid, hence the name retardation coefficient for R_d. For Equation (8.62) there is no analytical solution is available for the moment being. In the discussion to follow attention will be, therefore, limited to a simple one-dimensional Dirichlet boundary condition problem.

8.7.1 Solution of generalized form of advection dispersion equation via Adomian decomposition and Variational Iteration methods

As V.M. Alexandrov wrote in the foreword of a popular science book ‘‘Asymtotology: ideas, methods, and applications’’, asymptotic methods belong to the, perhaps, most romantic area of modern mathematics (Andrianov and Manevitch, 2003). Though computer science is growing very fast, and numerical simulation is applied everywhere, non-numerical issues will still play a large role (Andrianov and Awrejcewicz, 2000; (Bender *et al.*, 1989); Delamotte, 1993; He, 1999). There exists some alternative analytical asymptotic approaches, such as the non-perturbative method, modified Lindstedt–Poincare method (Delamotte, 1993), variational iteration method (He, 1999), Adomian decomposition method (ADM), homotopy perturbation method (He, 1999; He, 2000), book-keeping artificial parameter perturbation method (He, 2001) and the homotopy decomposition method by Atangana see in (Atangana and Alabaraoye, 2013) (Atangana *et al*., 2013) and (Atangana and Secer, 2013b) . Our concern here is to make use of VIM and ADM to provide asymptotic solutions to the fractional advection dispersion equations. For the case of generalized form of advection dispersion equation, two different methods will be used to investigate a possible analytical solution, including the Adomian Decomposition and variational iteration methods. The equation under investigation is the one-dimensional space-time fractional advection dispersion equation as shown below.

$$\partial_t^\alpha c(x,t) + \mathrm{q_r}\partial_x^\beta \mathrm{c}(x,t) - \mathrm{D_r}\partial_x^\mu c(x,t) + \lambda c(x,t) = 0. \tag{8.63}$$

Subject to the initial condition

$$c(x,0) = 0$$

and boundary conditions

$$\partial_x^{\beta} c(x,t) = 0 \qquad (x \to \infty),$$

here the operator $o\partial_x^{\beta}$ is fractional derivative in Caputo -Weyl sense which, because we want our solution to vanish at infinity and

$$c(0,t) = c_0 \exp(-\gamma t) \qquad (t > 0),$$

where $0 < \alpha \leq 1$,$0 < \beta \leq 1$ and $1 < \mu \leq 2$; c_0 is the initial concentration and γ a is positive constant.

Adomian Decomposition method

Hence the method is based on applying the operator J^{β}, the inverse operator of ∂_x^{β}, on both sides of the Equation (7.63) to obtain: (8.64)

$$\mathrm{q_r} c(x,t) = \sum_{k=0}^{m-1} \frac{\partial^{\beta} c(0,t) x^k}{\partial x^k} + J_x^{\beta}\left[\mathrm{D_r} \partial_x^{\mu} c(x,t) - \partial_t^{\alpha} c(x,t) - \lambda c(x,t)\right].$$

The Adomian decomposition method (Adomian, 1988) assumes a series solution for $c(x,t)$ given by

$$c(x,t) = \sum_{n=0}^{\infty} c_n(x,t),$$

where the component $c_n(x,t)$ will be determined recursively, substituting this in Equation (8.64) yields (8.65)

$$\mathrm{q_r} \sum_{n=0}^{\infty} c_n(x,t) = \sum_{k=0}^{m-1} \frac{\partial^{\beta} c(0,t) x^k}{\partial x^k} + J_x^{\beta}\left[\mathrm{D_r} o\partial_x^{\mu} \sum_{n=0}^{\infty} c_n(x,t) - \infty \partial_t^{\alpha} \sum_{n=0}^{\infty} c_n(x,t) - \lambda \sum_{n=0}^{\infty} c_n(x,t)\right].$$

To the following decomposition method we introduce the recursive relation as

$$c_{n+1}(x,t) = \frac{1}{\mathrm{q_r}} J_x^{\beta}\left[-o\partial_t^{\alpha} c_n(x,t) + \mathrm{D_r} o\partial_x^{\mu} c_n(x,t) - \lambda c_n(x,t)\right], \tag{8.66}$$

$$c_0(x,t) = \sum_{k=0}^{m-1} \frac{\partial^{\beta} c(0,t) x^k}{\partial x^k}.$$

It is worth noting that if the zero's component $c_0(x,t)$ is known then the remaining

components $c_n(x,t)$, $n \geq 1$, can be completely determined such that each term is determined by using the previous terms, and the series solutions are entirely determined. Finally, we approximate the solution $c(x,t)$by the truncated series

$$c_N(x,t) = \sum_{n=0}^{N-1} c_n(x,t) \text{ and } \quad \lim_{N\to\infty} c_N(x,t) = c(x,t). \tag{8.67}$$

For our purpose, we used the Dirichlet initial and boundary conditions as defined previously. Therefore the recursive relation is given as

$$c_0(x,t) = c(0,t) = c_0 \exp(-\gamma t)\,, \quad t > 0\,.$$

Following the discussion presented earlier, we obtain the recurrence relation

$$c_{n+1}(x,t) = \frac{1}{\mathrm{q_r}} J_x^{\beta}\left[-o\partial_t^{\alpha} c_n(x,t) + \mathrm{D_r} o\partial_x^{\mu} c_n(x,t) - \lambda c_n(x,t)\right], \tag{8.68}$$

It follows from the above recurrence formula that.

$$c_1(x,t) = \frac{1}{\mathrm{q_r}} J_x^{\beta}\left[-o\partial_t^{\alpha} c_0(x,t) + \mathrm{D_r} o\partial_x^{\mu} c_0(x,t) - \lambda c_0(x,t)\right]$$

$$= \frac{1}{\mathrm{q_r}} J_x^{\beta}\left[-o\partial_t^{\alpha} c_0 \exp(-\gamma t) + \mathrm{D_r} o\partial_x^{\mu} c_0 \exp(-\gamma t) - \lambda c_0 \exp(-\gamma t)\right]$$

$$= \frac{1}{\mathrm{q_r}} J_x^{\beta}\left[-o\partial_t^{\alpha} c_0 \exp(-\gamma t) - \lambda c_0 \exp(-\gamma t)\right]$$

$$= \frac{1}{\mathrm{q_r}} J_x^{\beta}\left[(-\gamma)^{\alpha} c_0 \exp(-\gamma t) - \lambda c_0 \exp(-\gamma t)\right]$$

$$= \frac{1}{\mathrm{q_r}} c_0 \exp(-\gamma t)\,(-(\gamma)^{\alpha} - \lambda)\frac{x^{\beta}}{\Gamma(1+\beta)}.$$

$$c_2(x,t) = \frac{1}{\mathrm{q_r}} J_x^{\beta}\left[-o\partial_t^{\alpha} c_1(x,t) + \mathrm{D_r} o\partial_x^{\mu} c_1(x,t) - \lambda c_1(x,t)\right]$$

$$= \left(\frac{1}{\mathrm{q_r}}\right)^2 \{-(\gamma)^{\alpha} - \lambda\} c_0 \exp(-\gamma t)\left[\{-(-\gamma)^{\alpha} - \lambda\}\frac{x^{2\beta}}{\Gamma(2\beta+1)} + \mathrm{D_r}\frac{x^{2\beta-\mu}}{\Gamma(2\beta-\mu+1)}\right].$$

$$c_3(x,t) = \frac{1}{\mathrm{q_r}} J_x^{\beta}\left[-o\partial_t^{\alpha} c_2(x,t) + \mathrm{D_r} o\partial_x^{\mu} c_2(x,t) - \lambda c_2(x,t)\right]$$

$$o\partial_x^{\mu} c_2(x,t) = \left(\frac{1}{\mathrm{q_r}}\right)^2 \{-(\gamma)^{\alpha} - \lambda\} \exp(-\gamma t)\left[\frac{x^{2\beta-\mu}}{\Gamma(2\beta-\mu+1)} + \mathrm{D_r}\frac{x^{2\beta-2\mu}}{\Gamma(2\beta-2\mu+1)}\right].$$

$$o\partial_t^{\alpha} c_2(x,t) = (-\gamma)^{\alpha}\left(\frac{1}{\mathrm{q_r}}\right)^2 \{-(\gamma)^{\alpha} - \lambda\} c_0 \exp(-\gamma t)\left[\{-(\gamma)^{\alpha} - \lambda\}\frac{x^{2\beta}}{\Gamma(2\beta+1)}\right.$$

$$\left. + \mathrm{D_r}\frac{x^{2\beta-\mu}}{\Gamma(2\beta-\mu+1)}\right].$$

Thus

$$c_3(x,t) = \left(\frac{1}{\mathrm{q_r}}\right)^3 \{-(\gamma)^\alpha - \lambda\} \exp(-\gamma t) \left[\mathrm{D_r} \left[\frac{x^{3\beta-\mu}}{\Gamma(3\beta-\mu+1)} + \mathrm{D_r} \frac{x^{3\beta-2\mu}}{\Gamma(3\beta-2\mu+1)} \right] + \{-(\gamma)^\alpha - \lambda\} \left[\{-(\gamma)^\alpha - \lambda\} \frac{x^{3\beta}}{\Gamma(3\beta+1)} + \mathrm{D_r} \frac{x^{3\beta-\mu}}{\Gamma(3\beta-\mu+1)} \right] \right].$$

In this case, four components of the decomposition series of Equation (8.66) were obtained, of which $c(x,t)$ was evaluated to have the following asymptotic expansion. But is very important to know that, for practise purpose, one will need compute the number terms that will fit the experimental data.

$$c(x,t) = c_0(x,t) + c_1(x,t) + c_2(x,t) + c_3(x,t) + \cdots + \tag{8.69}$$

Using the package mathematica, we roughly approximate the above series solution to:

$$c(x,t) = \frac{exp(-\gamma^\alpha t)}{2} \left[E_{\mu,\beta} \left[\frac{x(q_r - u_r)}{2D_r} \right] erfc \frac{x - u_r t}{2\sqrt{D_r t}} + E_{\mu,\beta} \left[\frac{x(q_r + u_r)}{2D_r} \right] erfc \frac{x + u_r t}{2\sqrt{D_r t}} \right]$$

Where $E_{\mu,\beta}$ is the generalized Mittag-Leffler function

Variation Iteration Method

To solve the generalized hydrodynamic dispersion equation by means of variational iteration method (He, 1977), we rewrite Equation (8.61) in the form (8.70)

$$(c(x,t))_{\alpha t} + \mathrm{q_r}(\mathrm{c}(x,t))_{x\beta} - (c(x,t))_{x\mu} + \lambda c(x,t) = 0$$

Where α, β and μ are the parameters defined previously. The correction functional for the above equation can be approximately expresses as follows (8.71)

$$c_{n+1}(x,t) = c_n(x,t) + \int_0^x \tau(\zeta) \left(\frac{\partial}{\partial \zeta} c_n(\zeta,t) + (\tilde{c}(\zeta,t))_{\alpha t} - (\tilde{c}(\zeta,t))_{x\mu} + \lambda \tilde{c}(\zeta,t) \right) d\zeta,$$

where τ is a general Lagrange multiplier (Inokuti *et al*, 1978), which can be identified optimally via variational theory, here $(\tilde{c}(t,\zeta))_{\alpha t}$, $(\tilde{c}(t,\zeta))_{x\mu}$ and $\tilde{c}(t,\zeta)$ are considered as restricted variations. Making the above functional stationary,

$$\delta c_{n+1}(x,t) = \delta c_n(x,t) + \delta \int_0^x \tau(\zeta) \frac{\partial}{\partial \zeta} c_n(\zeta,t) d\zeta$$

yields the following Lagrange multiplier $\tau = -1$. Therefore we obtain the following iteration formula: (8.72)

$$c_{n+1}(x,t) = c_n(x,t) - \int_0^x \left((c_n(\zeta,t))_{\alpha t} + \mathrm{q_r}(\mathrm{c_n}(\zeta,t))_{x\beta} - (c_n(\zeta,t))_{x\mu} + \lambda c_n(\zeta,t) \right) d\zeta.$$

In this case we begin with the initial approximation

$$c_0(0,t) = c_0 \exp(-\gamma t),$$

By the above iteration formula, begin with$c_0(0,t)$, we can obtain the following approximation (8.73)

$$c_0(0,t) = c_0 \exp(-\gamma t)$$

$$c_1(x,t) = c_0(x,t) - \int_0^x \Big((c_0(\zeta,t))_{\alpha t} + \mathrm{q_r}(c_0(\zeta,t))_{x\beta} - \mathrm{D_r}(c_0(\zeta,t))_{x\mu} + \lambda c_0(\zeta,t) \Big) d\zeta$$

$$= c_0 \exp(-\gamma t) + (-(-\gamma)^{\alpha} - \lambda) c_0 \exp(-\gamma t) x$$

$$= c_0 \exp(-\gamma t)\,[1 + (-(-\gamma)^{\alpha} - \lambda)x].$$

$$c_2(x,t) = c_1(x,t) - \int_0^x \left[-2\gamma^{\alpha} - \mathrm{q_r}(\gamma^{\alpha} - \lambda) \frac{\Gamma(2)\zeta^{1-\beta}}{\Gamma(2-\beta)} + \lambda[1 + (\gamma^{\alpha} - \lambda)\zeta] \right] d\zeta$$

$$= c_1(x,t) - c_0 \exp(-\gamma t) \left[-2\gamma^{\alpha} x - \mathrm{q_r}(\gamma^{\alpha} - \lambda) \frac{\Gamma(2)x^{2-\beta}}{\Gamma(2-\beta)(2-\beta)} + \lambda[x + (\gamma^{\alpha} - \lambda)\frac{x^2}{2}] \right]$$

$$= c_0 \exp(-\gamma t) \left[1 + (\gamma^{\alpha} - \lambda)x + 2\gamma^{\alpha} x + \mathrm{q_r}(\gamma^{\alpha} - \lambda) \frac{\Gamma(2)x^{2-\beta}}{\Gamma(2-\beta)(2-\beta)} - \lambda[x + (\gamma^{\alpha} - \lambda)\frac{x^2}{2} \right].$$

In this case three components of the series Equation (8.43) were obtained of which $c(x,t)$ was evaluated to have the following asymptotic expansion

$$c(x,t) = c_0(x,t) + c_1(x,t) + c_2(x,t) + \cdots + \quad (8.74)$$

It is worth noting that the solution obtained via Variation Iteration Method has repeated terms. To reduce the repeated terms in this solution one need to cancel the repeated terms or while calculating c_n component, and then, the last component gives the approximated solution of the differential equation. The following example is used as illustration. Consider the differential equation describing the rate at which the radioactive material disintegrates, that is

$$DN(t) = -\gamma N(t).$$

The analytical solution of the above differential equation is given as

$$N(t) = N(0) \exp(-\gamma t).$$

For the Variation iteration method the following recursive formula is considered

$$N_{n+1}(t) = N_n(t) - \int_0^t \big(DN_n(\zeta) - \gamma N_n(\zeta) \big) d\zeta,$$

with $N_0(t) = N(0)$

Here for any $\geq 1, N_n(t) = N(0)[1 + \sum_{k=1}^{n} \frac{(-\gamma t)^k}{k!}]$, it follows that when n is approaching infinity $N_{\infty}(t) = N(0) \sum_{k=0}^{\infty} \frac{(-\gamma t)^k}{k!} = N(0) \exp(-\gamma t)$, which is the exact solution of the

equation.

8.7.2 Analytical solution of space-time fractional derivative of hydrodynamic advection-dispersion equation in term of Mittag-Leffler function

In this section a straight fort method will be used to give an analytical solution of space-time fractional derivative of hydrodynamic advection-dispersion equation in term of Mittag-Leffler function. The method is based on Laplace transform, due to the complexity of the Mittag-Leffler function, the graphical representation will not be given in this thesis. We start this analysis with the fractional derivative according to Riemann-Liouville, following by the fractional derivative according to Caputo (Atangana and Kilicman, 2013).

Case 1 Fractional derivative in Riemann-Liouville sense

The method here consists of applying the Laplace transform with respect to the time variable on both sides of equation (8.63) to have

$$D\frac{\partial^{\alpha}c(x,s)}{\partial x^{\alpha}} - v\frac{\partial^{\beta}c(x,s)}{\partial x^{\beta}} - R(\lambda + s)c(x,s) = Rc(x,0), \tag{8.75}$$

with the initial condition and further transformation, the above equation can then be in the following-form (8.76)

$$\frac{\partial^{\alpha}c(x,s)}{\partial x^{\alpha}} - \mu\frac{\partial^{\beta}c(x,s)}{\partial x^{\beta}} - \tau\, c(x,s) = 0,$$

where s is the Laplace variable, $\mu = \frac{v}{D}$ and $\tau = \frac{R(\lambda+s)}{D}$. Let $c(x,s) = y(x)$, the equation (8.76) becomes: (8.77)

$$\frac{\partial^{\alpha}y(x)}{\partial x^{\alpha}} - \mu\frac{\partial^{\beta}y(x)}{\partial x^{\beta}} - \tau\, y(x) = 0.$$

Applying the Laplace operator respect to the space variable on both sides of equation (7.77), on the space component and replacing we have the following equation:

$$\mathcal{L}(y)(p) = \sum_{i=1}^{l} h_i \frac{p^{i-1}}{p^{\alpha} - \mu\, p^{\beta} - \tau} \tag{8.78}$$

where p is the Laplace variable for the space varaible and $h_i = \partial_x^{\alpha-i}c(0^+)$.

For $p \in \mathbb{C}$ and $\left|\frac{\tau p^{-\beta}}{p^{\alpha-\beta}-\mu}\right| < 1$, we have the following expression $\frac{1}{p^{\alpha}-\mu\, p^{\beta}-\tau}$ can be writing as follows:

$$\frac{p^{i-1}}{p^{\alpha} - \mu\, p^{\beta} - \tau} = p^{i-1}\sum_{j=0}^{\infty}\frac{\tau^n p^{-\beta-\beta n}}{(p^{\alpha-\beta}-\mu)^{n+1}},$$

and hence replacing the above expression in equation (8.78) yields to the following representation: (8.79)

$$(\mathcal{L}y)(p) = \sum_{i=1}^{l} h_i \sum_{j=0}^{\infty} \frac{\tau^n p^{-\beta-\beta n+i-1}}{(p^{\alpha-\beta}-\mu)^{n+1}}.$$

The above expression is then simplified further, for $p \in \mathbb{C}$ and $\left|\mu p^{\beta-\alpha}\right| < 1$, we have that first,

$$\frac{\tau^n p^{-\beta-\beta n+i-1}}{(p^{\alpha-\beta}-\mu)^{n+1}} = \frac{\tau^n p^{(\alpha-\beta)-(\alpha+\beta n-i+1)}}{(p^{\alpha-\beta}-\mu)^{n+1}},$$

and secondly the above equation can now be expressed as follows (8.80)

$$= \frac{1}{n!}\mathcal{L}\left\{x^{\alpha n+\alpha-i}\left(\frac{\partial}{\partial x}\right)^n E_{\alpha-\beta,\alpha+n\beta+1-i}(\mu x^{\alpha-\beta})\right\}$$

where

$$\left(\frac{\partial}{\partial x}\right)^n E_{\alpha,\beta}(x) = \sum_{j=0}^{\infty} \frac{\Gamma(n+j+1)}{\Gamma(n\alpha+\beta+\alpha j)} \frac{x^j}{j!}.$$

Hence the solutions of equation (8.77) can be given as follows (8.81)

$$y_i(x) = \sum_{n=0}^{\infty} \frac{\tau^n}{n!} x^{\alpha n+\alpha-i}\left(\frac{\partial}{\partial x}\right)^n E_{\alpha-\beta,\ \alpha+\beta n+1-i}(\mu x^{\alpha-\beta})$$

Thus it follows that the solution of equation (8.63) is given as: (8.82)

$$y(x) = \sum_{i=1}^{l} h_i y_i\,(x)$$

In our case here $l = 2$ so that

$$c(x,s) = \sum_{i=1}^{2} h_i c_i\,(x,s)$$

Thus the series solution of equation (7.63) can be now given by applying the inverse Laplace operator on $c(x,s)$ to have: (8.83)

$$c_i(x,t) = \mathcal{L}^{-1}\left(\sum_{n=0}^{\infty} \frac{\tau^n}{n!} x^{\alpha n+\alpha-i}\left(\frac{\partial}{\partial x}\right)^n E_{\alpha-\beta,\ \alpha+\beta n+1-i}(\mu x^{\alpha-\beta})\right).$$

Since the inverse Laplace operator is a linear operator it follows that (8.84)

$$c_i(x,t) = \sum_{n=0}^{\infty} \frac{\mathcal{L}^{-1}(\tau^n)}{n!} x^{\alpha n+\alpha-i}\left(\frac{\partial}{\partial x}\right)^n E_{\alpha-\beta,\ \alpha+\beta n+1-i}\left(\mu x^{\alpha-\beta}\right).$$

Replacing $\tau^n = \left(\frac{R(\lambda+s)}{D}\right)^n = \left(\frac{R}{D}\right)^n (\lambda+s)^n$ so that (8.85)

$$\mathcal{L}^{-1}\{\tau^n\} = \left(\frac{R}{D}\right)^n \mathcal{L}^{-1}\{(\lambda+s)^n\} = \left(\frac{R}{D}\right)^n \frac{\exp\{-\lambda t\} t^{-1-n}}{\Gamma(-n)}$$

$$c_i(x,t) = \sum_{n=0}^{\infty} \frac{\left(\frac{R}{D}\right)^n \frac{\exp\{-\lambda t\} t^{-1-n}}{\Gamma(-n)}}{n!} x^{\alpha n+\alpha-i} \left(\frac{\partial}{\partial x}\right)^n E_{\alpha-\beta,\ \alpha+\beta n+1-i}\left(\mu x^{\alpha-\beta}\right).$$

(8.86)

$$c(x,t) = \sum_{i=1}^{2} h_i c_i\,(x,t)$$

$$c_1(x,t) = \sum_{n=0}^{\infty} \frac{\left(\frac{R}{D}\right)^n \frac{\exp\{-\lambda t\} t^{-1-n}}{\Gamma(-n)}}{n!} x^{\alpha n+\alpha-1} \left(\frac{\partial}{\partial x}\right)^n E_{\alpha-\beta,\ \alpha+\beta n}(\mu x^{\alpha-\beta})$$

(8.89)

$$c_2(x,t) = \sum_{n=0}^{\infty} \frac{\left(\frac{R}{D}\right)^n \frac{\exp\{-\lambda t\} t^{-1-n}}{\Gamma(-n)}}{n!} x^{\alpha n+\alpha-2} \left(\frac{\partial}{\partial x}\right)^n E_{\alpha-\beta,\ \alpha+\alpha n-1}(\mu x^{\alpha-\beta}).$$

To find the coefficient h_i, $i = 1,2$, we need to apply the boundary and initial conditions on $c(x,t)$ yields to :

$$h_i = \frac{c_0}{2}.$$

Example 1

Our concern here is to consider equation (8.63) when $\alpha = 2$ and $0 < \beta \leq 1$. Following the discursion presented earlier, the analytical solution ofspace-time fractional derivative of hydrodynamic advection-dispersion equation has its two solutions given by:

$$c_1(x,t) = \sum_{n=0}^{\infty} \frac{\exp\{-\lambda t\}\, t^{-1-n}}{\Gamma(-n)n!} x^{2n+1} \left(\frac{\partial}{\partial x}\right)^n E_{2-\beta,2}\left(\frac{R}{D} x^{2-\beta}\right)$$

(8.90)

$$c_2(x,t) = \sum_{n=0}^{\infty} \frac{\exp\{-\lambda t\}\, t^{-1-n}}{\Gamma(-n)n!} x^{2n} \left(\frac{\partial}{\partial x}\right)^n E_{2-\beta,2}\left(\frac{R}{D} x^{2-\beta}\right)$$

The above solutions form the fundamental system of solution when $\beta < 1$.

Case 2 Fractional derivative in Caputo sense

The Riemann-Liouville derivative has certain disadvantages when trying to model real-world phenomena with fractional differential equations. Therefore, investigate the solution of space-time Caputo fractional derivative of hydrodynamic advection-dispersion equation.

For the Caputo derivative, the Laplace transform is based on the formula:

$$(\mathcal{L}\, cD^{\alpha} y)(s) = s^{\alpha}(\mathcal{L}y)(s) - \sum_{i=0}^{2-1} h_i\, s^{\alpha-i-1}$$

with (8.91)

$$h_i = y^{i}(0) \quad (i = 0,1)$$

Thus applying the Laplace transform in both side of equation (8.63) on the component of time, and applying again the Laplace transform on the component of space yields to: (8.92)

$$\mathcal{L}(y)(p) = \sum_{i=0}^{2-1} h_i \frac{p^{\alpha-i-1}}{p^{\alpha} - \mu\, p^{\beta} - \tau} - \mu \sum_{i=0}^{1-1} h_i \frac{p^{\beta-i-1}}{p^{\alpha} - \mu\, p^{\beta} - \tau}.$$

For $p \in \mathbb{C}$ and $\left|\frac{\tau p^{-\beta}}{p^{\alpha-\beta}-\mu}\right| < 1$, in analogy of the discussion presented earlier for the case of Riemann-Liouville, we have the following (8.93)

$$\mathcal{L}(y)(p) = \sum_{i=0}^{2-1} h_i \sum_{n=0}^{\infty} \tau^n \frac{p^{(\alpha-\beta)-(\beta n+i+1)}}{(p^{\alpha-\beta} - \mu)^{n+1}} - \mu \sum_{i=0}^{1-1} \tau^n \frac{p^{(\alpha-\beta)-(\beta n+i+1+\alpha-\beta)}}{(p^{\alpha-\beta} - \mu)^{n+1}}$$

Hence for $p \in \mathbb{C}$and $\left|\mu p^{\beta-\alpha}\right| < 1$, we have that

$$\frac{p^{(\alpha-\beta)-(\beta n+j+1)}}{(p^{\alpha-\beta} - \mu)^{n+1}} = \frac{1}{n!}\left(\mathcal{L}\left[x^{n\alpha+i}\left(\frac{\partial}{\partial x}\right)^{n} E_{\alpha-\beta,\beta n+i+1}\left(\mu x^{\alpha-\beta}\right)\right]\right)$$

and (8.94)

$$\frac{p^{(\alpha-\beta)-(\beta n+j+1+\alpha-\beta)}}{(p^{\alpha-\beta} - \mu)^{n+1}} = \frac{1}{n!}\mathcal{L}\left[x^{n\alpha+i+\alpha-\beta}\left(\frac{\partial}{\partial x}\right)^{n} E_{\alpha-\beta,\beta n+i+1+\alpha-\beta}\left(\mu x^{\alpha-\beta}\right)\right]$$

Thus from the above expression we derive the following solution to the space-time Caputo fractional derivative of advection-dispersion equation (8.63): (8.95)

$$c(x,t) = \sum_{i=0}^{2-1} h_i c_i(x,t) - \mu \sum_{i=0}^{1-1} h_i c_i(x,t)$$

where for $i = 0$ (8.96)

$$c_i(x,t) = \sum_{n=0}^{\infty} \frac{\exp\{-\lambda t\}\, t^{-1-n}}{\Gamma(-n)n!} x^{n\alpha+i}\left(\frac{\partial}{\partial x}\right)^{n} E_{\alpha-\beta,\beta n+i+1}\left(\mu x^{\alpha-\beta}\right)$$

$$- \mu \sum_{n=0}^{\infty} \frac{\exp\{-\lambda t\}\, t^{-1-n}}{\Gamma(-n)n!} x^{n\alpha+i+\alpha-\beta}\left(\frac{\partial}{\partial x}\right)^{n} E_{\alpha-\beta,\beta n+i+1+\alpha-\beta}\left(\mu x^{\alpha-\beta}\right)$$

and for $i = 1$ (8.97)

$$c_i(x,t) = \sum_{n=0}^{\infty} \frac{\exp\{-\lambda t\}\, t^{-1-n}}{\Gamma(-n)n!} x^{n\alpha+i}\left(\frac{\partial}{\partial x}\right)^{n} E_{\alpha-\beta,\beta n+i+1}\left(\mu x^{\alpha-\beta}\right)$$

Further the coefficients h_i are found by applying the initial and boundary conditions on $c(x,t)$.

Example 2

Our concern here is to consider equation (8.63) when $\alpha = 2$ and $0 < \beta \leq 1$. Following the discursion presented earlier, the analytical solution of space-time fractional derivative of hydrodynamic advection-dispersion equation has its two solutions given by: (8.98)

$$c_1(x,t) = \sum_{n=0}^{\infty} \frac{\exp\{-\lambda t\}\, t^{-1-n}}{\Gamma(-n)n!} x^{2n} \left(\frac{\partial}{\partial x}\right)^n E_{2-\beta,\beta n+1}\left(\mu x^{2-\beta}\right) - \mu \sum_{n=0}^{\infty} \frac{\exp\{-\lambda t\}\, t^{-1-n}}{\Gamma(-n)n!} x^{2n+2-\beta} \left(\frac{\partial}{\partial x}\right)^n E_{2-\beta,\beta n+3-\beta}\left(\mu x^{2-\beta}\right)$$

and (8.99)

$$c_2(x,t) = \sum_{n=0}^{\infty} \frac{\exp\{-\lambda t\}\, t^{-1-n}}{\Gamma(-n)n!} x^{2n+1} \left(\frac{\partial}{\partial x}\right)^n E_{2-\beta,\beta n+2}\left(\mu x^{2-\beta}\right).$$

These solutions are linearly independent and they provide the fundamental system of solutions to space-time Caputo fractional derivative of hydrodynamic advection-dispersion equation. We have to prove that the series are convergent. Note that the below series is convergent and converges to:

$$\sum_{j=0}^{\infty} \frac{\Gamma(n+j+1)}{\Gamma(\alpha+m\alpha+\beta)j!} x^j = -\frac{(1-x)^{-n}\Gamma(1+n)}{(-1+x)\Gamma(\alpha+n\alpha+\beta)}$$

or (8.100)

$$\sum_{j=0}^{\infty} \frac{\Gamma(n+j+1)}{\Gamma(\alpha+m\alpha+\beta)j!} x^j \geq \sum_{j=0}^{\infty} \frac{\Gamma(n+j+1)}{\Gamma(\alpha j+m\alpha+\beta)j!} x^j$$

Because the series of left hand side is convergent it follows that the series of the right hand is convergent and $c_2(x,t)$ and $c_1(x,t)$ are convergent. Due to the complexity of these solutions, the graphical representation of these solutions will not be given in this thesis.

8.7.3 Approximated solution via Fourier transform

In order to be consistent in comparison, one need to propose an analytical solution to the fractional version of the advection dispersion equation, and one compare the two solutions by mean of experimental data. Solutions to common solute transport boundary value problems (BVP) are usually obtained by means of Laplace or Fourier transforms. We will solve the BVP for instantaneous injection of a "spike" of solute, i.e. the Green's function. The

fractional-in-space equation is solved via Fourier transform. To start here we choose the fractional advection dispersion equation governed by:

$$\partial_t c(x,t) + \mathrm{q_r}\partial^{\alpha}{}_x \mathrm{c}(x,t) - \mathrm{D_r} o \partial_x^{\mu} c(x,t) + \lambda c(x,t) = 0 \tag{8.102}$$

Applying the Fourier transform in x-direction on both sites of the above equation, we obtained the following ordinary differential equation: (8.103)

$$\frac{d\check{c}(p\,,t)}{dt} = -[\mathrm{q_r}(ip)^{\alpha}\check{c}(p\,,t) - \mathrm{D_r}(ip)^{\mu}\check{c}(p\,,t) + \lambda\check{c}(p\,,t)]$$

And the solution of the above ordinary differential equation is given as: (8.104)

$$\check{c}(p\,,t) = \exp[-[\mathrm{q_r}(ip)^{\alpha} - \mathrm{D_r}(ip)^{\mu} + \lambda]t]$$

Using the trigonometry properties $i = e^{i\pi/2}$, the above expression is transformed to

$$\check{c}(p\,,t) = \exp[-\lambda t]\exp\left[-\left[\mathrm{q_r}(ip)^{\alpha} - \mathrm{D_r}e^{i(sign(p))^{\pi\mu}/_2}\right]t\right]. \tag{8.105}$$

This Fourier transform does not have a closed form inverse. However following the work done by Benson in 1998, the expression can be put it in the form of the characteristic function by substituting -p for p, the density can be manipulated into the canonical form of the characteristic function for μ-stable densities (Benson, 1998).

The solution to the classical ADE with the continuous source initial condition is generally written in "closed form" using the error function. The error function itself is twice the integral of the positive half of a Gaussian density with variance $= 1/2$, or standard deviation of $\sqrt{2}/2$ (Benson, 1998). The analytical solution the ADE was given by (Cleary and Ungs, 1978), is

$$c(x,t) = \frac{c_0 \exp[-\gamma t]}{2}\left[exp\frac{x(q_r - u_r)}{2D_r}erfc\frac{x - u_r t}{2\sqrt{D_r t}} + exp\frac{x(q_r + u_r)}{2D_r}erfc\frac{x + u_r t}{2\sqrt{D_r t}}\right]$$

where

$$u_r = \sqrt{q_r^2 + 4D_r(\lambda - \gamma)}$$

and

$$erfc(x) = \frac{2}{\sqrt{\pi}}\int_x^{\infty} \exp(-t^2)dt$$

is known as complementary error function. For the generalisation of this widely-used formula, a similar solution to the Fractional Advection Dispersion Equation is given by:

$$c(x,t) = \frac{c_0 \exp(-\gamma t)}{2}\left[exp\frac{x(q_r - u_r)}{2D_r} SERF_\mu c\left[\frac{x - u_r t}{2(D_r t)^{\frac{1}{\mu}}}\right] + exp\frac{x(q_r + u_r)}{2D_r} SERF_\mu c\left[\frac{x + u_r t}{2(D_r t)^{\frac{1}{\mu}}}\right]\right],$$

where (8.106)

$SERF_\mu c = 1 - SERF_\mu c, SERF_\mu$ was defined by (Benson , 1998) as the μ-stable error function ($SERF_\mu$) function similarly to the error function, that is, twice the integral of a symmetric μ-stable density from 0 to the argument (z): (8.107)

$$SERf_\mu[z] = 2\int_0^z f_\mu(x)dx$$

where $f_\mu(x)$ is the standard, symmetric, μ-stable density. The factor of 2 in the denominator of the $SERF$ argument has been dropped from equation (8.107) for simplicity. The μ-stable density is defined in series form as: (8.108)

$$f_\mu(z) = \frac{1}{\pi}\sum_{n=0}^{\infty}\frac{(-1)^n}{(2n+1)!}\Gamma\left[\frac{2n+1}{\mu}+1\right]z^{2n}$$

Or in integral form we have: (8.109)

$$f_\mu(z) = \frac{z^{(1/\mu-1)}\mu}{2|1-\mu|}\int_0^1 U_\mu(\theta) exp\left[-z^{(\mu/\mu-1)}U_\mu(\theta)\right]d\theta$$

$$U_\mu(\theta) = \left[\frac{sin\left[\frac{\pi\theta\mu}{2}\right]}{cos\left[\frac{\pi\mu}{2}\right]}\right]^{\mu/(1-\mu)}. \quad (8.110)$$

Up to this day the analytical expression of the μ-stable density is not well known in general but for some specific case that may not be relevant for our problem, therefore we propose the following alternative expression as solution of the Fractional Advection Dispersion Equation (Atangana, and Kilicman , 2013): (8.111)

$$c(x,t) = \frac{c_0 \exp(-\gamma t)}{2}\left[exp\left(\frac{x^\alpha(q_r - u_r)}{2D_r}\right) erfc\left(\frac{x^\alpha - u_r t}{2(D_r t)^{\frac{1}{\mu}}}\right) + exp\left(\frac{x^\alpha(q_r + u_r)}{2D_r}\right) erfc\left(\frac{x^\alpha + u_r t}{2(D_r t)^{\frac{1}{\mu}}}\right)\right].$$

Here, note that if $\alpha = 1$ and $\mu = 2$, we recover ADE. In order to see the possible effect of the fractional order into the solution, we present the graphical representation for several values of $\alpha, and\ \mu$ for the same theoretical values of the problem. Now having both analytical solutions of the two versions of the advection dispersion equation, one can proceed with the comparison and this will be done below. The following figures 8-1 to 8-5 show the density plot of the approximate solutions of the fractional advection dispersion equation. The theoretical values used for these simulations are recorded in table below.

Table 8-1: Theoretical parameters used for numerical simulation

Parameters	$\boldsymbol{c_0}$	$\boldsymbol{\gamma}$	$\boldsymbol{D_r}$	$\boldsymbol{q_r}$	$\boldsymbol{\underline{\lambda}}$
Values	100	0.94	0.89	0.9	1

The below figure show the numerical simulation of the concentration through the geological formation as function of space, time and fractional order derivatives. The figures are obtained via the software Mathematica.

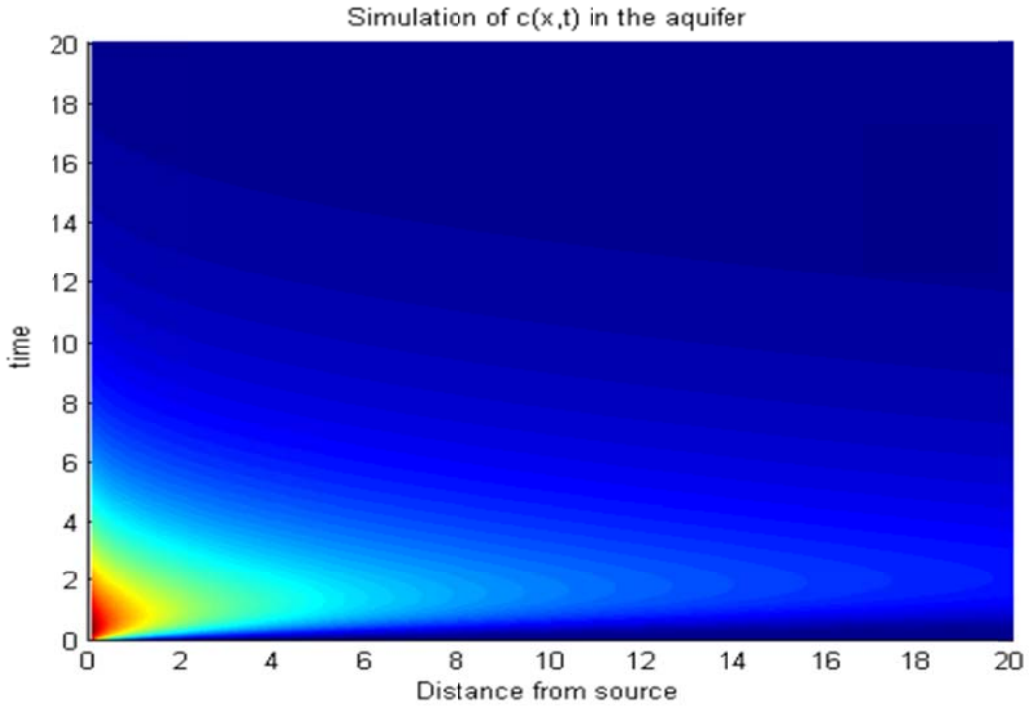

Figure 8-1: Simulation of the FADE ($\boldsymbol{c_0 = 100, \alpha = 0.45, \beta = 2, D = 2}$; $\boldsymbol{q = 1, \gamma = 0.25\ and\ \lambda = 1}$)

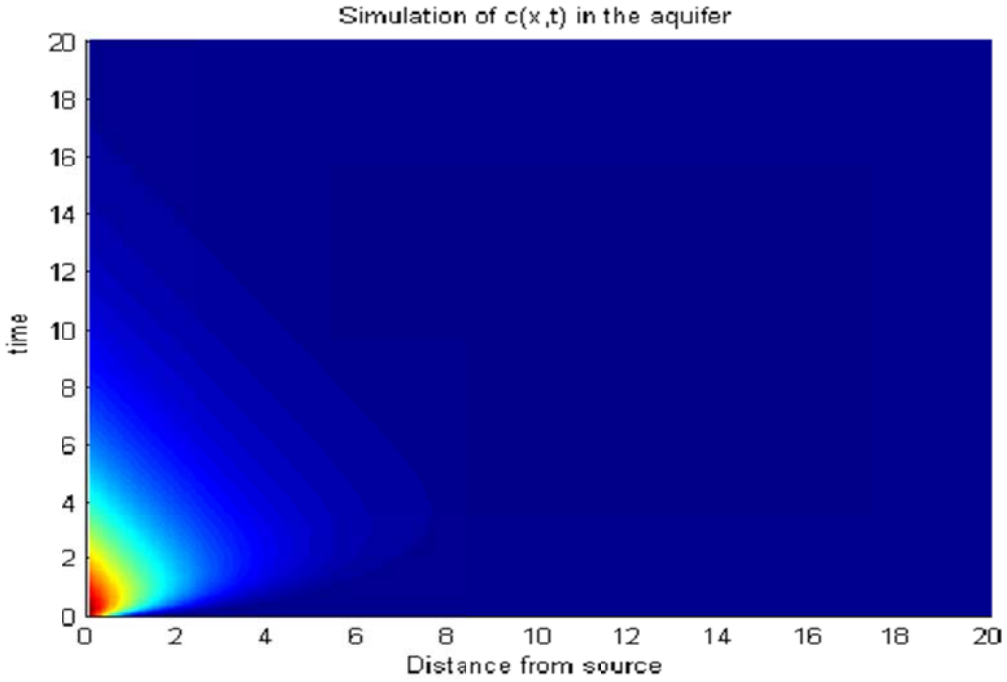

Figure 8-2: Simulation of the ADE $\boldsymbol{c_0 = 100, \alpha = 1, \beta = 2, D = 2}$; $\boldsymbol{q = 1, \gamma = 0.25}$ $\boldsymbol{and}$ $\boldsymbol{\lambda = 1}$

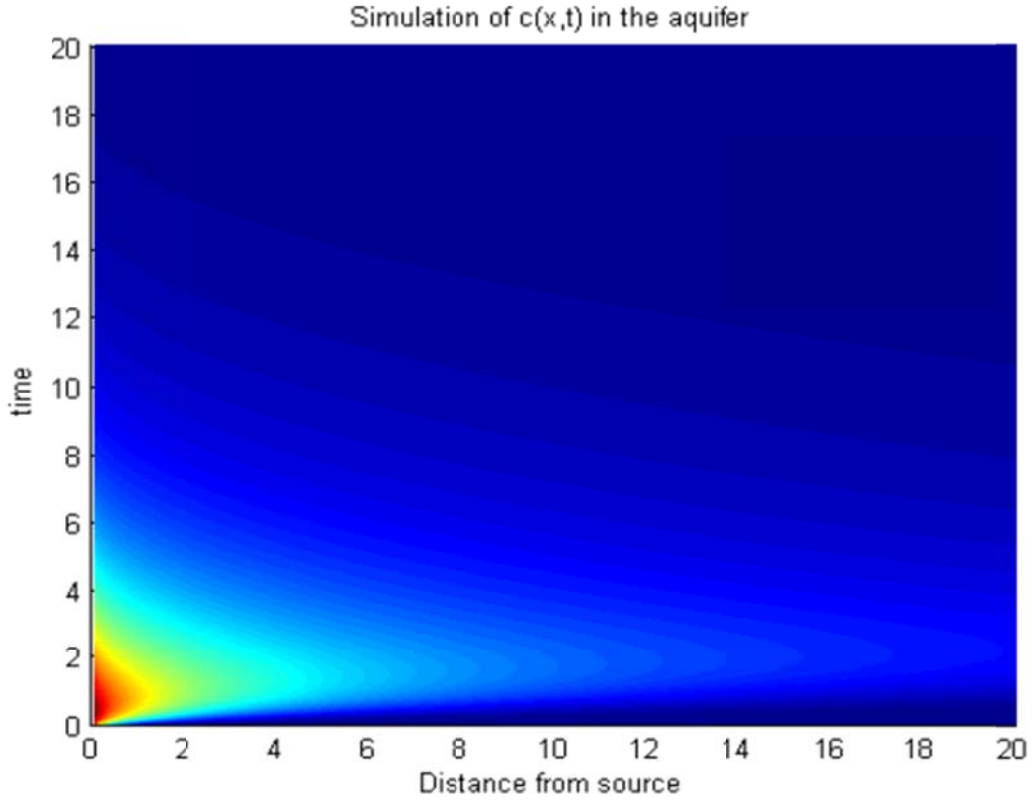

Figure 8-3: FADE $\boldsymbol{c_0 = 100, \alpha = 0.55, \beta = 1.55, D = 2}$; $\boldsymbol{q = 1, \gamma = 0.25}$ $\boldsymbol{and}$ $\boldsymbol{\lambda = 1}$

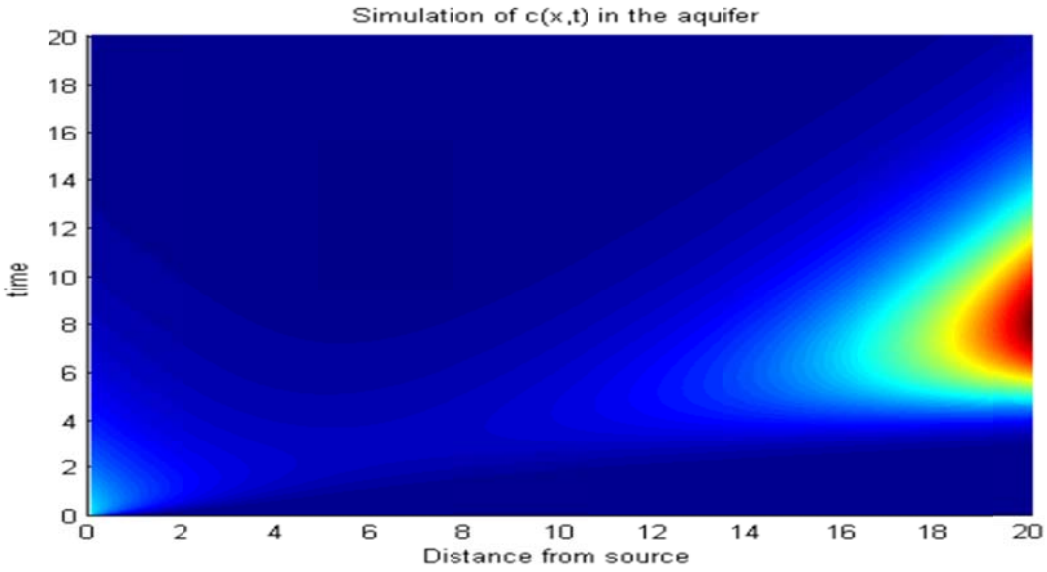

Figure 8-4: $\boldsymbol{c_0 = 100, \alpha = 0.25, \beta = 1.55, D = 2}$; $\boldsymbol{q = 1, \gamma = 0.25}$ ***and*** $\boldsymbol{\lambda = 1}$

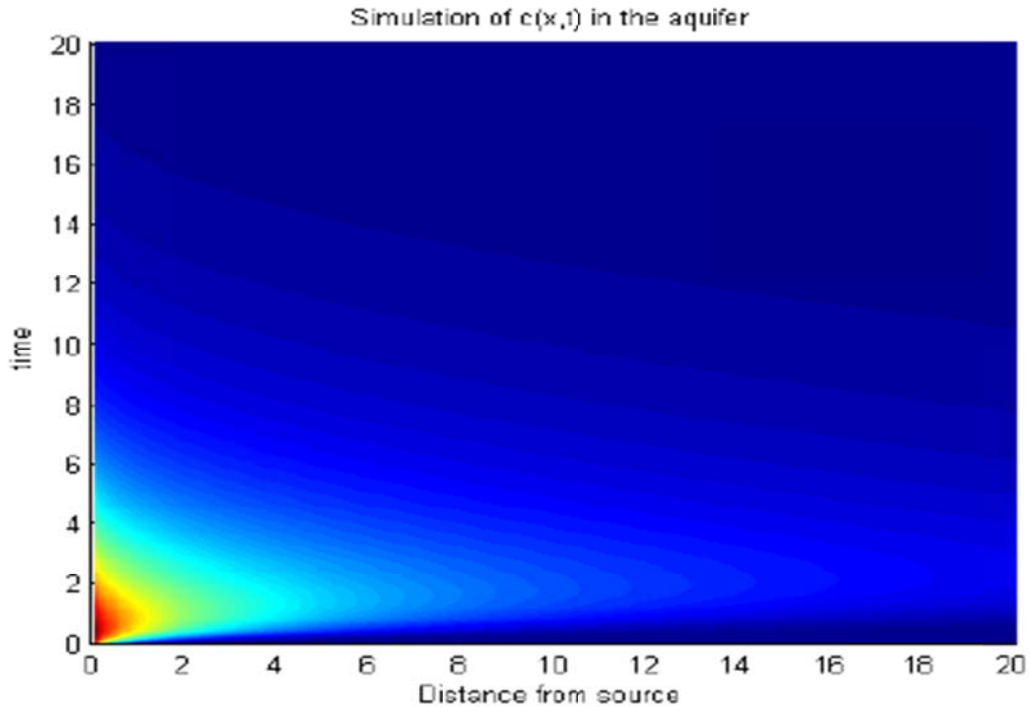

Figure 8-5: Simulation of the FADE $\boldsymbol{c_0 = 100, \alpha = 0.55, \beta = 1.95, D = 2}$; $\boldsymbol{q = 1, \gamma = 0.25}$ **and** $\boldsymbol{\lambda = 1}$

The above simulation let no choice than to believe that the order of the derivative plays an important role while simulation the plume of the pollution in the aquifer.

Several studies have been done for this concern, more precisely when the parameter $\lambda = 0$, see for example (Benson *et al.*, 2000), however the approach used is their studies is rather stochastic than deterministic. In this thesis we deal with the deterministic approach .To test the accuracy and efficiency of FADE, we compare the solution of FADE, ADE and the experimental data from field observation. The following figures 8-6 and 8-7 show the comparison between FADE, ADE, and measured data from real field for different values of α and μ. The equations compared here are (8.111) and the solution by (Cleary and Ungs, 1978). A plume observed in natural systems is used in this section to distinguish further the time and space non-localities. Realistic data from natural systems provide the most important criteria for distinguishing the space- and time-nonlocal processes and evaluating the applicability of the FADE models. Three experiments are selected, where tracer transport through regional-scale natural systems with very different hydraulic properties including, a natural two confined aquifers, were monitored. The observed anomalous phenomena were studied extensively and modelled using the space FADE by different researchers in the last several years. Analysis, comparison and application of various FADEs in this study are intended to provide a general guidance for model selection.

The below simulation let no choice than to believe that the order of the derivative plays an important role while simulation the plume of the pollution in the aquifer. The comparison revealed that, the fractional advection dispersion equation is compatible with observations of the plume in the laboratory and the field. It predicts power law, faster than the apparent plume variance. It is shown that the traditional 2^{nd} –order advection equation does not adequately describe the movement of solute trace in the aquifer. On the basis this assertion we conclude that, the fractional advection dispersion equation is better than the classical version of advection dispersion equation (Abdon and Kilicman, 2013).

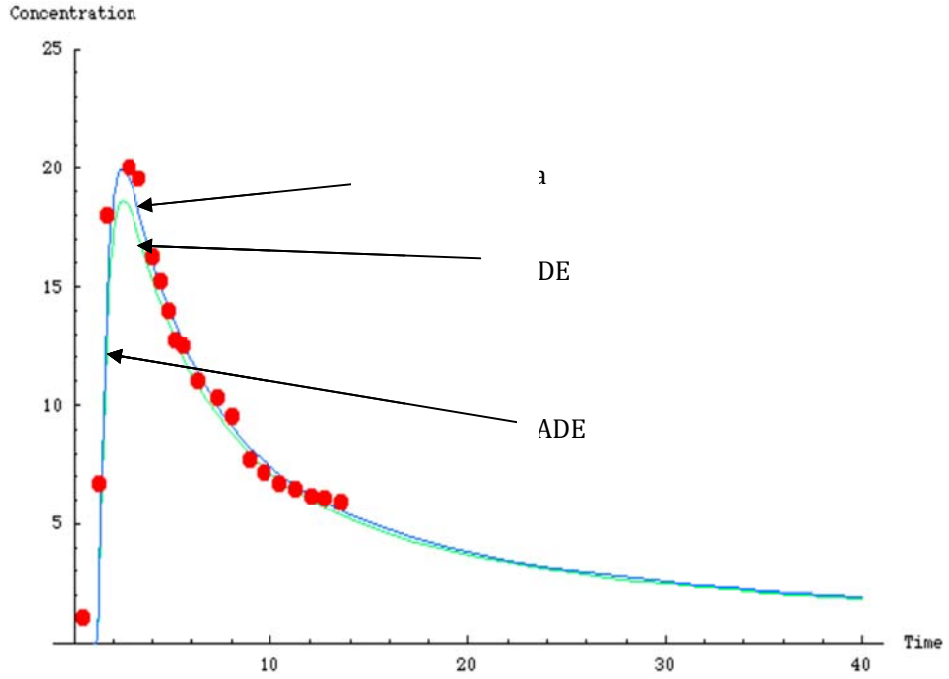

Figure 8-6: Comparison of FADE, ADE and experimental data from real world, Dr = 4.5 ,$\boldsymbol{\mu = 1.95}$,$\boldsymbol{\alpha = 0.99}$ and qr =0.51

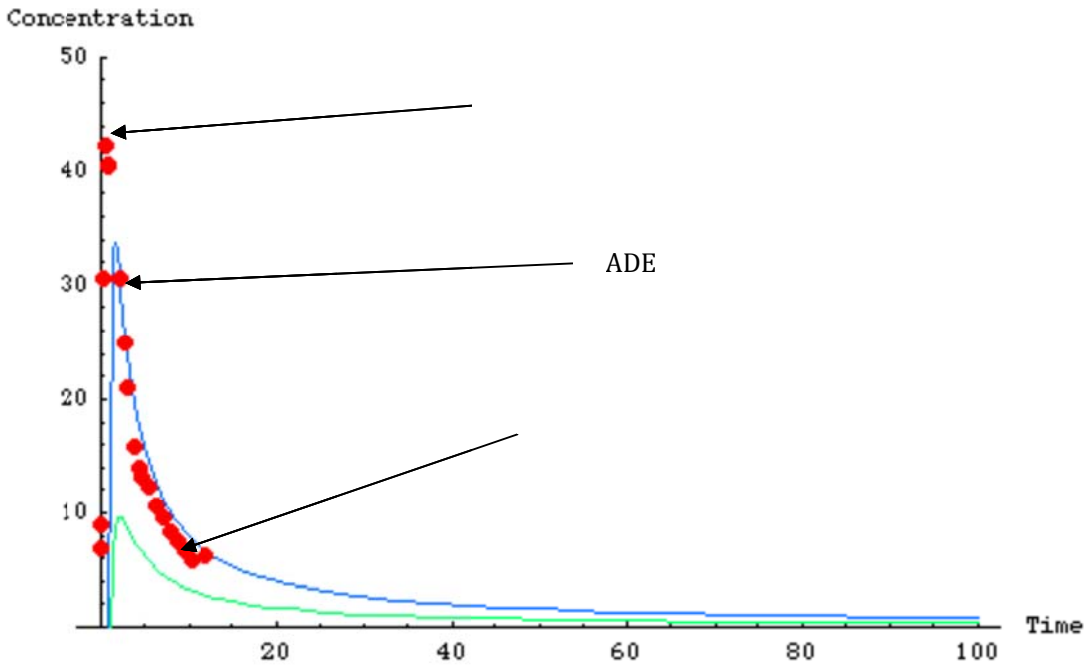

Figure 8-7: Comparison of FADE, ADE and experimental data from real world, Dr = 2.5 ,$\boldsymbol{\mu = 1.36}$,$\boldsymbol{\alpha = 0.3}$ and qr =0.4, c0 = 150

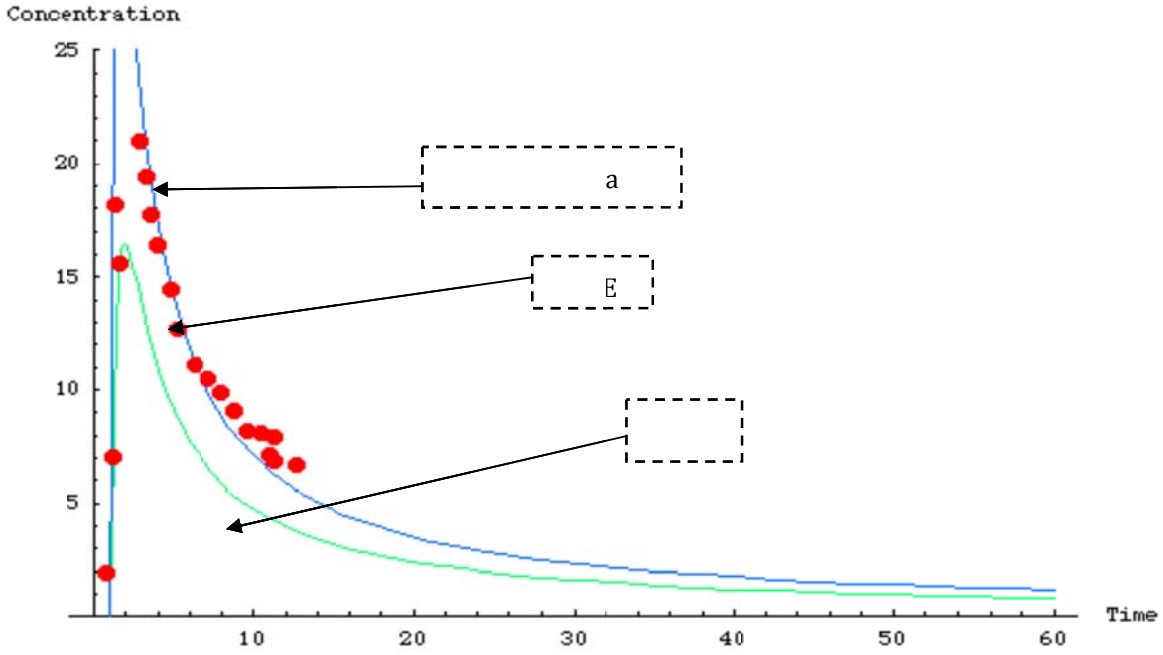

Figure 8-8: Comparison of FADE, ADE and experimental data from real world, Dr = 0.5 , $\boldsymbol{\mu = 1.68}$, $\boldsymbol{\alpha = 0.64}$ and qr =0.5, c0 = 155.

8.7.4 Discussions

Natural geological deposits with highly contrasting permeability may form mobile and relatively immobile zones, where the potential mass exchange between mobile and immobile zones results in a wide time distribution for solute ‘‘trapping”. The transport process, groundwater is, by its very nature, always in contact with the matrix of an aquifer. There is thus a possibility that the solutes may interact with the rock matrix, and one another. A true mathematical model for groundwater pollution must therefore be able to account for interactions between the dissolved solids and matrix of the aquifer. It will thus be advantageous to look at the nature of the interactions between dissolved solids and a porous medium that may be expected in groundwater pollution. Experimental evidence indicates that when a dissolved solid comes in contact with the matrix of a porous medium it may (a) pass through the medium with no apparent effect, (b) be absorbed by the porous matrix and (c) reacts with the porous matrix and other substances dissolved in the fluid. The dissolved solids encountered in porous flow are, for this reason, often classified as conservative, non-conservative and reactive tracers. This behaviour implies that the quantity of dissolved solids in a porous medium depends not only on the flow pattern, but also the nature of the porous matrix and the solution. These situations (a) (b) and (c) can be characterized efficiently by the time-nonlocal model, including the time FADE. If the high-

permeable material tends to form preferential flow paths, such as the interconnected paleo-channels observed in alluvial depositional systems, then the solute transport may show a heavy leading edge, which can be described by the space FADE with maximally positive skewness as shown in Figures 8-1 , 8-2 , 8-3 and 8-4. Development of partial differential equations such as the advection-dispersion equation (ADE) begins with assumptions about the random behaviour of a single particle: possible velocities it may experience in a flow field and the length of time it may be immobilized. When assumptions underlying the ADE are relaxed, a fractional ADE (FADE) can arise, with a non-integer-order derivative on time or space terms. Fractional ADEs are nonlocal; they describe transport affected by hydraulic conditions at a distance. Space fractional ADEs arise when velocity variations are heavy tailed and describe particle motion that accounts for variation in the flow field over the entire system. Time fractional ADEs arise as a result of power law particle residence time distributions and describe particle motion with memory in time. As shown, the best-fitting curve from the classical radial flow model greatly under-estimated early arrival. We also remark that this solute flow model and its numerical solution match the test data closely only up to the peak.

An excellent literatures review revealed that, the fractional advection dispersion equation has proven useful in modelling contaminant flow in heterogeneous porous media (Benson *et al.*, 2000 a, 2000 b and 2000 c). The fractional advection dispersion equation is known to be a special case of a general transport equation with convolution flux (Cushman and Ginn TR, 2000)and a limit case of the continuous time random walk with power-law particle jumps (Berkowitz *et al.*, 2006) (Meerschaert and Scheffler, 2004). It is a simple matter to derive the fractional advection dispersion equation from the fractional conservation of mass equation using a moving coordinate system at the plume centre of mass, in exactly the same way that the usual advection dispersion equation follows from the traditional conservation of mass equation see (Meerschaert *et al.*, 2006). This approach validates the utility of the fractional advection dispersion equation and related theories, by highlighting the scaling factor that renders the fractional equation scale invariant. We believe that this scaling captures the fractal nature of the porous medium (Wheatcraft and Tyler 1988).

Chapter 9

CONCLUSIONS AND RECOMMENDATIONS

9.1 CONCLUSIONS

A large number of cities in tropical and subtropical areas of the earth depend on both groundwater and surface water resources for their supply of drinking water. As discussed in Chapter 2, one problem is that both sources are often highly polluted, a situation that is particularly important for the city of Douala in the Cameroon. The present thesis is an attempt to draw attention to this problem and to provide preliminary guidelines for the future remediation of the groundwater resources at Douala. There is no doubt that to achieve this will be an immense task. Nonetheless, the discussion also shows that such an action should be undertaken urgently.

While it would be possible to instigate "trial–and–error" methods for the remediation of the groundwater resources at Douala, past experiences worldwide have shown that the best approach to remediate an aquifer is to have a good knowledge of the problem at hand and use it to develop an appropriate conceptual model of the site. This conceptual model is then translated into a mathematical model and implemented either analytically or numerically on a computer and then used to simulate the expected future behaviour of the contaminated aquifer with the view to devise an appropriate method to clean up the aquifer.

There is not much quantitative information available on the Douala aquifer at the moment. Nevertheless, an analysis of the available information in Chapter 3 provided some guidance in developing a preliminary conceptual and mathematical model of the aquifer, which was implemented numerically with the computer package FEFLOW (Diersch, 2009) as discussed in Chapter 6. Although there exists a large number of technologies that can be used to clean up an aquifer, the investigation was limited to the so-called Deep Aquifer Remediation Tools (DARTs) in particular it shallow aquifer equivalent to the Permeable Reaction Barriers. In this technique the groundwater is allowed to pass through a permeable reactive barrier (PRB), which transform the contaminant into a non-toxic form by a variety of chemical reactions and then immobilized it. The reasons for this choice were twofold. The first is that the Douala aquifer occurs at relatively shallow depths and the second that the technique does not require constant active supervision. These expectations are largely supported by the results of the FEFLOW model in Chapter 6. As discussed in Chapter 6, the barrier can be emplaced either in a series of non-pumping wells or in a trench. Although not investigated in detail, the FEFLOW model in Chapter 6 suggests that trenches might be particularly useful at

Douala.

Mathematical models are only as effective in describing a contaminated aquifer as the underlying conceptual model, which can never be complete. Results derived from groundwater models are consequently always subject to uncertainties. While these uncertainties have regularly been neglected in the past, it is nowadays imperative that a groundwater model, whether it a flow or mass transport model, be accompanied by an estimates of uncertainties associated with the model. Although a large number of approaches are available for this purpose, they often require exorbitant computing resources. The present investigation was consequently limited to the application of Latin Hypercube Sampling method to the analytical solution of the conventional hydrodynamic dispersion equation, discussed in Chapter 6. The discussion there showed that the Latin Hypercube Sampling method might provide one with uncertainty estimates that might be quite useful, especially during preliminary investigations.

It has been known for years that the hydrodynamic dispersion equation discussed in Chapter 4, is not able to account for the long-tail plumes often observed in studies of contaminated fractured-rock aquifers. One approach that has become quite fashionable in recent years to account for this is to replace the ordinary spatial and temporal derivatives in the hydrodynamic equation of Chapter 5, separately or simultaneously, with fractional derivatives. As shown by the exploratory discussion of the approach in Chapter 8, the method seems to be able to account for long tail plumes. However, an analysis of the computations reported in Chapter 8 with the mathematical computer package *Mathematica* revealed that the results depend not only on the definition of the fractional derivative used in the computation, but also on how the derivatives are computed.

9.2 RECOMMENDATIONS

The most important factor for the successful implementation of the DART technology is an adequate site characterization. Site characterizations typical of remedial feasibility investigations, are usually not enough. This is not surprising given that the PRB (part of DART) cannot be moved once installed. It will therefore be necessary to develop and perform a detailed site characterization of the Douala area before the method can be applied. Such an exercise should concentrate include detailed studies of:

a) the nature, origin and positions of the existing and expected future pollution sources and their evolution over time

b) the stratigraphy and geochemistry of the contaminated area.

c) the prevailing surface– and groundwater flow patterns laterally and at depth

The possibility of course always exists that a project of this nature may fail at sometime in the future, with unexpected consequences. However, this can be avoided to some extend by the keeping a fully documented history of the evolution of the project and the development of a continuously updated contingency plan detailing corrective actions that needed to be taken should the system fail.

There is no doubt that the success with a remediation scheme for the Douala aquifer will depend to a large extent on the development of an accurate numerical model for the aquifer. However, as shown by the discussion in Chapter 7, any such model will be subject to uncertainties. It is therefore important that the model used with the implementation of the technology and the contingency plan be based on a sound uncertainty analysis supplemented by an appropriate risk analysis.

There is little doubt that fractional derivatives may account for properties of mass transport in the subsurface of the earth, that cannot be accommodate in the classical hydrodynamic equation. However, the computations of fractional derivatives in Chapter 8, indicated that it may be necessary to pay more attention to their definition and implementation than suggested in the existing literature.

The framework and recommendations provided in this thesis, may not fully address the problems associated with the pollution of the groundwater resources of Douala. However, but it is hoped that it can serve as a basis for a more detailed project to create a cleaner and healthier environment, if not for the present population of Douala, then for future generations.

Appendix

4-Table of fractional order derivative for some functions

We shall present for the Liouville fractional derivative (Atangana and Secer, 2013):

Functions	L-fractional derivative
$x^{\beta}, \beta > -1$	$\frac{x^{-\alpha+\beta}\Gamma(1+\beta)}{\Gamma(1-\alpha+\beta)}$
$Cos(a\,x), a \in \mathbb{R}$	$\frac{x^{-\alpha} HypergeometricPFQ\left[\{1\},\left\{1-\frac{\alpha}{2},\frac{3}{2}-\frac{\alpha}{2},\right\}-\frac{1}{4}a^2x^2\right]}{\Gamma(1-\alpha)}$
$Sin(a\,x), a \in \mathbb{R}$	$-\frac{a^2x^{2-\alpha} HypergeometricPFQ\left[\{2\},\left\{2-\frac{\alpha}{2},\frac{5}{2}-\frac{\alpha}{2},\right\}-\frac{1}{4}a^2x^2\right]}{\Gamma(4-\alpha)}$
$ln(x)$	$\frac{ax^{1-\alpha}(2-\alpha) HypergeometricPFQ\left[\{1\},\left\{2-\frac{\alpha}{2},\frac{3}{2}-\frac{\alpha}{2},\right\}-\frac{1}{4}a^2x^2\right]}{\Gamma(2-\alpha)}$ $-\frac{2a^3x^{3-\alpha} HypergeometricPFQ\left[\{2\},\left\{\frac{5}{2}-\frac{\alpha}{2},3-\frac{\alpha}{2},\right\}-\frac{1}{4}a^2x^2\right]}{\Gamma(5-\alpha)}$
$e^{ax}, a \in \mathbb{R}$	$-\frac{x^{-\alpha}(EulerGamma+\pi Cot[\pi\,\alpha]-ln(x)+PolyGamma[0,\alpha])}{\Gamma(1-\alpha)}$
$Sinh(a\,x)$	$\left(\frac{a^{\alpha}\left((a\,x)^{-\alpha}+e^{ax}\left(\Gamma(1-\alpha)-\Gamma(1-\alpha,ax)\right)\right)}{\Gamma(1-\alpha)}\right)$
$Cosh(ax)$	$\left(\frac{e^{-ax}(-a^2x^2)^{-\alpha}}{2\Gamma(1-\alpha)}((-a^2x^2)^{\alpha})\left((-a)^{\alpha}\left(\alpha\Gamma(-\alpha)+\Gamma(1-\alpha,-ax)\right)\right.\right.$ $\left.\left.+a^{\alpha}e^{2ax}\left(\Gamma(1-\alpha)-\Gamma(1-\alpha,ax)\right)\right)\right)$
$Arcsin(x)$, $0<x<1$	$\left(\frac{1}{2\Gamma(1-\alpha)}\left(e^{-ax}(-a^2x^2)^{-\alpha}\left((-a)^{\alpha}(ax)^{\alpha}(e^{ax}+axExpIntegralE[\alpha,-ax])\right.\right.\right.$ $\left.+a^{\alpha}e^{ax}(-ax)^{\alpha}(1-ae^{ax}xaxExpIntegralE[\alpha,ax])\right.$ $\left.\left.\left.+((-a)^{\alpha}+a^{\alpha}e^{2ax})(-a^2x^2)^{\alpha}\Gamma(1-\alpha)\right)\right)\right)$
	$\left(\frac{x^{1-\alpha} HypergeometricPFQ\left[\left\{\frac{1}{2},\frac{1}{2},1\right\},\left\{\frac{3}{2}-\frac{\alpha}{2},2-\frac{\alpha}{2}\right\},x^2\right]}{\Gamma(2-\alpha)}\right.$ $\left.+\frac{2x^{3-\alpha} HypergeometricPFQ\left[\left\{\frac{3}{2},\frac{3}{2},2\right\},\left\{\frac{5}{2}-\frac{\alpha}{2},3-\frac{\alpha}{2}\right\},x^2\right]}{\Gamma(5-\alpha)}\right)$

$Arccos(x)$, $0 < x < 1$	$\left(-\frac{x^{-\alpha}\left(\pi(-2+\alpha)+2xHypergeometricPFQ\left[\left\{\frac{1}{2},\frac{1}{2},1\right\},\left\{\frac{3}{2}-\frac{\alpha}{2},2-\frac{\alpha}{2}\right\},x^2\right]\right)}{2(2-\alpha)\Gamma(1-\alpha)}\right.$ $-\frac{x^{1-\alpha}HypergeometricPFQ\left[\left\{\frac{1}{2},\frac{1}{2},1\right\},\left\{\frac{3}{2}-\frac{\alpha}{2},2-\frac{\alpha}{2}\right\},x^2\right]}{2(2-3\alpha+\alpha^2)\Gamma(1-\alpha)}$ $\left.-\frac{x^{3-\alpha}HypergeometricPFQ\left[\left\{\frac{3}{2},\frac{3}{2},2\right\},\left\{\frac{5}{2}-\frac{\alpha}{2},3-\frac{\alpha}{2}\right\},x^2\right]}{2(2-3\alpha+\alpha^2)\Gamma(1-\alpha)\left(\left(\frac{3}{2}-\frac{\alpha}{2}\right)\left(2-\frac{\alpha}{2}\right)\right)}\right)$
$Arctan(x)$	$-\frac{x^{1-\alpha}}{\Gamma(5-\alpha)}\left((-4+\alpha)(-3+\alpha)(-2\right.$ $+\alpha)HypergeometricPFQ\left[\left\{\frac{1}{2},1,1\right\},\left\{\frac{3}{2}-\frac{\alpha}{2},2-\frac{\alpha}{2}\right\},-x^2\right]$ $\left.+4x^2HypergeometricPFQ\left[\left\{\frac{3}{2},2,2\right\},\left\{\frac{5}{2}-\frac{\alpha}{2},3-\frac{\alpha}{2}\right\},-x^2\right]\right)$
$\int_x^\infty \frac{e^{-y}}{y}dy$	$\frac{1}{\Gamma(3-\alpha)}\left(e^{-x}x^{-1-\alpha}\left((-x)^\alpha(-2+\alpha)\left(\Gamma(2-\alpha)-\Gamma(2-\alpha,-x)\right)\right.\right.$ $+e^x x(-1$ $\left.\left.+\alpha)\left(xHypergeometricPFQ[\{1,1\},\{2,,3-\alpha\},-x](-2\right.\right.\right.$ $\left.\left.\left.+\alpha)\left(\pi Cot(\pi\alpha)-ln(x)+PolyGamma(0,\alpha)\right)\right)\right)\right)$
$E_\alpha(-t^\alpha)$	$\frac{x^{-\alpha}}{\Gamma(1-\alpha)}-E_\alpha(-t^\alpha)$
$J_n(x)\ ,Re[n]>-1$	$\frac{2^{-n}x^{n-\alpha}(1+n-\alpha)}{\Gamma(2+n-\alpha)}HypergeometricPFQ\left[\left\{\frac{1}{2}+\frac{n}{2},1+\frac{n}{2}\right\},\left\{1+n,1+\frac{n}{2}-\frac{\alpha}{2},\frac{3}{2}+\frac{n}{2}\right.\right.$ $\left.\left.-\frac{\alpha}{2}\right\},\frac{-x^2}{4}\right]$ $+\frac{2^{-1-n}\left(\frac{1}{2}+\frac{n}{2}\right)\left(1+\frac{n}{2}\right)x^{2+n-\alpha}}{(1+n)\left(1+\frac{n}{2}-\frac{\alpha}{2}\right)\left(\frac{3}{2}+\frac{n}{2}-\frac{\alpha}{2}\right)\Gamma(2+n-\alpha)}HypergeometricPFQ\left[\left\{\frac{3}{2}+\frac{n}{2},2\right.\right.$ $\left.\left.+\frac{n}{2}\right\},\left\{2+n,2+\frac{n}{2}-\frac{\alpha}{2},\frac{5}{2}+\frac{n}{2}-\frac{\alpha}{2}\right\},\frac{-x^2}{4}\right]$
$K_n(x)\ ,1>Re[n]>-1$	

$Y_n(x), -1 < Re[n] < 1$	$2^{-1-n}\pi x^{1-n-\alpha} Csc(n\pi)\left(\frac{4^n}{\Gamma(2+n-\alpha)} HypergeometricPFQ\left[\left\{\frac{1}{2}-\frac{n}{2}, 1-\frac{n}{2}\right\}, \left\{1-n, 1-\frac{n}{2}-\frac{\alpha}{2}, \frac{3}{2}-\frac{n}{2}-\frac{\alpha}{2}\right\}, \frac{x^2}{4}\right] + \frac{x^{2n}}{\Gamma(2+n-\alpha)} HypergeometricPFQ\left[\left\{\frac{1}{2}+\frac{n}{2}, 1+\frac{n}{2}\right\}, \left\{1+n, 1+\frac{n}{2}-\frac{\alpha}{2}, \frac{3}{2}+\frac{n}{2}-\frac{\alpha}{2}\right\}, -\frac{x^2}{4}\right]\right)$
$Zeta[x]$	$2^{-1-n}x^{1-n-\alpha}\left(-\frac{Csc(n\pi)4^n}{\Gamma(2+n-\alpha)} HypergeometricPFQ\left[\left\{\frac{1}{2}-\frac{n}{2}, 1-\frac{n}{2}\right\}, \left\{1-n, 1-\frac{n}{2}-\frac{\alpha}{2}, \frac{3}{2}-\frac{n}{2}-\frac{\alpha}{2}\right\}, -\frac{x^2}{4}\right] + \frac{x^{2n}}{\Gamma(2+n-\alpha)} HypergeometricPFQ\left[\left\{\frac{1}{2}+\frac{n}{2}, 1+\frac{n}{2}\right\}, \left\{1+n, 1+\frac{n}{2}-\frac{\alpha}{2}, \frac{3}{2}+\frac{n}{2}-\frac{\alpha}{2}\right\}, -\frac{x^2}{4}\right]\right)$
$Erf(t)$	$\sum_{n=1}^{\infty}\left[\frac{(-1)^{\alpha}(-x)^{-\alpha}}{\Gamma(1-\alpha)} - \frac{n^{-x}\alpha\Gamma(-\alpha)\left(-ln(n)\right)^{\alpha}}{\Gamma(1-\alpha)} - -\frac{n^{-x}\alpha\Gamma(1-\alpha, -xln(n))\left(-ln(n)\right)^{\alpha}}{\Gamma(1-\alpha)}\right]$
	$2^{-1+x}x^{1-\alpha}(2-\alpha) HypergeometricPFQRegularized\left[\left\{\frac{1}{2}, 1\right\}, \left\{\frac{3}{2}-\frac{\alpha}{2}, 2-\frac{\alpha}{2}\right\} - x^2\right] + 2^{-1+x}x^{3-\alpha} HypergeometricPFQRegularized\left[\left\{\frac{3}{2}, 2\right\}, \left\{\frac{5}{2}-\frac{\alpha}{2}, 3-\frac{\alpha}{2}\right\} - x^2\right]$

Here:

HypergeometricPFQ [{},{},{}] is the generalized hypergeometric function which is defined as follow in the Euler integral representation:

$$ {}_2F_1(a,b,c,z) = \frac{\Gamma(a)}{\Gamma(b)\Gamma(c-b)}\int_0^1 t^{b-1}(1-t)^{c-b-1}(1-zt)^{-a}dt, c \in \mathbb{C}\backslash\mathbb{Z}_0^-,\ a,b \in \mathbb{C} $$

$$ (0 < Re[b] < Re[c]; |arg(1-z)| < \pi) $$

The PolyGamma[n, z] and PolyGamma[z] are the logarithmic derivative of gamma function given by

$$ PolyGamma[n,z] = \frac{d^n}{dz^n}\left(\frac{\Gamma'(z)}{\Gamma(z)}\right), PolyGamma[z] = PolyGamma[0,z] $$

These functions are meromorphic of z with no branch cut discontinuities.

$E_\alpha(-t^\alpha)$is the generalized Mittag-Leffler function and is defined as

$$E_\alpha(-t^\alpha) = \sum_{k=0}^{\infty} \frac{(-t^\alpha)^k}{\Gamma(k\alpha + 1)}$$

Γis denotes the gamma function, which is the Mellin transform of exponential function and is defined as:

$$\Gamma(z) = \int_0^\infty t^{z-1}\, e^{-t} dt, Re[z] > 0$$

$J_n(x), K_n(x)$and$Y_n(x)$are Bessel functions first and second kind.

Zeta[s] is the zeta function, has no branch cut discontinuities and is defined as:

$$Zeta[x] = \sum_{n=1}^{\infty} n^{-x}$$

Chapter 10

REFERENCES

I was standing on the shoulders of giants

Abriola, L.M. and Pinder, G.F. (1985a) *A multiphase approach to the modelling of porous media contamination by organic componounds.1 Equation development*. Water resources research; 21, 11-18.

Abriola, L.M. and Pinder, G.F. (1985b) *A multiphase approach to the modelling of porous media contamination by organic componounds1 Numerical simulation*; Water resources research; 21, 19-26.

Abdon Atangana, (2012) *Numerical solution of space-time fractional derivative of groundwater flow equation*, International conference of algebra and applied analysis, June 20-24 Istanbul, pp 20.

Abdon Atangana and Botha JF (2012) *Analytical Solution of the Groundwater Flow Equation obtained via Homotopy Decomposition Method*. J Earth Sci Climate Change 3:115. doi:10.4172/2157-7617.1000115.

Abdon Atangana and Adem Kilicman, "*Analytical Solutions of the Space-Time Fractional Derivative of Advection Dispersion Equation*," *Mathematical Problems in Engineering*, vol. 2013, Article ID 853127, 9 pages, 2013. doi:10.1155/2013/853127.

Abdon. Atangana, E. Alabaraoye, (2012) *Groundwater flow model described by prolate spheroid coordinates and new analytical solution for the flow model in a confined aquifer under Theis conditions*. Accepted for publication in international Journal of Advance Applied Mathematics and Mechanics in press.

Abdon Atangana and Aydin Secer, "*A Note on Fractional Order Derivatives and Table of Fractional Derivatives of Some Special Functions*," Abstract and Applied Analysis, vol. 2013, Article ID 279681, 8 pages, 2013. doi:10.1155/2013/279681.

Abdon Atangana and Ernestine Alabaraoye **(**2013) "*Solving system of fractional partial differential equations arisen in the model of HIV infection of CD4+ cells and attractor one-dimensional Keller-Segel equation* " Advances in Difference Equations 2013, 2013:94 doi:10.1186/1687-1847-2013-94.

Abdon Atangana, O. Aden Ahmed, and Necdet Bıldık, **(**2013) "*A Generalized Version of a Low Velocity Impact between a Rigid Sphere and a Transversely Isotropic Strain-Hardening Plate Supported by a Rigid Substrate Using the Concept of Noninteger Derivatives*," Abstract and Applied Analysis, vol. 2013, Article ID 671321, 9 pages,

Abdon Atangana and Botha J.F **(**2013) " *Generalized groundwater flow equation using the concept of variable order derivative*" Boundary Value Problems, **2013**:53 doi:10.1186/1687-2770-2013-53, 2013.

Abdon Atangana and A.H.Cloot **(**2013) "*Stability and convergence of the space fractional variable-order Schrodinger equation"* Advances in Difference Equations vol.2013,:80 doi:10.1186/1687-1847-2013-80.

Adams EE, Gelhar LW.(1992) Field study of dispersion in a heterogeneous aquifer: 2. Spatial moment analysis. Water Resour Res;28(12):3293–307.

Adomian, G. (1988), *A review of the decomposition method in applied mathematics*, J Math Anal Appl 135, 501–544.

Air Sparging, *The Centre for Public Environmental Oversight (CPEO*). Retrieved 2009-11-29.

AndrianovI., L. Manevitch, Asymptotology*: (*2003) *Ideas, Methods, and Applications*, Kluwer Academic Publishers,

Andrianov I., J. Awrejcewicz, (2000) *Construction of periodic solution to partial differential equations with nonlinear boundary conditions*, International Journal of Nonlinear Sciencesand Numerical Simulation 1 (4) pp 327–332.

Asaah VA, Abimbola AF, Suh CE (2006) *Heavy metal concentration and distribution in surface soils of the Bassa Industrial Zone 1 Douala Cameroon*. Arabian J SciEng 31(2A):147–158.

Asangwe, C. K. A. (2006) *The Douala Coastal Lagoon Complex, Cameroon*: Environmental Issues. Barcelona Field Studies Centre; Industry Location Factors, 2008:

Atheull, AN; Din, N; Longonje, SN; Koedam, N; Dahdouh-Guebas, F (2009-11-17). "*Commercial activities and subsistence utilization of mangrove forests around the Wouri estuary and the Douala-Edea reserve (Cameroon).". Ethnobiol Ethnomed* **5**: 35.

Asangwe, C. K. A. (2006) *The Douala Coastal Lagoon Complex, Cameroon*: Environmental Issues. Barcelona Field Studies Centre; Industry Location Factors, 2008:

Azevedo, E. N., de Sousa, P. L., de Souza, R. E.,Engelsberg, M., Miranda, M.deN.do N. & Silva, M. A. (2006) "*Concentration-dependent diffusivity and anomalous diffusion: A magnetic resonance imaging study of water ingress in porous zeolite*," *Phys.Rev. E* **73**, 011204.

Bear, J. (1979) *hydraulics of Groundwater*; Water Resources and Environmental Engineering; McGraw-Hill, Book Co., New York.

Bear, J. (1972) *Dynamic of fluids in porous media*. American Elsevier Environmental science series; American Elsevier Publishing Company, Inc., New York

Becker-Kern P, Meerschaert MM, Scheffler HP. (2004)Limit theorems for coupled continuous time random walks. Ann Probab;32(1B):730–56.

Benson DA, Wheatcraft SW, Meerschaert MM. (2000) *Application of a fractional advection–dispersion equation.* Water Resour Res;36(6):1403–12.

Benson DA, Schumer R, Meerschaert MM, Wheatcraft SW. (2001) *Fractional dispersion, Lévy motion, and the MADE tracer tests*. Transport Porous Med;42:211–40.

Benson DA, Wheatcraft SW, Meerschaert MM. (2000) *The fractional-order governing equation of Lévy motion*. Water Resour Res; 36(6):1413–23.

Bender C.M., K.S. Pinsky, L.M. Simmons, (1989) *A new perturbative approach to nonlinear problems*, Journal of Mathematical Physics 30 (7), pp 1447–1455.

Berkowitz B, Cortis A, Dentz M, Scher H. (2006) Modeling non-Fickian *transport in geological formations as a continuous time random walk*. Rev Geophys;44:RG2003.

Berkowitz B, Scher H. (1998) *Theory of anomalous chemical transport in random fracture network*. Phys Rev E;57(5):5858–69.

Berkowitz B, Emmanuel S, Scher H.(2008) *Non-Fickian transport and multiple-ratemass transfer in porous media*. Water Resour Res;44:W03402.

Bob Thibodeau , (2006) *The Alternative To Pump And Treat, Water Online Magazine*, December 27.

Bouchaud JP, Georges A.(1990) *Anomalous diffusion in disordered media: statistical mechanism and physical applications*. Phys Rep;195:127–293

Bradford S.A., M. Bettahar, J. Simunek, M.T.V. Genuchten.(2004) *Straining and attachment of colloids in physically heterogeneous porous media*, Vadose Zone Journal 3, 384–394.

Botha, J. F. (1985) *Ground-water modelling: Present and future*. Transactions of the Geological Society of South Africa. **88**, 549–552.

Botha. J. F. (1996); *Principle of groundwater motion, Institute for groundwater study, University of the Free State*, Bloemfontein. Unpublished Lecturer note.

Botha, J.F, Buys, J. Verwey, J.P, Tredoux, G., Moodie, J.W. and Hodgkiss, M.(1990*) Modelling Groundwater Contamination in the Atlantics Aquifer*. WRC Report No 175/1/90. Water Research Commission, P.O. Box 824, Pretoria 0001.

Bromly M, Hinz C.(2004) *Non-Fickian transport in homogeneous unsaturated repacked sand*. Water Resour Res;40:W07402.

Brusseau ML, Gerstl Z, Augustijn D, Rao PSC. (1994)*Simulating solute transport in an aggregated soil with the dual-porosity model: measured and optimized parameter values*. J Hydrol;163:187–93.

Carrera J, Sanchez-Vila X, Benet II, Medina A, Galarza G, Guimera J. (1998) *On matrix diffusion: formulations, solution methods, and qualitative effects*. Hydrogeol. J.;6:178–90.

Caputo M. (1967) *Linear models of dissipation whose Q is almost frequency independent*. Part II, J Roy AstrSoc 13 , 529–539.

Chapman DV (1996) *Water quality assessments: a guide to the use of biota, sediments and water in environmental monitoring*, 2nd .Spon Press, Taylor and Francis Group, London, 525.

Chechkin, A. V., Gorenflo, R. & Sokolov, I. M (2005) "*Fractional diffusion in inhomogeneous media,"* J. Phys. A: Math. Gen. **38**, L679–L684.

Clarke D, Meerschaert MM, Wheatcraft SW. (2005) *Fractal travel time estimates for dispersive contaminants.* Ground Water;43(3):401–7.

Cleary, R.W. and Ungs, M.J, (1978) *Groundwater Pollution and Hydrology. Mathematical Models and Computer programs;* Water Resources Programs, Princeton University, Princeton, New Jersey, 08540

Coimbra, C. F. M. (2003) "*Mechanics with variable-order differential operators*," *Ann. Phys. (Leipzig) Math.Sci.***12**, 692–703.

Cortis A, Berkowitz B (2004). *Anomalous transport in "classical" soil and sand columns*. Soil Sci Soc Am J;68:1539–48.

Coats KH, Smith BD. (1964) *Dead-end pore volume and dispersion in porous media*. Soc Petrol Eng J (March):73–84.

Cushman JH, Ginn TR. (2000) *Fractional advection–dispersion equation: a classical mass balance with convolution-Fickian flux*. Water Resour Res;36(12):3763–6.

Cushman JH, Ginn TR. (2000) *Fractional advection-dispersion equation: a classical mass balance with convolution-Fickian flux*. Water Resour Res;36(12): 3763–6

David L. Naftz and James A. Davis, (1999) *Deep Aquifer Remediation Tools (DARTs): A new technology for ground-water remediation,* Science for changing world, pp 1-2.

Davies, J. T. (1973); *The Scientific Approach*. (2nd Ed) Academic Press, London.

Delamotte B., (1993) *Non-perturbative method for solving differential equations and finding limit cycles*, Physical Review Letters 70 pp 3361–3364.

Deng ZQ, Singh VP, Bengtsson L.(2004) *Numerical solution of fractional advection–dispersion equation*. J Hydraul Eng;130(5):422–31.

Dent, J. E. (2012) *Climate and Meteorological Information Requirements for Water Management. A Review of Issues*. Technical Report Series No. 1. WMO-No. 1094. World Meteorological Organization, Geneva.

Dentz M, Berkowitz B. (2003) *Transport behavior of a passive solute in continuous time random walks and multirate mass transfer*. Water Resour Res;39(5):1111.

Dentz M, Cortis A, Scher H, Berkowitz B. (2004) *Time behaviour of solute transport in heterogeneous media: transition from anomalous to normal transport*. Adv.Water Resour.;27: pp 155–73.

Din N, Priso RJ, Kenne M, Ngollo, DE, Blasco F (2002). *Early growth stages and natural regeneration of Avicennia germinans (L.) Stearn in the Wouri estuarine mangroves (Douala-Cameroon).* Wetlands,Ecology and Management 10 (6):461-472.

Diersch, H.-J. G. (2009) *FEFLOW® Finite Element Subsurface Flow & Transport Simulation System. Reference Manual*. DHI-WASY Gmbh, Berlin.

Djeuda-Tchapnga HB, Tanawa E, Ngnikam E. (2001) *L'eau au Cameroun*; Presses Universitaires, Yaoundé, 115–129

Dumort JC (1968) *Notice explicative sur la feuille de Douala-Quest*, Direction Mines et de la Geologie du Cameroun. Yaoundé, 69 – 56

Eneke, G. T., Ayonghe, S. N., Chandrasekharam, D., Ntchancho, R., Ako, A. A., Mouncherou, O. F. and Thambidurai, P. (2011) *Controls on groundwater chemistry in a highly urbanised coastal area*. International Journal of Environmental. Research. **5** (2), 475-490.

EPA (1996) *Documenting Ground-Water Modeling at Sites Contaminated with Radioactive Substances.* EPA 540-R-96-003. U.S. Environmental Protection Agency, Washington, D.C

Essex C. And M. Davison. (1998) *Fractional differential equations and initial value problems*. Math. *Scientist*, 23:108–106.

Eggleston J, Rojstaczer S.(1998) *Identification of large-scale hydraulic conductivity trends and the influence of trends on contaminant transport*. Water Resour Res;34(9):2155–68

Feynman, R. P. (1956). *The Meaning of It All I, the Uncertainty of Science*

Fonteh, M. F. (2003) *Water for people and the environment: Cameroon water development report*. Background paper for African Water Development Report, Addis Ababa, Economic Commission for Africa.

Gabche, C.E.; Smith, V.S. (2007) *Water, Salt and Nutrients Budgets of Two Estuaries in the Coastal Zone of Cameroon*.West African Journal of Applied Ecology**3**.

Garrels, R.M. and Christ, C.L. (1965) *Solution, Minerals and Equilibrium;* Harper and Row, New York

Gerke HH, van Genuchten MT. (1993) *A dual-porosity model for simulating the preferential movement of water and solutions in structured porous media*. Water Resour

Res;29(2):305–20.

Gillham, R.W., and Burris, D.R. (1992) *Recent developments in permeable in situ treatment walls for remediation of contaminated groundwater*: Proceedings, Subsurface Restoration Conference, June 21-24, 1992,Dallas, Tex.

Grabasnjak M. *Random particle motion and fractional-order dispersion inhighly heterogeneous aquifers*. MS thesis, University of Nevada, Reno, 2003.

Guévart, E., Noeske, J., Solle, J., Essomba, J.-M., Edjen guele, M., Bita, A., Mouangue, A. and Manga, B. (2006) *Déterminant du cholera a´Douala*. Médecin Tropical. **66**, 283–291.

Haggerty R, McKenna SA, Meigs LC. (2000) *On the late-time behavior of tracer test breakthrough curves*. Water Resour Res;36(12):3467–79.

Haggerty R, Wondzell SM, Johnson MA. (2002) *Power-law residence time distribution in the hyporheic zone of a 2nd-order mountain stream*. Geophys Res Lett;29(13):1640.

Harvey CF, Gorelick SM. (1995);*Temporal moment generating equations: modelling transport and mass transfer in heterogeneous aquifers*. Water Resour. Res. ;31(8):pp 1895–911.

Harvey CF, Gorelick SM. (2000) *Rate-limited mass transfer or macrodispersion:which dominates plume evolution at the Macro dispersion Experiment (MADE) site*? Water Resour Res;36(3):637–50.

Herrick MG, Benson DA, Meerschaert MM, McCall KR. (2002) *Hydraulic conductivity, velocity, and the order of the fractional dispersion derivative in a highly heterogeneous system*. Water Resour Res;38(11):1227.

Hatano Y, Hatano N. (1998) *Dispersive transport for ions in column experiments: an explanation of long-tailed profiles*. Water Resour Res;34(5):1027–33.

Hayman, M, & Dupont, R. R. (2001). *Groundwater and Soil Remediation: Process Design and Cost Estimating of Proven Technologies*. Reston, Virginia: ASCE Press.

He J. H., (1997),*Variational iteration method for delay differential equations*, Commun Nonlinear Sci NumerSimulat 2, 235–236.

He J.H., (1999) *Homotopy perturbation technique*, Computer Methods in Applied Mechanics andEngineering 178 pp 257–262.

He, J.H. (2000) *A coupling method of homotopy technique and perturbation technique for nonlinear problems*, International Journal of Nonlinear Mechanics 35 (1) pp 37–43.

He J. H., (2001) *Book-keeping parameter in perturbation methods*, International Journal of Nonlinear Science and Numerical Simulation 2 (3) pp 257–264.

He J.H., (1999) *Variational iteration method*: *a kind of nonlinear analytical technique: some examples*, International Journal of Nonlinear Mechanics 34 (4), pp 699–708.

Hem, J.D. (1970) *Study and interpretation of the Chemical Characteristics of Natural Water*. Water supply; Paper No.1473 (2nd Ed); US Geology Survey, Washington.

Helton, J. C. and Davis, F. J. (2003) *Latin hypercube sampling and the propagation of uncertainty in analyses of complex systems.* Reliability Engineering and System Safety. **81**, 23–69. [doi:10.1016/S0951-8320(03)00058-9.

Helton J.C. (1997) *Uncertainty and sensitivity analysis in the presence of stochastic and subjective uncertainty*. Journal of Statistical Computation and Simulation, 3–76.

Helton . J.C. (1993) *Uncertainty and sensitivity analysis techniques for use in performance assessment for radioactive waste disposal*. Reliability Engineering & System Safety 42, 327–367.

Hocevar D. E., M. R. Lightner, and T. N. Trick, (1983*) A study of variance reduction techniques for estimating circuit yields*.IEEE Trans.Computer-Aided Design, vol. CAD-2, no. 3,180-192

Hughes, R. H.; Hughes, J. S. (1992).*A directory of African wetlands*; IUCNISBN 2880329493, 466

Hudak, P. F. (2009) *Efficiency comparison of variably-spaced, non-pumped wells for filtering polluted groundwater*. Journal of Environmental Protection Science. **3**, 107–110.

IAEA (2004a) *Safety Assessment Methodologies for Near Surface Disposal Facilities. Results of a co-ordinated research project*. International Atomic Energy Agency. Vienna. Report Number Volume 1. Review and Enhancement of Safety Assessment Approaches and Tools. 408 p.

IAEA (2004b) *Safety Assessment Methodologies for Near Surface Disposal Facilities. Results of a co-ordinated research project*. International Atomic Energy Agency. Vienna. Report Number Volume 2. Test cases. 336 p.

Iman R.L., J.C. Helton. (1988)*An investigation of uncertainty and sensitivity analysis techniques for computer models*, Risk Analysis 8, 71–90

Iman R.L., J.C. Helton. (1985)*Comparison of uncertainty and sensitivity analysis techniques for computer models, other information*: Risk analysis 8, 116.

Iman R. L. and W. J. Conover. (1980)*Small sample sensitivity analysis technique for computer models, with an application to risk assessment*. Communications in Statistics, 1749-1874.

Iman R. L. and J. C. Helton. (1988)*An investigation of uncertainty and sensitivity analysis techniques for computer models*, Risk Analysis, vol. 8, no. 1, 71-90.

Iman R. L. and W. J. Conover. (1982) *A distribution-free approach to inducing rank correlation among input variables*.Communications in Statistics Simulation and Computation. 311-334.

Ingman, D. & Suzdalnitsky, J. (2005) "*Application of differential operator with servo-order function in model of viscoelastic deformation process*," *J. Eng. Mech.* 131, 763–767.

Inokuti M., H. Sekine, and T. Mura, (1978) *General use of the Lagrange multiplier in non-linear mathematical physics, S. Nemat-Nasser*, editor, Variational method in the mechanics of solids, Oxford, Pergamon Press, pp. 156–162.

Isukapalli, S. S. and Georgopoulos, P. G. (2001) *Computational Methods for Sensitivity and Uncertainty Analysis for Environmental and Biological Models*. Report prepared for the US Environmental Protection Agency National Exposure Research Laboratory. Research Triangle Park, NC 27711. Report Number EPA/600/R-01-068. 155 p.

ITRC (Interstate Technology & Regulatory Council) (2011) *Permeable Reactive Barrier: Technology Update. PRB-5*. Interstate Technology & Regulatory Council, PRB: Technology Update Team, Washington, D.C. http://www.itrcweb.org..

Jacob, C.E. and S.W. Lohman (1952). *Non-steady flow to a well of constant drawdown in an extensive aquifer*. Trans. Amer. Geophys. Union, Vol. 33, pp. 559-56.

James, R.C. (1966) *Advanced Calculus*. Belmont, CA, Wadsworth.

Javandel, I., Doughty, C. and Tsang, C.F (1984) *Groundwater transport: Handbook of Mathematical Models*. Water resources Monographs Series, Vol. 10 American Geophysical union, Washington, D.C.

Jousma, G. and Roelofsen, F. J. (2003) *Inventory of Existing Guidelines and Protocols for Groundwater Assessment and Monitoring.* International Groundwater Resources Assessment Centre (IGRAC). Utrecht. Report Number Report Number GP 2003-1. 22 p.

Jumarie G., (2005) *On the representation of fractional Brownian motion as an integral with respect to* $(dt)^{\alpha}$, Appl. Math. Lett. 18 (2005), no. 7, 739–748.

Jumarie G.,(2006) *Modified Riemann-Liouville derivative and fractional Taylor series of non-differentiable functions further results*, Comput. Math. Appl. 51, no. 9-10, 1367–1376

Kamta GA .(1999) *Contribution a l'etude hydrogeologique du basin de Douala; Essai de correlation des niveau captes dans l'aquifere quaternaire*, Rapport, 36.

Katte VY, Fonteh MF, Guemuh GN (2003). *Domestic water quality in urban centres in Cameroon: a case of study of Dschang in the West Province*. African Water Journal, December 2003, pp. 43-54.

Kauskopf, K.B. (1967) *Introduction to geochemistry*. McGraw-Hill book company, New York.

Keramat M.,(1996) "*Theoretical bases of Latin hypercube sampling Monte Carlo (LHSMC)estimators for statistical circuit design*," Ecole Superieure d'Electricite (SUPELEC), Paris, France, Tech. Rep. No. SUP-0696-11.

KilbasA. A., H. H. Srivastava, and J. J. Trujillo, (2006) *Theory and Applications of Fractional Differential Equations*, Elsevier, Amsterdam, The Netherlands.

Klise KA, Tidwell VC, McKenna SA, Chapin MD. (2004) *Analysis of permeability controls on transport through laboratory-scale cross-bedded sandstone*. Geol Soc Am Abstr Program;36(5):573.

Kohlbecker M, Wheatcraft SW, Meerschaert MM. (2006) *Heavy tailed log hydraulic conductivity distributions imply heavy tailed log velocity distributions*. Water Resour Res;42:W04411.

Lakin Mike . (2010) *Onshore Cameroon Douala basin*. Bomono Permit (OLHP-1&OLHP-2),173 www.envoi.co.uk.

Lee, Phyllis C. (1988) *Threatened Primates of Africa*. The Iucn Red Data Book; IUCN; ISBN 2880329558; 17.

Louie, A. H. (1983) *Categorical system theory*. Bulletin of Mathematical Biology; 45 (6), 1047–1072.

Magin, R. L. (2006) *Fractional Calculus in Bioengineering* (Begell House Publisher, Inc., Connecticut).

Magin, R. L., Abdullah, O., Baleanu, D. & Zhou, X. J.(2008) "*Anomalous diffusion expressed through fractional order differential operators in the Bloch-Torrey equation*," *J. Magn. Reson.* 190, 255–270.

Manz, C., and Quinn, K., (1997*) Permeable treatment wall design and cost analysis*: International Contaminant Technology Conference Proceedings, February 9-12, 1997, St. Petersburg, Flor., 788-794.

Mafany (1999), *Impact of the geology and seawater intrusion on groundwater quality in Douala*; M.Sc. Thesis, Unpublised, Buea University, Cameroon, 100

McInnes, Robin G.; Jakeways, Jenny (2002); *Instability: planning and management: seeking sustainable solutions to ground movement problems*. Thomas Telford.; pp. 143.

McKay M. D, R. J. Beckman, and W. J. Conover.(1979a) *A comparison of three methods for selecting values of input variables in analysis of output from a computer code*. Techno metrics, vol. 21, no. 2, 239-245.

McKay M.D, J.D. Morrison, S.C. Upton. (1999b).*Evaluating prediction uncertainty in simulation models*. Computer Physics Communications 117, 44–51.

Meerschaert MM, Scheffler HP. (2004) *Limit theorems for continuous time random walks with infinite mean waiting times*. J Appl Probab; 41(3):623–38.

Meerschaert MM, Mortensen J, Wheatcraft SW. *Fractional vector calculus for fractional advection–dispersion*. Physica A 2006;367:181–90.

Miller K. S. and B. Ross, (1993)*An introduction to the fractional calculus and fractional differential equations*; Wiley, New York,.

Miller, W. D. (1980). *Waste Disposal Effects on Groundwater: A Comprehensive Survey of the Occurrence and Control of Ground-Water Contamination Resulting from Waste Disposal Particles*. Berkeley, California: Premier Press.

Morris, B. L., Lawrence, A. R. L., Chilton, P. J. C., Adams, B., Calow, R. C. and Klinck, B. A. (2003) *Groundwater and its Susceptibility to Degradation: A Global Assessment of the Problem and Options for Management. Early Warning and Assessment*. United Nations Environment Programme. Nairobi, Kenya. Report Number Report Series, RS. 03-3. pp 126 .

Montroll EW, Weiss GH. *(*1965) *Random walks on lattices*: II. J Math Phys;6(2):167–81.

Munde, Walters. *Pesticide Use in Cameroon*. PESTICIDEUSE IN CAMEROON; pdf. Retrieved 2011-02-27.

NAS (2004) *Analytical Methods and Approaches for Water Resources Project Planning. National Academies Press*, Washington, DC(http://www.nap.edu/catalog/10973.html).

NAS (2006) *Improving the Regulation and Management of Low-Activity Radioactive Wastes*. National Academies Press, Washington, DC (http://www.nap.edu/catalog/11595.html).

National Aeronautics and Space Administration (NASA) (2010) *Measurement Uncertainty Analysis Principles and Methods. NASA Measurement Quality Assurance Handbook* – ANNEX 3. National Aeronautics and Space Administration. Washington DC. Report Number NASA-HDBK-8739.19-3. 275 p. (http://ebookbrowse.com/nhbk873919-3-pdf-d48180039)

National Academy of Sciences (2007), *Models in Environmental Regulatory Decision Making. Committee on Models in the Regulatory Decision Process* The National Academies Press, Washington, DC 20055. http://www.nap.edu/catalog/11972.html..

Neuman SP. (1993) *Eulerian–Lagrangian theory of transport in space–time non-stationary velocity fields: exact nonlocal formalism by conditional moments and weak approximation*. Water Resour Res.;29(3): 633–45.

Ngea, Peter, (2010) *Douala – Edea Reserve: the last refuge of hope for man and natur*e (Part 2). EnviroMend, 19.

Nguyen, V.V. and Pinder, G.F. (1981) *Is Dispersive Solute Transport in Porous Media Scale-dependent*? Report Number 81-WR-12. Water Resources Program, Princeton University, Princeton, N.J.

Ninan, Karachepone Ninan (2009). "*Marine and coastal resources in Cameroon: Interplay of climate and climate change". Conserving and valuing ecosystem services and biodiversity: economic, institutional and social challenges*. Earths can. ISBN 1-84407-651-2.

Ramsar Wetlands. Cameroon. http://ramsar.wetlands.org/Portals/15/CAMEROON.pdf. Retrieved 2011-03-01*Protection of Cameroon estuary mangroves through improved smoke houses*".United Nations Framework Convention on Climate Change. 01/07/2010. Retrieved 2011-03-01.

Regnoult J.M (1986) *Synthe`se Ge´ologique du Cameroun. Yaounde, Ministere de Mine et de L'energy*. Re´publique du Cameroun, 119.

Ritchey, T. (1996) *Analysis and Synthesis, 0n Scientific Method – Based on a Study by Bernhard Riemann*; Systems Research; 8 (4), 21–41

Ross, B. and Samko, S. G. (1995) "*Fractional integration operator of variable order in the* Holder space $H\lambda(x)$," *Int. J. Math. Math. Sci.* **18**, 777–788.

Olivry JC (1986) *Fleuve et rivie`re du Cameroun. Collection Monographie Hydrologie*, MESRE/ORSTOM.

K. B. Oldham and J. Spanier. (1974) *The fractional calculus*, Academic Press, New York,

Olvery, F. W. J.; Maximon, L. C. (2010), *"Mittag-Leffler function*", in Olver, Frank W. J.; Lozier, Daniel M.; Boisvert, Ronald F. et al., NIST Handbook of Mathematical Functions, Cambridge University Press.

Pinder, G. F. and Gray, W. G. (1977) *Finite Element Simulation in Surface and Subsurface Hydrology*. Academic Press, Inc., New York, N.Y.

Podlubny I., (1999) *Fractional differential equations,* Academic Press, San Diego, CA,.

Podlubny I.,(2002)*Geometric and physical interpretation of fractional integration and fractional differentiation*, Fract Calculus Appl Anal 5, 367–386

Princeton University Water Resources Program (1984) *Groundwater Contamination from Hazardous Wastes*. Prentice-Hall Inc., Englewood Cliffs, New Jersey.

Sama, Dudley Achu. (1996) *The Constraints in Managing the Pathways of Persistent Organic Pollutants into the Large Marine Ecosystem of the Gulf of Guinea--The Case of Cameroon*. Intergovernmental Forum on Chemical Safety, pp 17–19.

Samko S. G., A. A. Kilbas and O. I. Marichev, (1993) *Fractional integrals and derivatives, Translated from the 1987 Russian original,* Gordon and Breach, Yverdon.

Santamaria, F., Wils, S., de Schutter, E. & Augustine,G. J. (2006) "Anomalous diffusion in Purkinje cell dendrites caused by spines," *Neuron* **52**, 635–648.

Schmithorst, W.L., and Vardy, J.A., (1997), RCRA *corrective measures using a permeable reactive iron wall*, U.S .Coast Guard Support Center, Elizabeth City, North Carolina: International Contaminant Technology Conference Proceedings, February 9-12, 1997, St. Petersburg, Flor., 794-813.

Schumer R, Benson DA, Meerschaert MM, Baeumer B. (2001) *Eulerian derivation of the fractional advection–dispersion equation*. J Contam Hydrol;48:69–88

Schumer R, Benson DA, Meerschaert MM, Baeumer B. (2003) *Fractal mobile/immobile solute transport*. Water Resour Res.;39(10):1296.

Sin G. K.V. Gernaey, A.E. Lantz. (2009a) *Good modelling practice for PAT applications: propagation of input uncertainty and sensitivity analysis*, Biotechnology Progress 25, 1043–1053.

Sin G. K.V. Gernaey, M.B. Neumann, M.C.M. van Loosdrecht, W. Gujer. (2009b) *Uncertainty analysis in WWTP model applications: a critical discussion using an example from design*. Water Research, 2894–2906.

Solomon, T. H., Weeks, E. R. & Swinney, H. L. (1993)"Observation of anomalous diffusion and L´evy flights in a two-dimensional rotating flow," *Phys. Rev. Lett.***71**, 3975–3978.

Sun, H. G., Chen, W. & Chen, Y. Q. (2009) "Variable order fractional differential operators in anomalous diffusion modeling," *Phys. A* **388**, 4586–4592.

Sun, H. G., Chen, Y. Q. & Chen, W. (2011) "Random order fractional differential equation models," *Sign.Process.* **91**, 525–530.

Steinberg H. A.. (1963) *Generalized quota sampling*. Nuc. Sci. and Engr., vol. 15, 142-145.

Sudicky, E.A. (1983); *An advection-Diffusion Theory of Contamination transport for Stratified Porous Media. Unpublished Ph.D*. Thesis, Department of Earth sciences, University of Waterloo Ontario.

Suthersan, S. S. (1999) *In situ air Sparging. Remediation Engineering*: Design Concepts. S. S. Suthersan (ed.) CRC Press. Boca Raton.

Stewart, Robert. *Groundwater Remediation*, Retrieved on 2009-11-29.

Stumm, W. and Morgan, J.J.(1996): *Aquatic Chemistry, Chemical Equilibria and Rates in Natural Waters,* 3rd ed. John Wiley & Sons, Inc., New York, 1022p.

Takem Gloria Eneke Dornadula Chandrasekharam, Samuel N. Ayonghe, P. Thambidurai. (2010) *Pollution characteristics of alluvial groundwater from springs and bore wells in semi-urban informal settlements of Douala, Cameroon, Western Africa*. Environ EarthSci 61 DOI 10.1007/s12665-009-0342-8, 287–298.

Tamfu S, Batupe M (1995) *Geologic setting, stratigraphy and hydrocarbon habitat of the Douala Basin Cameroon*. Natl Hydrocarbon J Cameroon, pp 3-6.

Tanawa E, Djeuda Tchapnga HB, Ngnikam E, Temgoua E, Siakeu E (2002) *Habitat and protection of water resources in suburban areas in African cities*. Build Environ vol.37, pp 269–275.

TERZAGHI, K., (1923), *Die Berechnung der Durchla¨ssigkeitsziffer des Tones aus dem Verlaug der Hydrodynamischen Spannungsercheinungen: Akademie der Wissenchaften in Wein, Sitzungsberichte, Mathematisch-Naturwissenschaftliche Klasse*, Part IIa, v. 132, no. 3/4, p.125–128.

Theis, C.V. (1935). *The relation between the lowering of the piezometric surface and the rate and duration of discharge of a well using groundwater storage*. Trans. Amer. Geophys. Union, Vol. 16, pp. 5 19-524.

Travis, C.C., and Doty, C.B., (1990), *Can contaminated aquifers at Superfund sites be remediated? Environmental Science and Technology*, vol. 24, 1464-1466.

Trefry MG, Ruan FP, McLaughlin D. (2003) Numerical simulations of pre-asymptotic transport in heterogeneous porous media: departure from the Gaussian limit. Water Resour Res;39(3):1063

(UBC) (2007) *The Uniform Building Code* (UBC) lists Cameroon.

Umarov, S. & Steinberg, S. (2009) "Variable order differential equations and diffusion with changing modes,"*Zeitschrift fr Analysis und ihre Anwendungen* **28**,431–450.

UNFCCC (2011) *Douala Landfill gas recovery and flaring project Version 1.5. Project 4175, Clean Development Mechanism Project Design Document*, Version 03. 62 p. United Nations Framework Convention on Climate Change.

U.S. Environmental Protection Agency (EPA) (2012) *Technologies: Remediation*. http://www.clu-in.org/remediation/. (Date accessed: 2013-01-23.).

U. S. Geological Survey (USGS) (1999) *Deep Aquifer Remediation Tools (DARTs): A new technology for ground-water remediation*. U.S.Department of the Interior, U.S. Geological Survey. Washington, DC. Report Number USGS Fact Sheet 156-99. 2 p.

USEPA (U.S. Environmental Protection Agency). 1988. *Guidance for Conducting Remedial Investigations and Feasibility Studies under CERCLA (Interim Final).* OSWER Directive 9355.3-01, EPA/540/G-89/004.

USEPA. (1998a). *Permeable Reactive Barrier Technologies for Contaminant Remediation*. EPA/600/R-98/125.

USEPA. (1998b). *Technical Protocol for Evaluating Natural Attenuation of Chlorinated Solvent sin Groundwater*: EPA/600/R-98/128. Cincinnati: Office of Research and Development National Risk Management Research Laboratory.

USEPA. (2000a). *Engineered Approaches to In Situ Bioremediation of Chlorinated Solvents: Fundamentals and Field Applications.* EPA/542/R-00/008. Office of Solid Waste and Emergency Response, Division of Solid Waste and Emergency Response.

USEPA. (2000b). *Field Demonstration of Permeable Reactive Barriers to Remove Dissolved Uranium from Groundwater, Fry Canyon, Utah. Interim Report, September 1997–September1998.* EPA/402/C-00/001.

USEPA. (2008a). *Green Remediation: Incorporating Sustainable Practices into the Remediation of Contaminated Sites.* EPA/542/R-08/002.

Van Tonder, Botha J F, Chiang W H, Kunstmann H and XU Y. (2001) Estimation of sustainable yields of boreholes in fractured rock formations. *J. Hydrol.* **241** 70-90.

Van Der Voort I,I (2001) *Risk-Based Decision Tools for Managing and Protecting Groundwater Resources. Ph.D.* Dissertation, University of the Free State, PO Box 339, Bloemfontein.

Wheatcraft SW, Tyler SW. (1988) *An explanation of scale-dependent dispersivity in heterogeneous aquifers using concepts of fractal geometry*. Water Resour Res;24(4):566–78

Wilson, R.D., and Mackay, D.M., (1997), *Arrays of un-pumped wells: An alternative to permeable walls for in situ treatment: International Contaminant Technology Conference Proceedings*, February 9-12, St. Petersburg, Flor. 888 - 894.

Wisegeek (2012) *What is Groundwater Pollution*? http://www.wisegeek.com/what-is-groundwater-pollution.htm. (Date accessed: 2012-07-09).

Wolfram Research Inc. (2012) *Mathematica, Version* 9.0. Champaign, Illinois

World Meteorological Organization (2008) *Guide to Hydrological Practices. Volume I Hydrology–From Measurement to Hydrological Information*. WMO-No. 168. Geneva.

World Weather Information Service (2012) - Douala". *World Meteorological Organization.* Retrieved December 6.

Yerima, Bernard P.K.; Van Ranst, E. (2005); *Major Soil Classification Systems Used in the Tropics: Soils of Cameroon*. Trafford Publishing. ISBN 1412057892, 144.

Zaslavsky G. M., *Hamiltonian Chaos and Fractional Dynamics, Oxford University Press, 2005.*

Zhang XX, Mouchao L. (2007) *Persistence of anomalous dispersion in uniform porous media demonstrated by pore-scale simulations*. Water Resour Res;43: W07437

Zhang Y, Benson DA, Meerschaert MM, LaBolle EM. (2007) *Space-fractional advection–dispersion equations with variable parameters: diverse formulas, numerical solutions, and application to the MADE-site data*. Water Resour. Res;43:W05439

Zhang Y, Baeumer B, Benson DA. *The relationship between flux and resident concentrations for anomalous diffusion*. Geophys Res Lett 2006;33: L18407

Zheng C, Gorelick SM. (2003) *Analysis of the effect of decimeter-scale preferential flow paths on solute transport. GroundWater*;41(2):142–55.

Zinn B, Harvey CF. (2003) *When good statistical models of aquifer heterogeneity gobad: a comparison of flow, dispersion, and mass transfer in connected and multivariate Gaussian hydraulic conductivity fields*. Water Resour. Res; 39(3):1051.

Zoeteman, B.C.J and Piet, G.J (1980*) Organic water quality changes during sand band and dune filtration of surface waters in the Netherlands*. Journal of the American Water Workers Association, 72,400-404

Abstract

One reason why groundwater, so often constitutes the main source of drinking water in many cities and towns around the world, is because it is frequently present in sufficient quantities at the point of demand. However, this seemingly advantage may sometimes be its greatest disadvantage, especially in situations where the groundwater occurs at shallow depths and the area overlying the aquifer is populated densely. This problem is particularly relevant in the present technological age with its vast quantities of waste that is often disposed in an uncontrolled manner. Such a situation occurs at Douala the economic capital of Cameroon in central Africa. The city not only host more than 80% of industries in the country, but also has the largest urban population of approximately 3 000 000 with a population density of approximately 350 persons per square kilometre, which continue to increase at a rate of approximately 120 000 migrants per year from the rural areas, while the groundwater level is very shallow and may sometimes rise above the soil surface, especially during floods, which occur not too infrequently.

Although the pollution problem is not restricted to groundwater as such, it is aggravated here, because of the ancient belief that wastes are safely disposed of, if buried below the earth's surface. It took disasters like Love Canal and the Price Landfill to discover the detrimental effects that this practice may have on the population living on or near polluted aquifers. Extreme care therefore should be exercised to prevent the pollution of any aquifer that may pose problems to living organisms or to try and restore a polluted aquifer threatening the natural environment. Groundwater pollution should therefore receive urgent attention when discovered.

This thesis describes an attempt to develop a set of guidelines for the restoration of the groundwater resources at Douala, based on the relatively new technique of permeable reactive barriers for groundwater remediation—a technique that is also increasingly applied in the restoration of the Superfund sites in the United States of America.

Modern attempts to clean up contaminated aquifers, relies heavily on the use of suitable computational numerical models. Such models have in the past always been based on the classical hydrodynamic dispersion equation. However, an analysis of the equation in this thesis has shown that the equation cannot account for the long-tail contamination plumes characteristic of fractured rock aquifers. Fortunately, it is not too difficult to develop a more suitable equation. For, as shown in the thesis, all that one has to do is to replace the ordinary

derivatives in the classical equation with fractional derivatives.

Mechanistic modeling of physical systems is often complicated by the presence of uncertainties, which was in the past usually neglected in the models used in the restoration of aquifers.While these uncertainties have regularly been neglected in the past, it is nowadays imperative that any groundwater model be accompanied by estimates of uncertainties associated with the model. Although a large number of approaches are available for this purpose, they often require exorbitant computing resources. The present investigation was consequently limited to the application of the Latin Hypercube Sampling method applied to an analytical solution of the hydrodynamic dispersion equation.

It has been known for years that the hydrodynamic dispersion equation discussed in Chapter 5, is not able to account for the long-tail plumes often observed in studies of contaminated fractured-rock aquifers. An approach frequently used to account for this is to replace the ordinary spatial and temporal derivatives in the hydrodynamic equation with fractional derivatives—a procedure confirmed in this thesis.

Keywords and phrases: Groundwater pollution, Douala City, hydrodynamic dispersion equation, groundwater flow equation, uncertainty and sensitivity analyses, groundwater remediation; fractional derivatives, mathematical, analytical and numerical models.

OPSOMMING

Een van die redes waarom grondwater gereeld die primêre bron van drinkwater in baie stede en dorpe in die wêreld is, is omdat dit teenwoordig is in voldoende hoeveelhede wanneer dit benodig word. Ongelukkig is hierdie voordeel dikwels ’n groot nadeel, veral in digsbevolkte gebiede met vlak grondwatervlakke. Hierdie probleem kom veral voor in digsbevolkte gebiede wat voortdurend groot hoeveelhede afval genereer en dit op ’n ongekontroleerde wyse wegdoen. Dit is onder andere die geval in Douala, die ekonomiese hoofstad van die staat Kameroen in sentraal Afrika. Die stad huisves meer as 80% van die industrie in die land en het ook die grootste stedelike bevolking van ongeveer 3 000 000 met ’n digtheid van plus minus 350 persone per km^2 wat elke jaar met sowat 120 000 vanaf die landelike gebiede toeneem. Die grondwatervlak is baie vlak en dagsoom dikwels tydens vloede watgereeld voorkom.

Alhoewel die besoedelingsprobleem nie beperk is tot grondwater as sulks nie, word dit hier vererger deur die historiese geloof dat afval veilig gestort word as dit in die grond begrawe word. onder die. Dit het rampe soos die Love Canal en die Price stortingsterrein gekos om

mense te besef dat hierdie praktyk uiters negatiewe impakte op die bevolking in die onmiddellike omgewing van besoedelde akwifere mag hê. Uiterste voorsorg moet dus getref word om te verhoed dat akwifere besoedel word.

Hierdie proefskrif beskryf ’n poging om ’n stel riglyne daar te stel vir die herstel van die besoedelde grondwaterbronne van te Douala, wat gebaseer word op die redelike nuwe tegniek van deurlaatbare reagerende versperrings—’n tegniek wat ook in die skoonmaak van die sogenaamde “Superfund” terreine in die VSA toegepas word.

Hedendaagse pogings om besoedelde akwifere skoon te maak, steun geweldig op die gebruik van geskikte rekenaar gebaseerde numeriese modelle. Hierdie modelle is tot nogtoe gewoonlik op die klassieke hidrodinamiese dispersiewe vergelyking gebaseer. Die ondersoek wat vir hierdie proefskrif onderneem is, ondersteun egter die hedendaagse siening dat hierdie vergelyking nie besoedelingspluime met lang agterstukke—’n karakteristieke eienskap van besoedelingspluime in gekraakte akwifere—kan beskryf nie. Soos getoon in hierdie proefskrif, kan die probleem geredelik oorkom word deur klassieke afgeleides wat in die hidrodinamiese dispersievergelyking voorkom met breukafgeleides te vervang.

Meganistiese modellering van fisiese sisteme is altyd onderhewig aan onsekerhede wat in die verlede gewoonlik in modelle van sulke geïgnoreer is wat gebruik is in die restourasie van akwifere. Hierdie onsekerhede is in die verlede gewoonlik geïgnoreer. Deesdae is dit egter noodsaaklik dat modelle skattings van dié onsekerhede moet bevat. Alhoewel daar ’n groot verskeidenheid van metodes bestaan wat vir hierdie doel gebruik kan word, vereis dit dikwels buitensporige hulpbronne. Die huidige ondersoek is daarom beperk tot die aanwending van Latynse hiperkubus monsters, wat toegepas is op ’n analitiese oplossing van die hidrodinamiese dispersiewe vergelyking wat getoon het dat dit uiters geskik vir die doel is.

Sleutelwoorde en frases: Grondwaterbesoedeling, Douala Stad, hidrodinamiese dispersievergelyking, grondwatervloeivergelyking, herstel van besoedelde akwifere, onsekerheids- en sensitiwiteitsanalises, breukafgeleides, wiskundige, analitiese, en numeriese modelle.